Airport2030_TN_Supercritical_Airfoils_11-12-21

Aero – Aircraft Design and Systems Group
Department of Automotive and Aeronautical Engineering
Hamburg University of Applied Sciences
Berliner Tor 9
D - 20099 Hamburg

Survey of Experimental Data of Selected Supercritical Airfoils

Daniel Schiktanz
Dieter Scholz

2011-12-21

Technical Note

https://doi.org/10.48441/4427.2478

Report Documentation Page

1. Report-Number
Airport2030_TN_
Supercritical_Airfoils

2. Project Title
Efficient Airport 2030

3. ISSN / ISBN
N/A

4. Title and Subtitle
Survey of Experimental Data of Selected Supercritical Airfoils

5. Report Date
2011-12-21

6. Performing Org. Rep. No
Airport2030_TN_Supercritical_Airfoils

7. Author(s) (First Name, Last Name)
Daniel Schiktanz (Daniel.Schiktanz@haw-hamburg.de)
Dieter Scholz (info@ProfScholz.de)

8. Contract Code
03CL01G

9. Project Number
AP 2030 WT 4.1

10. Performing Agency (Name, Address)
Hamburg University of Applied Sciences (HAW)
Faculty of Engineering and Computer Science
Department of Automotive and Aeronautical Engineering
Berliner Tor 9
D - 20099 Hamburg

11. Report Type
Technical Note

12. Time Period
2008-12-01 – 2013-11-30

13. Number of Pages
236

14. Sponsoring / Monitoring Agency (Name, Address)
Bundesministerium für Bildung und Forschung
Heinemannstraße 2, D - 53175 Bonn

Projektträger Jülich, Forschungszentrum Jülich GmbH
D – 52425 Jülich

15. Number of References
16

16. Number of Tables
-

17. Number of Figures
-

18. Supplementary Notes
Language: German; URL: http://Airport2030.ProfScholz.de

19. Abstract

This survey was prepared for having a structured compendium about the aerodynamic characteristics of several supercritical airfoils. It may be used within the scope of the design of commercial airliners. The survey is based on published data coming from wind tunnel tests performed at the NASA Langley 0.3-Meter Transonic Cryogenic Tunnel. All of the referenced reports are published on the NASA Technical Reports Server (NTRS).

20. Subject Terms
supercritical airfoils, wind tunnel tests, aircraft design

21. Distribution
Department F+F, HAW Hamburg, Berliner Tor 9, D - 20099 Hamburg

22. Classification / Availability
unclassified - unlimited

23.

24. Price

Dokumentationsblatt nach DIN 1422 Teil 4

Abstract

This survey was prepared for having a structured compendium about the aerodynamic characteristics of several supercritical airfoils. It may be used within the scope of the design of commercial airliners. The survey is based on published data coming from wind tunnel tests performed at the NASA Langley 0.3-Meter Transonic Cryogenic Tunnel. All of the refe-renced reports are published on the NASA Technical Reports Server (NTRS).

Table of Contents

1 Introduction

This survey of selected supercritical airfoils was collocated in order to provide an easily to access and user-friendly compendium of experimental results of supercritical airfoil tests. Most of the pages are copies of the original publications coming from the NASA Technical Reports Server (**NTRS 2011**) which is open to the public. It has to be noted that, with two exceptions [NACA 65_1-214 and SC(2)-0714], all tests were conducted under cruise conditions at high Mach and Reynolds numbers.

Most of the tests were performed in the cryogenic tunnel at NASA Langley Research Center.

The use of the survey pages mostly is self-explanatory. Basic knowledge of geometry parameters of airfoils and of aerodynamic coefficients is required.

1.1 Included Data

For keeping the survey as clear as possible the presentation of each airfoil has the same structure. A new airfoil is presented with its name and the institution of its origin. Next there is a small table containing the most important data of the airfoil. The first two rows include the year of the referenced publication and the number of this reference. The following rows contain the maximum relative thickness of the airfoil, its design lift coefficient and Mach number and the type of boundary layer transition. For some airfoils not all of these data were available. A drawing of the airfoil together with its coordinates is presented as well.

On the following pages the lift, drag and pitching moment coefficients depending on the angle of attack are shown for several Reynolds and Mach numbers. Here the way of presentation may differ from airfoil to airfoil. For some airfoils some additional information (e.g. drag divergence Mach number vs. lift coefficient) is given.

1.2 Boundary Layer Transition

For each airfoil in this survey there is a statement included regarding transition. This refers to the position of the transition from laminar to turbulent boundary layer. This transition is either forced by a transition strip placed near the leading edge of the airfoil (fixed transition) or occurs naturally (free transition). The airfoils used for testing mostly have chord lengths between 7 and 20 cm, which is very small. With a free transition a huge portion of the boundary is laminar at low Reynolds numbers ($Re \sim 3 \cdot 10^6$) for such small airfoils. This does not reflect the conditions for a full scale airfoil at the same Reynolds numbers. Here the transition takes usually place close to the leading edge (hence most of the boundary layer is turbulent). Consequently a free transition at small chord lengths would result in lower drag coefficients than for full scale chord lengths. This is why for most of the tests transition strips were placed close to the leading edge of the airfoils for having the same conditions as for full scale airfoils. Note that these effects become more and more negligible for higher Reynolds numbers.

In **NACA TN 4279** (published in 1958) it is written about this topic:

> "*The extrapolation of small-scale test results to conditions that generally represent those of full scale continues to be one of the major problems encountered in properly interpreting wind-tunnel data. A vast majority of all high-speed tests in wind tunnels are conducted at Reynolds numbers below 4 million (based on the wing chord). For Reynolds numbers of this order, a large percentage of the boundary layer on the model can be laminar and changes in Reynolds number may cause rather large differences in the pressure distribution [...]. Tests at low Reynolds numbers can result in irregular lift and moment characteristics and changes in skin-friction drag with lift coefficient. Under full-scale conditions in flight, on the other hand, where the boundary layer is turbulent over most of the lifting surfaces, few, if any, of these irregular variations in aerodynamic characteristics found near zero lift would be expected.*"

2 Overview of Contained Airfoils

Airfoil	M_{design}	$C_{l,design}$	$(t/c)_{max}$	References	Page
BAC 1	n/a	n/a	0,1	NASA TM 87600, NASA TM 81922	10
CAST 7	0,76	0,573	0,118	AGARD AR-138	20
CAST 10-2 / DOA 2	n/a	n/a	0,121	NASA TM 86273	24
Cessna EJ Red. Airfoil	0,735[1)]	0,508[1)]	0,115	NASA TP 3579	40
DFVLR R4	n/a	n/a	0,135	NASA TM 85739	52
NACA 65_1-213[2)]	n/a	n/a	0,126	NASA TM 85732	106
NLR 7301	0,747[3)]	0,45[3)]	0,163	AGARD AR-138	114
NPL 9510	0,75	0,6	0,11	NASA TM 85663	117
SC(2)-0012	n/a	n/a	0,12	NASA TM 89102	171
SC(2)-0710	0,78	0,7	0,1	NASA TM X-72711	177
SC(2)-0714	0,74	0,7	0,14	NASA TM X-72712 (high speed)	196
				NASA TM X-81912 (low speed)	
SC(3)-0712(B)	0,76	0,7	0,12	NASA TM 86371	223
SKF 1.1	0,769	0,532	0,1207	AGARD AR-138	230
Airbus TA11	n/a	n/a	0,111	n/a	233

1) This airfoil has two design points, one for long range cruise and one for high speed cruise. The numbers given in the table are those for high speed cruise. The numbers for long range cruise are: M_{design} = 0,654; $C_{l,design}$ = 0,979.

2) This airfoil was actually developed for laminar flow. However, laminar flow airfoils also showed good characteristics at supercritical Mach numbers. This is why the airfoil NACA 65_1-213 is included in this survey.

3) The numbers given in the table are derived from the experimental results. According to the theoretic design point the numbers of this airfoil are: M_{design} = 0,721; $C_{l,design}$ = 0,6.

3 Drag Divergence Mach Number vs. Relative Thickness

Figure 3.1 shows analytical drag divergence Mach numbers determined for NASA phase 2 supercritical airfoils. Only the graph for a lift coefficient of 0,7 was validated, namely with the help of two experiments with the airfoils SC(2)-0710 and SC(2)-0714. Tests conducted with the phase 3 airfoil SC(3)-0712 showed a drag divergence Mach number of 0,76, which also matches the graph very well.

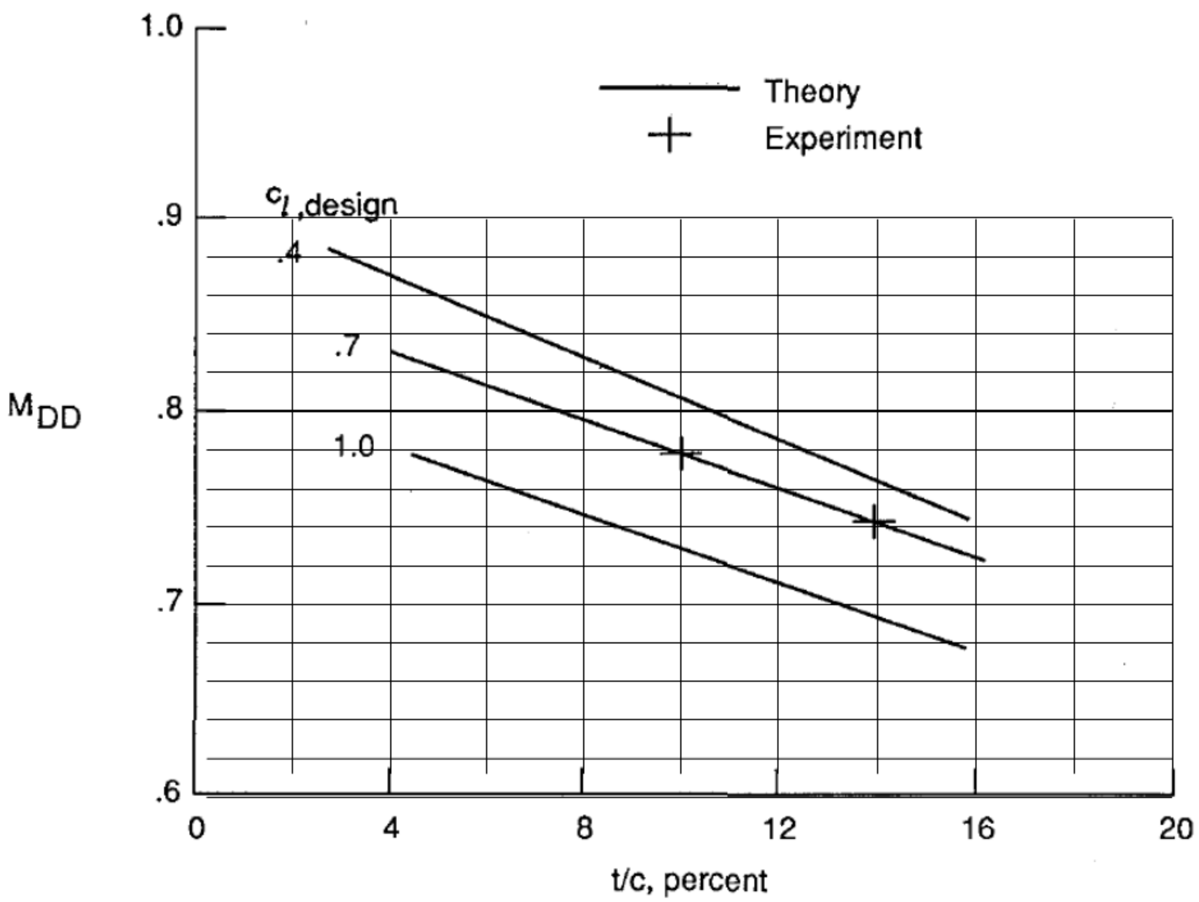

Figure 3.1 Analytical drag divergence Mach numbers for NASA phase 2 supercritical airfoils (acc. to **NASA TP 2969**)

4 Survey of Supercritical Airfoils

BAC 1

Boeing Aircraft Company

Year	1985
References	NASA TM-87600 (coordinates) NASA TM-81922 (figures)
t/c	0,1
Transition	fixed at 0,1c

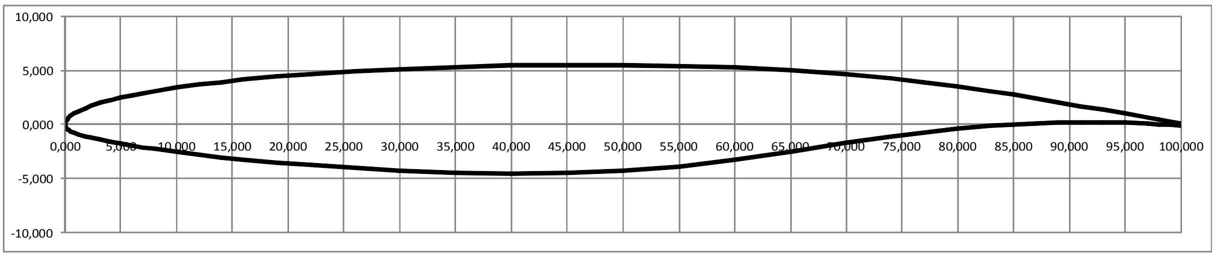

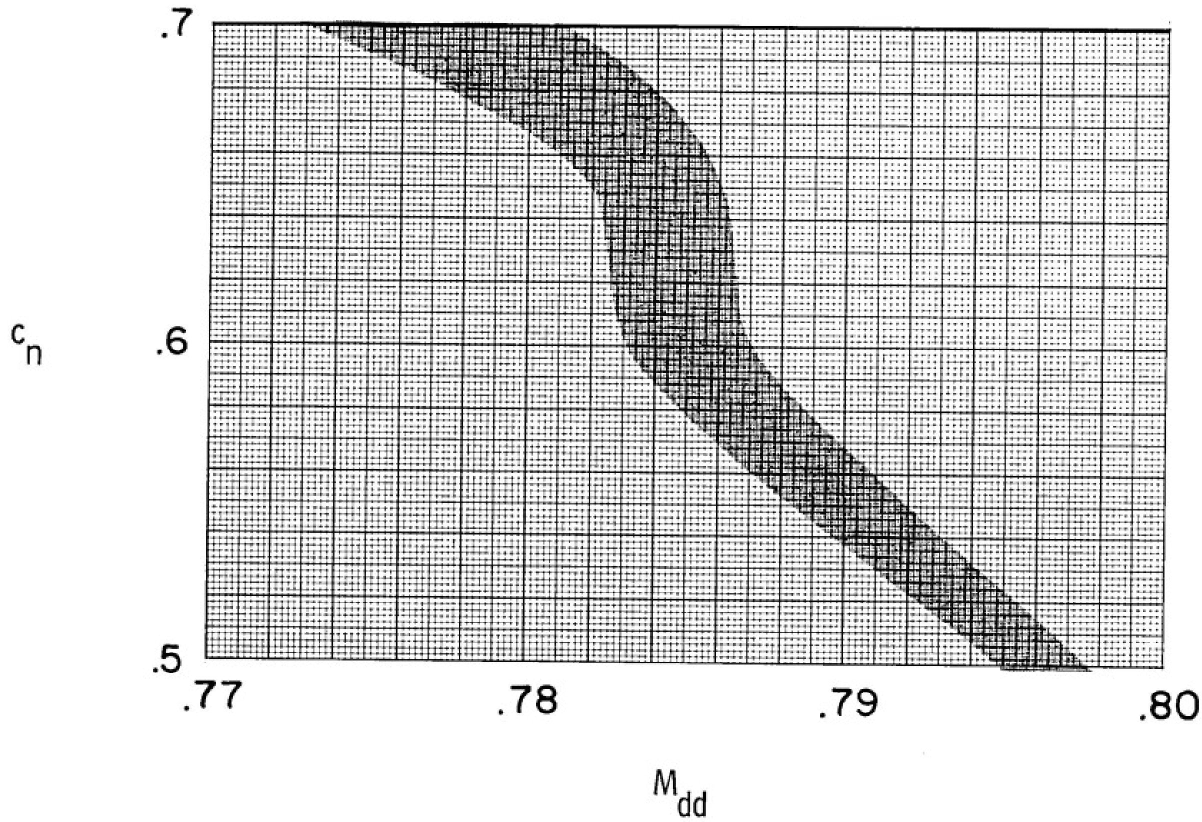

Figure 48.- Characteristic variation of normal-force coefficient with Mach number at drag divergence in Reynolds number range of 14.0×10^6 to 45.0×10^6. Free transition.

Airfoil Coordinates (in % chord)

x/c [%]	y_u/c [%]	x/c [%]	y_l/c [%]
0,000	0,000	0,000	0,000
0,050	0,242	0,050	-0,235
0,120	0,388	0,120	-0,349
0,200	0,504	0,200	-0,432
0,300	0,619	0,300	-0,508
0,500	0,798	0,500	-0,625
0,800	1,006	0,800	-0,758
1,200	1,229	1,200	-0,903
1,800	1,502	1,800	-1,084
2,400	1,731	2,400	-1,240
3,200	1,993	3,200	-1,424
4,000	2,222	4,000	-1,590
5,000	2,474	5,000	-1,779
6,000	2,697	6,000	-1,954
7,000	2,896	7,000	-2,116
8,000	3,079	8,000	-2,269
10,000	3,401	10,000	-2,548
12,000	3,678	12,000	-2,799
14,000	3,921	14,000	-3,028
16,000	4,134	16,000	-3,236
19,000	4,412	19,000	-3,519
22,000	4,647	22,000	-3,767
26,000	4,907	26,000	-4,048
30,000	5,113	30,000	-4,269
35,000	5,308	35,000	-4,463
40,000	5,436	40,000	-4,548
45,000	5,499	45,000	-4,501
50,000	5,498	50,000	-4,285
55,000	5,424	55,000	-3,875
60,000	5,269	60,000	-3,265
65,000	5,013	65,000	-2,508
70,000	4,638	70,000	-1,704
74,000	4,245	74,000	-1,107
77,000	3,896	77,000	-0,709
80,000	3,501	80,000	-0,379
83,000	3,060	83,000	-0,123
85,000	2,742	85,000	0,005
87,000	2,407	87,000	0,100
89,000	2,060	89,000	0,162
91,000	1,705	91,000	0,190
93,000	1,350	93,000	0,185
95,000	0,994	95,000	0,147
97,000	0,639	97,000	0,075
98,000	0,461	98,000	0,026
99,000	0,283	99,000	-0,030
100,000	0,106	100,000	-0,096

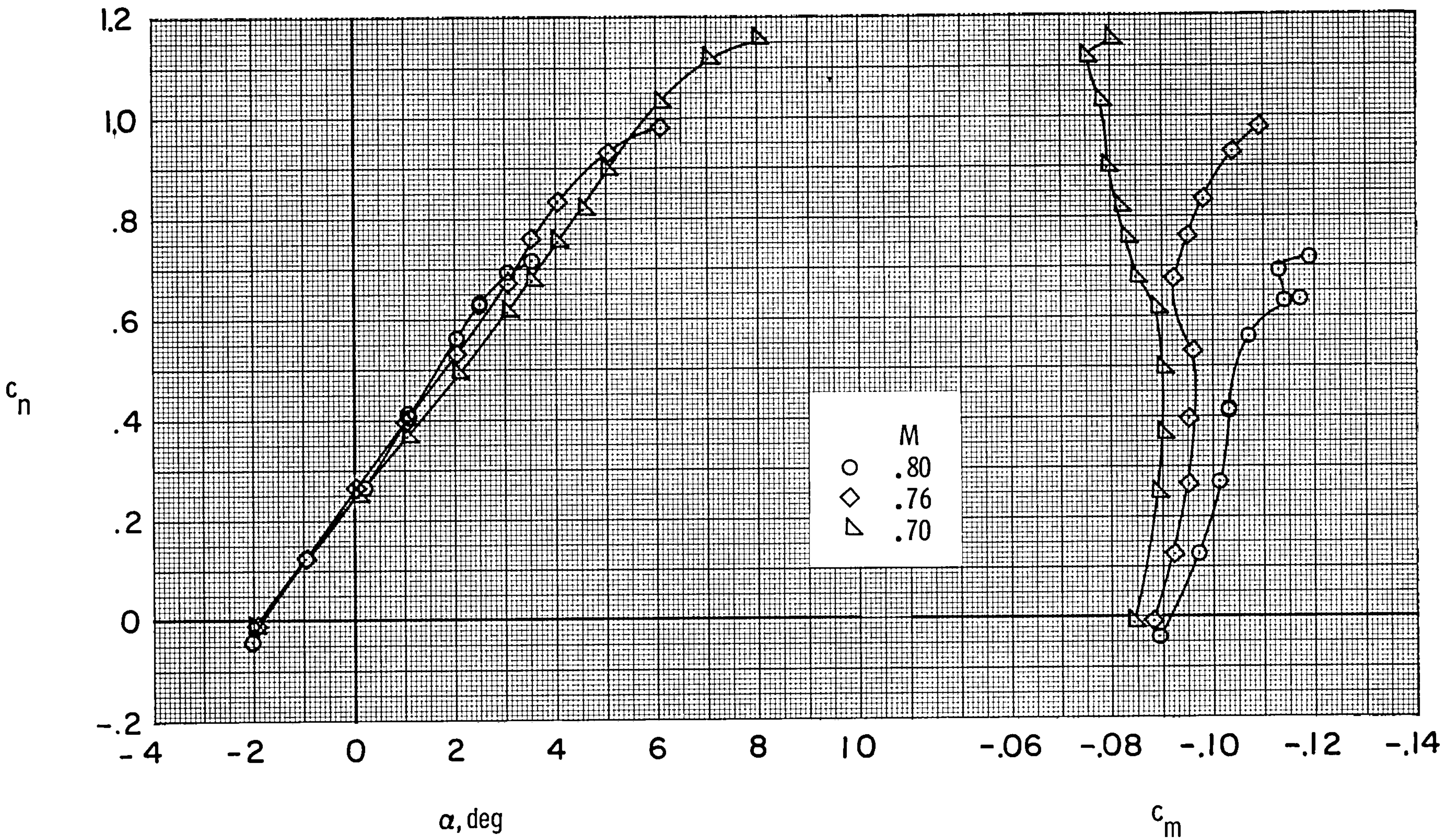

(a) c_n vs α and c_m.

Figure 31.- Effect of Mach number on aerodynamic characteristics of airfoil with fixed transition at $R \approx 4.4 \times 10^6$.

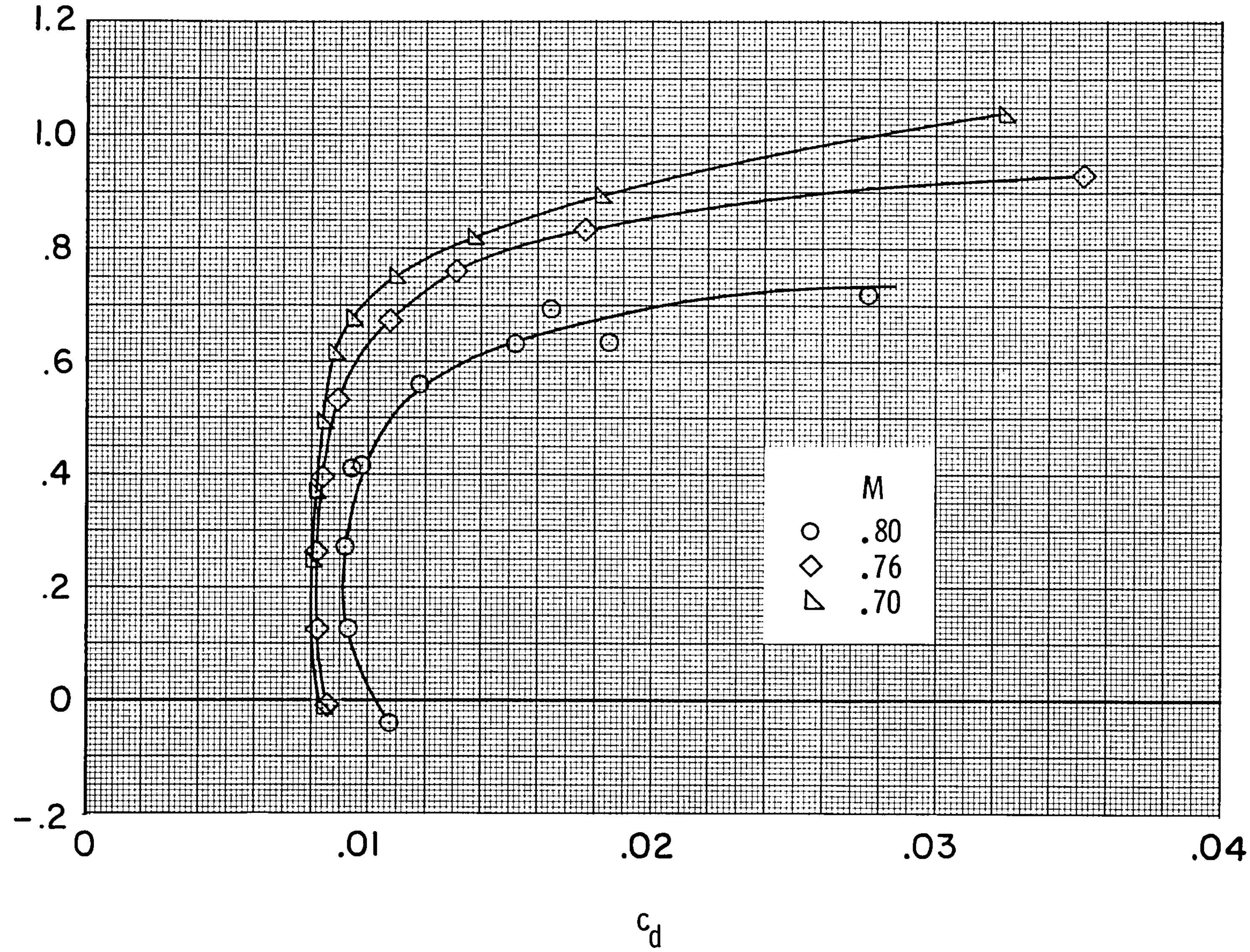

(b) c_n vs c_d.

Figure 31.- Concluded.

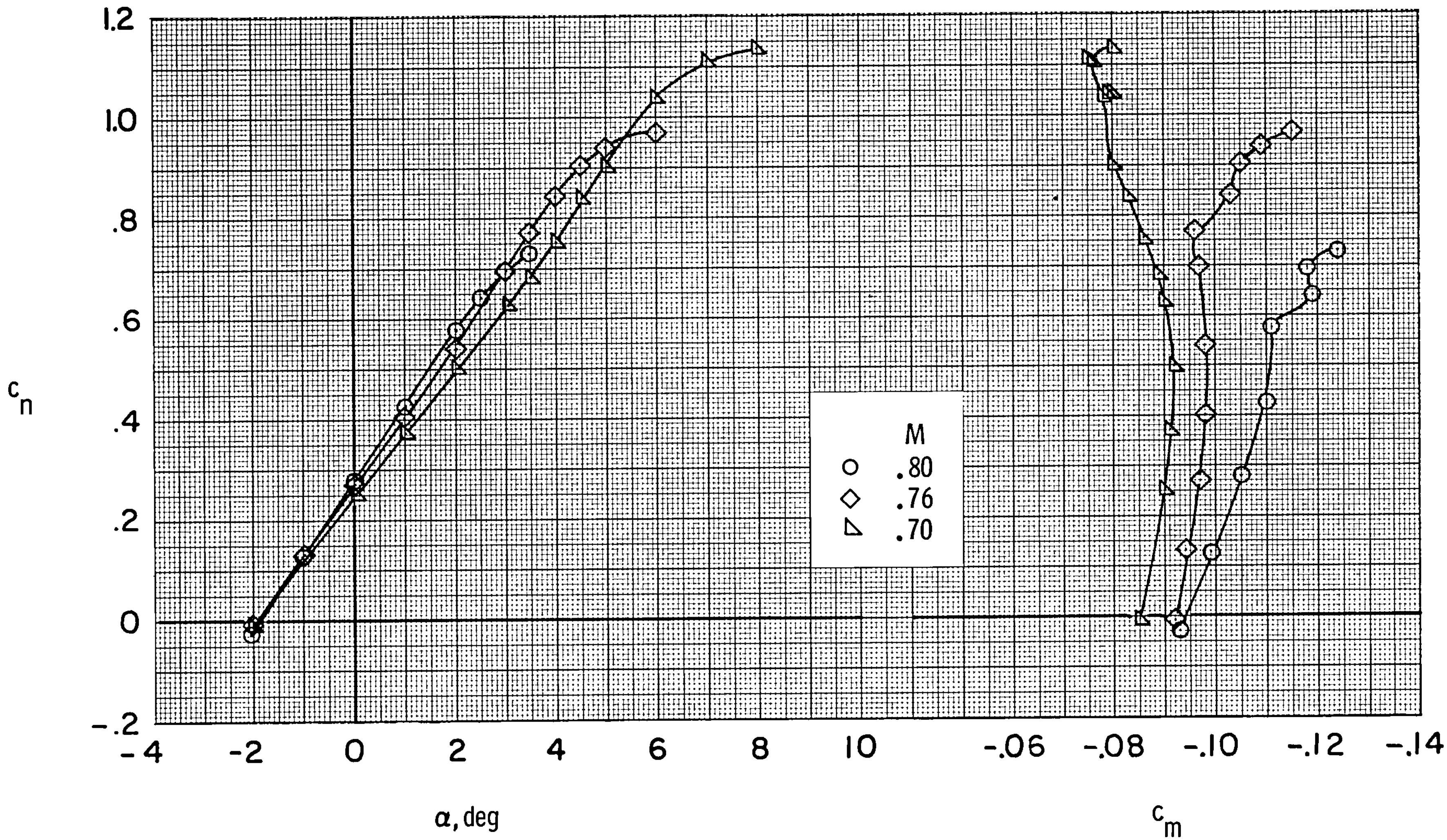

(a) c_n vs α and c_m.

Figure 32.- Effect of Mach number on aerodynamic characteristics of airfoil with fixed transition at $R \approx 7.7 \times 10^6$.

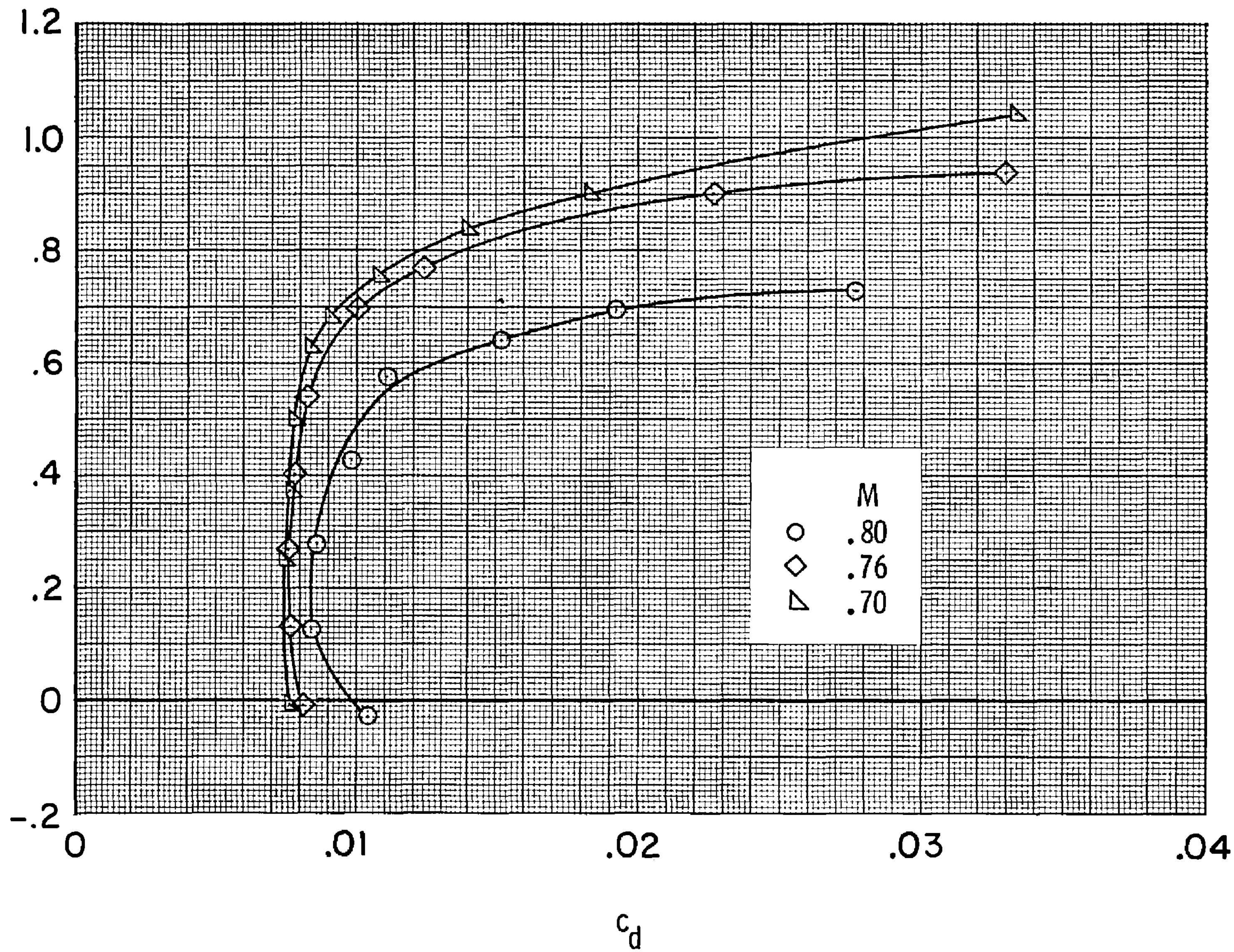

(b) c_n vs c_d.

Figure 32.- Concluded.

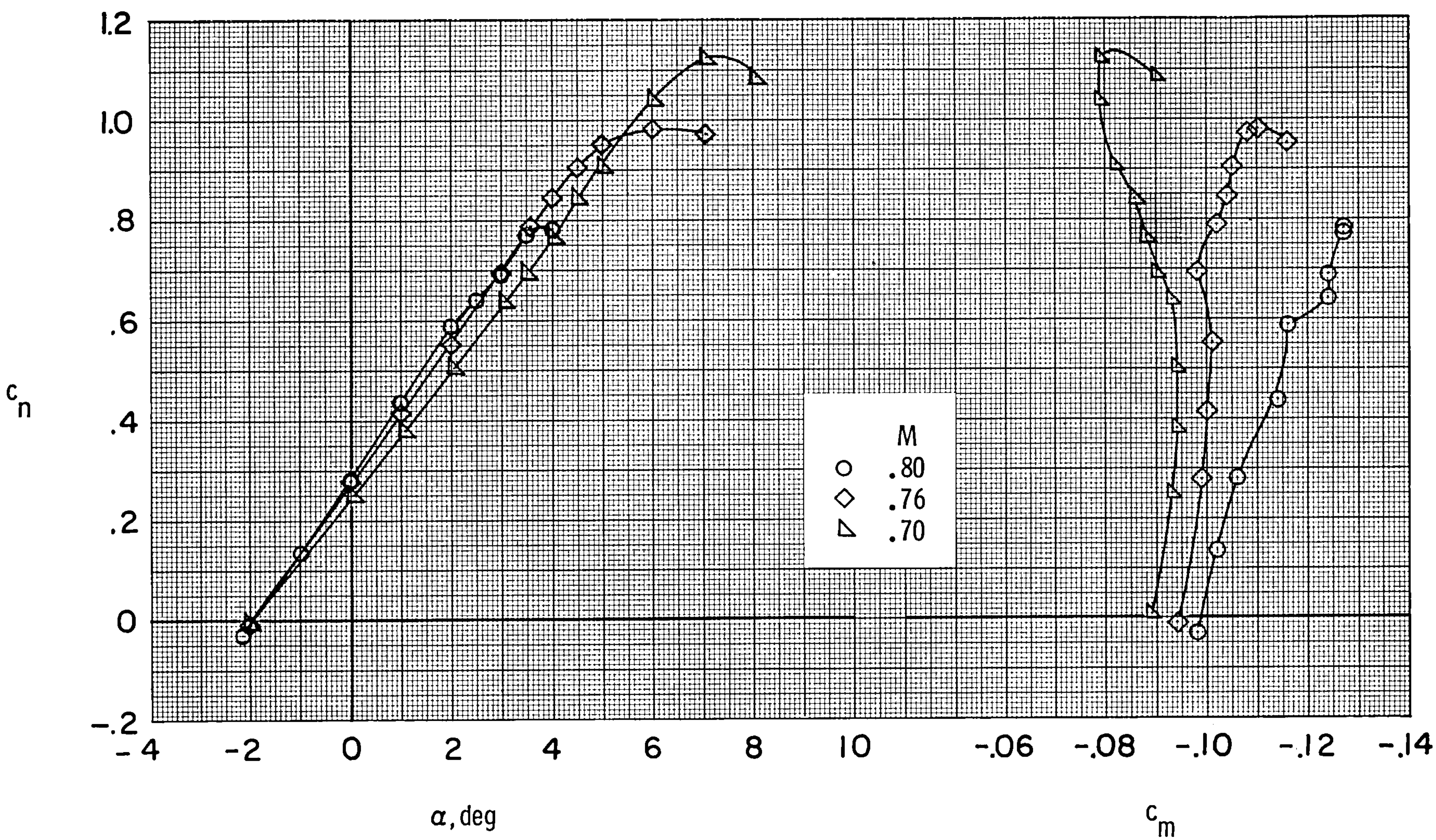

(a) c_n vs α and c_m.

Figure 33.- Effect of Mach number on aerodynamic characteristics of airfoil with fixed transition at $R \approx 14.0 \times 10^6$.

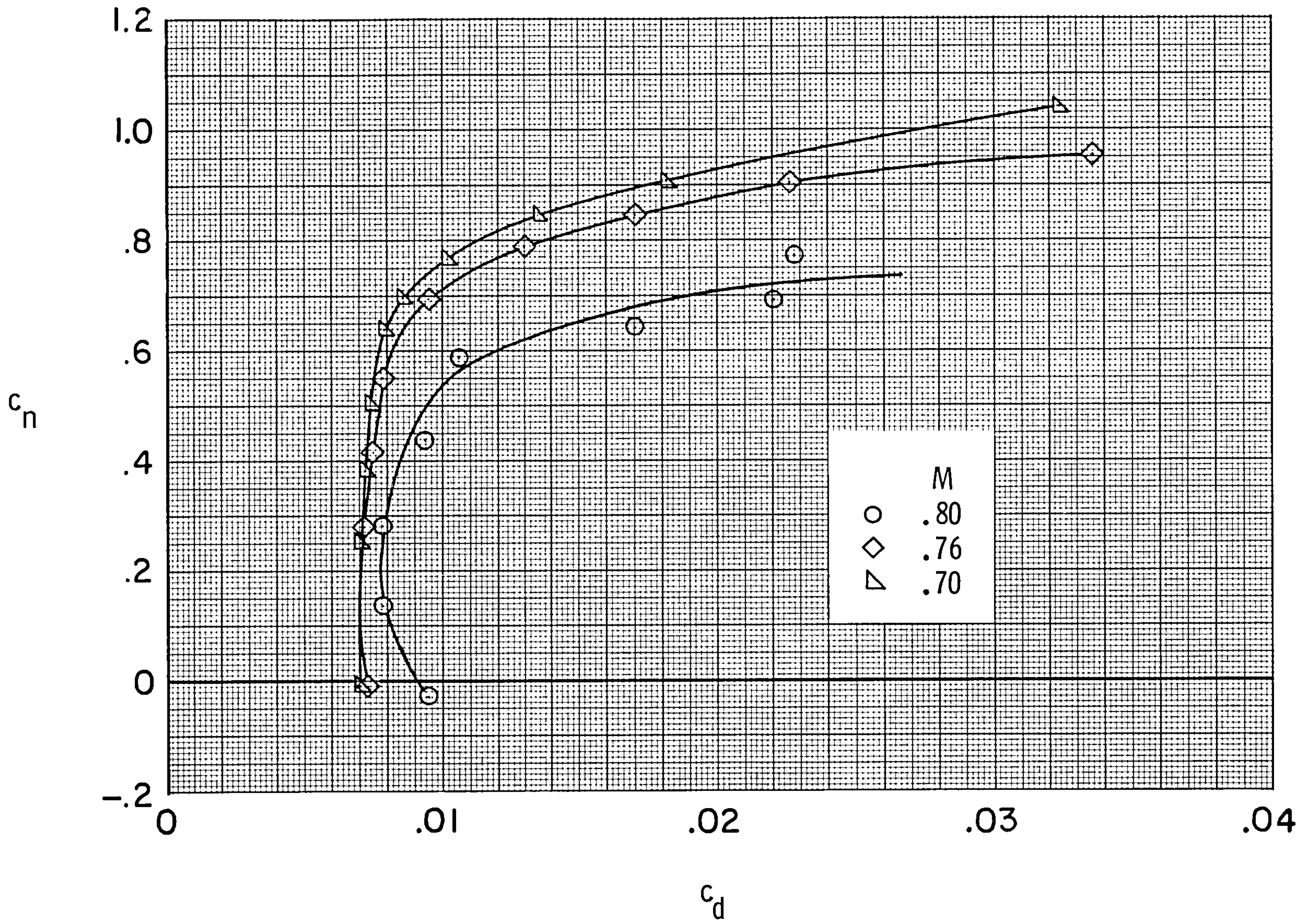

(b) c_n vs c_d.

Figure 33.- Concluded.

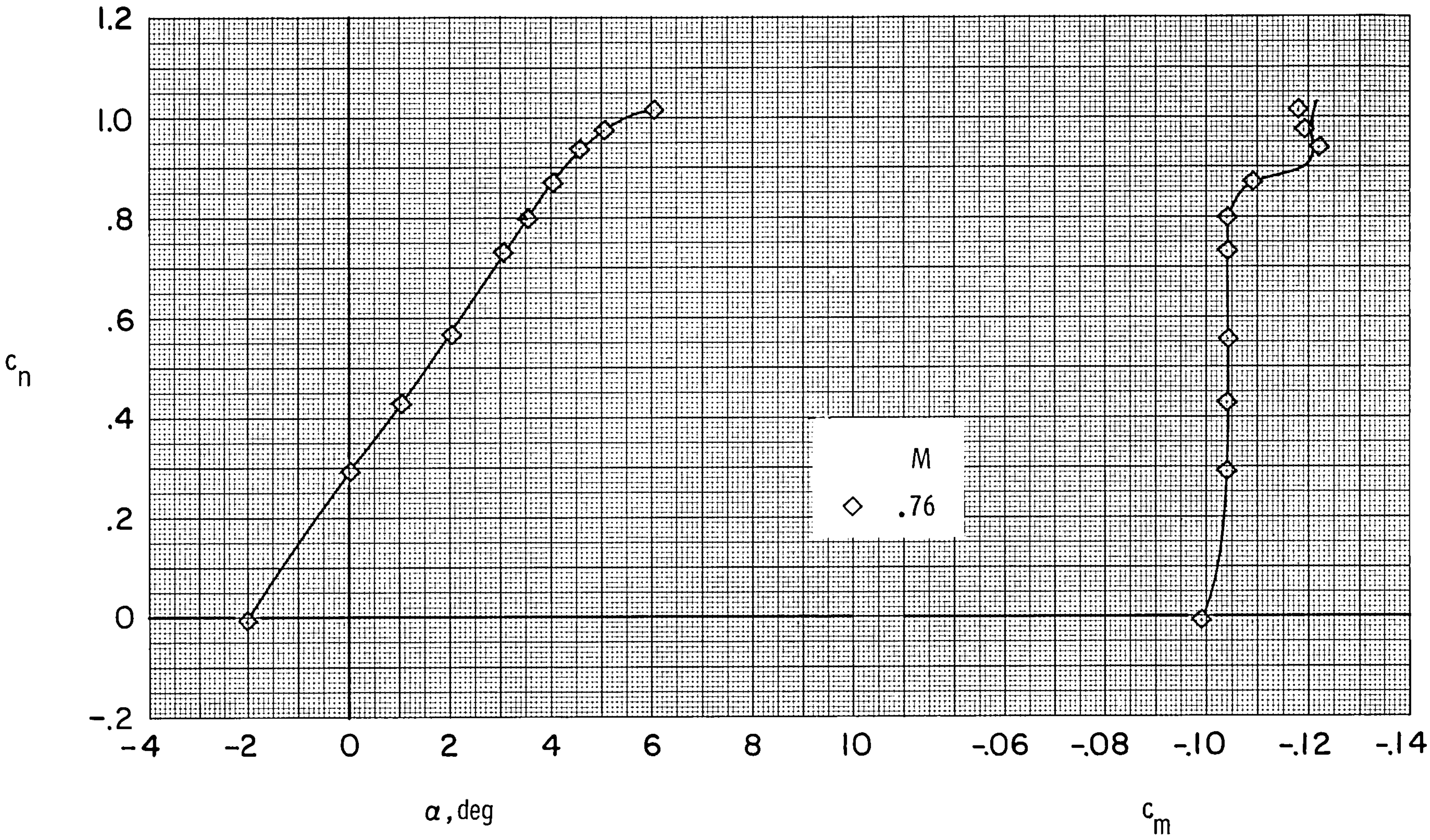

(a) c_n vs α and c_m.

Figure 34.- Effect of Mach number on aerodynamic characteristics of airfoil with fixed transition at $R \approx 30.0 \times 10^6$.

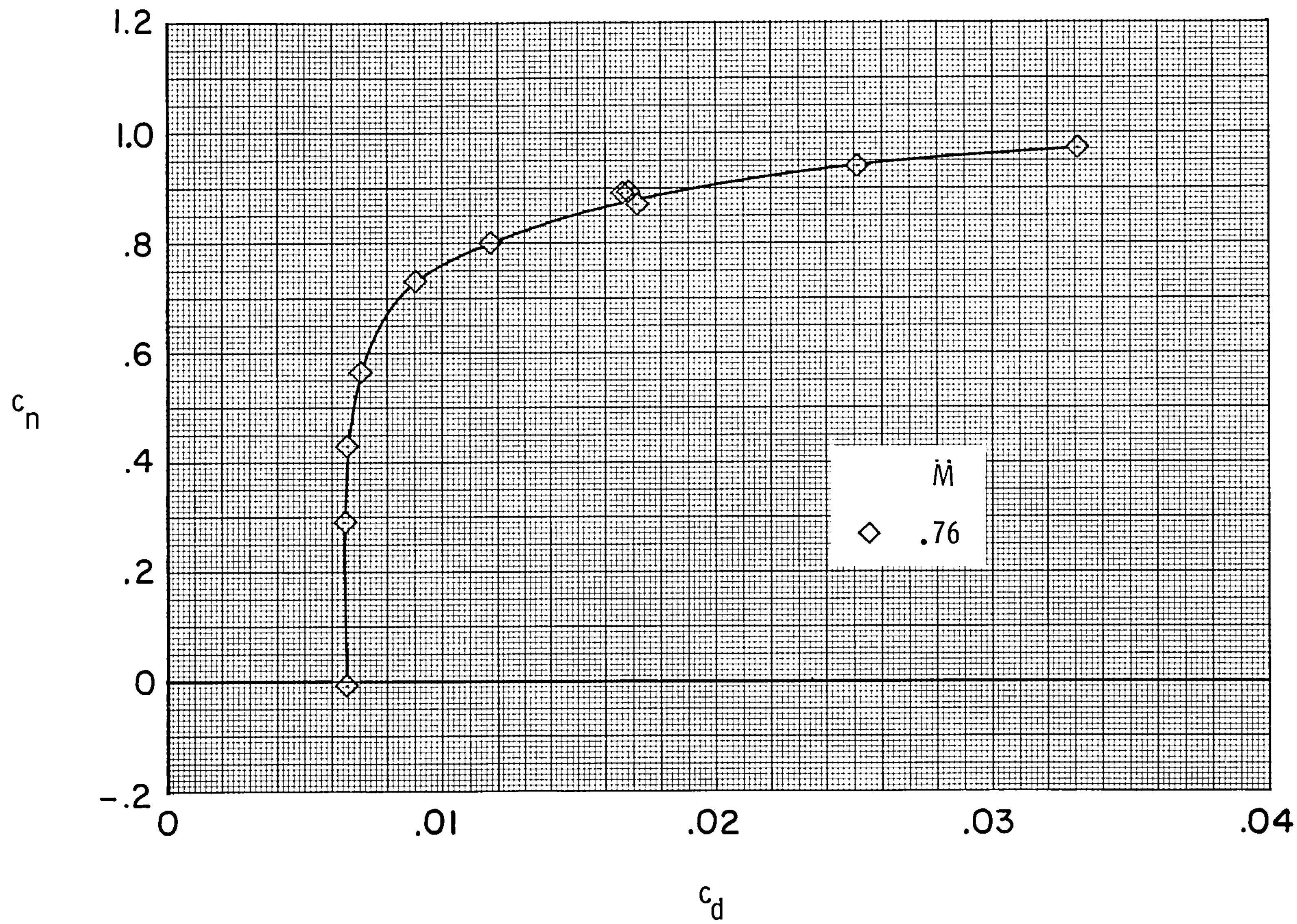

(b) c_n vs c_d.

Figure 34.- Concluded.

CAST 7

Versuchsanstalt für Luft- und Raumfahrt e.V. (DFVLR)

Year	1979
Reference	AGARD-AR-138
t/c	0,118
$c_{l,design}$	0,573
M_{design}	0,76
α_{design}	0°
Transition	fixed at 0,05c

Airfoil according to coordinates given in AGARD-AR-138

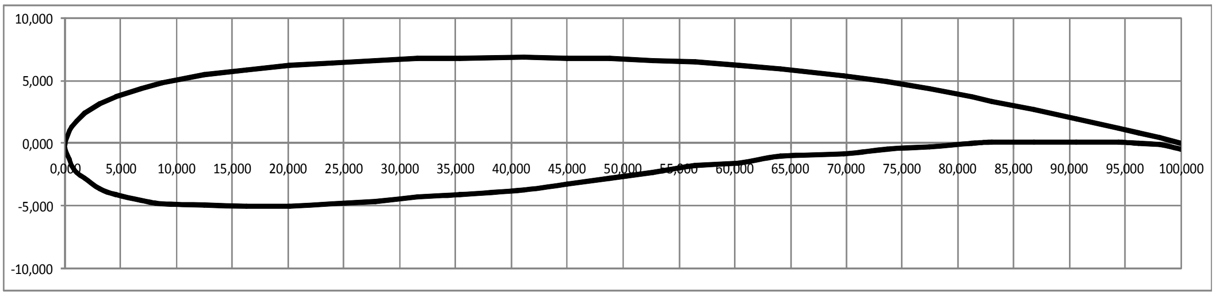

Airfoil according to drawing given in AGARD-AR-138

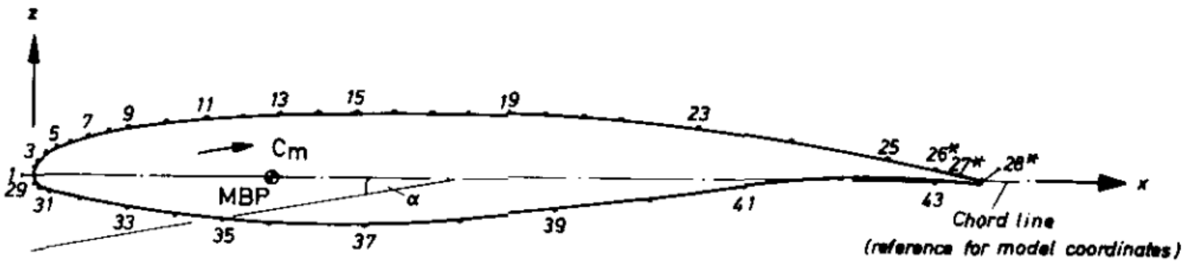

Airfoil Coordinates (in % chord)

(do not agree with drawing in AGARD-AR-138)

x/c [%]	y_u/c [%]	x/c [%]	y_l/c [%]
0,000	0,000	0,000	0,000
0,017	0,214	0,109	-0,526
0,356	1,021	0,867	-1,337
0,576	1,327	2,055	-1,743
1,001	1,791	4,508	-2,310
1,796	2,407	6,874	-2,781
3,131	3,110	12,533	-3,662
4,526	3,687	16,323	-4,135
6,839	4,394	20,122	-4,517
8,707	4,818	23,930	-4,799
12,485	5,443	27,744	-4,972
16,288	5,891	31,562	-5,036
20,106	6,217	35,381	-4,993
23,929	6,455	39,197	-4,851
27,756	6,626	43,008	-4,622
31,584	6,744	46,815	-4,317
35,414	6,817	48,716	-4,140
41,160	6,852	52,513	-3,743
44,990	6,823	56,306	-3,300
48,820	6,752	60,095	-2,821
52,649	6,637	63,880	-2,321
56,476	6,470	67,665	-1,812
60,300	6,245	69,557	-1,559
64,119	5,956	73,345	-1,070
69,836	5,384	75,240	-0,841
73,637	4,904	79,036	-0,429
77,426	4,344	80,937	-0,256
81,205	3,714	84,747	0,005
83,090	3,376	86,655	0,082
86,854	2,666	88,564	0,119
90,613	1,927	90,473	0,114
94,369	1,177	92,382	0,065
96,247	0,799	94,289	-0,022
98,124	0,419	96,195	-0,143
100,000	0,036	100,000	-0,466

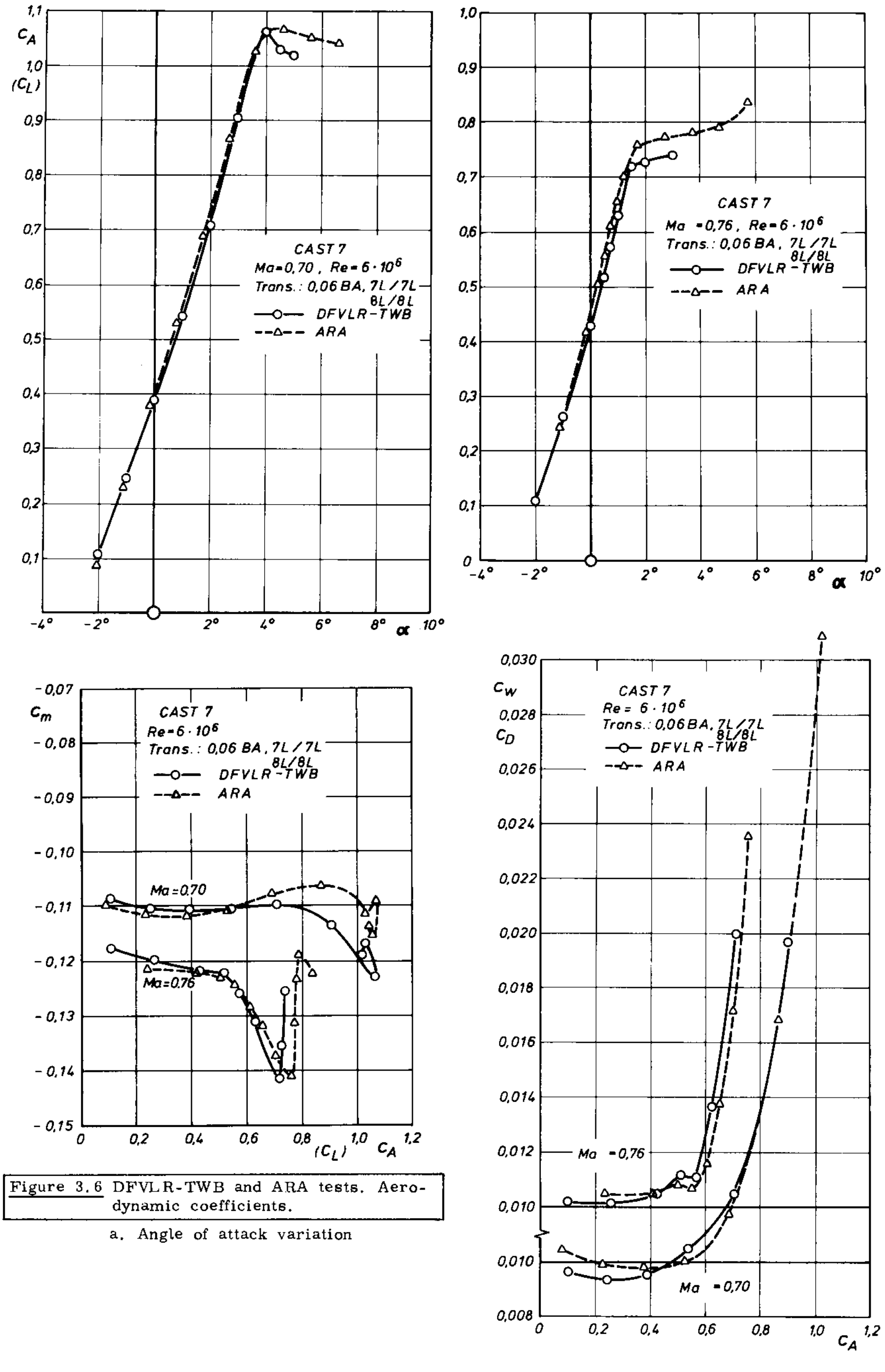

Figure 3.6 DFVLR-TWB and ARA tests. Aerodynamic coefficients.

a. Angle of attack variation

Aerodynamic Coefficients

NR.	MACH	E-6*RE	ALPHA	CA	CM	CW
2493	.697	5.80	-2.00	.1083	-.10867	.009632
2495	.701	6.06	-1.00	.2478	-.11050	.009341
2496	.703	5.90	.00	.3910	-.11076	.009554
2497	.701	5.97	1.00	.5422	-.11077	.010476
2498	.701	5.94	2.00	.7088	-.10979	.012468
2499	.702	5.96	3.00	.9057	-.11369	.021677
2500	.699	5.95	4.00	1.0637	-.12300	.039833
2501	.700	5.91	4.50	1.0297	-.11697	.060949
2502	.699	5.90	5.00	1.0187	-.11890	
2490	.761	5.98	-2.00	.1067	-.11769	.010196
2484	.761	5.97	-1.00	.2627	-.11974	.010101
2485	.759	5.98	.00	.4268	-.12195	.010441
2486	.761	6.00	.50	.5164	-.12232	.011146
2491	.760	5.99	.75	.5709	-.12591	.011030
2487	.760	5.92	1.00	.6297	-.13114	.013638
2488	.759	6.00	1.50	.7187	-.14159	.019940
2489	.760	5.94	2.00	.7258	-.13538	.041963
2492	.761	5.99	3.00	.7384	-.12548	.061552
2511	.407	5.40	.50	.3818	-.09001	.009730
2512	.499	5.76	.50	.3997	-.09495	.008745
2514	.602	5.86	.50	.4272	-.10208	.008973
2515	.650	5.80	.50	.4448	-.10659	.009466
2516	.702	5.88	.50	.4674	-.11216	.010174
2517	.717	5.81	.50	.4801	-.11450	.009983
2518	.739	5.87	.50	.4965	-.11774	.010352
2519	.751	5.96	.50	.5126	-.12174	.011314
2520	.759	5.97	.50	.5228	-.12355	.010731
2524	.765	5.88	.50	.5270	-.12508	.011194
2521	.770	5.99	.50	.5470	-.13323	.012007
2522	.779	5.89	.50	.5340	-.13716	.016398
2523	.801	5.92	.50	.4506	-.13480	.022780
2504	.759	4.11	.50	.5160	-.12051	.012377
2505	.761	5.10	.50	.5228	-.12249	.011555
2506	.760	5.81	.50	.5263	-.12340	.010599
2507	.763	7.63	.50	.5327	-.12652	.010580
2508	.762	10.07	.50	.5426	-.12923	.009927
2509	.758	11.77	.50	.5408	-.12904	.010398
2510	.760	13.41	.50	.5413	-.12921	.010124
2525	.760	4.09	2.00	.7116	-.13192	.042354
2526	.760	5.03	2.00	.7279	-.13535	.038594
2527	.760	5.94	2.00	.7387	-.13966	.038199
2531	.762	7.81	2.00	.7402	-.14236	.039436
2530	.759	9.96	2.00	.7718	-.14771	.031793
2529	.758	11.78	2.00	.7736	-.14793	.032559
2528	.759	13.49	2.00	.7772	-.14957	.031563

CAST 10-2/
DOA 2

Versuchsanstalt für Luft- und Raumfahrt e.V. (DFVLR)

Year	1984
Reference	NASA TM-86273
t/c	0,121
Transition	free

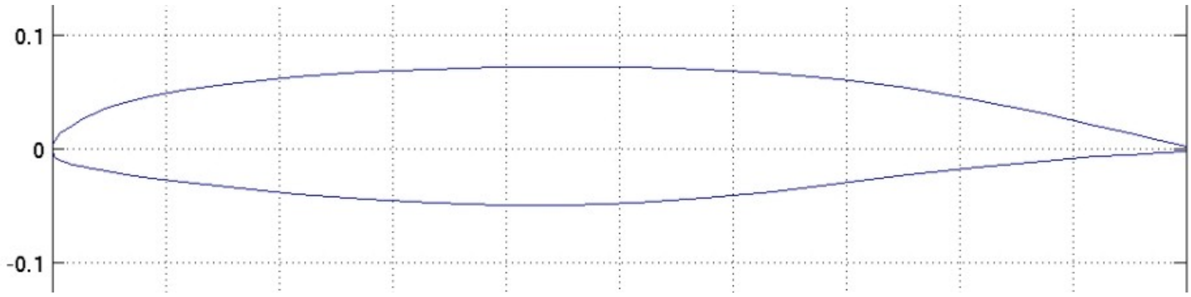

UIUU Airfoil Data Site

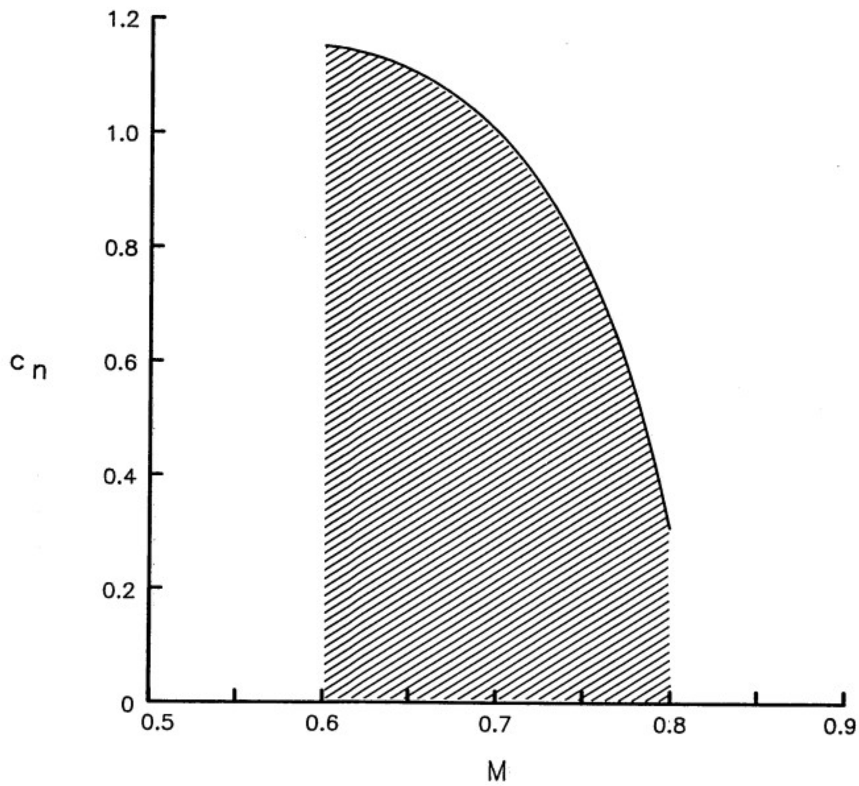

Figure 9.— "Usable" two–dimensional normal force data from tests of the CAST 10–2/DOA 2 airfoil in the 0.3–m TCT.

Airfoil Coordinates

Upper Surface

x/c	z/c	
	Design	Measured+
0.0	.0034	.0035
.0009	.0080	.0080
.0026	.0114	.0114
.0076	.0170	.0170
.0126	.0208	.0207
.0176	.0239	.0239
.0251	.0281	.0280
.0351	.0329	.0327
.0476	.0378	.0375
.0651	.0431	.0429
.0876	.0484	.0483
.1151	.0532	.0532
.1551	.0583	.0584
.2151	.0634	.0635
.2751	.0665	.0664
.3351	.0682	.0681
.3950	.0689	.0688
.4550	.0686	.0685
.5150	.0672	.0670
.5750	.0645	.0644
.6350	.0603	.0602
.6950	.0539	.0538
.7550	.0451	.0450
.8150	.0338	.0336
.8750	.0206	.0202
.9200	.0099	.0096
.9500	.0027	.0025
.9775	−.0040	−.0039
1.0000	−.0095	−.0089

Lower Surface

x/c	z/c	
	Design	Measured
.0011	−.0016	−.0018
.0026	−.0038	−.0039
.0076	−.0073	−.0072
.0126	−.0091	−.0090
.0176	−.0105	−.0105
.0251	−.0122	−.0123
.0351	−.0144	−.0144
.0476	−.0170	−.0169
.0651	−.0201	−.0200
.0876	−.0238	−.0237
.1151	−.0277	−.0276
.1551	−.0327	−.0326
.2151	−.0392	−.0391
.2751	−.0447	−.0445
.3351	−.0491	−.0490
.3950	−.0521	−.0520
.4550	−.0532	−.0531
.5150	−.0520	−.0519
.5750	−.0486	−.0485
.6350	−.0435	−.0433
.6950	−.0375	−.0374
.7550	−.0313	−.0312
.8150	−.0255	−.0254
.8750	−.0206	−.0204
.9200	−.0176	−.0175
.9500	−.0161	−.0161
.9775	−.0150	−.0153
1.0000	−.0145	−.0145

+ Measurements made by DFVLR.

CAST 10-2/
DOA 2

Lower Mach Numbers
(M = 0,6 ; M = 0,7)

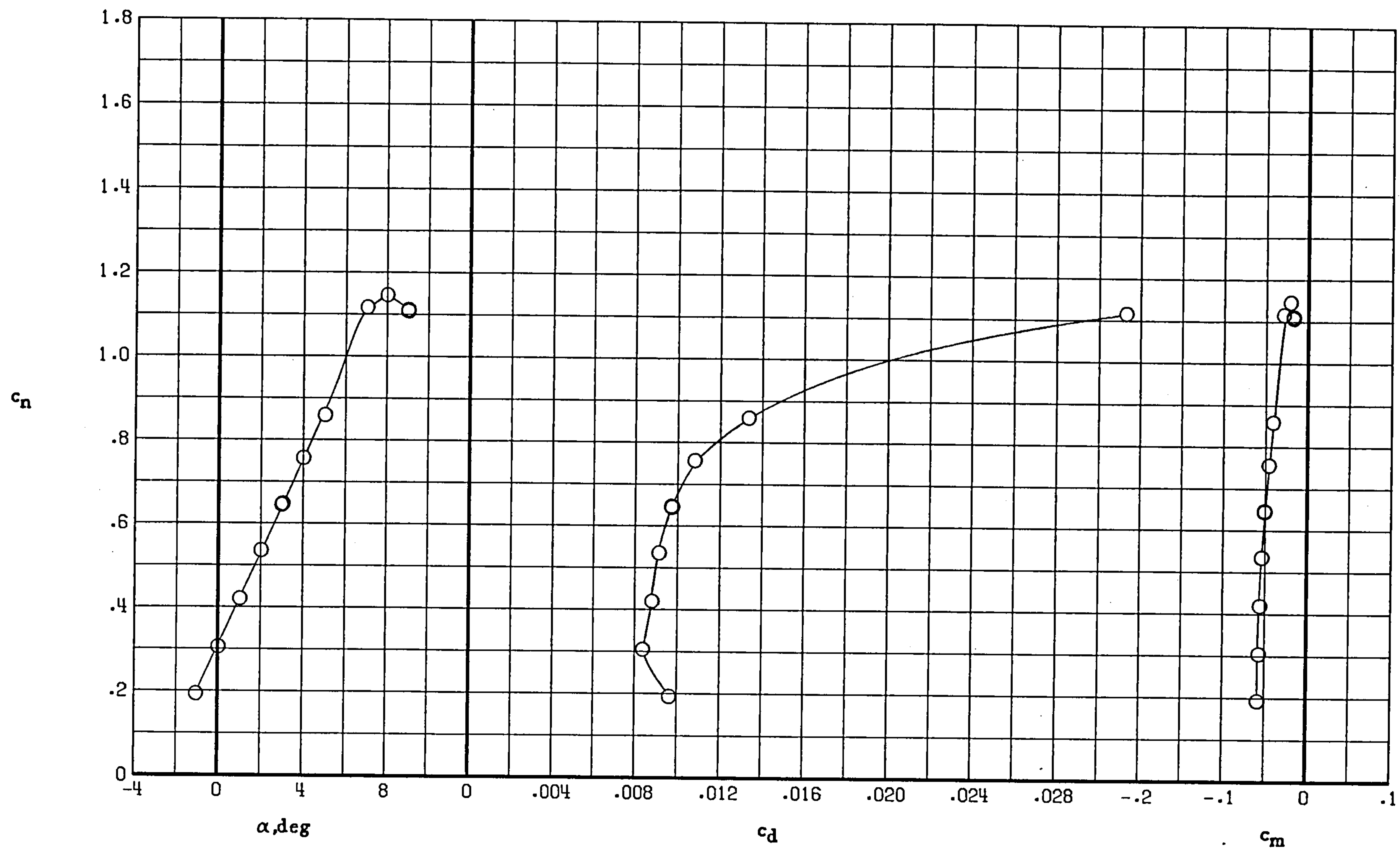

(a) M = 0.60

Figure 11.– Force and moment characteristics of CAST 10–2/DOA 2 airfoil. $R_c = 4.0 \times 10^6$, transition free.

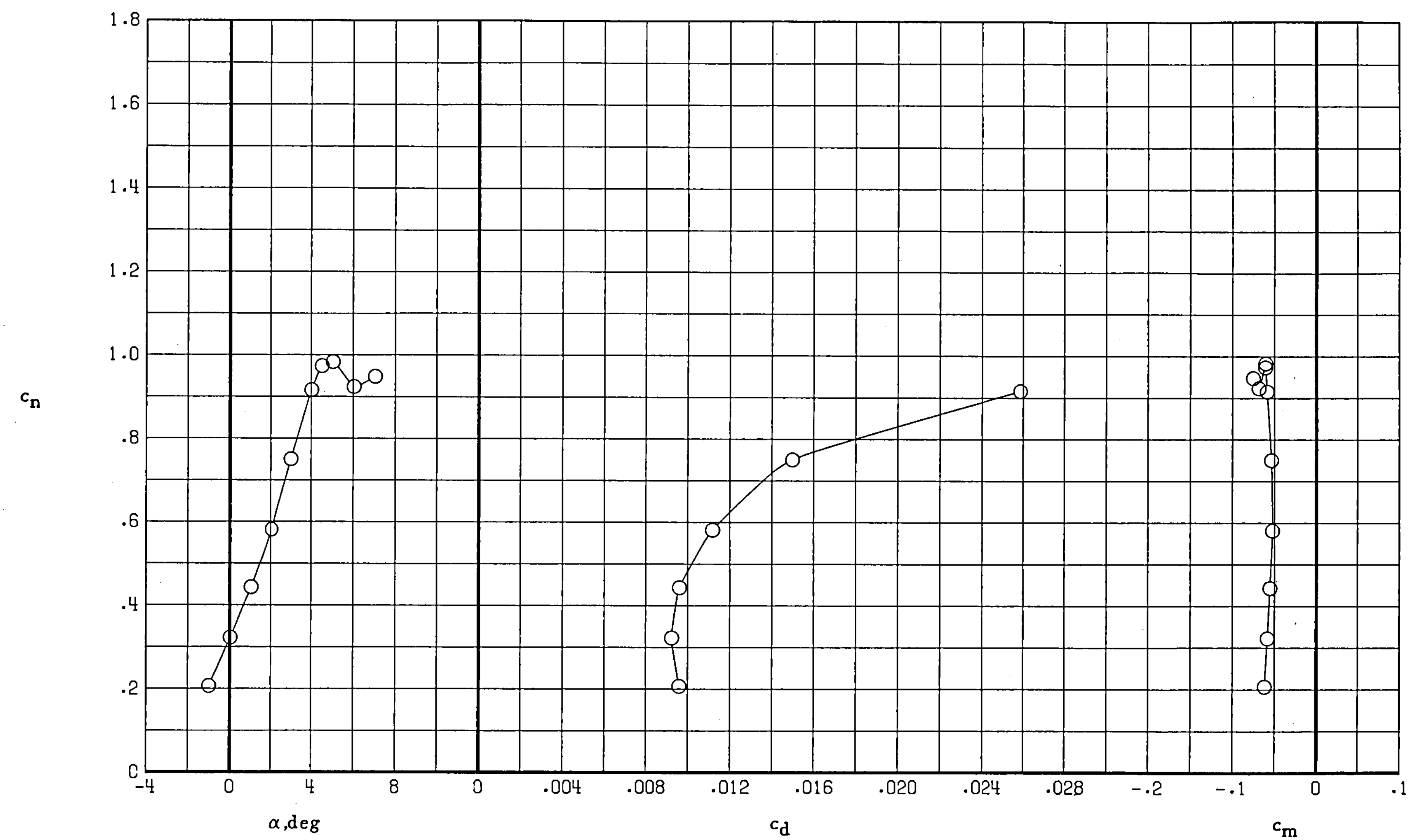

(b) M = 0.70

Figure 11.– Continued.

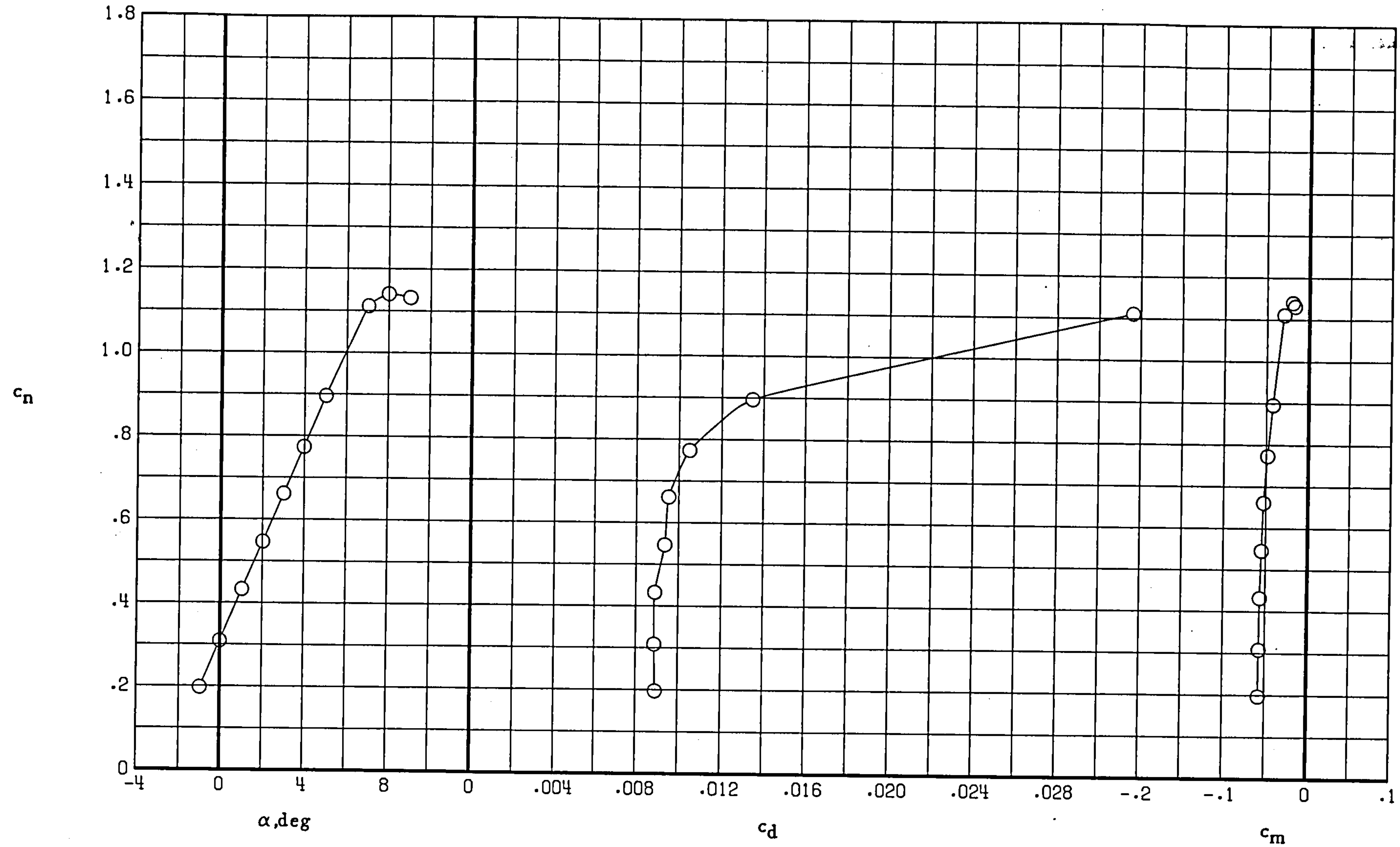

(a) M = 0.60

Figure 12.– Force and moment characteristics of CAST 10–2/DOA 2 airfoil. $R_c = 6.0 \times 10^6$, transition free.

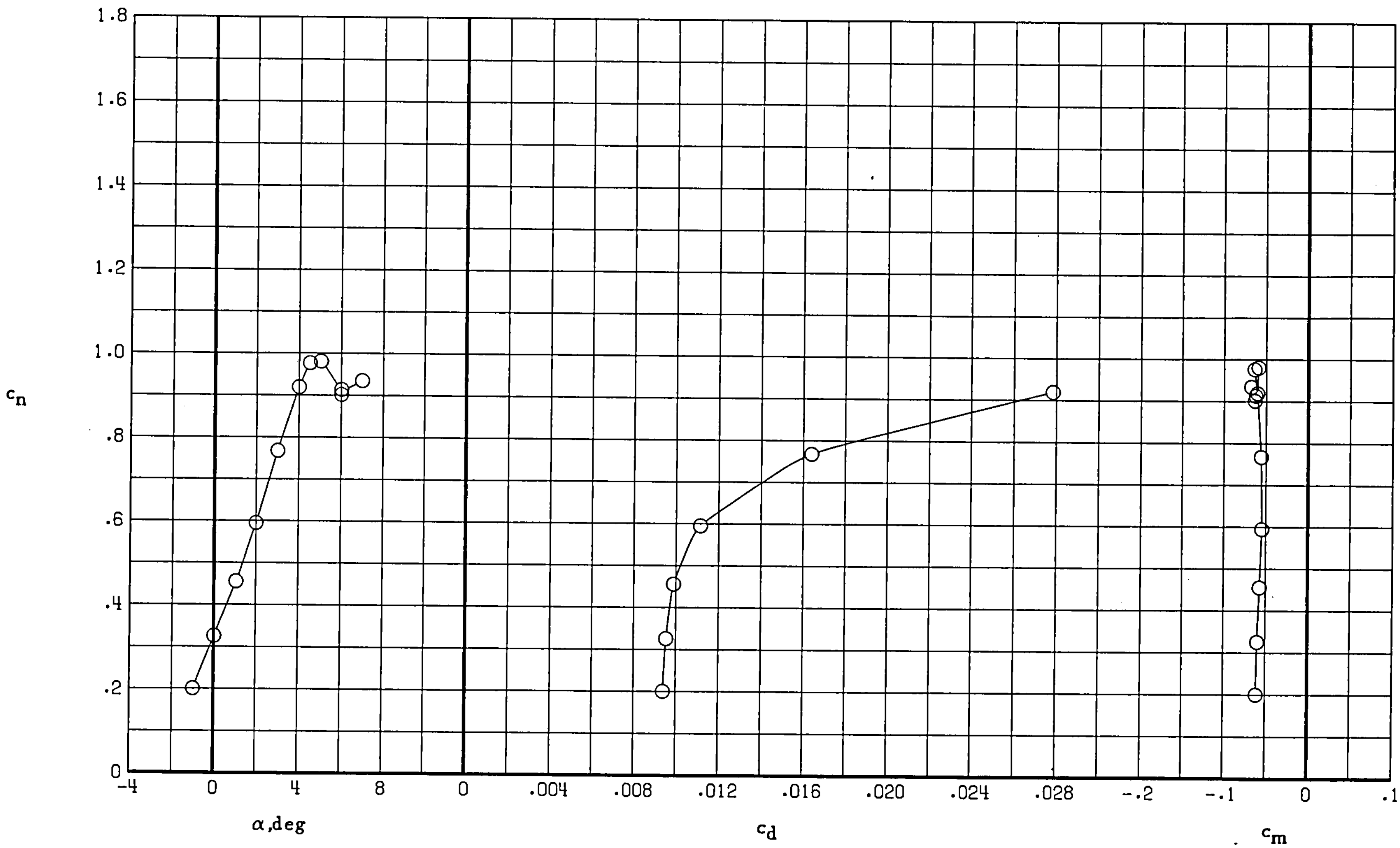

(b) M = 0.70

Figure 12.— Continued.

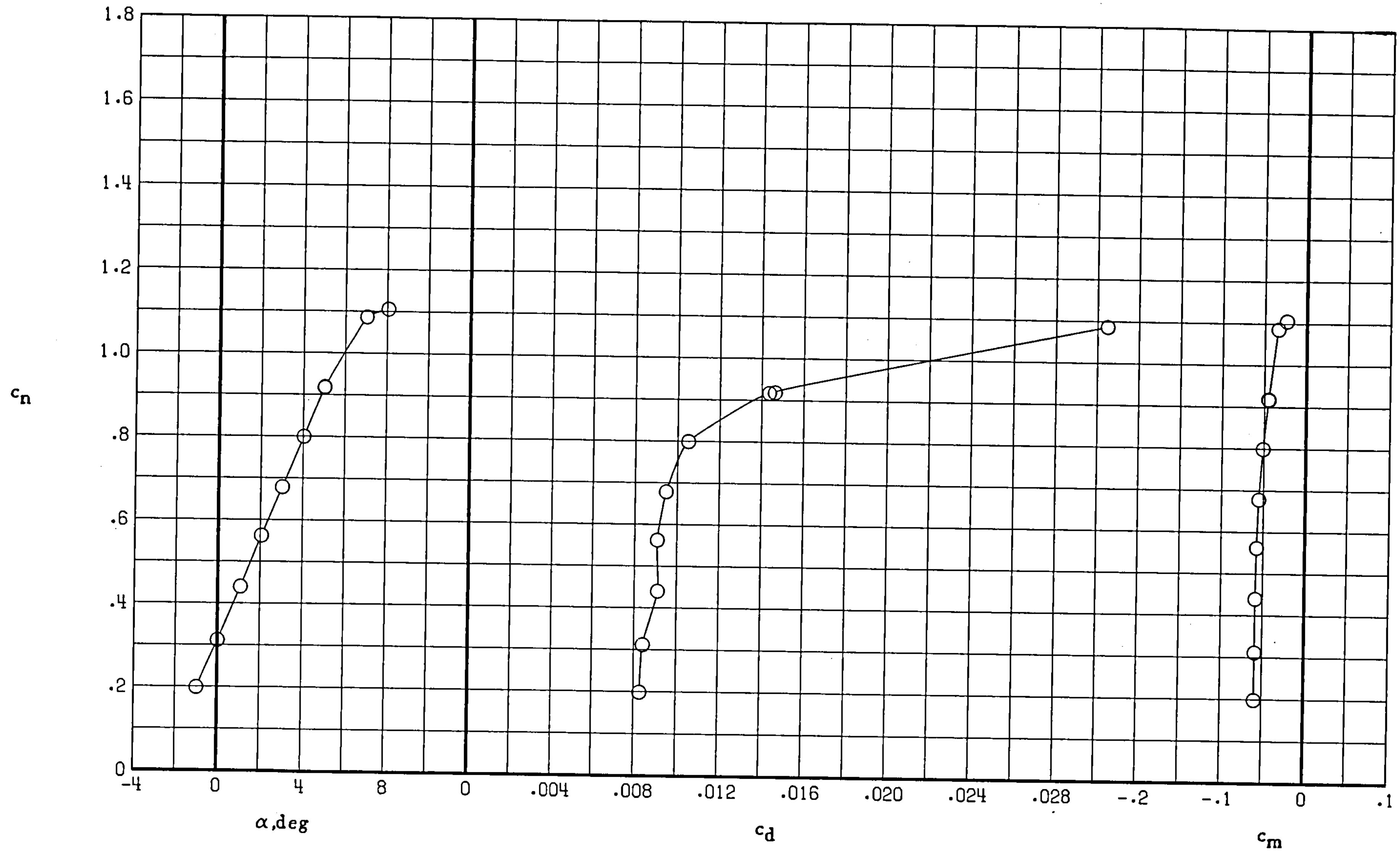

(a) M = 0.60

Figure 13.– Force and moment characteristics of CAST 10–2/DOA 2 airfoil. $R_c = 10.0 \times 10^6$, transition free.

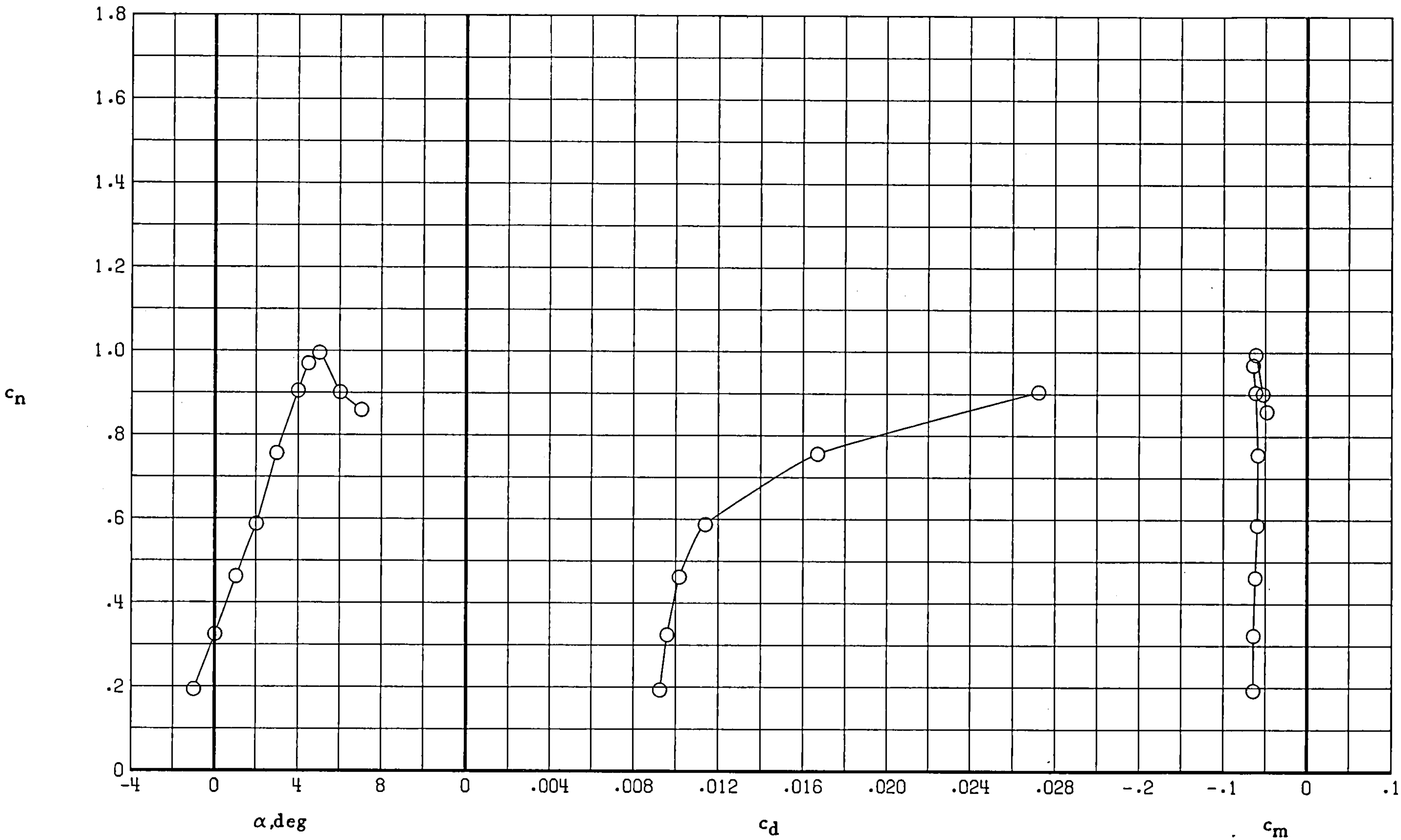

(b) M = 0.70

Figure 13.– Continued.

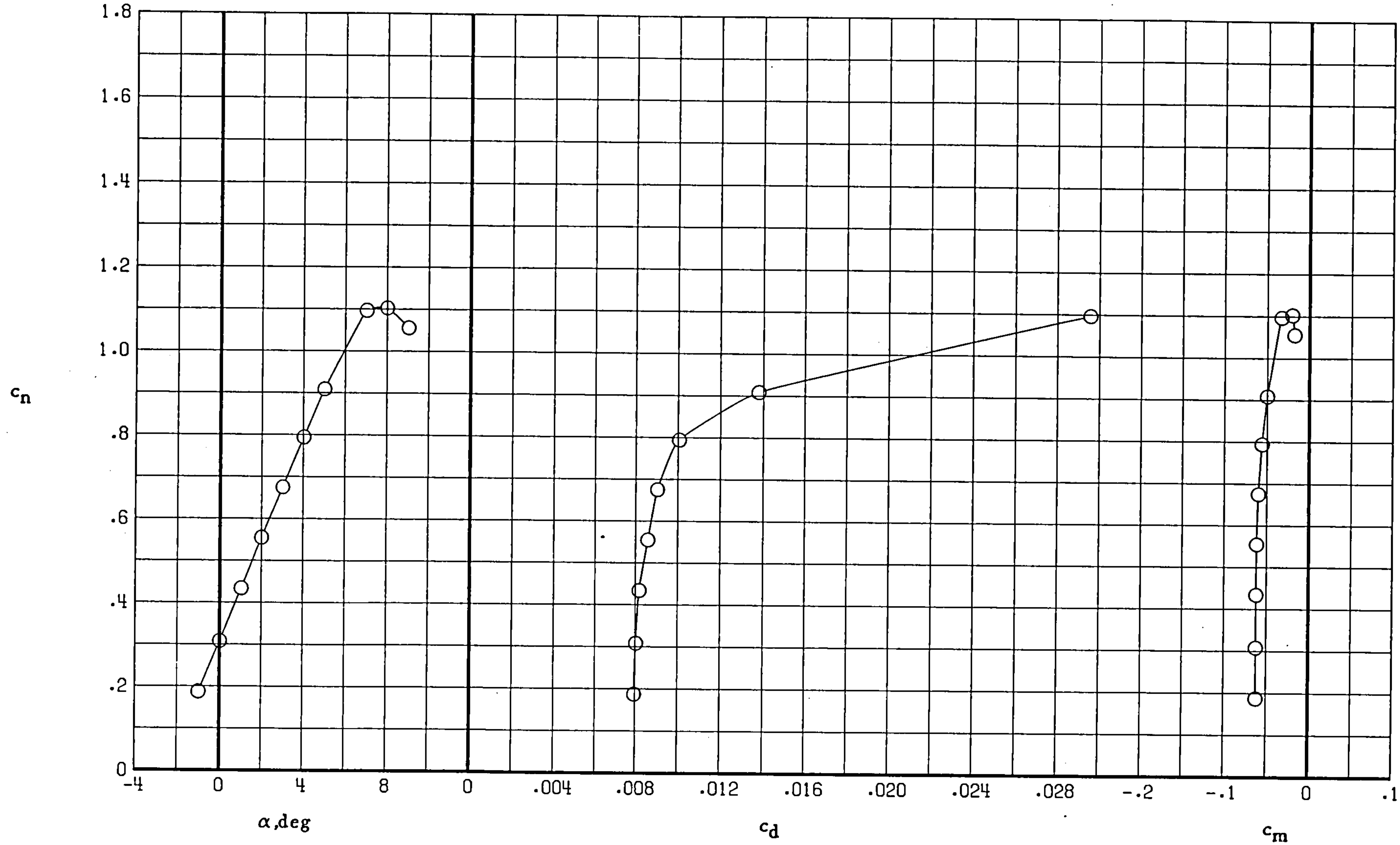

(a) M = 0.60

Figure 14.– Force and moment characteristics of CAST 10–2/DOA 2 airfoil. $R_c = 15.0 \times 10^6$, transition free.

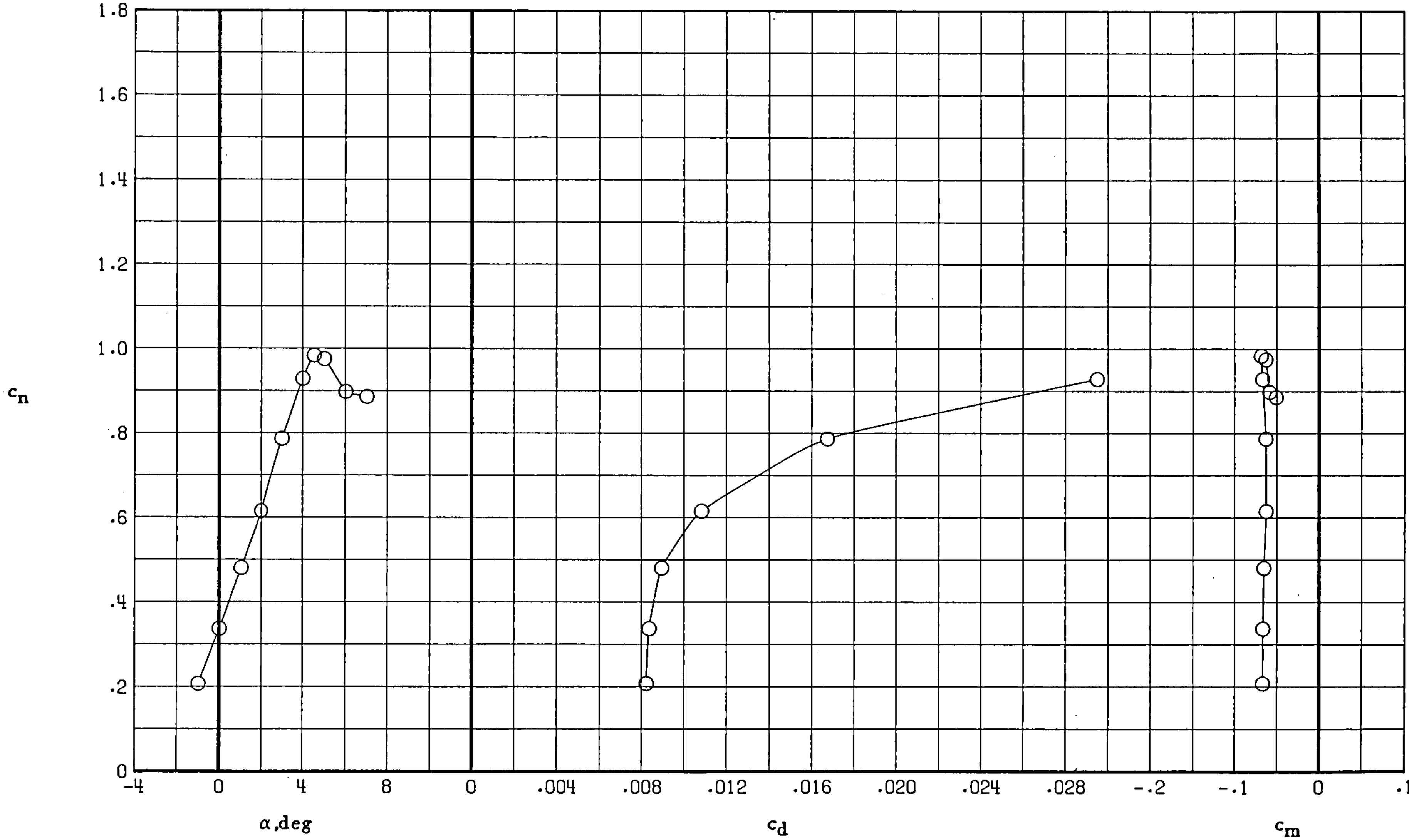

(b) M = 0.70

Figure 14.– Continued.

CAST 10-2/
DOA 2

Higher Mach Numbers
(M = 0,73 ; M = 0,75 ; M = 0,765 ; M = 0,78)

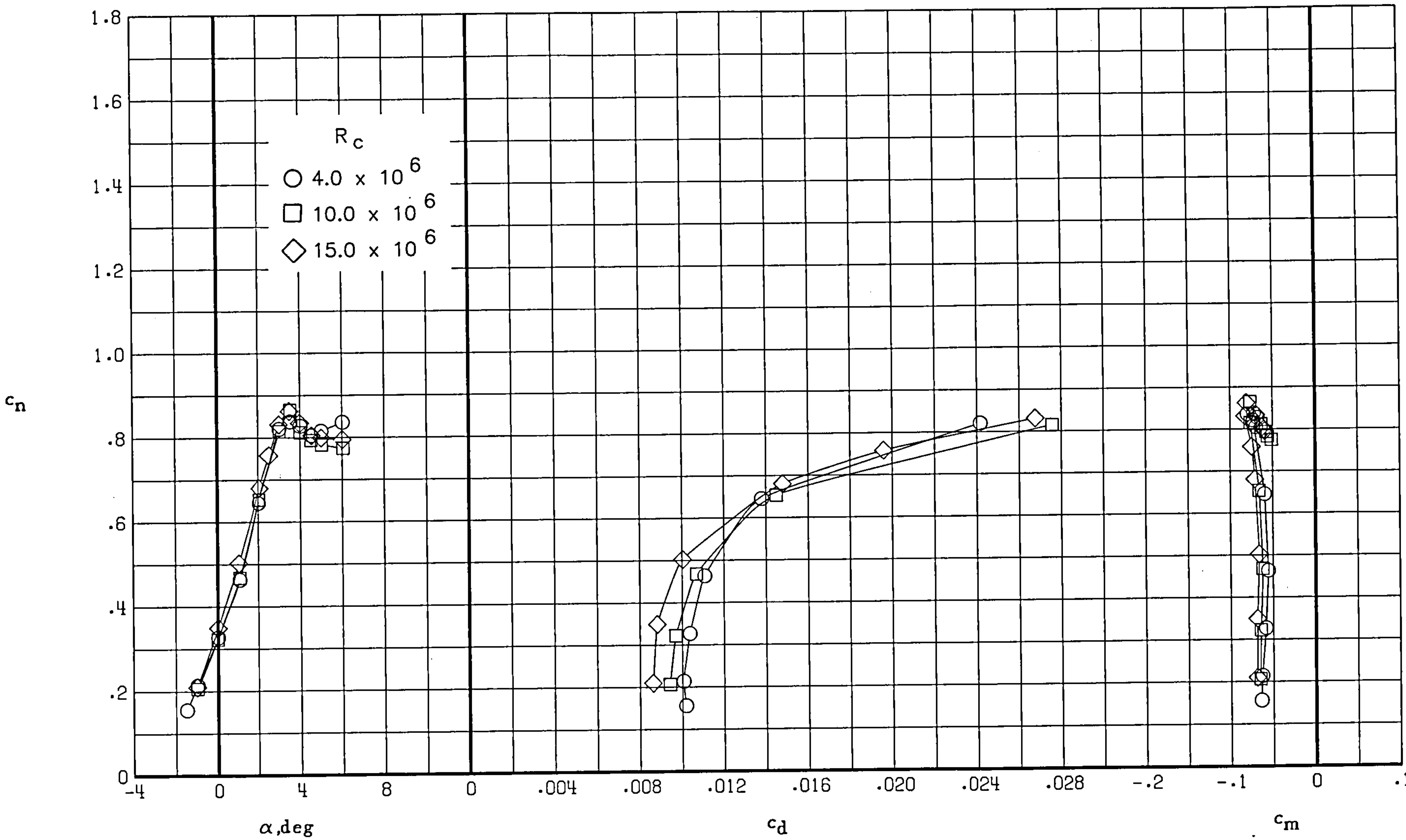

(a) M = 0.73

Figure 21.– Effect of Reynolds number on force and moment characteristics of CAST 10–2/DOA 2 airfoil. Transition free.

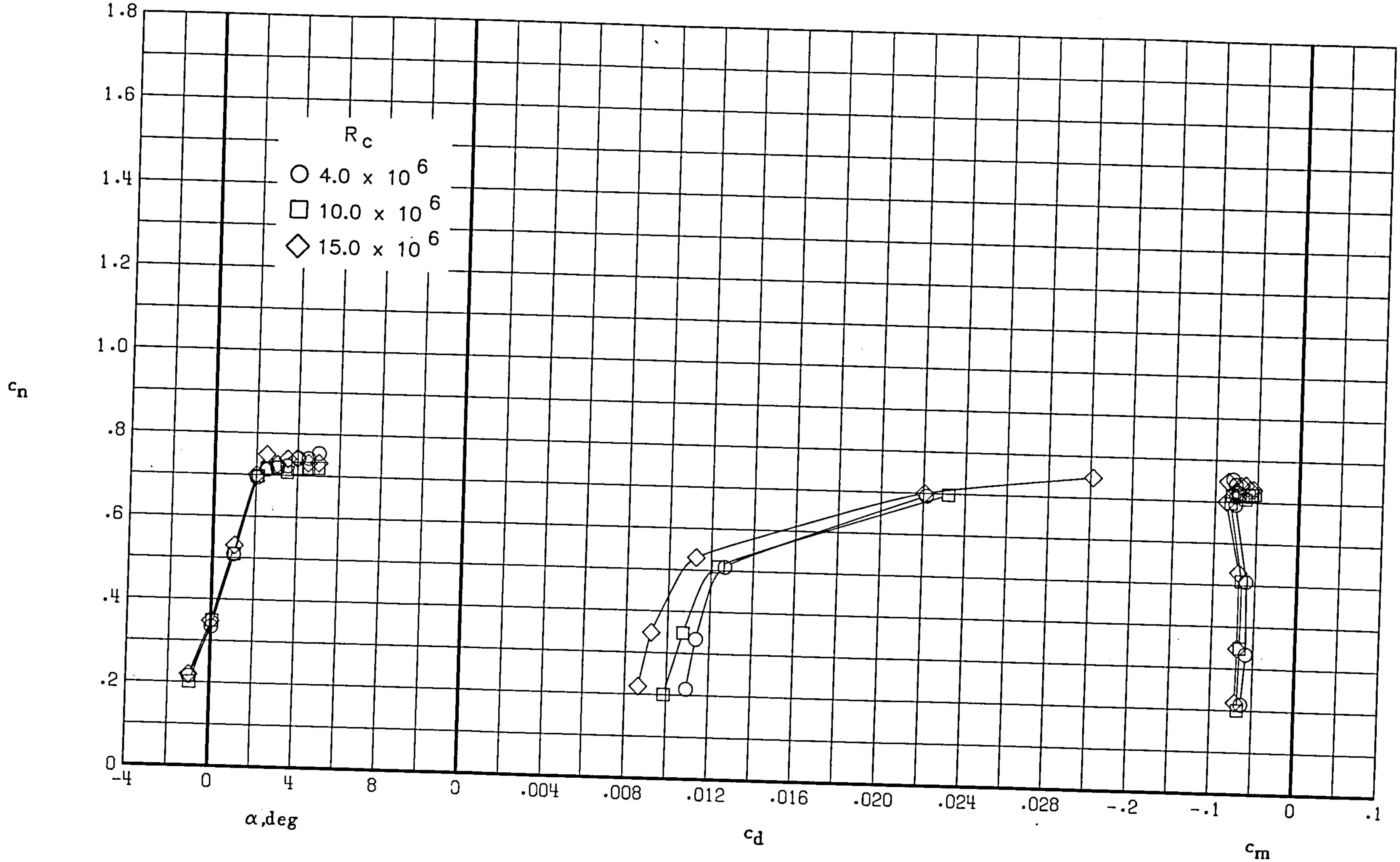

(b) M = 0.75

Fig. 21.– Continued.

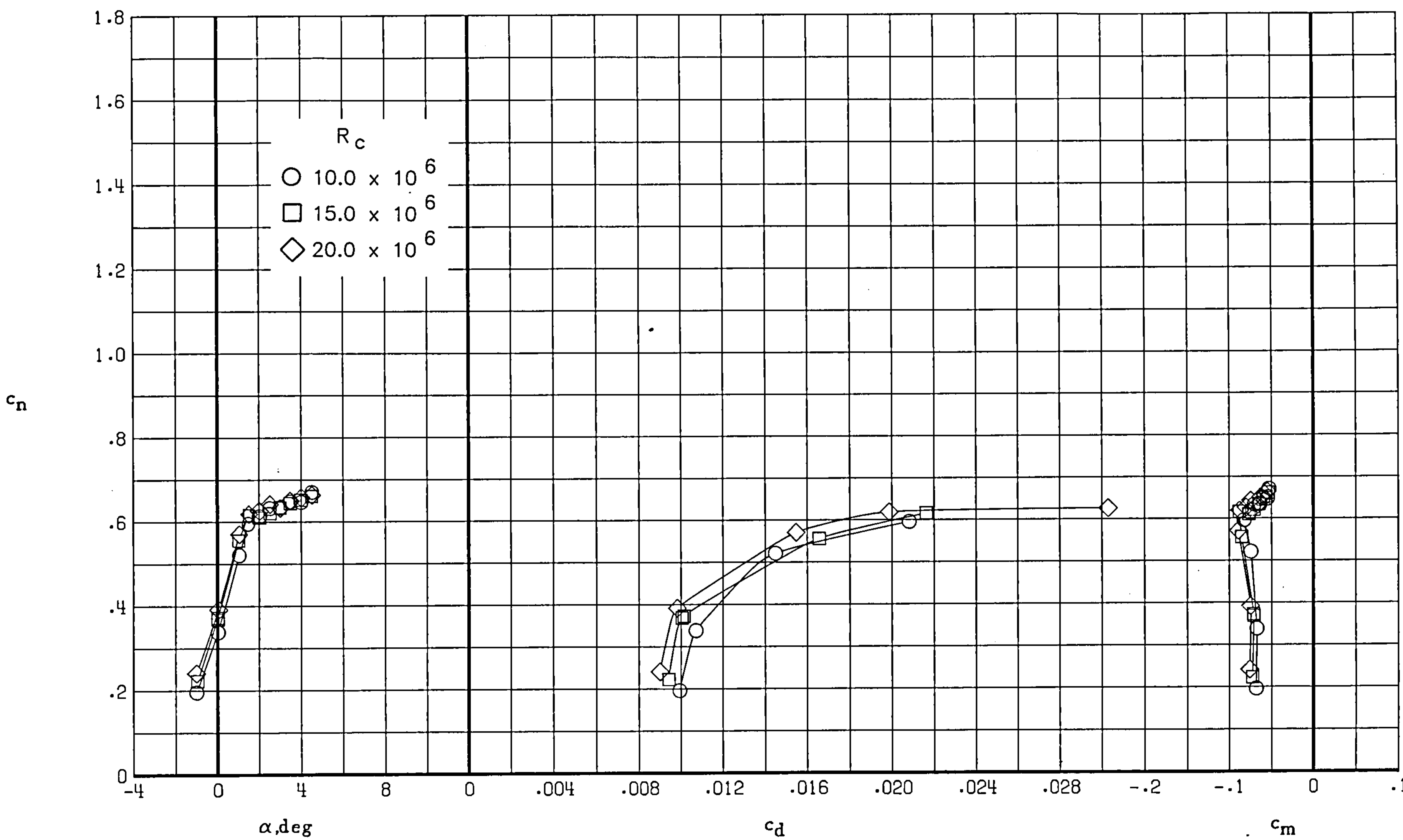

(c) M = 0.765

Fig. 21.– Continued.

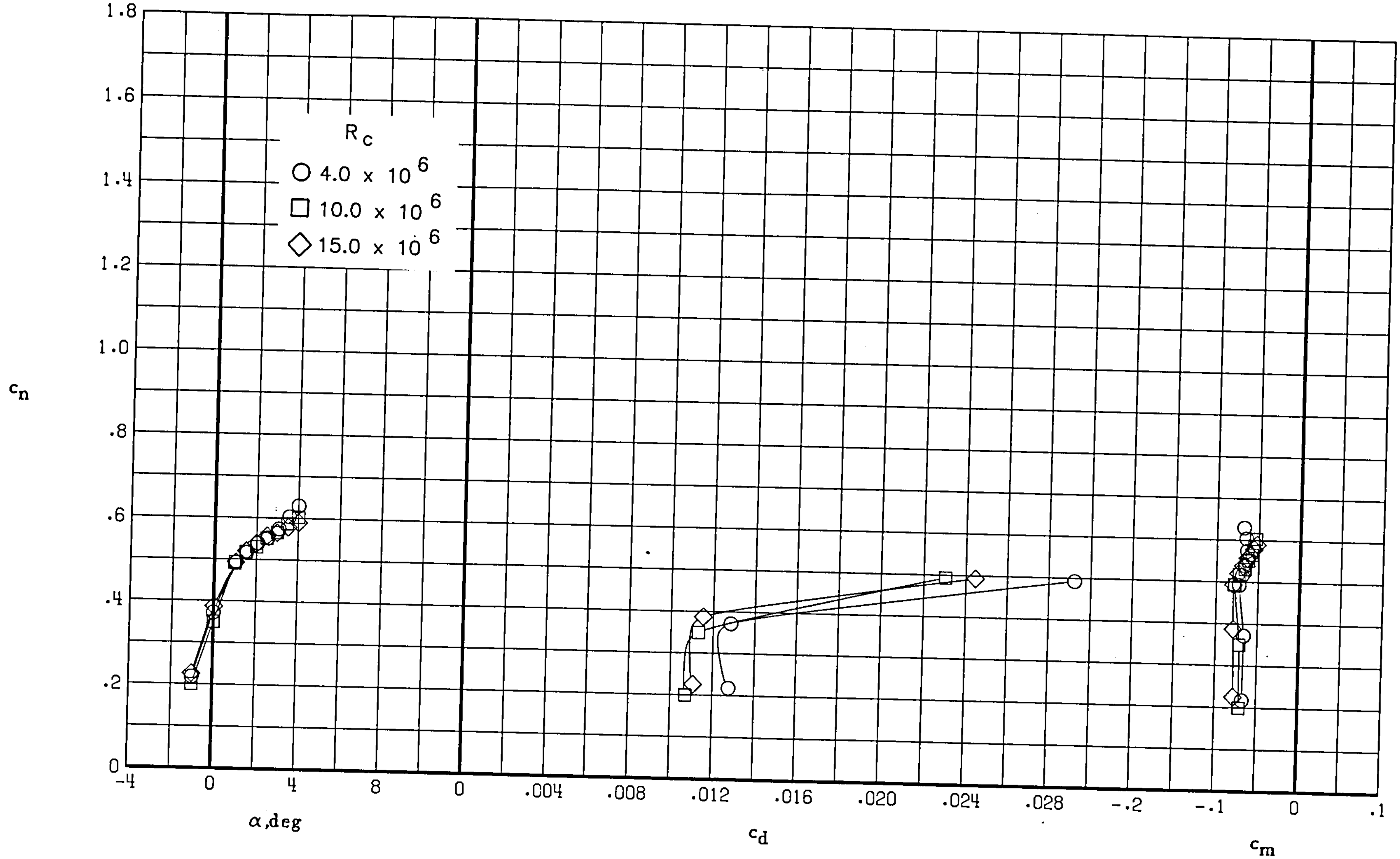

(d) M = 0.78

Fig. 21.– Concluded.

Cessna Executive Jet Modified Airfoil
(2 point design)

NASA and Cessna Aircraft Company

Year	1996
Reference	NASA TP-3579
t/c	0,115
$c_{l,design}$	long range: 0,979 high speed: 0,508
M_{design}	long range: 0,654 high speed: 0,735
Transition	fixed at 0,05c

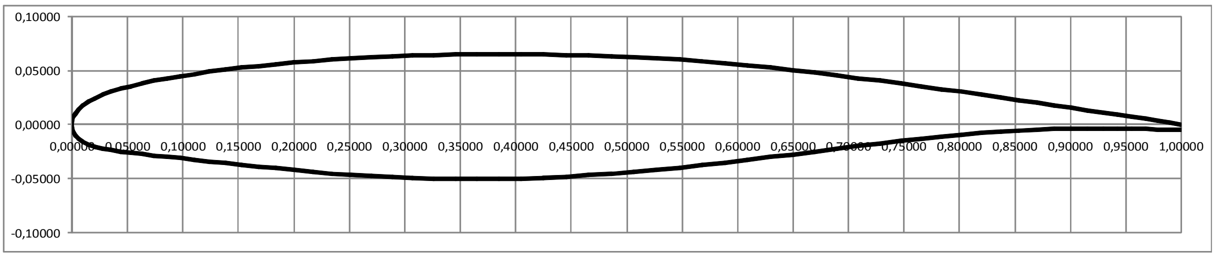

Table 2. Design Coordinates for Modified Airfoil

Upper surface		Lower surface	
x/c	*y/c*	*x/c*	*y/c*
0.00000	0.00000	0.00000	0.00000
.00099	.00620	.00099	−.00602
.00301	.01045	.00301	−.00987
.00604	.01431	.00604	−.01314
.01005	.01788	.01005	−.01595
.01500	.02122	.01500	−.01833
.02088	.02438	.02088	−.02033
.02764	.02740	.02764	−.02203
.03528	.03030	.03528	−.02351
.04374	.03308	.04374	−.02485
.05302	.03570	.05302	−.02609
.06308	.03816	.06308	−.02730
.07389	.04048	.07389	−.02853
.08543	.04269	.08543	−.02980
.09766	.04481	.09766	−.03113
.11056	.04685	.11056	−.03253
.12411	.04881	.12411	−.03400
.13826	.05068	.13826	−.03553
.15300	.05247	.15300	−.03713
.16830	.05420	.16830	−.03878
.18413	.05585	.18413	−.04047
.20045	.05743	.20045	−.04215
.21725	.05891	.21725	−.04376
.23450	.06025	.23450	−.04526
.25216	.06143	.25216	−.04662
.27021	.06244	.27021	−.04780
.28863	.06326	.28863	−.04880
.30737	.06390	.30737	−.04960
.32642	.06436	.32642	−.05018
.34575	.06466	.34575	−.05052
.36533	.06481	.36533	−.05060
.38513	.06485	.38513	−.05042
.40512	.06478	.40512	−.04995
.42527	.06462	.42527	−.04920
0.44557	0.06434	0.44557	−0.04819
.46597	.06391	.46597	−.04692
.48646	.06330	.48646	−.04541
.50699	.06248	.50699	−.04369
.52756	.06143	.52756	−.04178
.54812	.06014	.54812	−.03971
.56865	.05862	.56865	−.03749
.58912	.05686	.58912	−.03514
.60950	.05489	.60950	−.03268
.62977	.05274	.62977	−.03014
.64990	.05043	.64990	−.02754
.66986	.04803	.66986	−.02491
.68962	.04555	.68962	−.02231
.70915	.04304	.70915	−.01976
.72843	.04050	.72843	−.01730
.74742	.03794	.74742	−.01498
.76611	.03538	.76611	−.01284
.78445	.03283	.78445	−.01090
.80243	.03029	.80243	−.00919
.82002	.02775	.82002	−.00773
.83718	.02521	.83718	−.00650
.85389	.02269	.85389	−.00551
.87013	.02019	.87013	−.00475
.88585	.01775	.88585	−.00420
.90105	.01539	.90105	−.00384
.91568	.01312	.91568	−.00365
.92972	.01096	.92972	−.00360
.94314	.00890	.94314	−.00367
.95592	.00694	.95592	−.00383
.96802	.00507	.96802	−.00405
.97942	.00329	.97942	−.00432
.99009	.00160	.99009	−.00460
1.00000	.00000	1.00000	−.00489

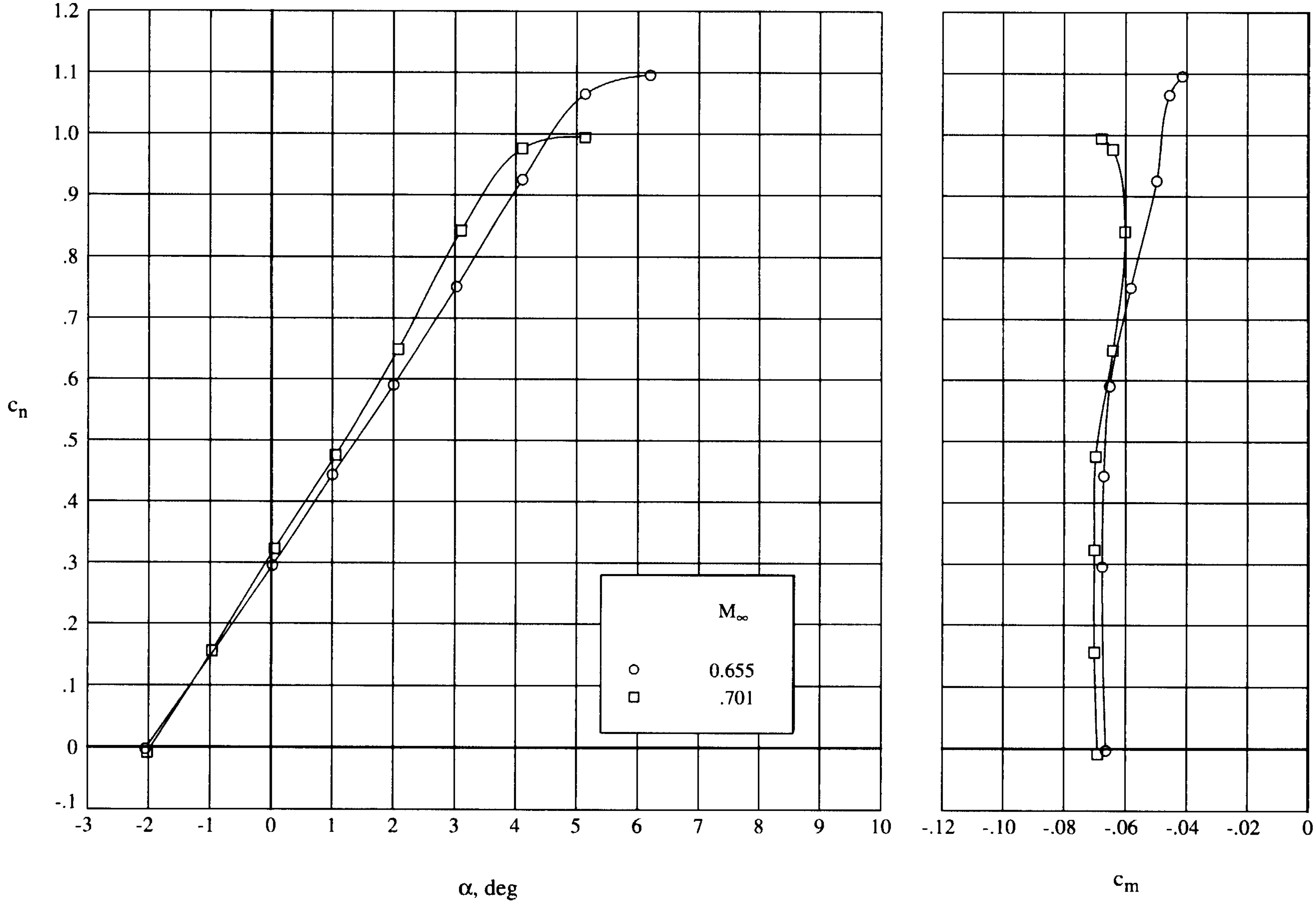

(a) Normal-force and pitching-moment coefficients. $R_c = 3.0 \times 10^6$.

Figure 13. Effect of free-stream Mach number on force and moment coefficients at constant Reynolds number for modified airfoil.

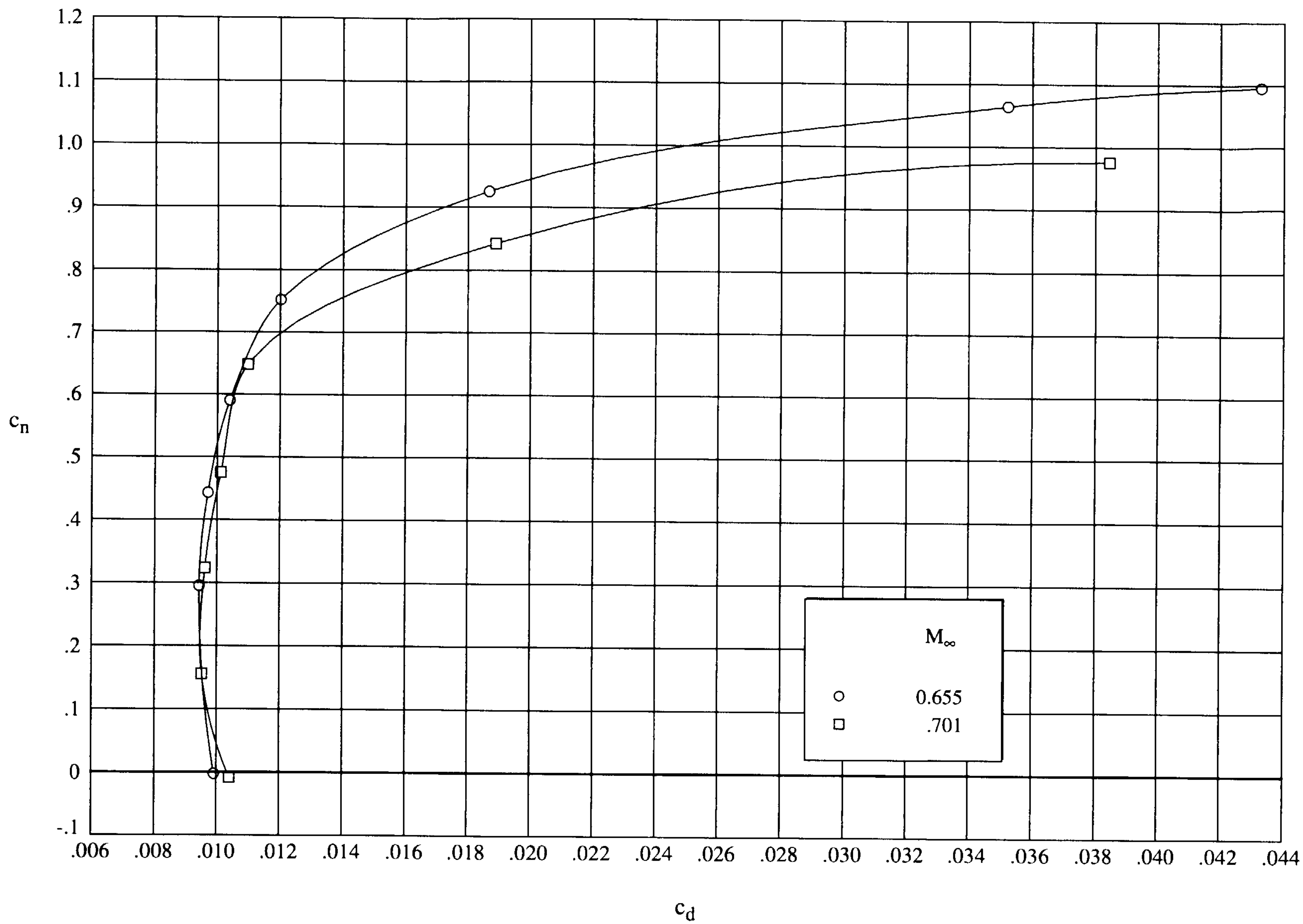

(b) Drag coefficient. $R_c = 3.0 \times 10^6$.

Figure 13. Continued.

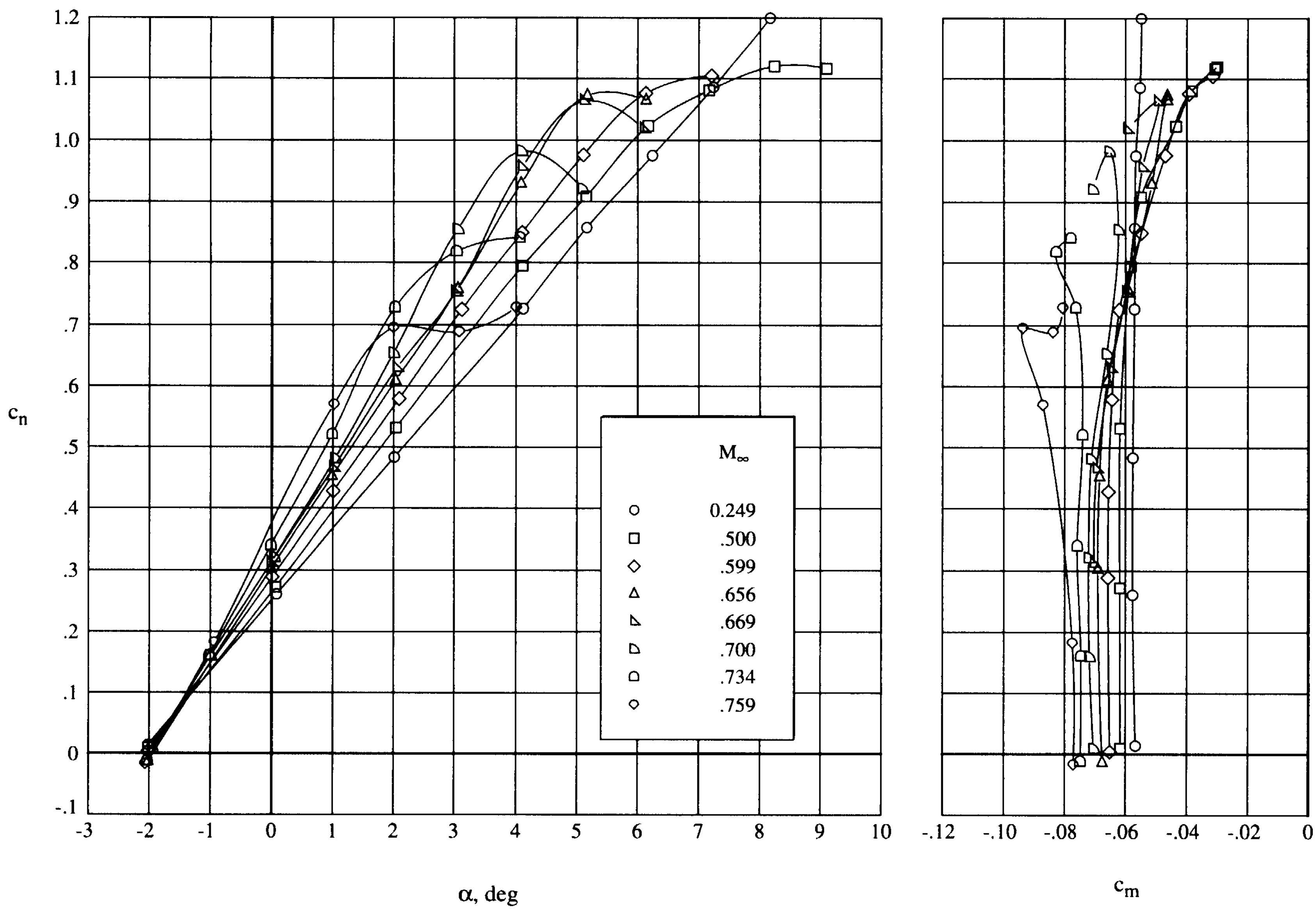

(c) Normal-force and pitching-moment coefficients. $R_c = 4.5 \times 10^6$.

Figure 13. Continued.

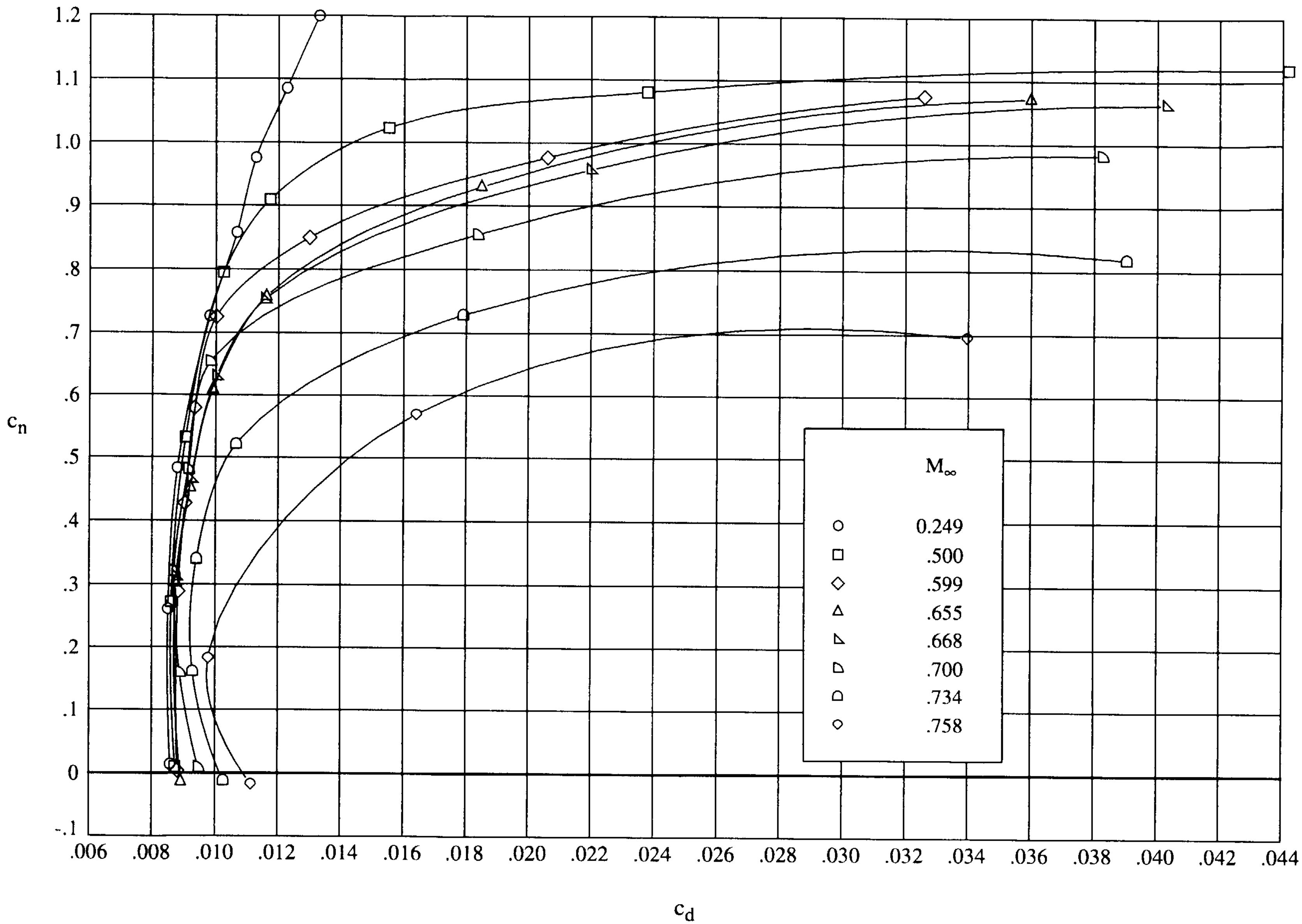

(d) Drag coefficient. $R_c = 4.5 \times 10^6$.

Figure 13. Continued.

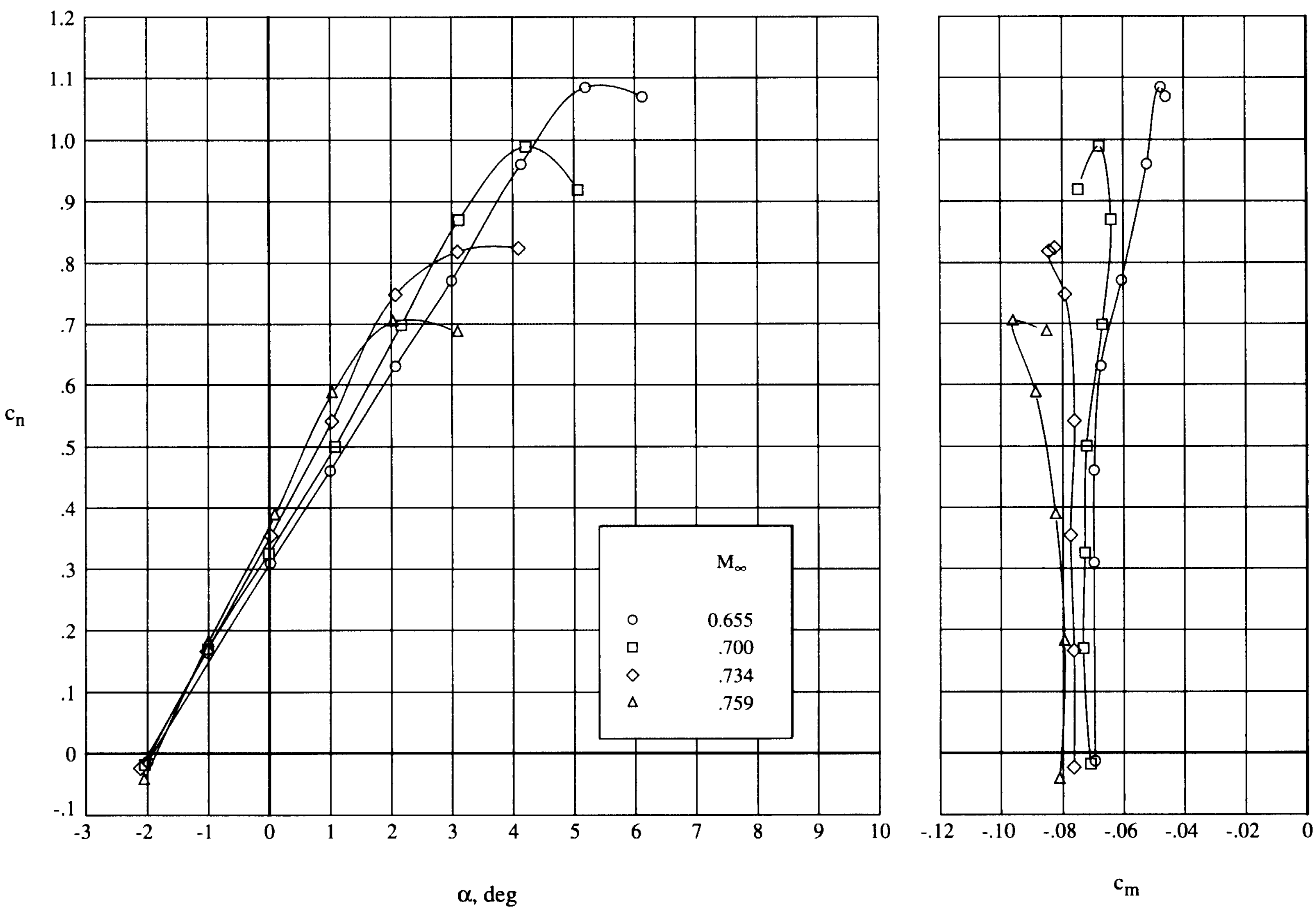

(e) Normal-force and pitching-moment coefficients. $R_c = 6.5 \times 10^6$.

Figure 13. Continued.

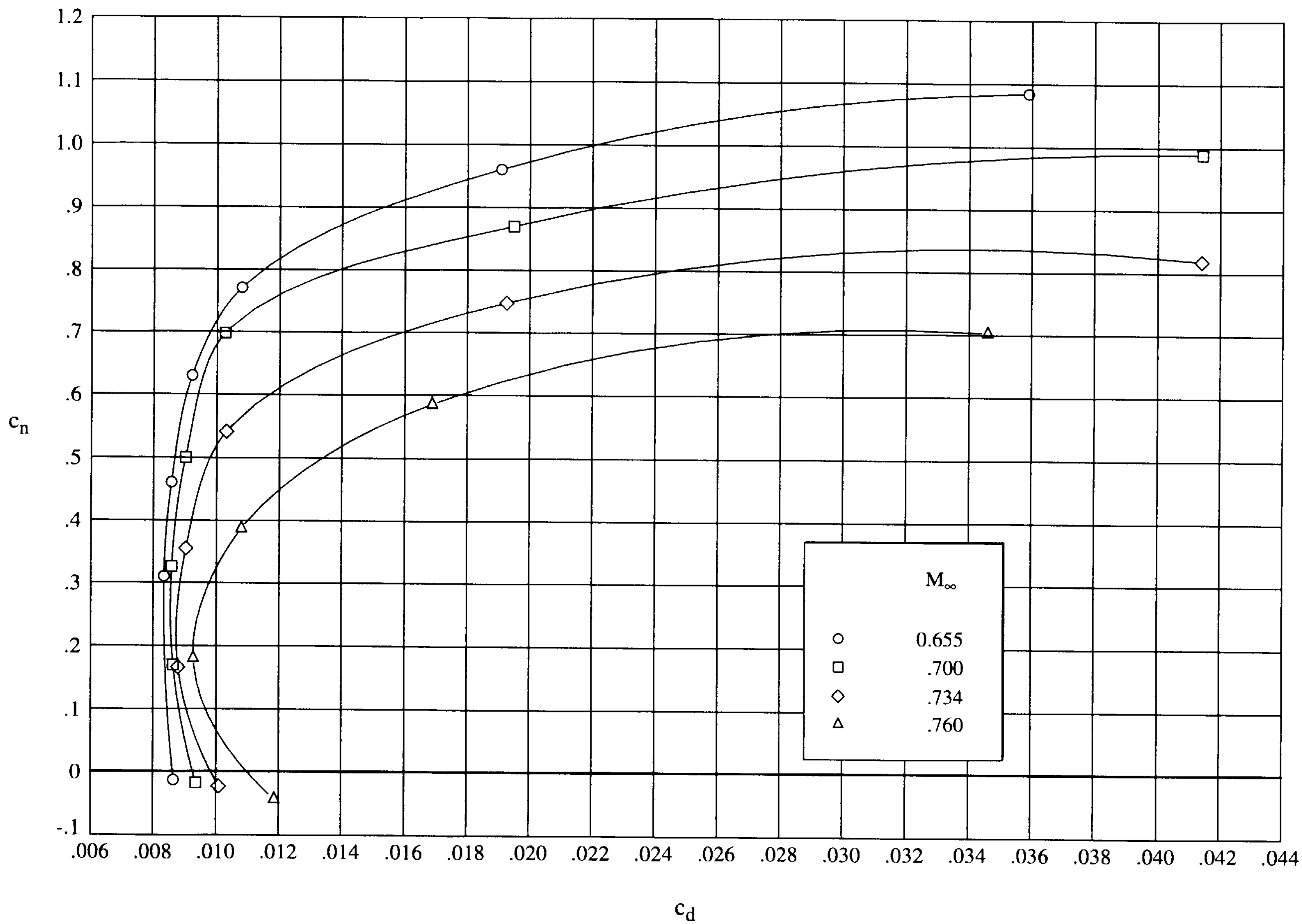

(f) Drag coefficient. $R_c = 6.5 \times 10^6$.

Figure 13. Continued.

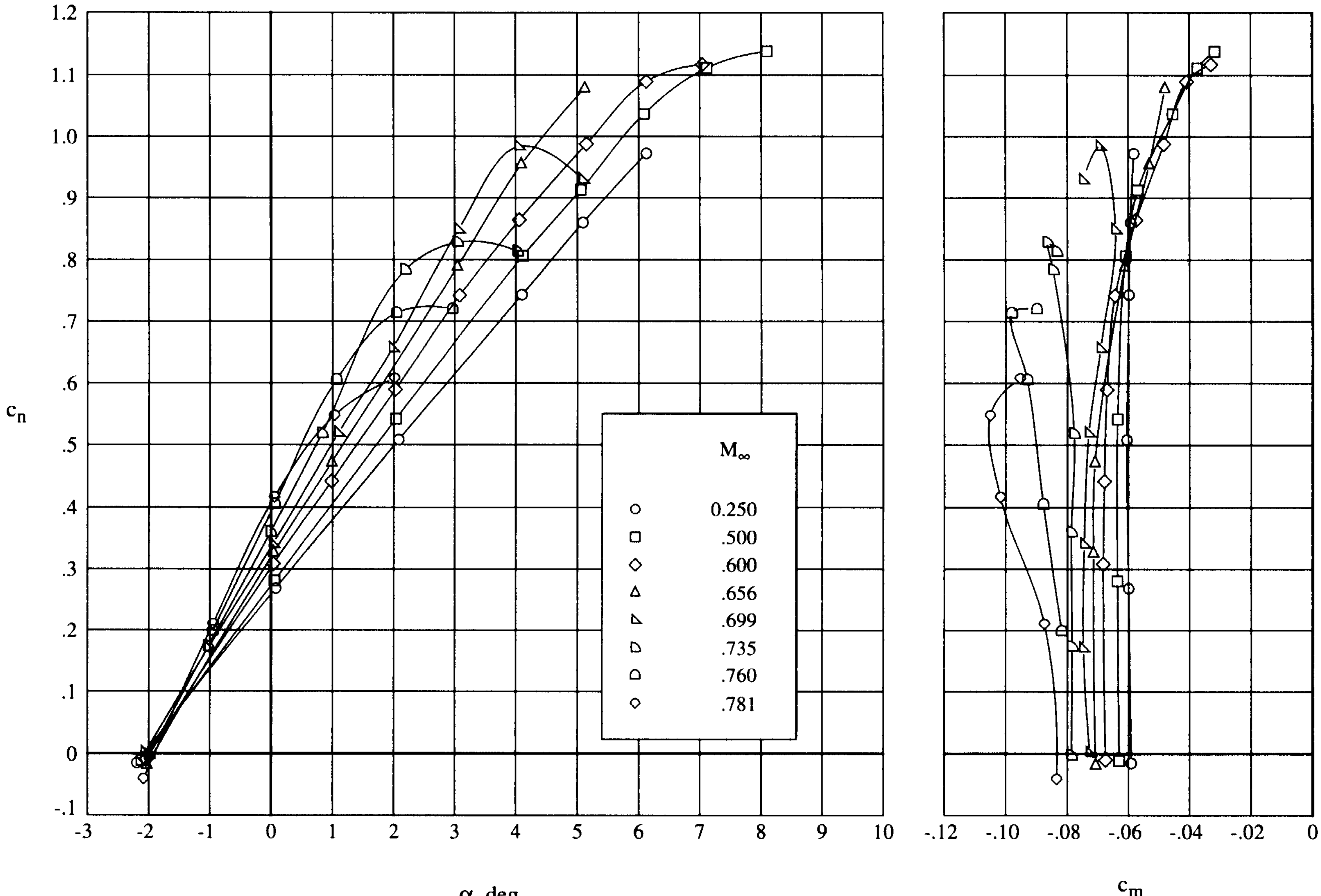

(g) Normal-force and pitching-moment coefficients. $R_c = 9.0 \times 10^6$.

Figure 13. Continued.

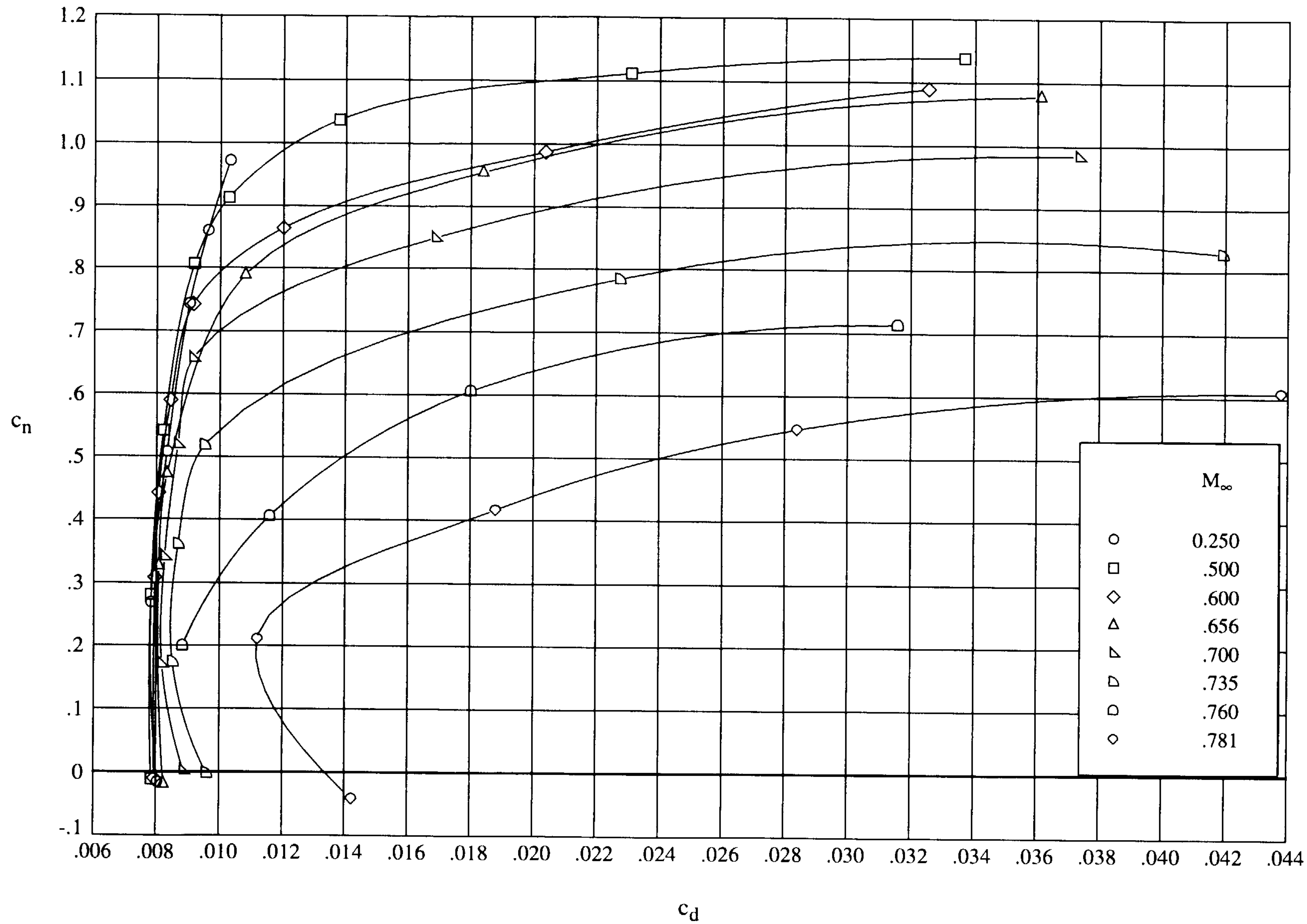

(h) Drag coefficient. $R_c = 9.0 \times 10^6$.

Figure 13. Continued.

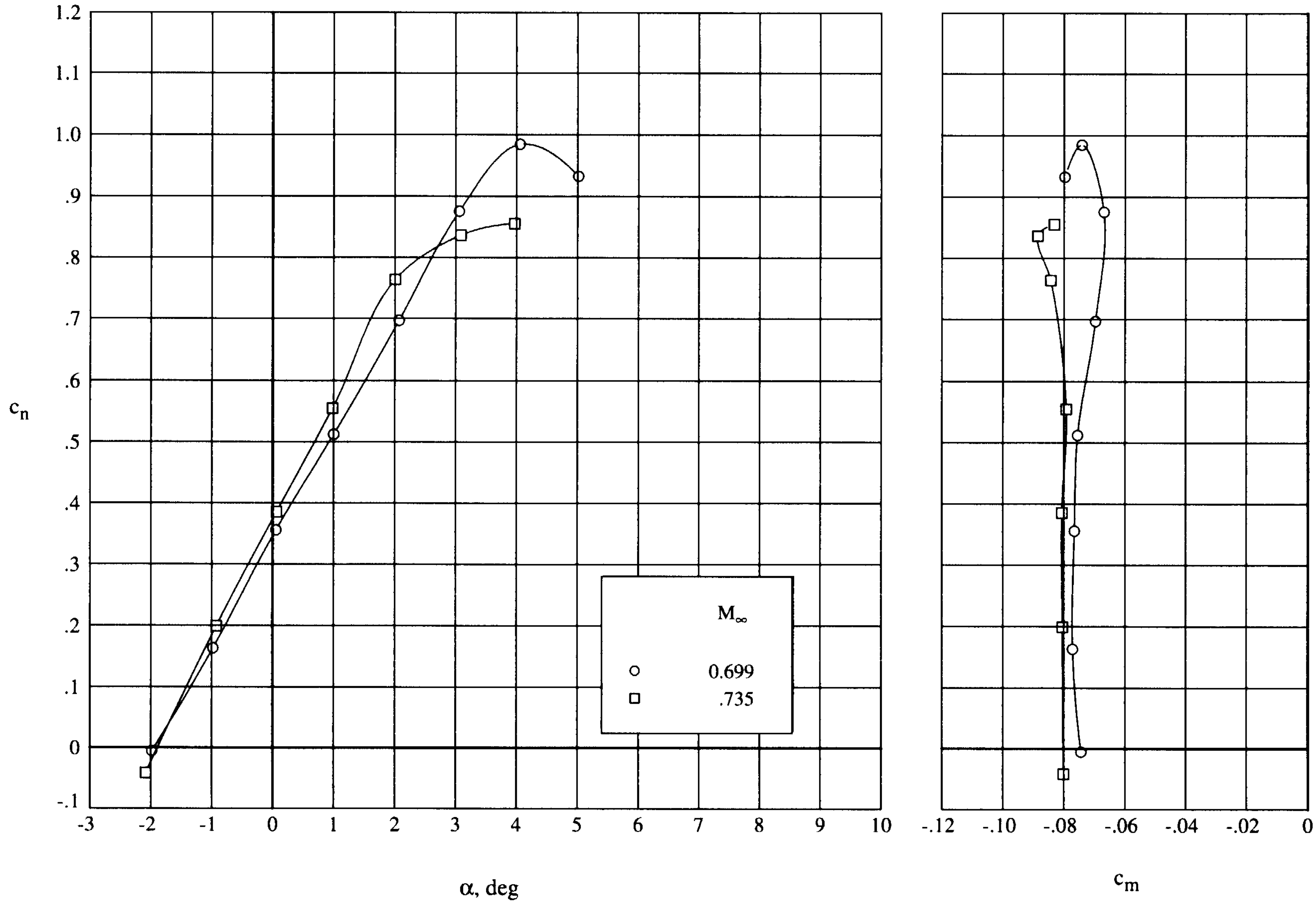

(i) Normal-force and pitching-moment coefficients. $R_c = 13.5 \times 10^6$.

Figure 13. Continued.

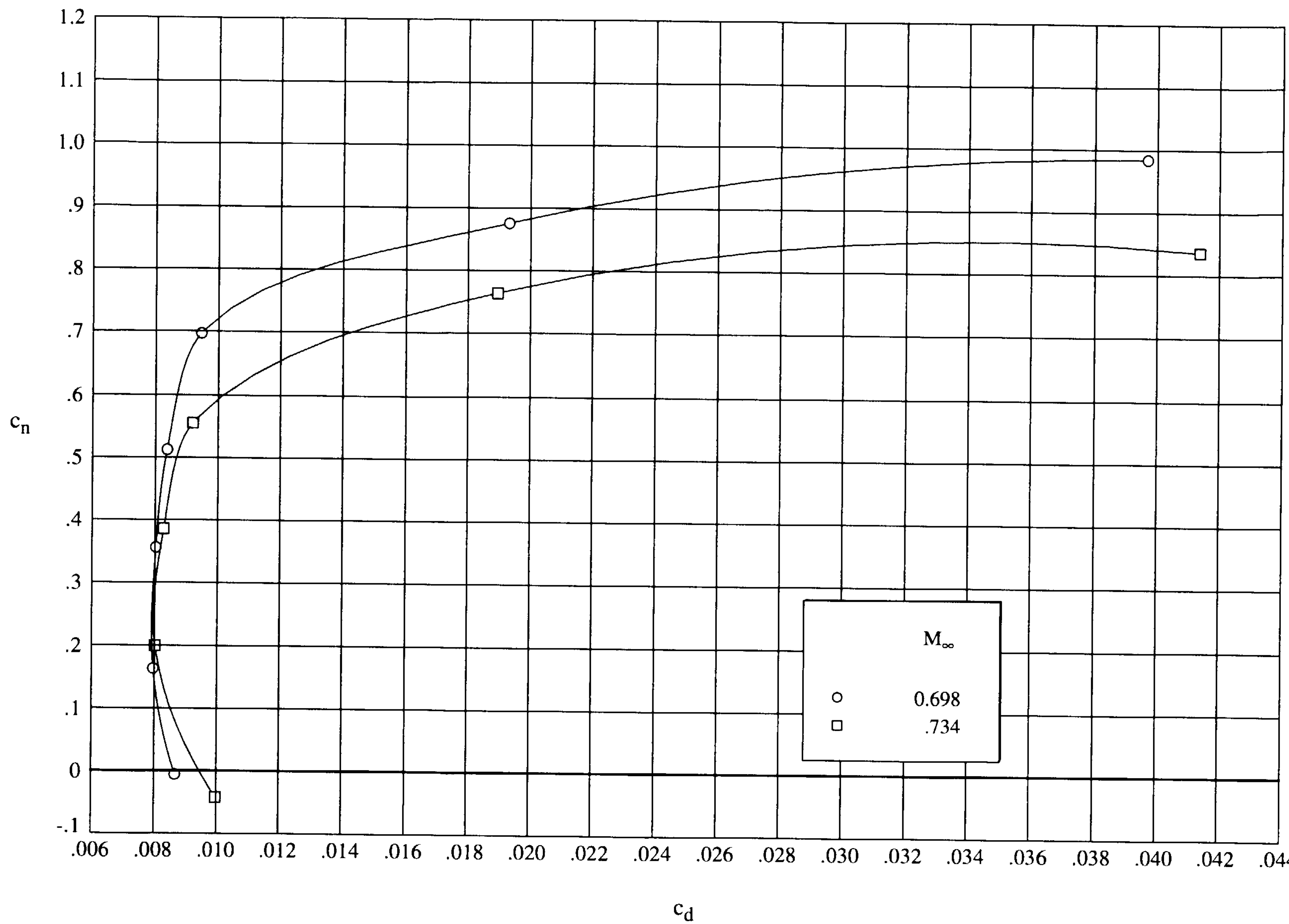

(j) Drag coefficient. $R_c = 13.5 \times 10^6$.

Figure 13. Concluded.

DFVLR R4

Deutsche Forschungs- und Versuchsanstalt für Luft- und Raumfahrt (DFVLR)

Year	1984
Reference	NASA TM-85739
t/c	0,135
Transition	n/a

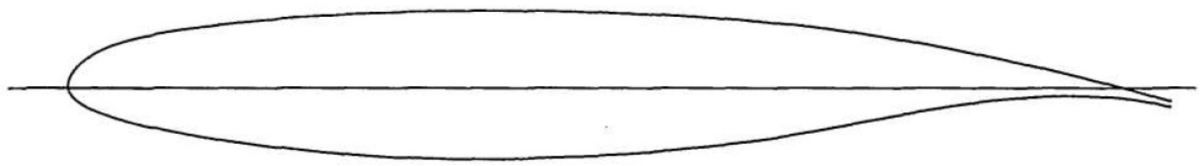

Note that UIUC Airfoil Data Site contains wrong coordinates

Proper Coordinates from Original Publication NASA TM-85739

x_u/c	z_u/c	x_l/c	z_l/c
0	0	0	0
0,0001	0,0043	0,0005	-0,0019
0,0005	0,0063	0,0011	-0,0033
0,0011	0,0079	0,0023	-0,0056
0,0016	0,0093	0,0045	-0,0084
0,0021	0,0103	0,0095	-0,0126
0,0045	0,014	0,0145	-0,0157
0,0095	0,0197	0,0195	-0,0184
0,0145	0,024	0,0245	-0,0207
0,0195	0,0276	0,0295	-0,0227
0,0245	0,0305	0,0345	-0,0245
0,0295	0,0332	0,0395	-0,0262
0,0345	0,0355	0,0445	-0,0278
0,0395	0,0376	0,0495	-0,0292
0,0445	0,0393	0,0545	-0,0306
0,0495	0,0409	0,0595	-0,0319
0,0545	0,0423	0,0645	-0,0331
0,0595	0,0436	0,0695	-0,0343
0,0645	0,0449	0,0745	-0,0354
0,0695	0,046	0,0795	-0,0364
0,0795	0,048	0,0995	-0,0404
0,0995	0,0515	0,1195	-0,0439
0,1195	0,0545	0,1395	-0,047
0,1395	0,057	0,1596	-0,0499
0,1596	0,0592	0,1796	-0,0525
0,1796	0,0611	0,1996	-0,0548
0,1996	0,0628	0,2196	-0,0569
0,2196	0,0643	0,2396	-0,0587
0,2396	0,0655	0,2596	-0,0603
0,2596	0,0666	0,2796	-0,0616
0,2796	0,0675	0,2996	-0,0627
0,2996	0,0683	0,3196	-0,0634
0,3196	0,0688	0,3597	-0,0639
0,3397	0,0692	0,3597	-0,0642
0,3597	0,0695	0,3797	-0,0642
0,3797	0,0696	0,3997	-0,064
0,3887	0,0696	0,4197	-0,0635
0,3997	0,0696	0,4397	-0,0629
0,4197	0,0695	0,4597	-0,0621
0,4397	0,0692	0,4797	-0,0611
0,4597	0,0688	0,4897	-0,0605
0,4797	0,0683	0,5047	-0,0596
0,4997	0,0676	0,5248	-0,0581
0,5197	0,0668	0,5448	-0,0564
0,5398	0,0659	0,5648	-0,0545
0,5598	0,0648	0,5848	-0,0524
0,5798	0,0636	0,6048	-0,05
0,5998	0,0622	0,6248	-0,0473
0,6198	0,0606	0,6448	-0,0444
0,6398	0,0588	0,6648	-0,0412
0,6598	0,0568	0,6848	-0,0377
0,6798	0,0545	0,7048	-0,0339
0,6998	0,0519	0,7249	-0,0302
0,7199	0,049	0,7449	-0,0264
0,7399	0,0459	0,7649	-0,0227
0,7599	0,0426	0,7849	-0,0192
0,7799	0,0391	0,8049	-0,0159
0,7999	0,0354	0,8249	-0,0131
0,8199	0,0315	0,8449	-0,0107
0,8399	0,0273	0,8649	-0,009
0,8599	0,0231	0,8849	-0,0079
0,8799	0,0186	0,905	-0,0074
0,8999	0,014	0,925	-0,0076
0,92	0,0093	0,945	-0,0085
0,94	0,0043	0,965	-0,0105
0,96	-0,0008	0,985	-0,0138
0,98	-0,0062	0,99	-0,0149
0,985	-0,0076	0,995	-0,0161
0,99	-0,009	1	-0,0172
0,995	-0,0104		
1	-0,0121		

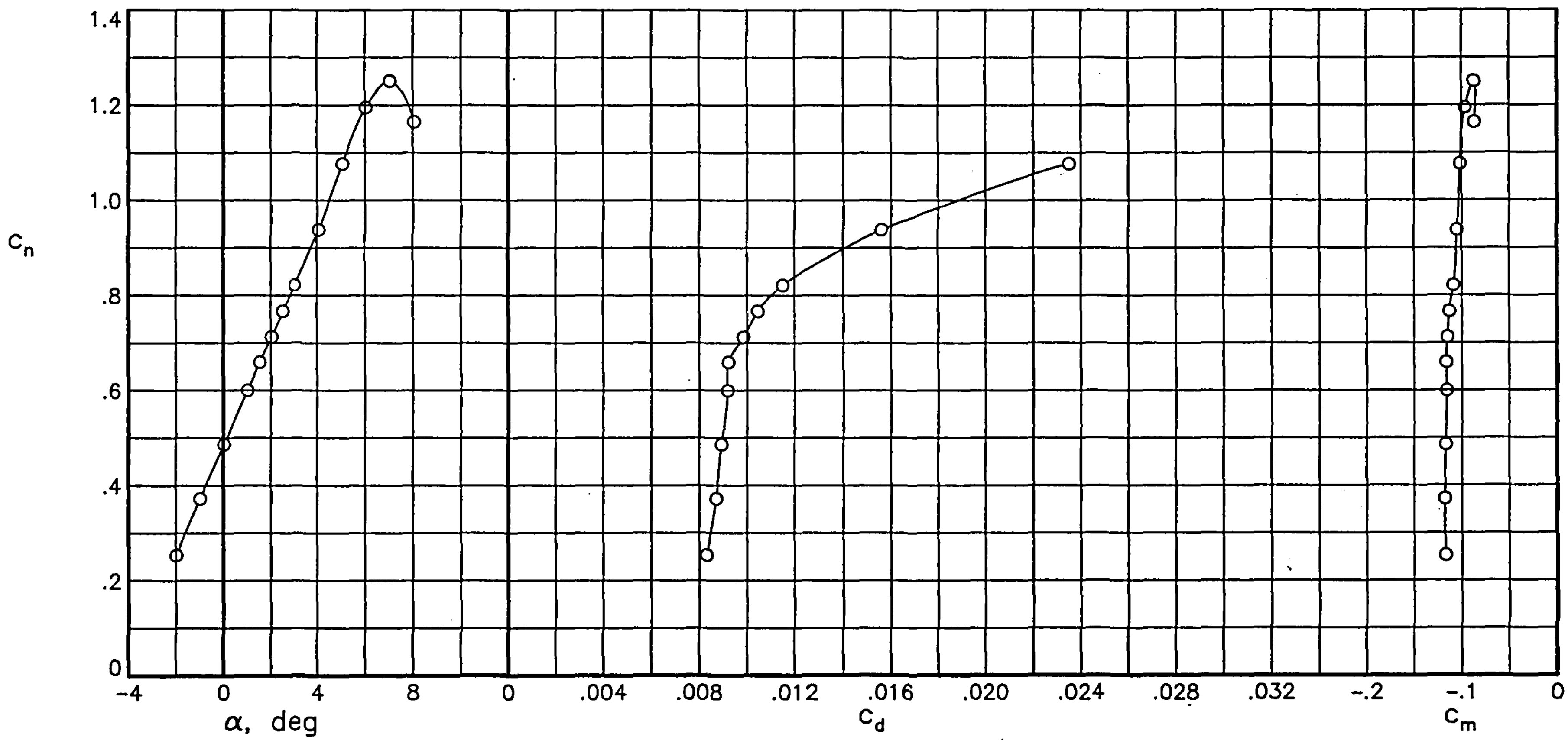

(a) $R = 4.01 \times 10^6$; $M = 0.6011$.

Figure 3.– Section characteristics at Reynolds numbers of 4×10^6.

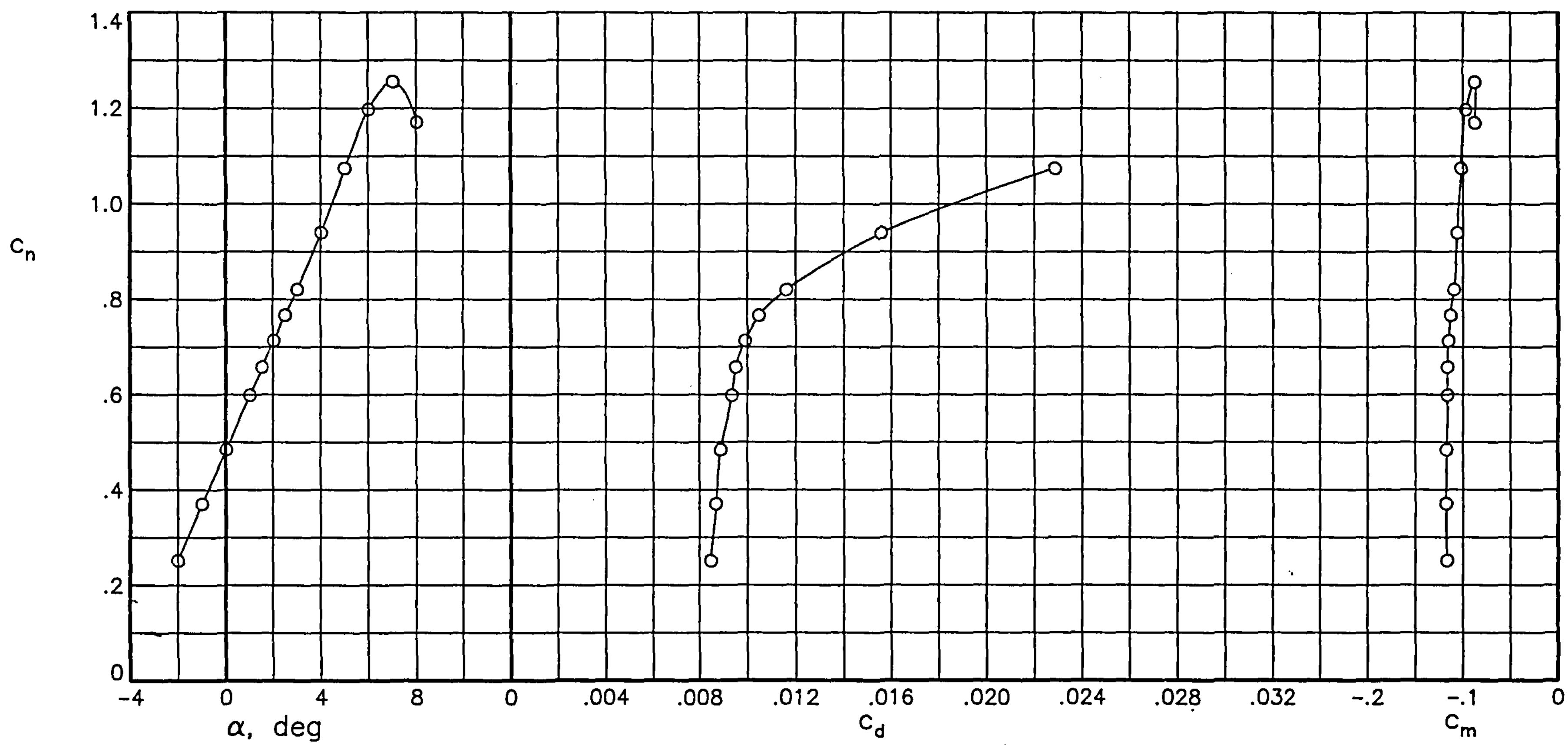

(b) $R = 4.05 \times 10^6$; $M = 0.5993$.

Figure 3.– Continued.

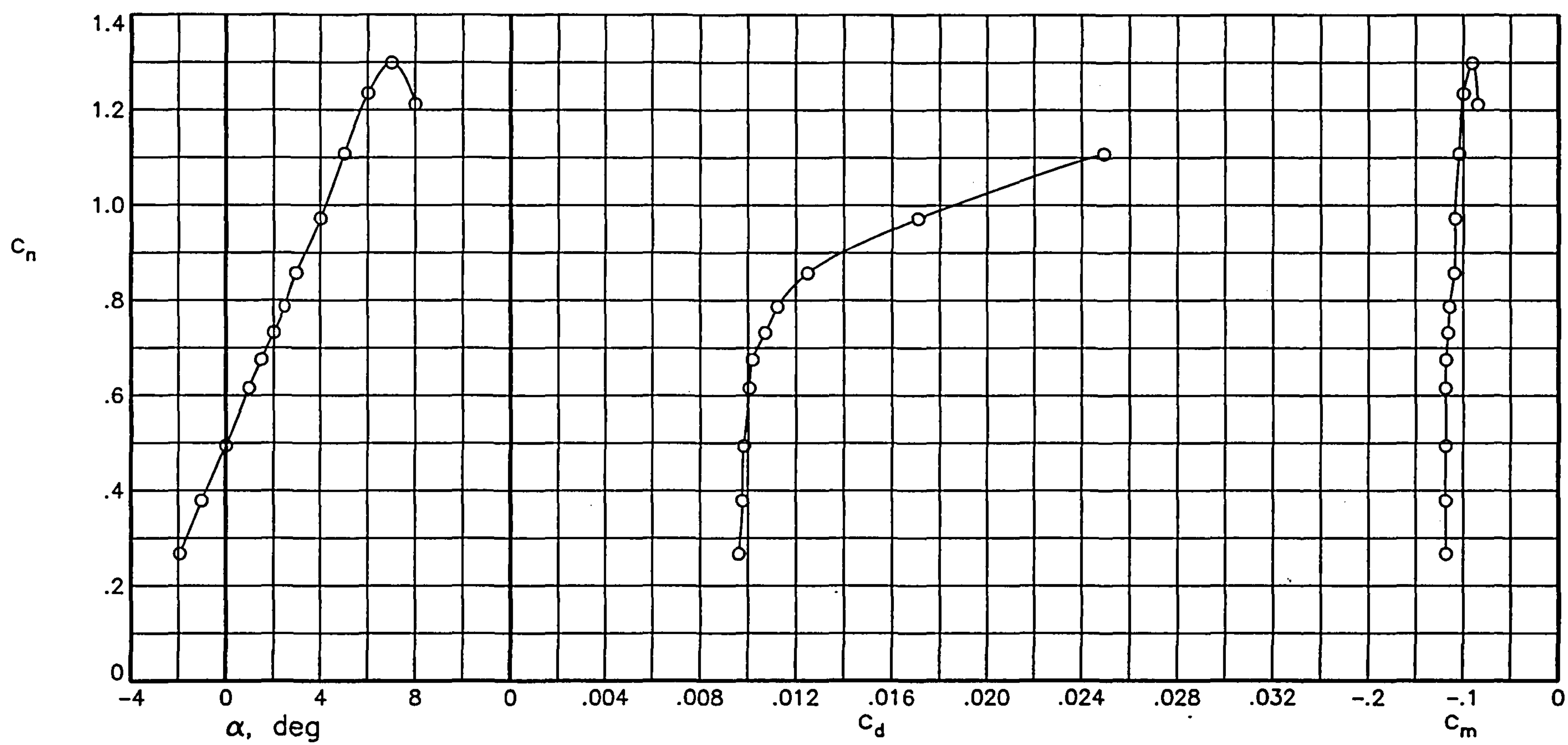

(c) R = 3.99 × 10 [6]; M = 0.5967

Figure 3.– Continued.

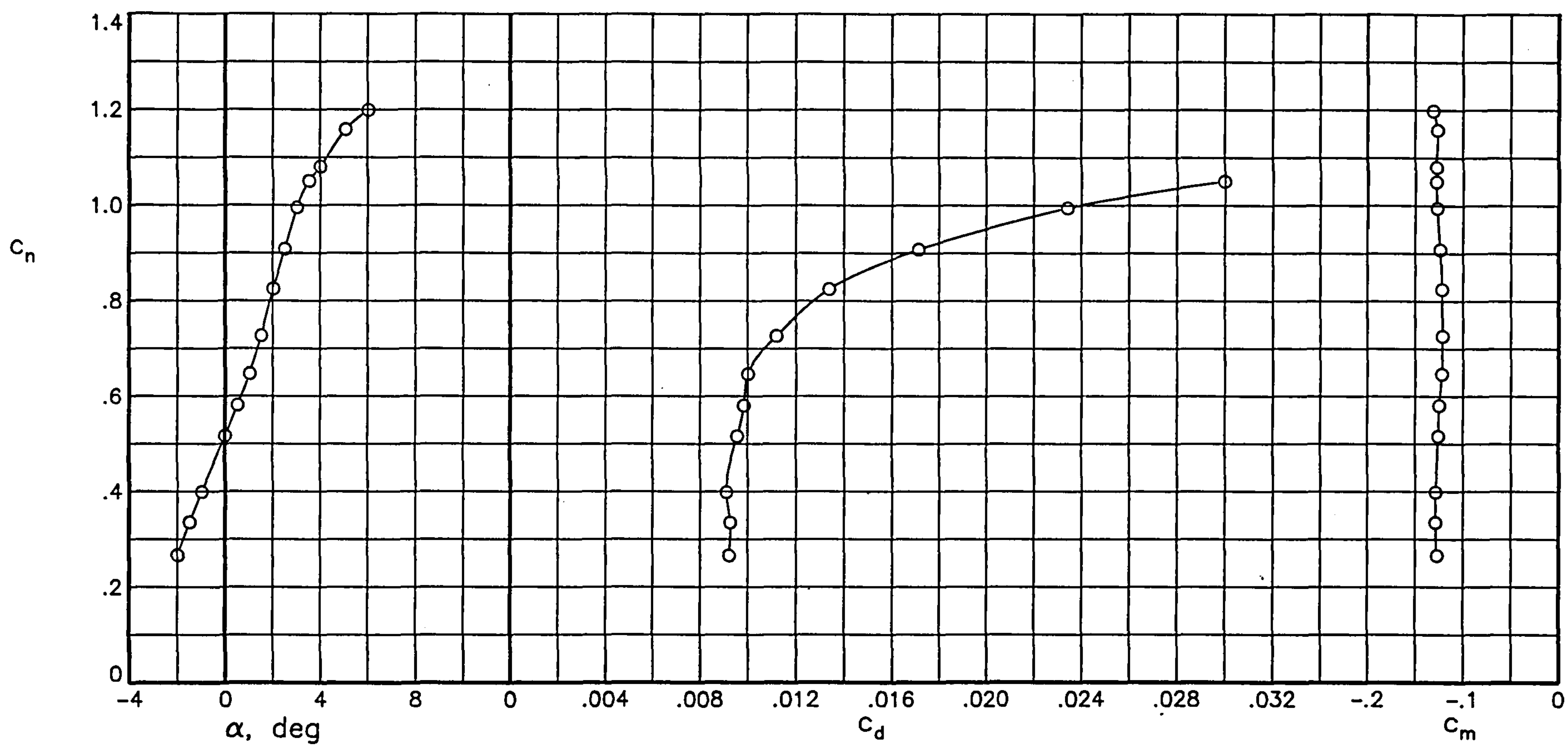

(d) $R = 4.03 \times 10^6$; $M = 0.6970$.

Figure 3.– Continued.

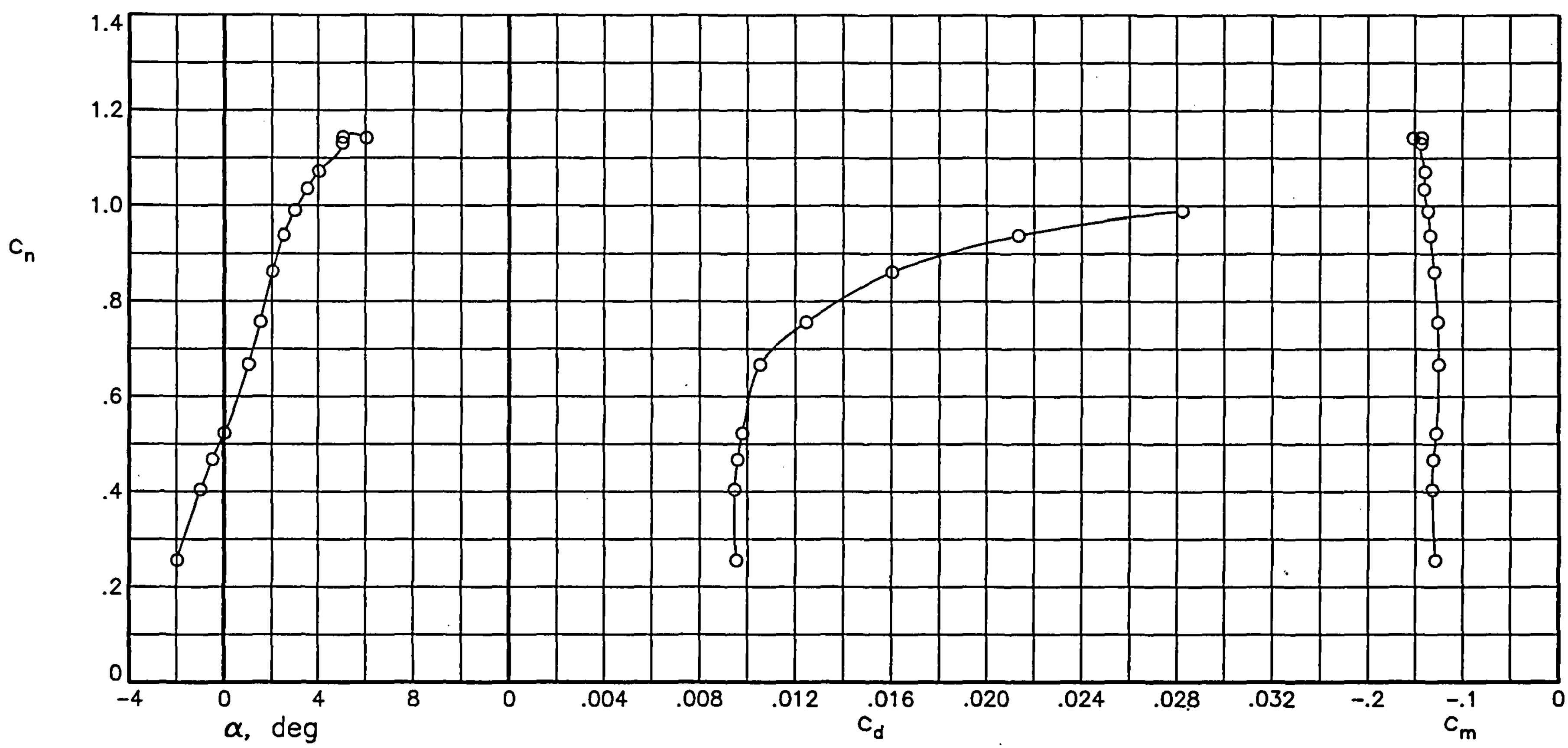

(e) $R = 4.02 \times 10^6$; $M = 0.7164$.

Figure 3.– Continued.

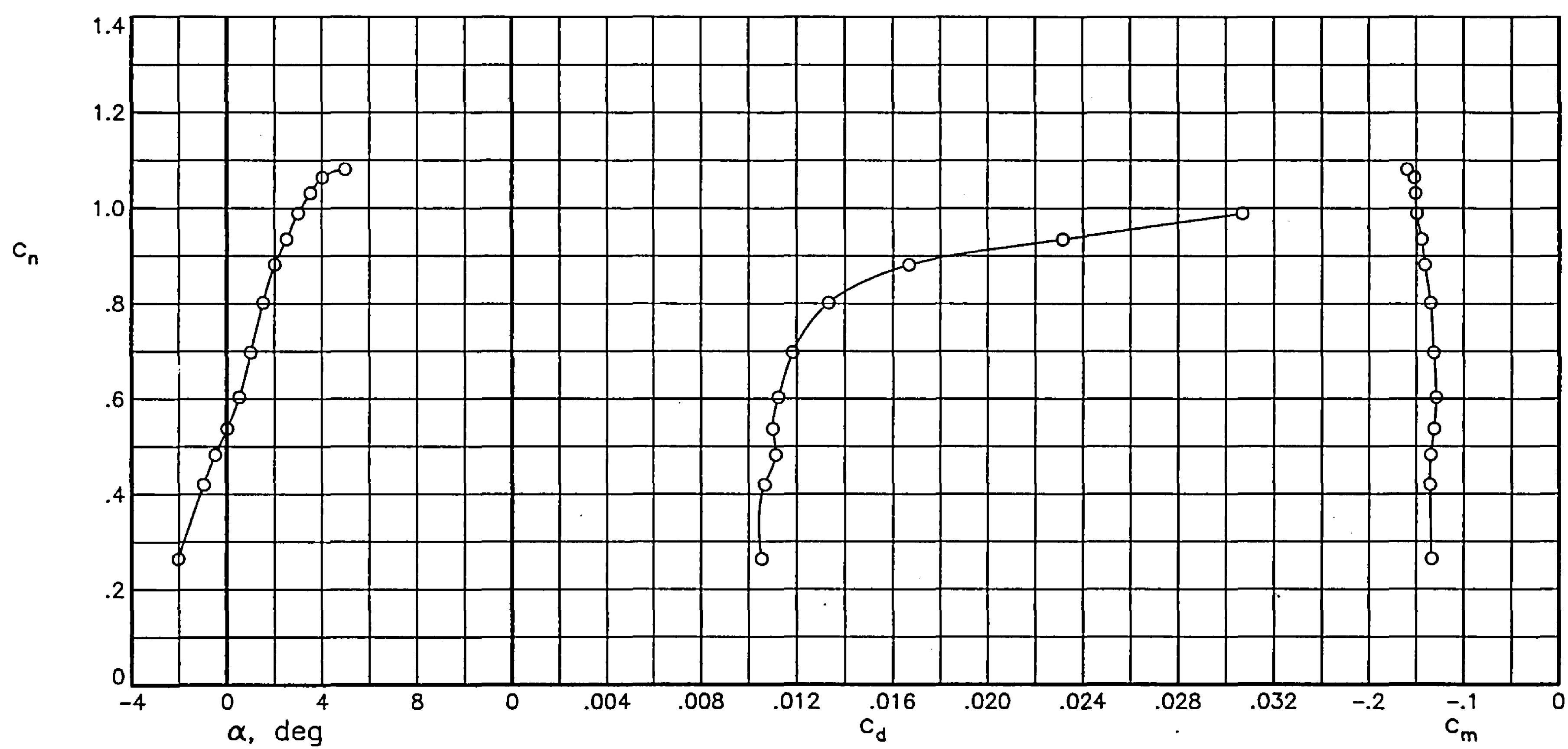

(f) $R = 4.03 \times 10^6$; $M = 0.7269$.

Figure 3.– Continued.

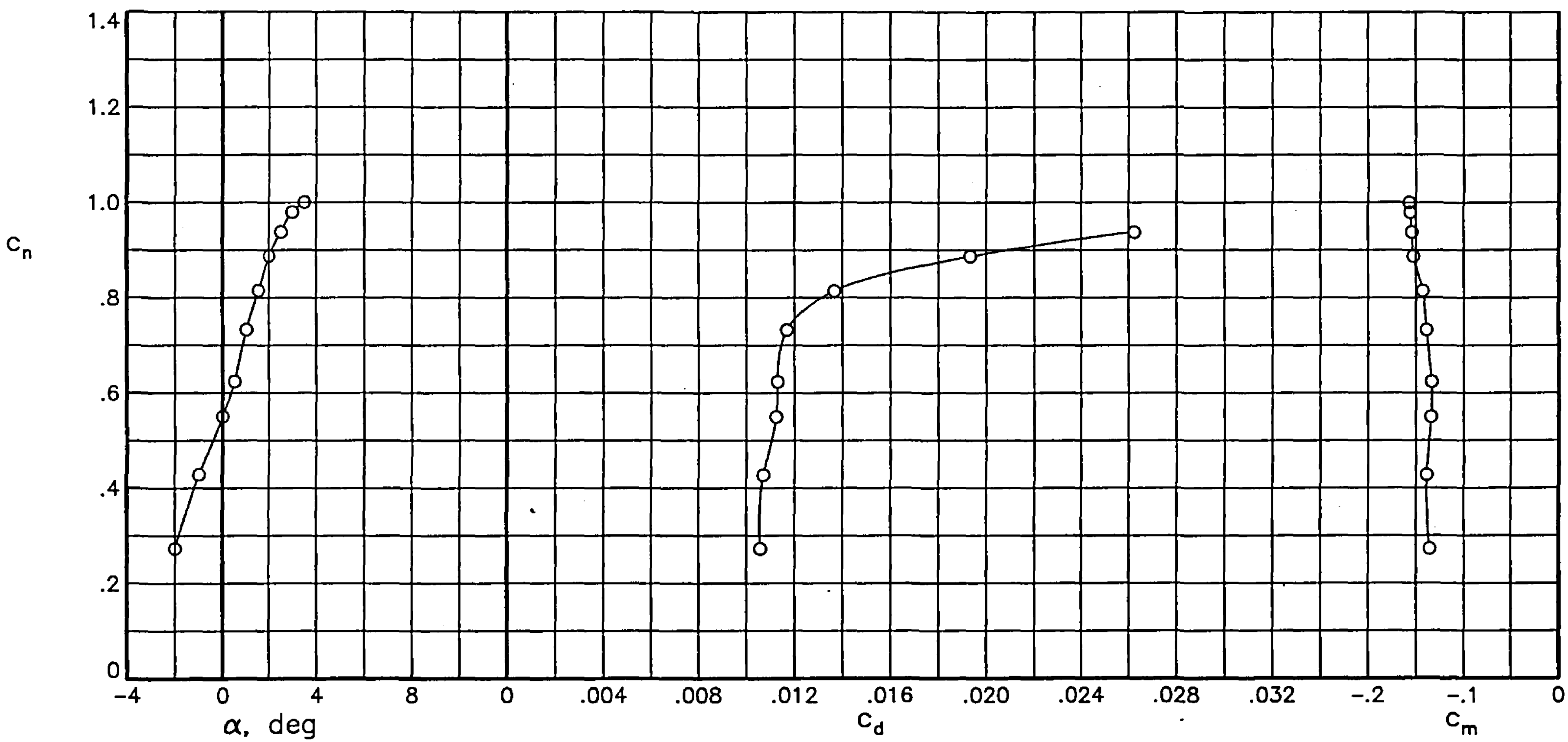

(g) $R = 4.04 \times 10^6$; $M = 0.7369$.

Figure 3.– Continued.

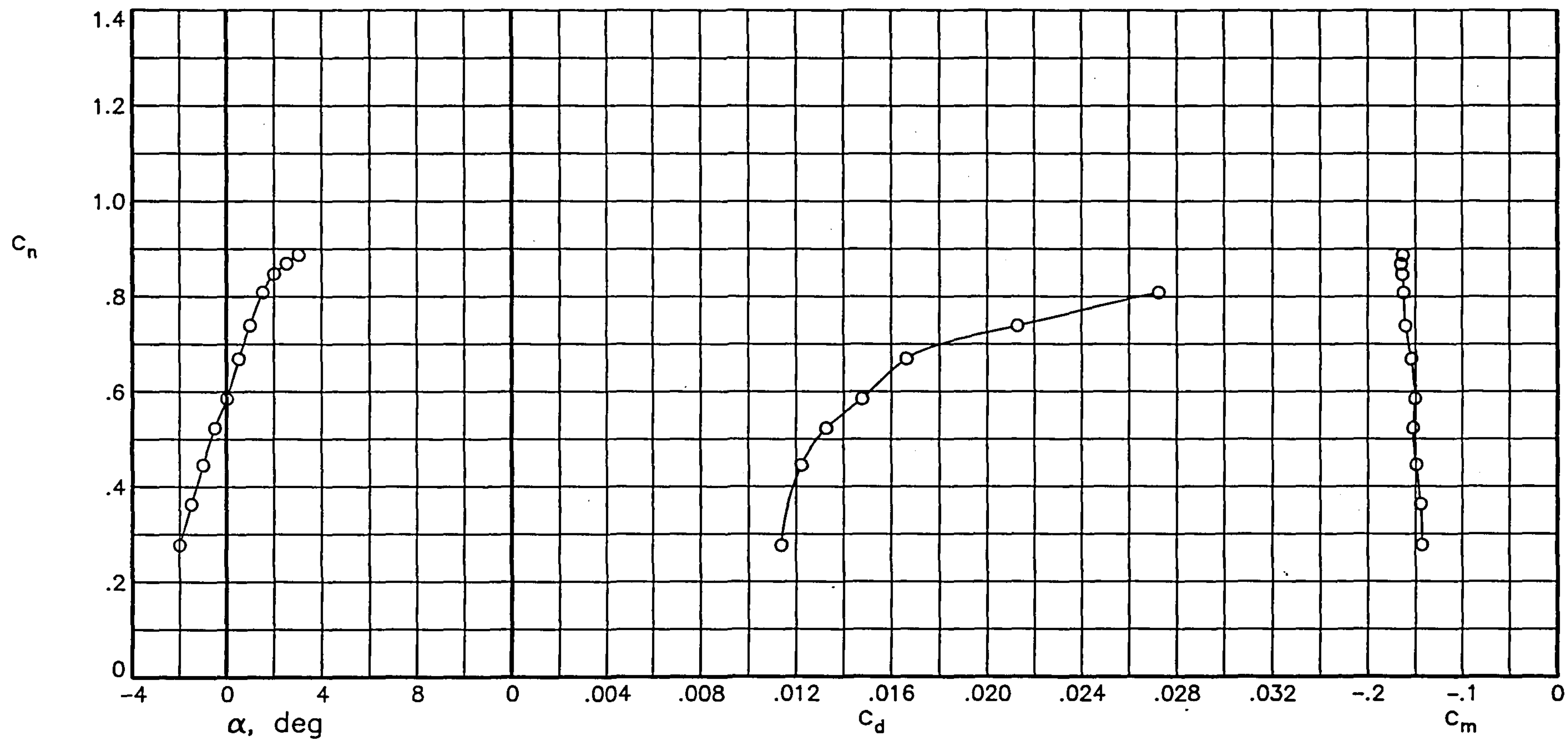

(h) $R = 4.09 \times 10^6$; $M = 0.7568$.

Figure 3.– Continued.

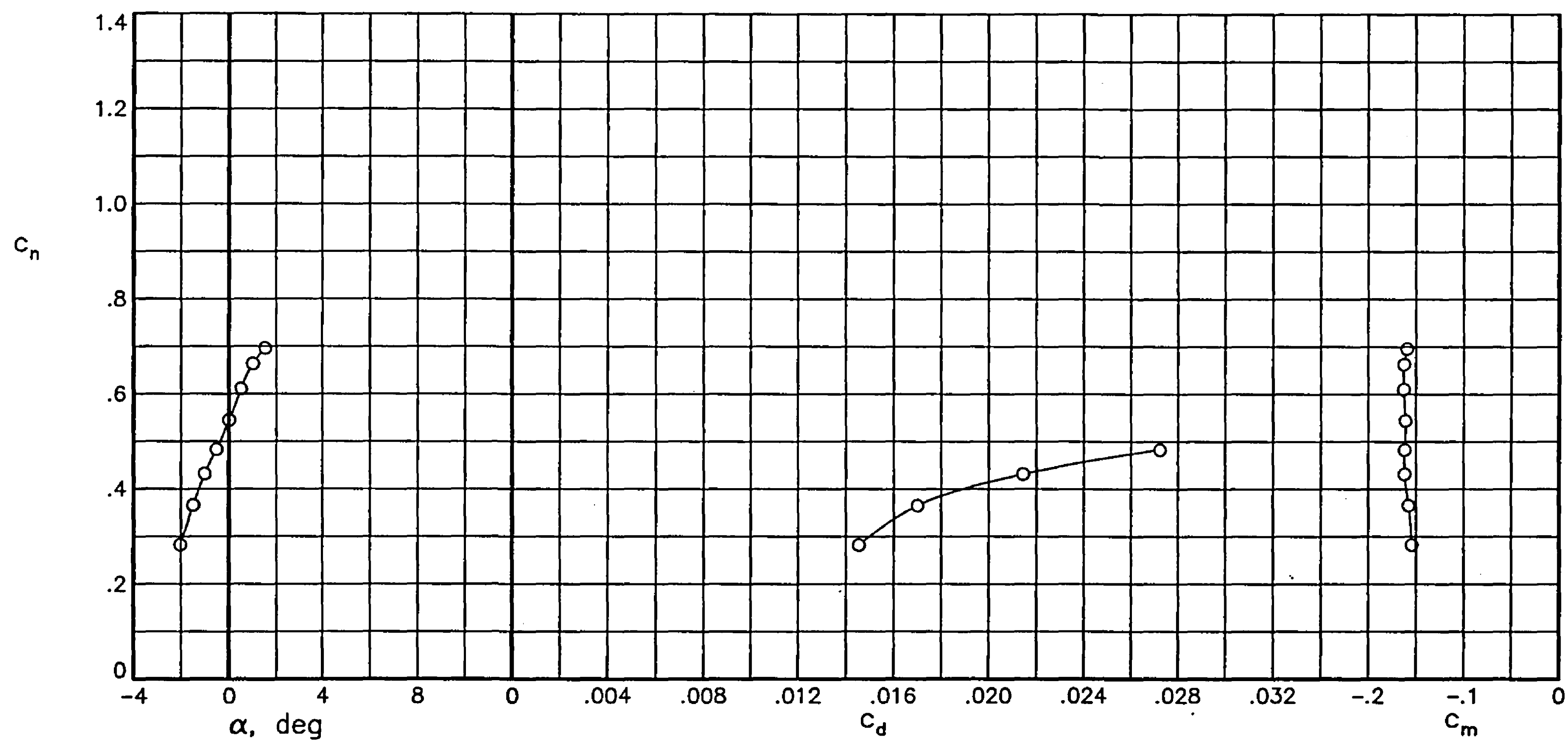

(i) $R = 4.07 \times 10^6$; $M = 0.7763$.

Figure 3.– Concluded.

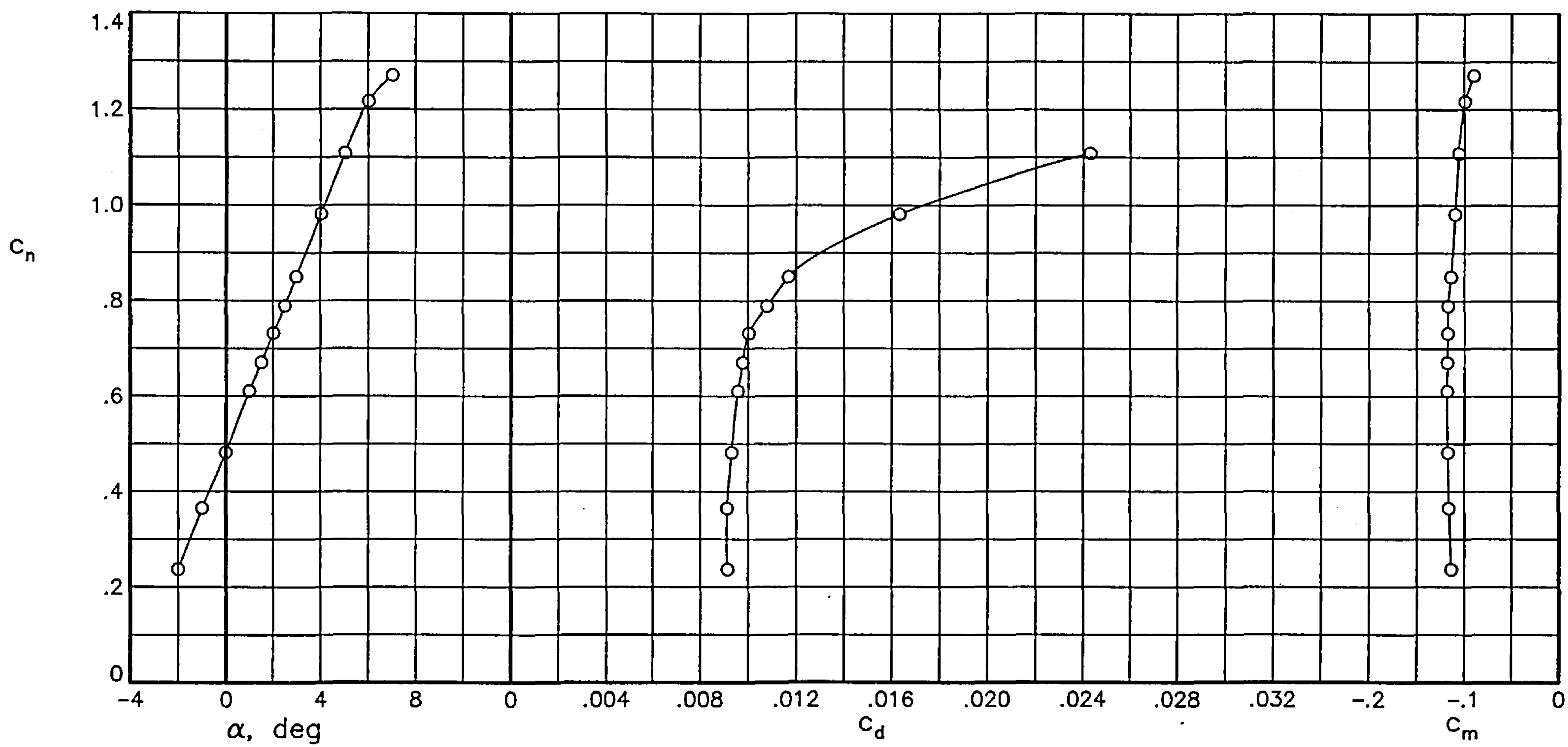

(a) R = 6.09×10^6; M = 0.6002.

Figure 4.— Section characteristics at Reynolds numbers of 6×10^6.

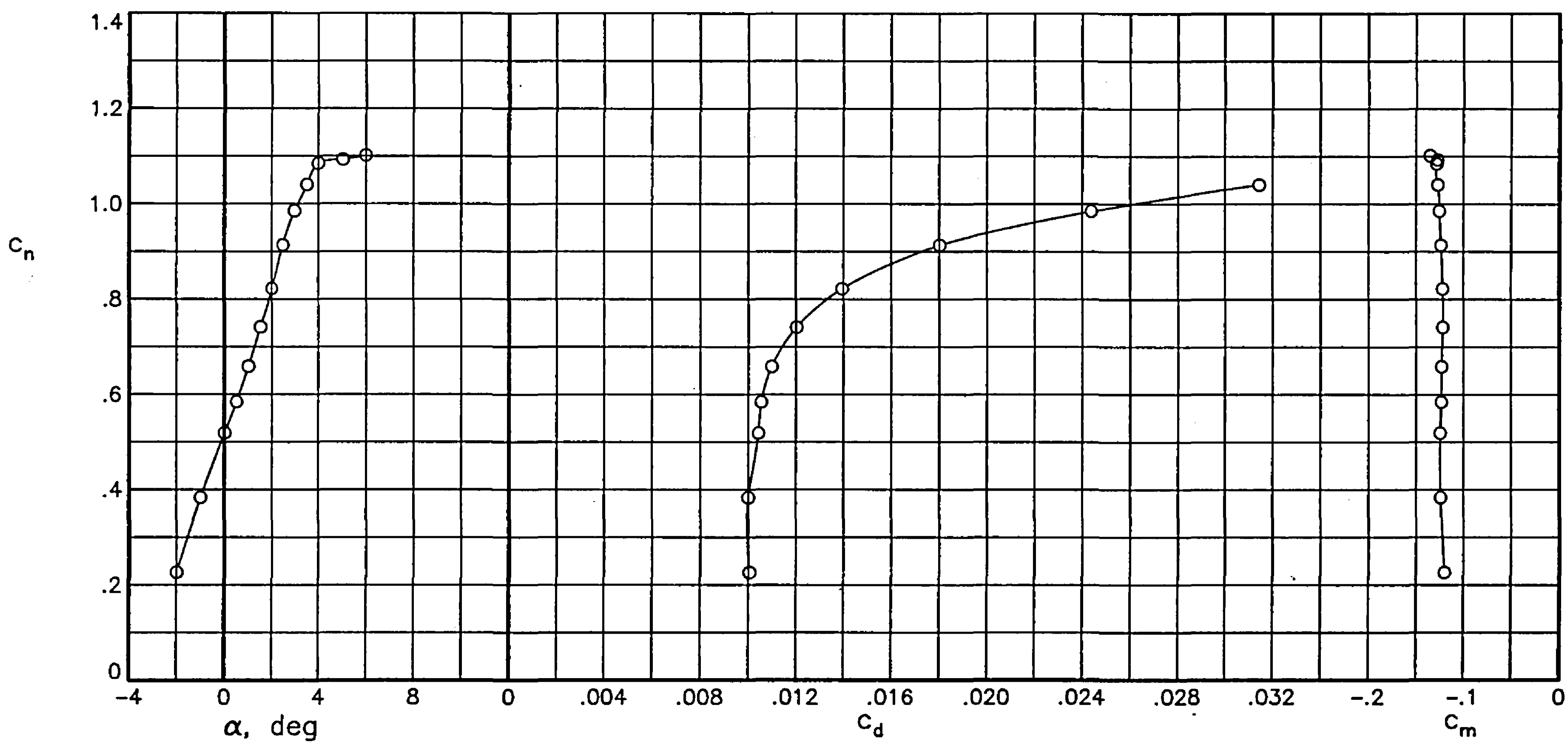

(b) $R = 6.07 \times 10^6$; $M = 0.6976$.

Figure 4.– Continued.

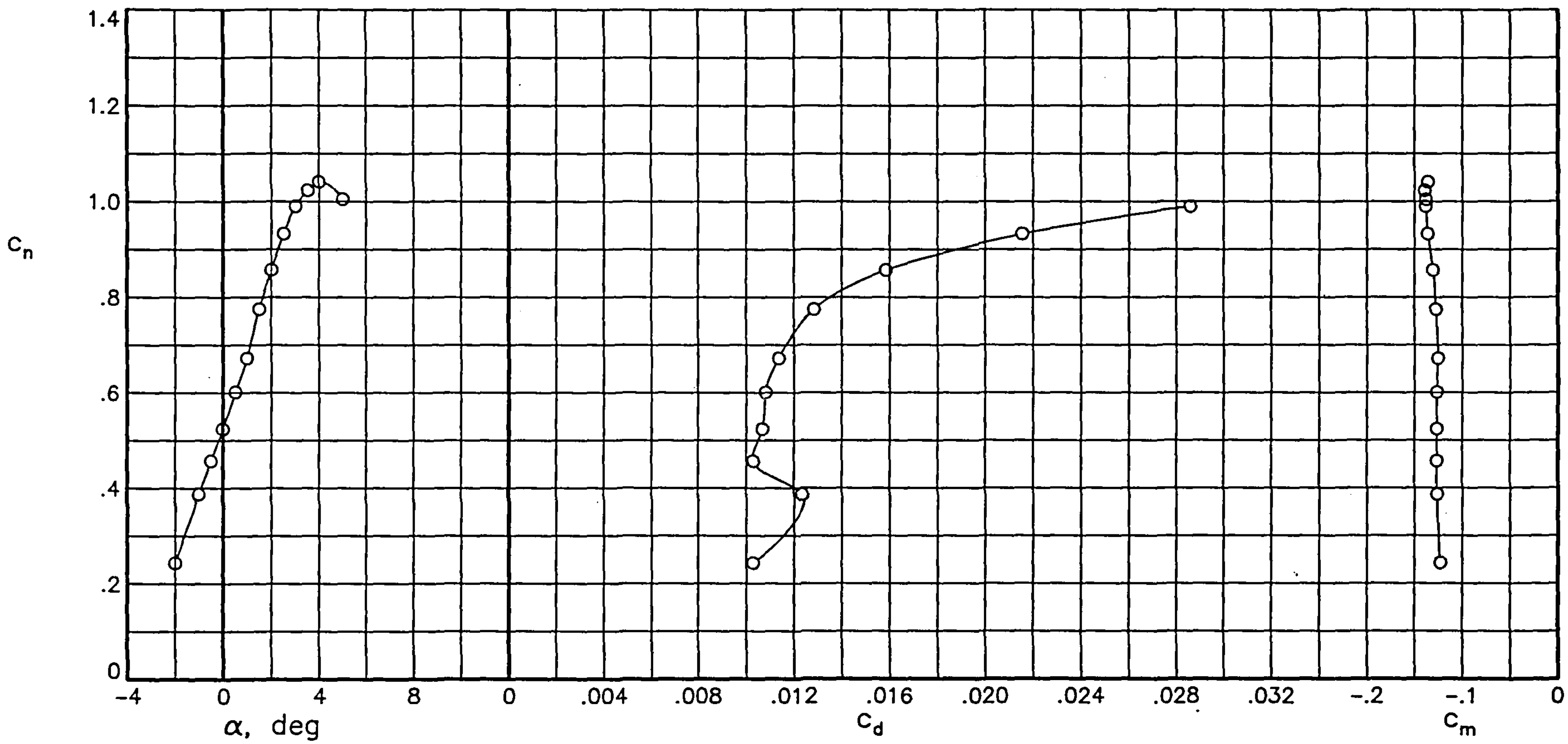

(c) $R = 6.06 \times 10^{6}$; $M = 0.7175$.

Figure 4.– Continued.

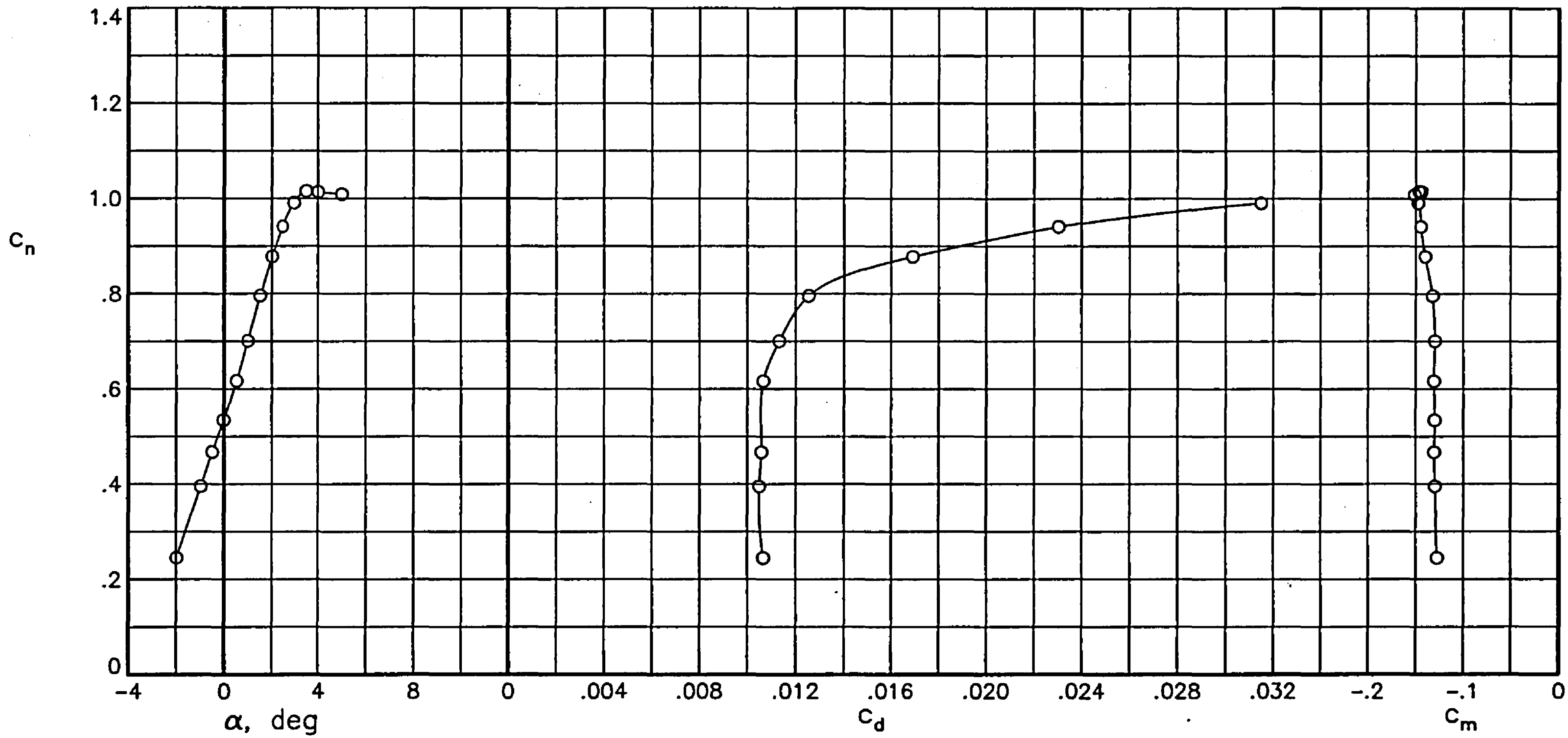

(d) $R = 6.04 \times 10^6$; $M = 0.7255$.

Figure 4.– Continued.

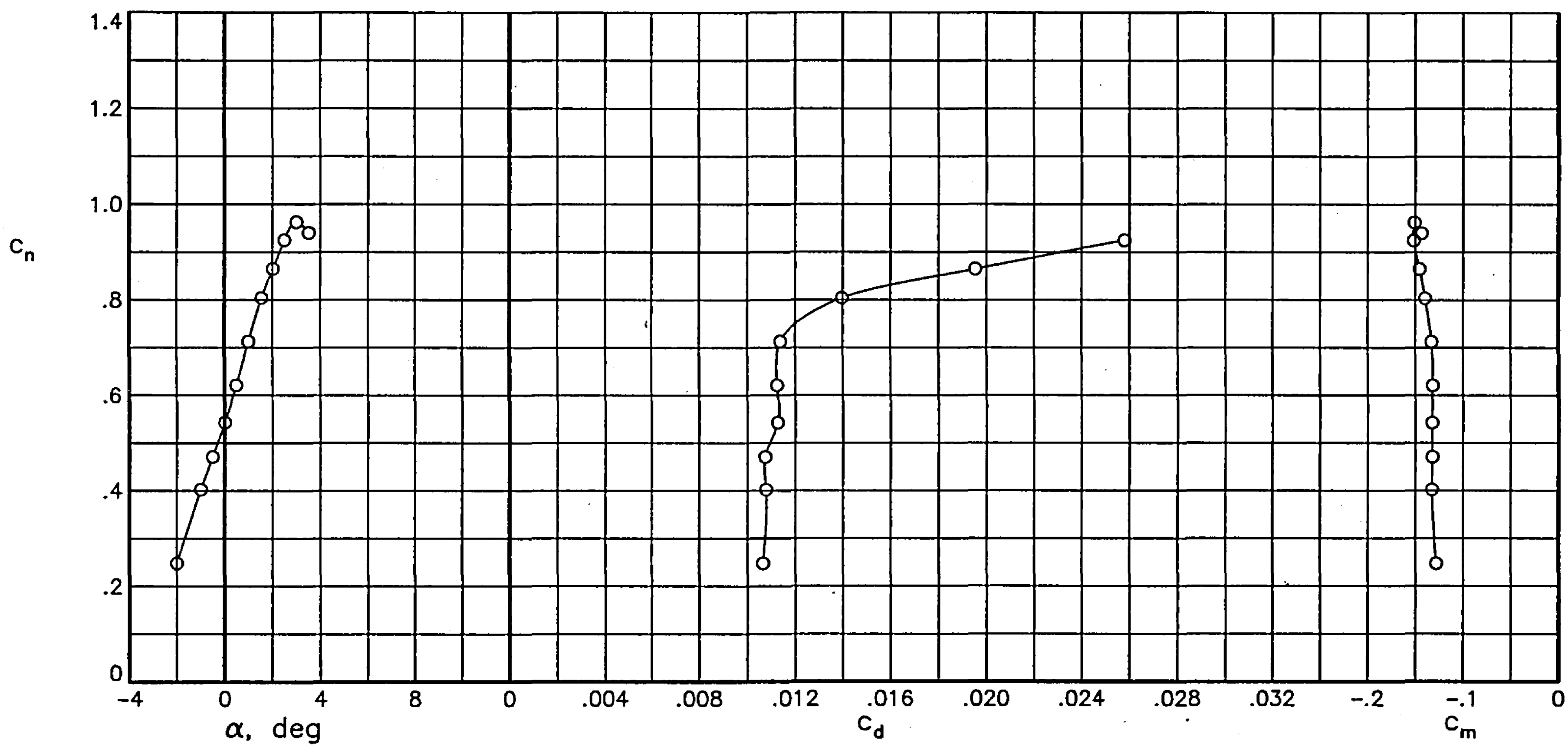

(e) $R = 6.01 \times 10^6$; $M = 0.7382$.

Figure 4.— Continued.

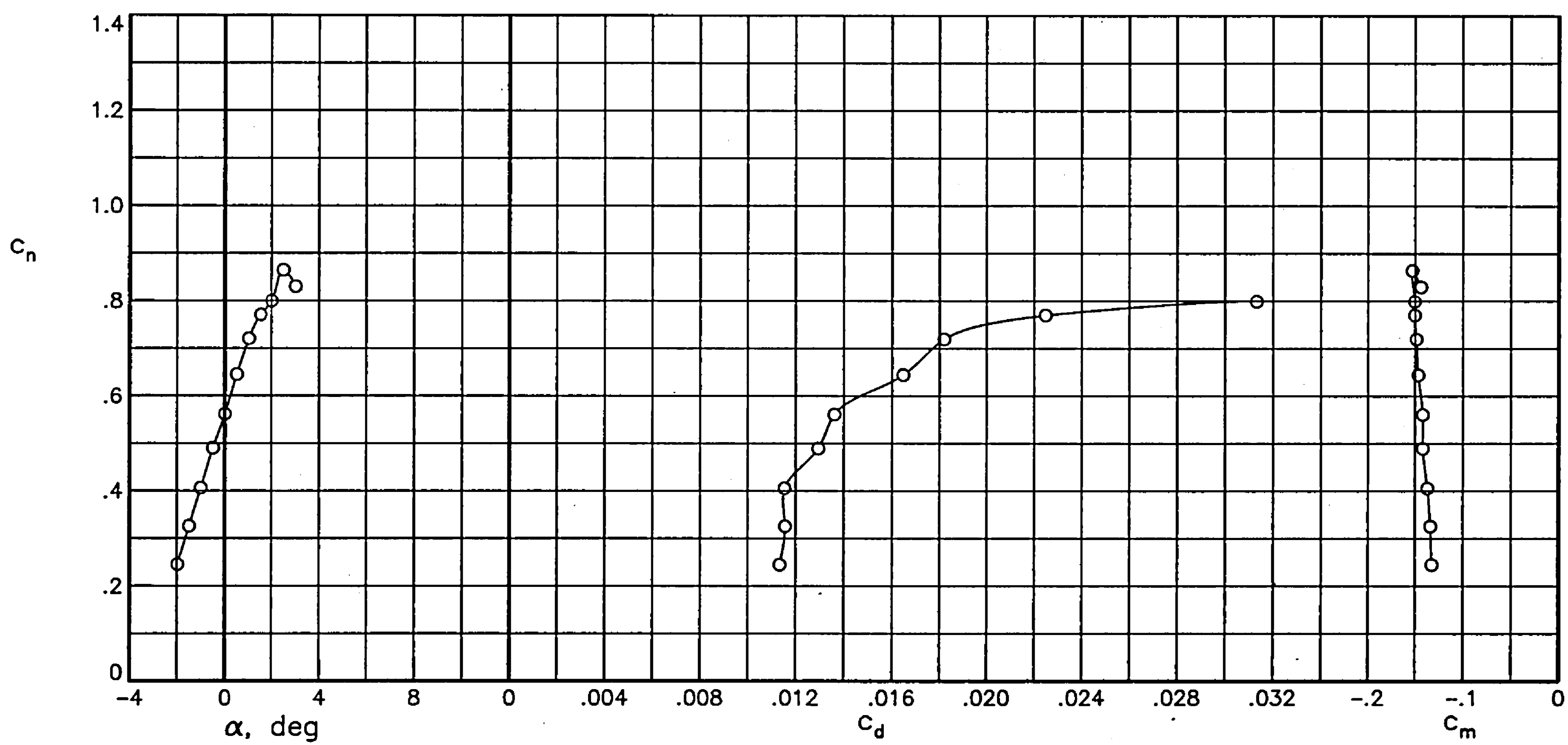

(f) R = 6.11 x 10 ^{6}; M = 0.7578.

Figure 4.– Continued.

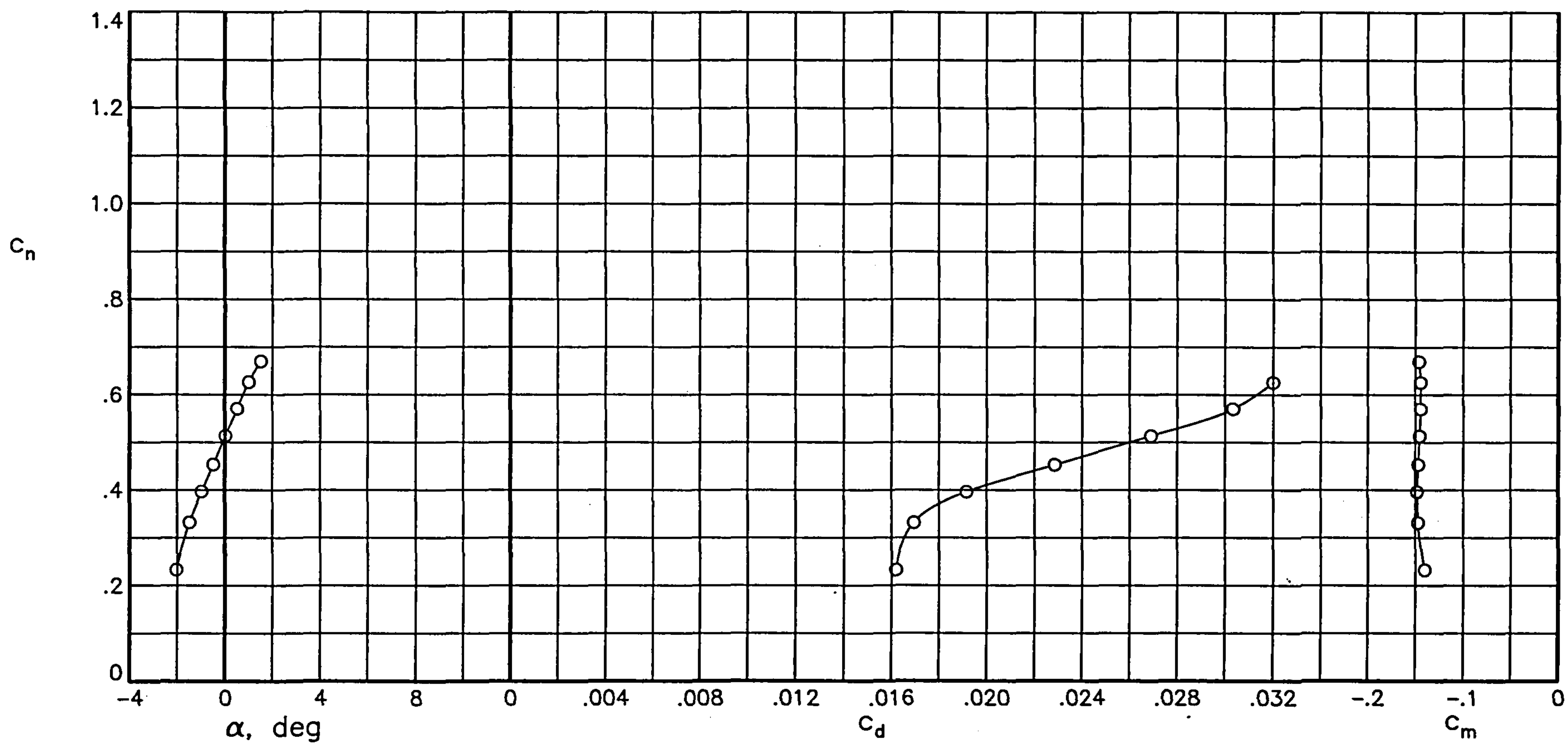

(g) $R = 6.07 \times 10^{6}$; $M = 0.7773$

Figure 4.— Concluded.

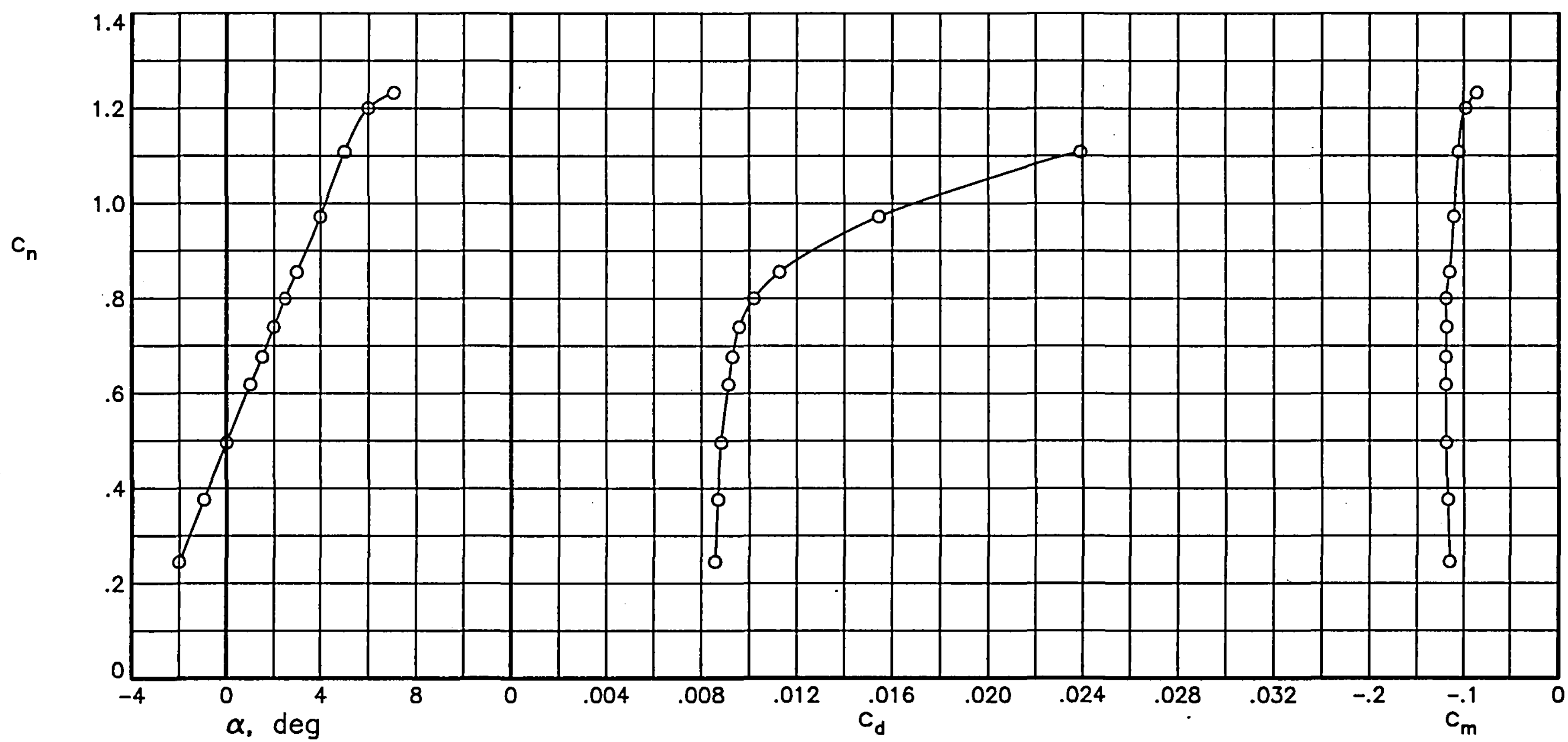

(a) $R = 10.07 \times 10^6$; $M = 0.6000$

Figure 5.– Section characteristics at Reynolds numbers of 10×10^6.

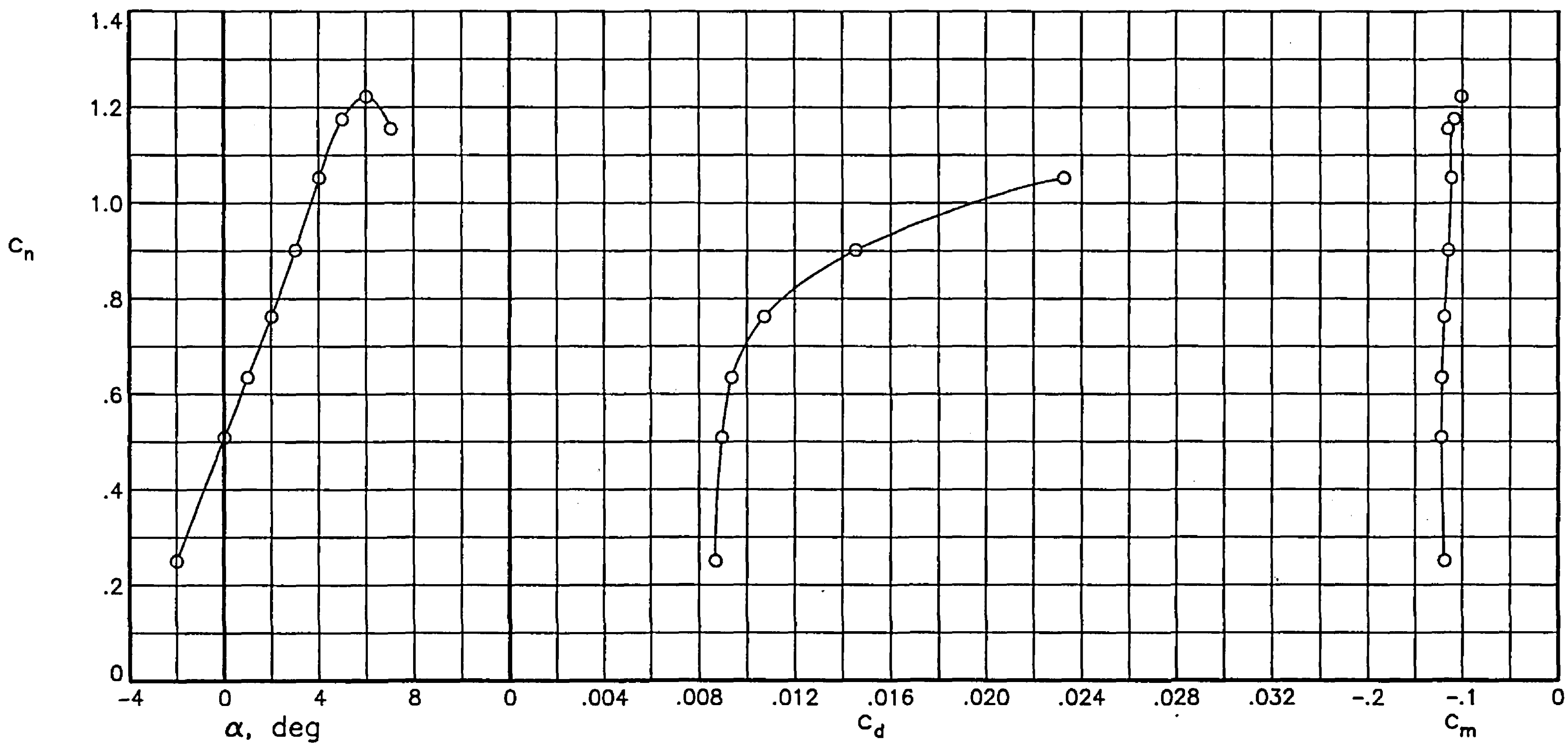

(b) $R = 10.12 \times 10^6$; $M = 0.6513$.

Figure 5.– Continued.

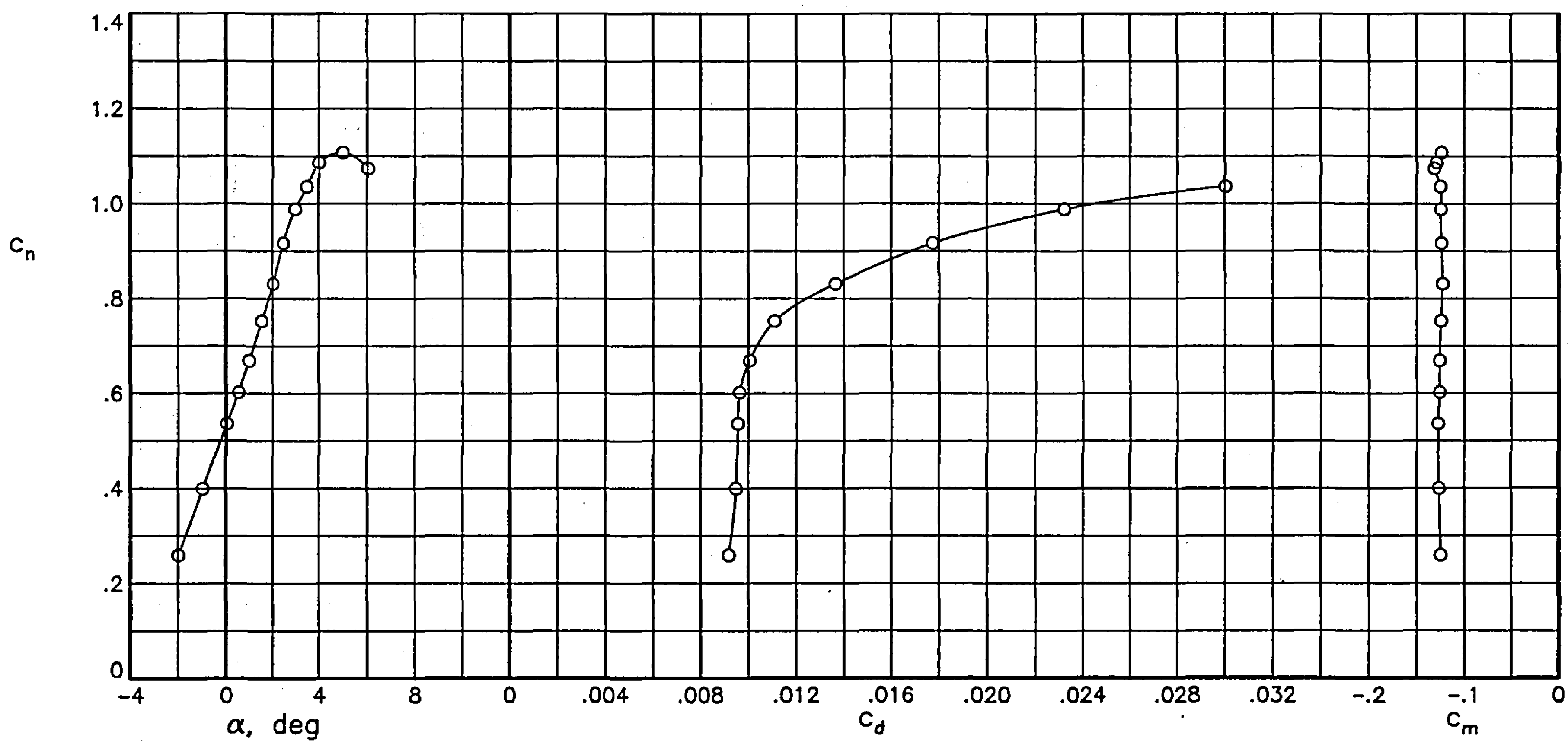

(c) $R = 10.07 \times 10^6$; $M = 0.7004$.

Figure 5.– Continued.

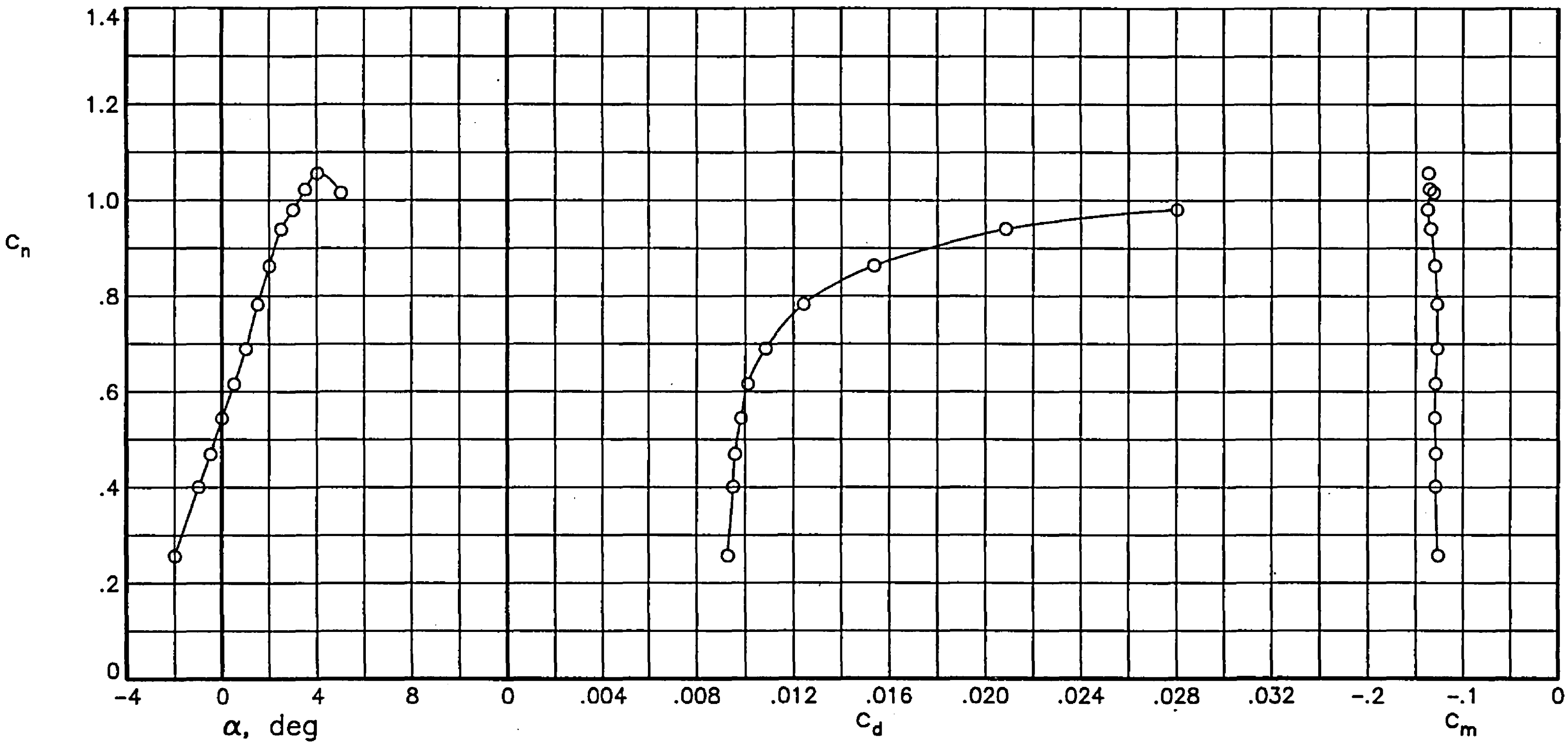

(d) $R = 10.08 \times 10^6$; $M = 0.7209$.

Figure 5.– Continued.

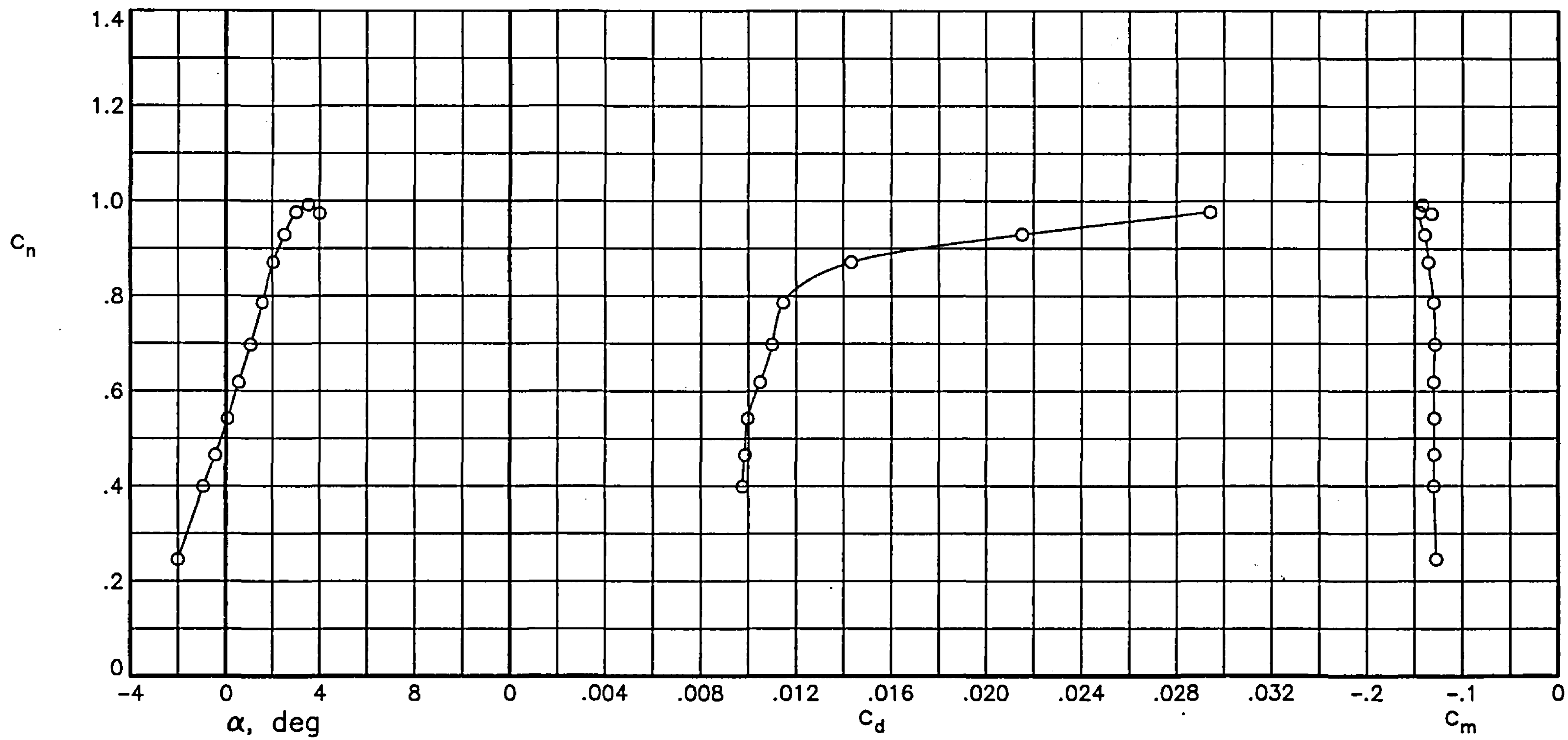

(e) R = 10.04 x 10^6; M = 0.7318.

Figure 5.– Continued.

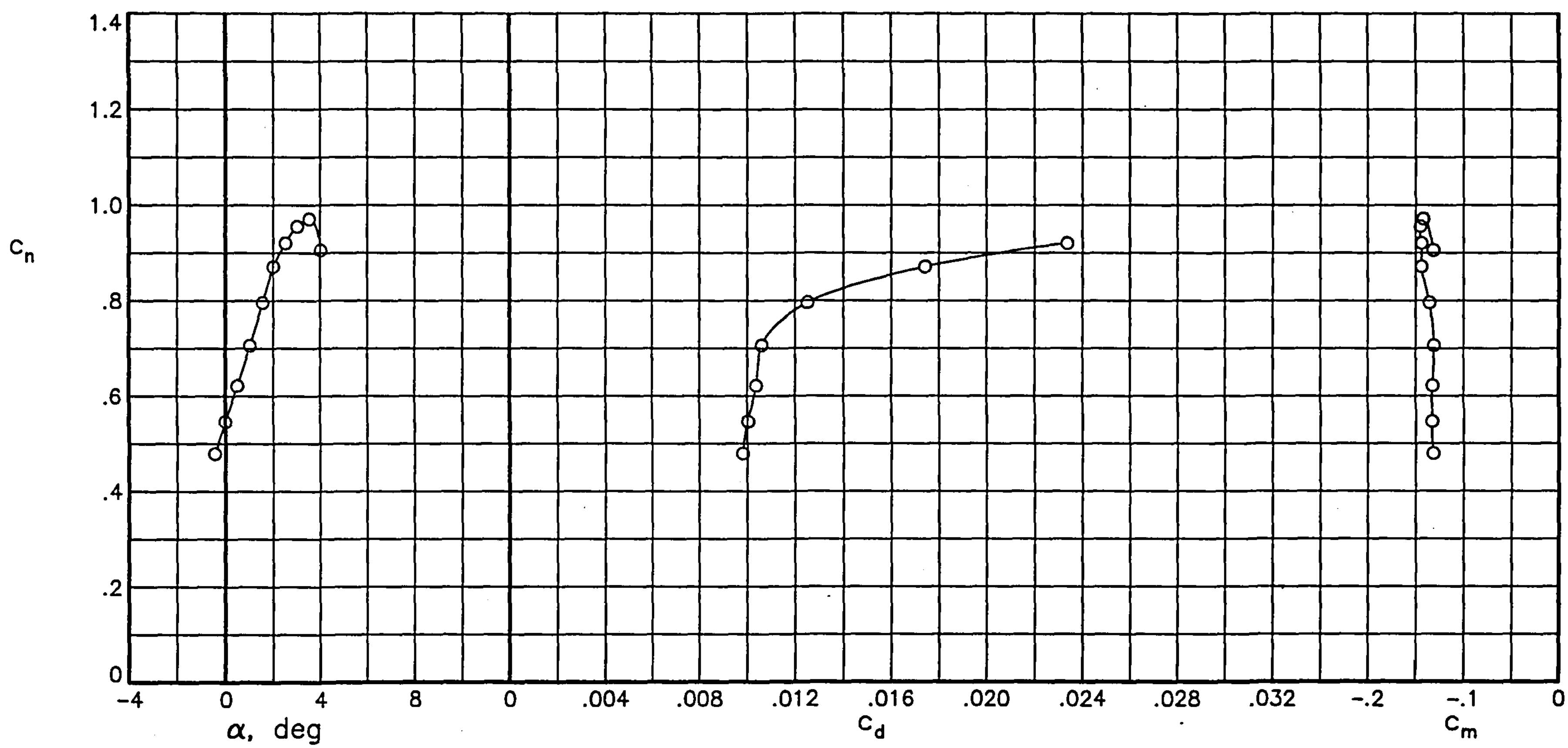

(f) $R = 10.05 \times 10^6$; $M = 0.7401$.

Figure 5.– Continued.

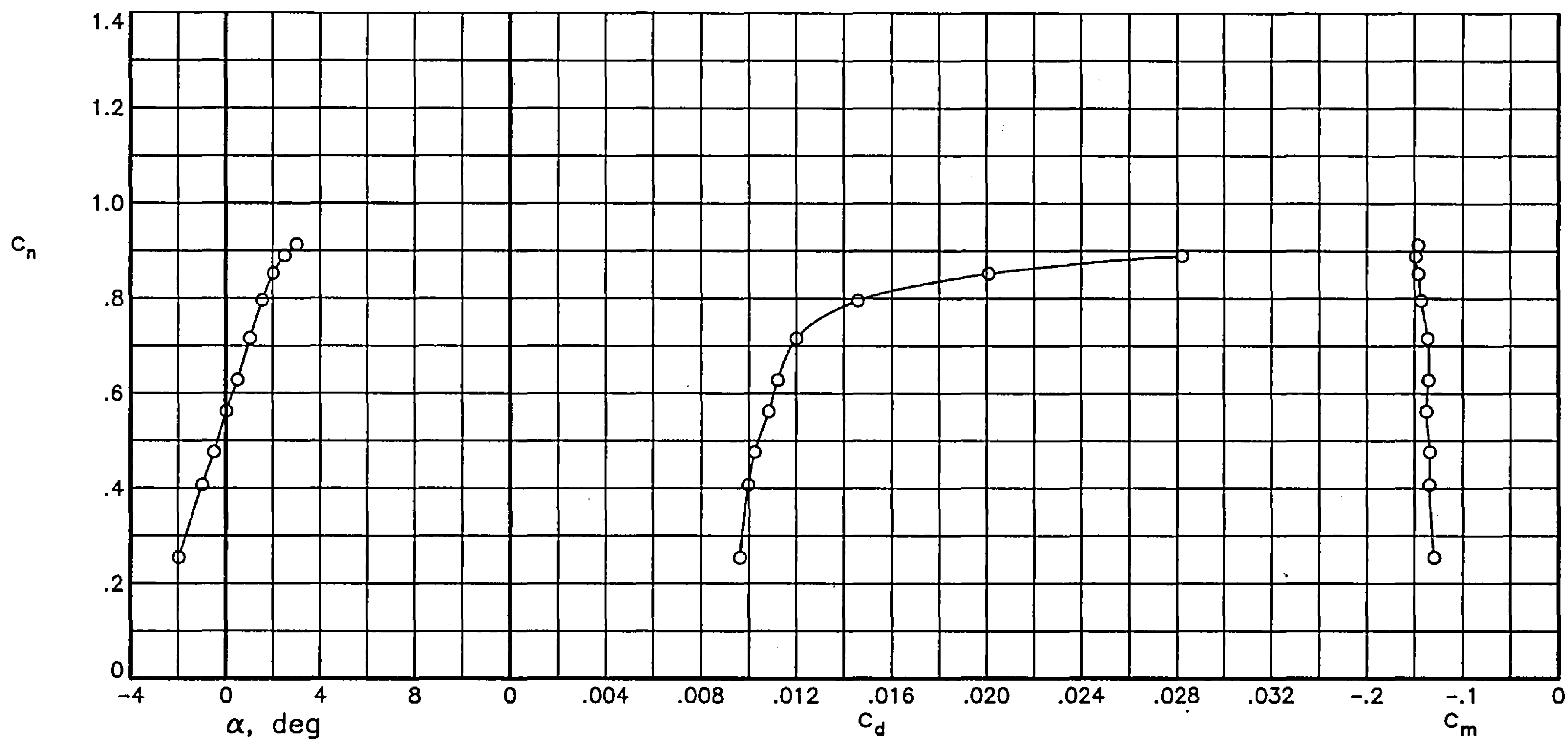

(g) $R = 10.07 \times 10^6$; $M = 0.7498$

Figure 5.– Continued.

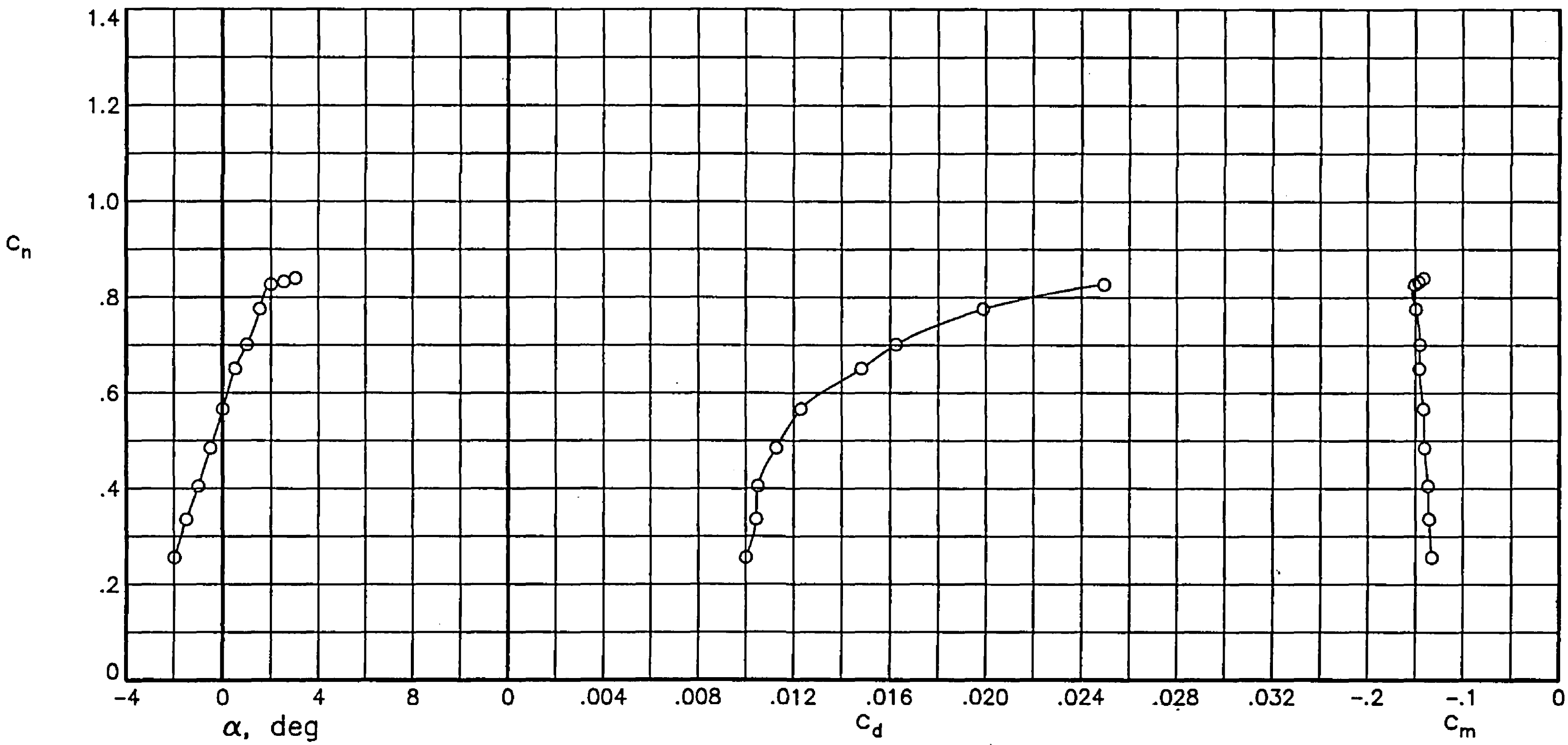

(h) $R = 10.03 \times 10^6$; $M = 0.7602$.

Figure 5.– Continued.

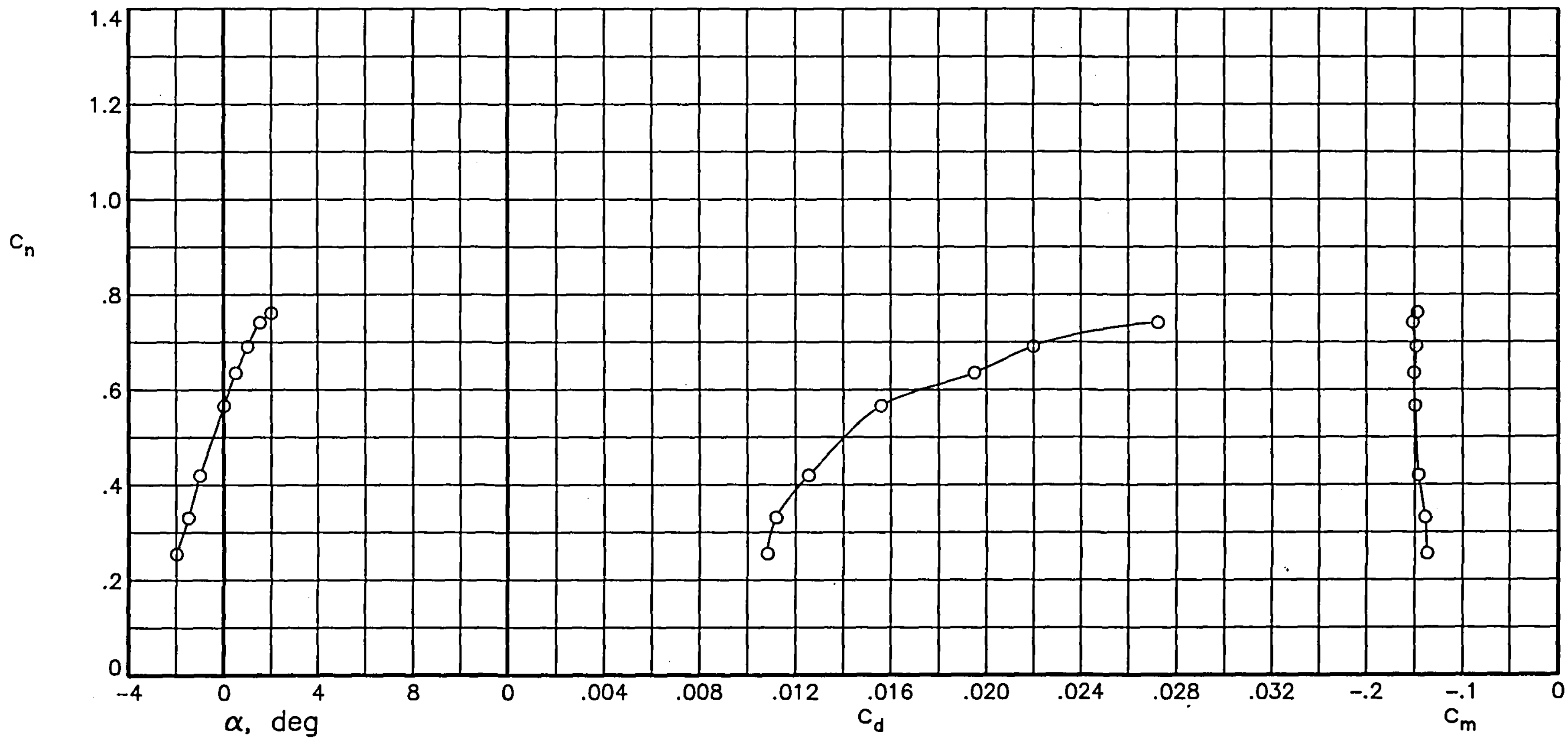

(i) $R = 9.99 \times 10^{6}$; $M = 0.7694$.

Figure 5.– Continued.

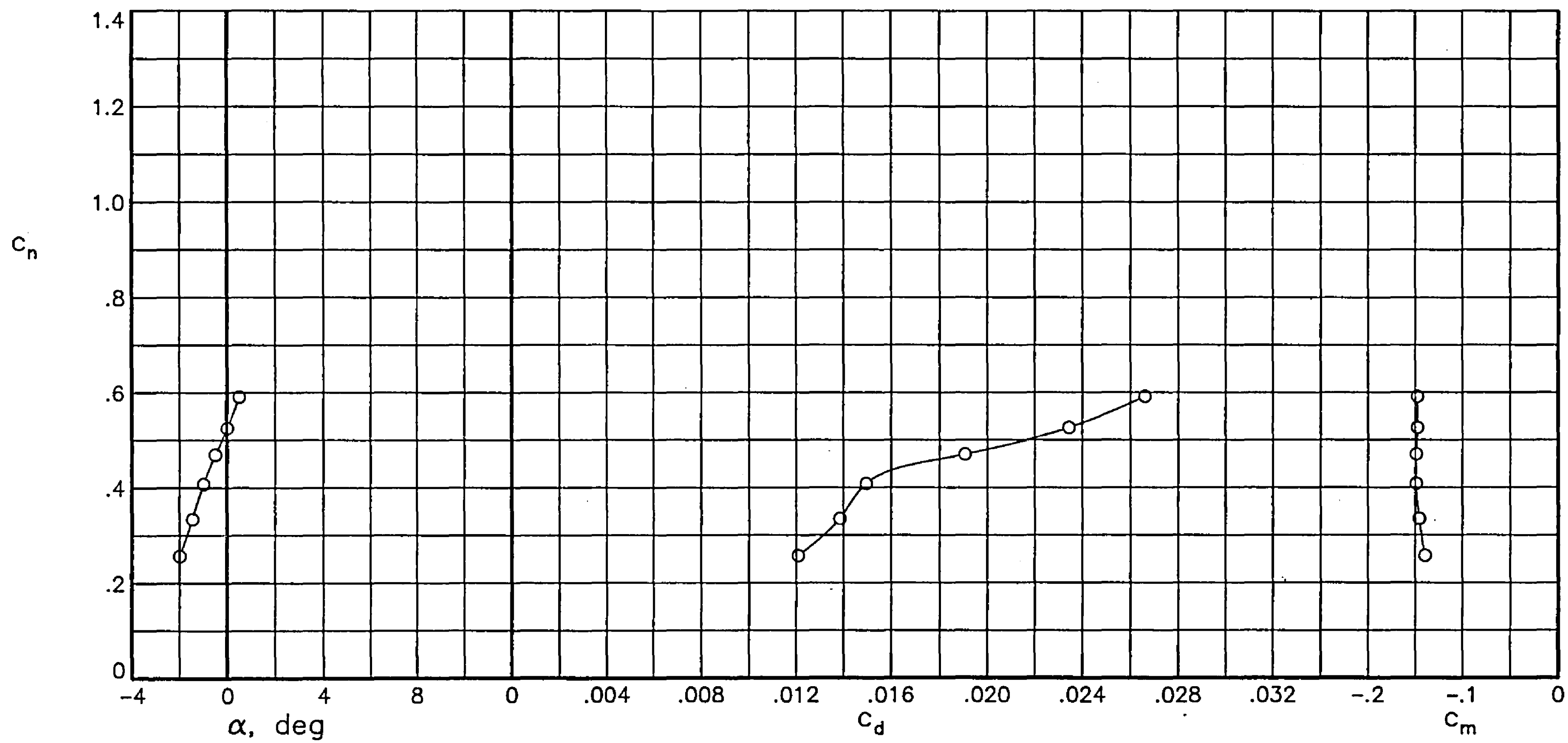

(j) $R = 9.96 \times 10^6$; $M = 0.7791$.

Figure 5.– Concluded.

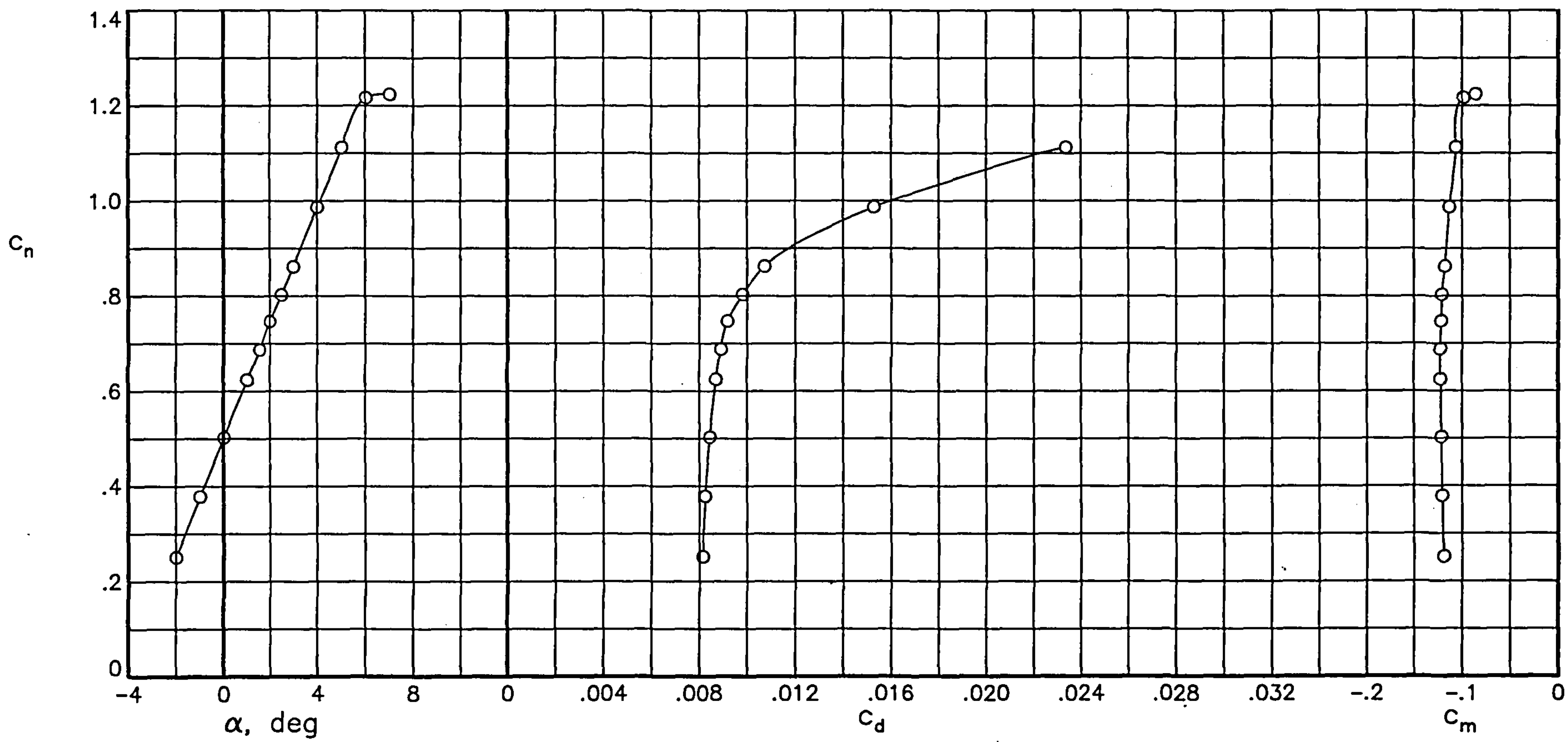

(a) $R = 14.95 \times 10^6$; $M = 0.5996$.

Figure 6.– Section characteristics at Reynolds numbers of 15×10^6.

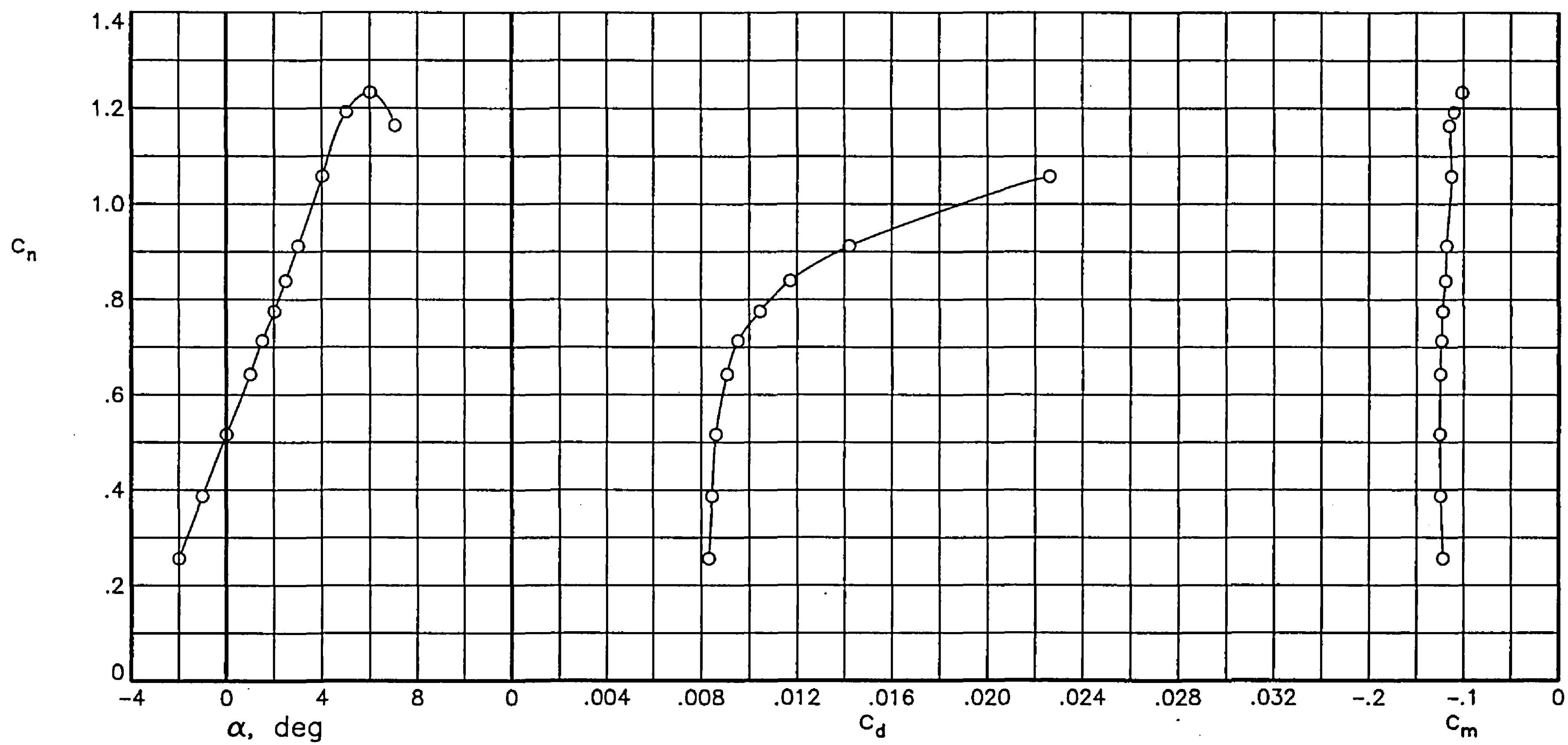

(b) $R = 15.02 \times 10^6$; $M = 0.6501$.

Figure 6.— Continued.

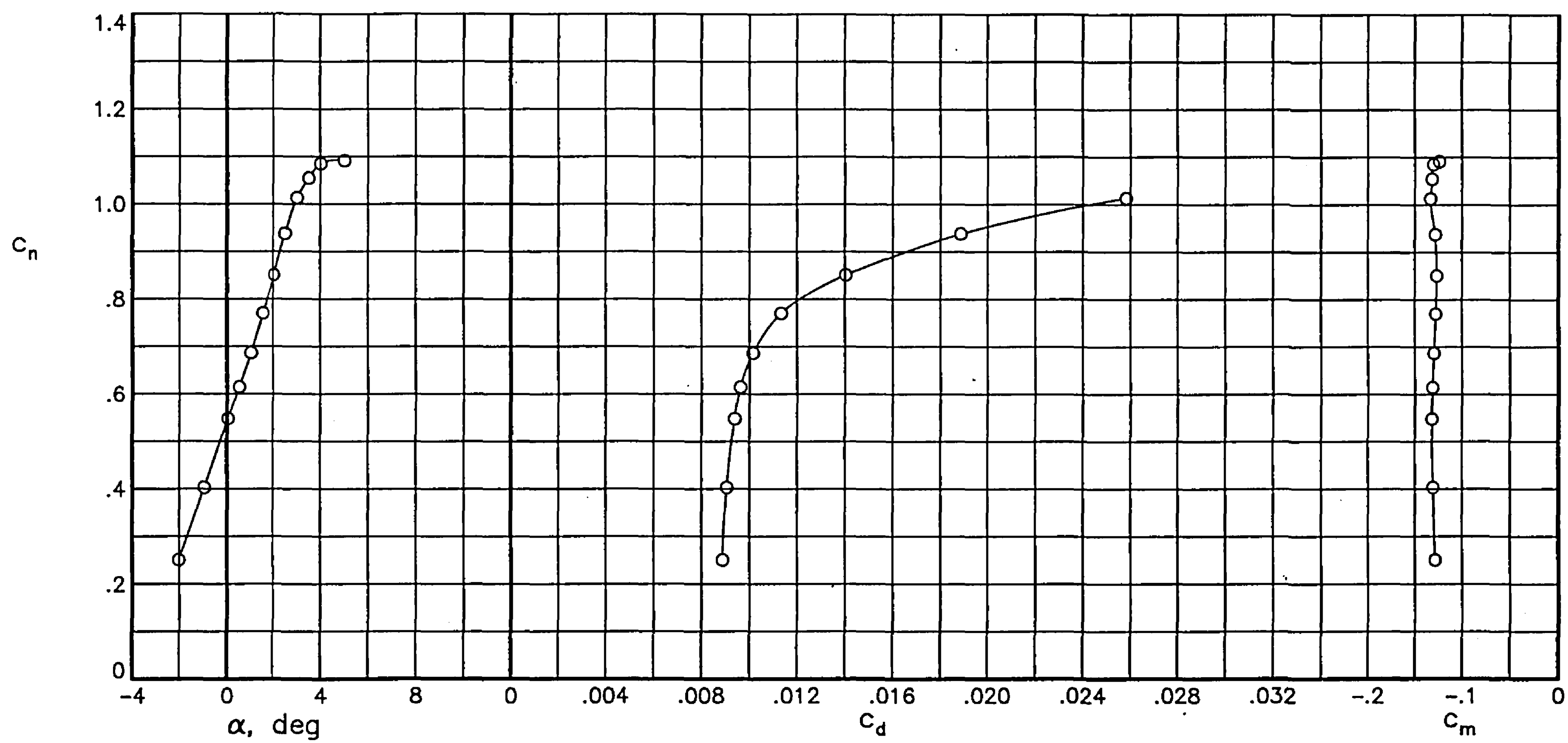

(c) $R = 15.12 \times 10^6$; $M = 0.7002$.

Figure 6.– Continued.

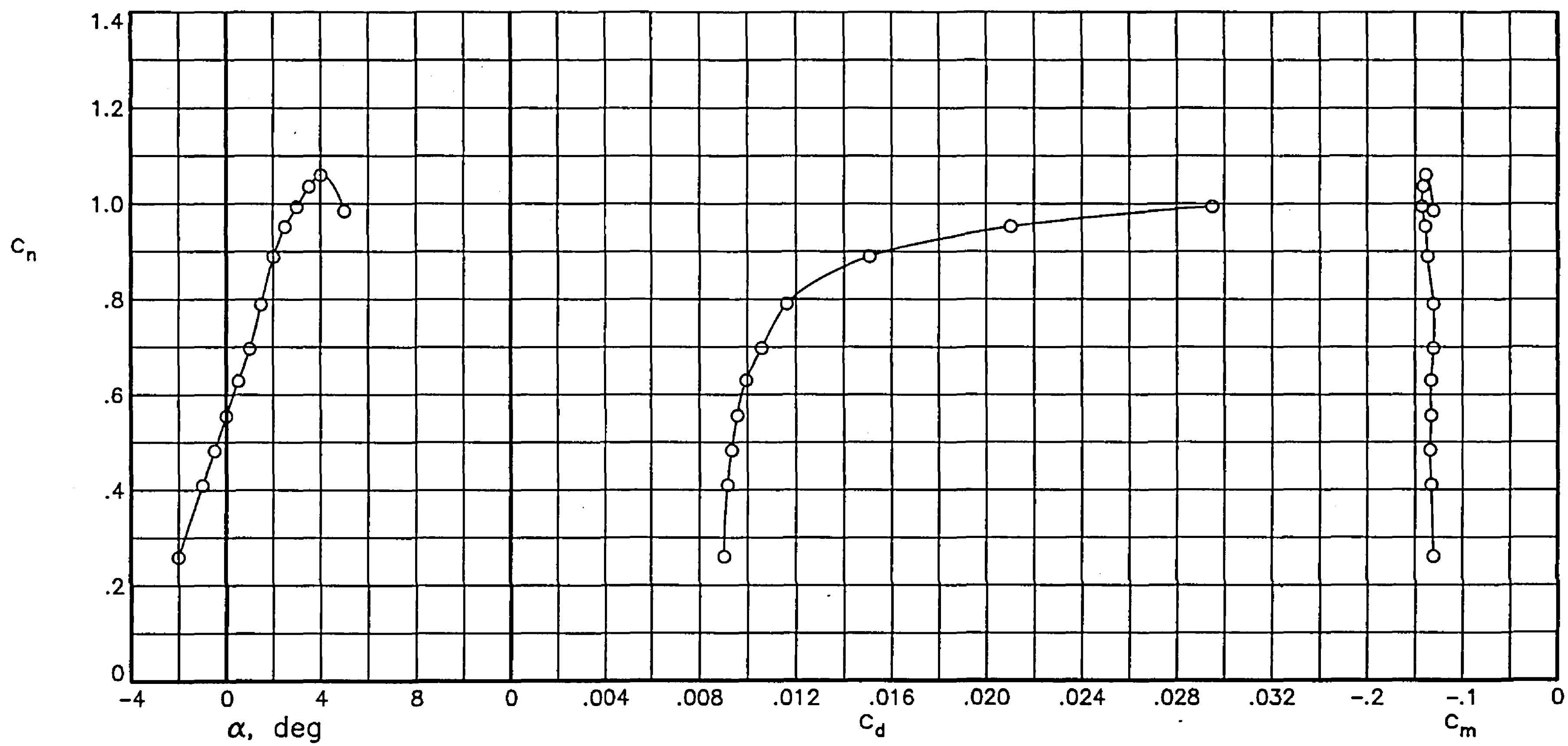

(d) $R = 15.05 \times 10^6$; $M = 0.7200$.

Figure 6.– Continued.

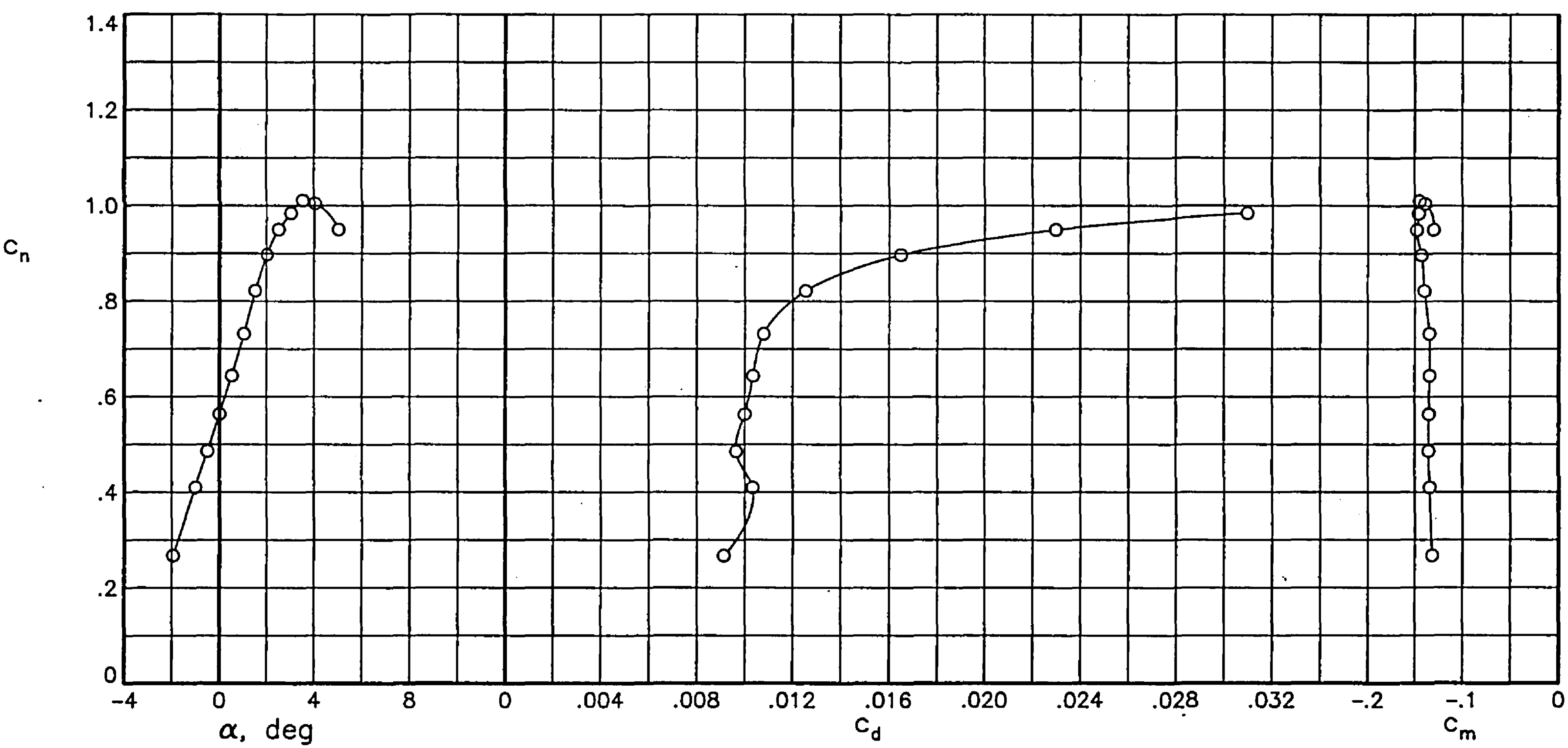

(e) $R = 14.99 \times 10^6$; $M = 0.7276$

Figure 6.– Continued.

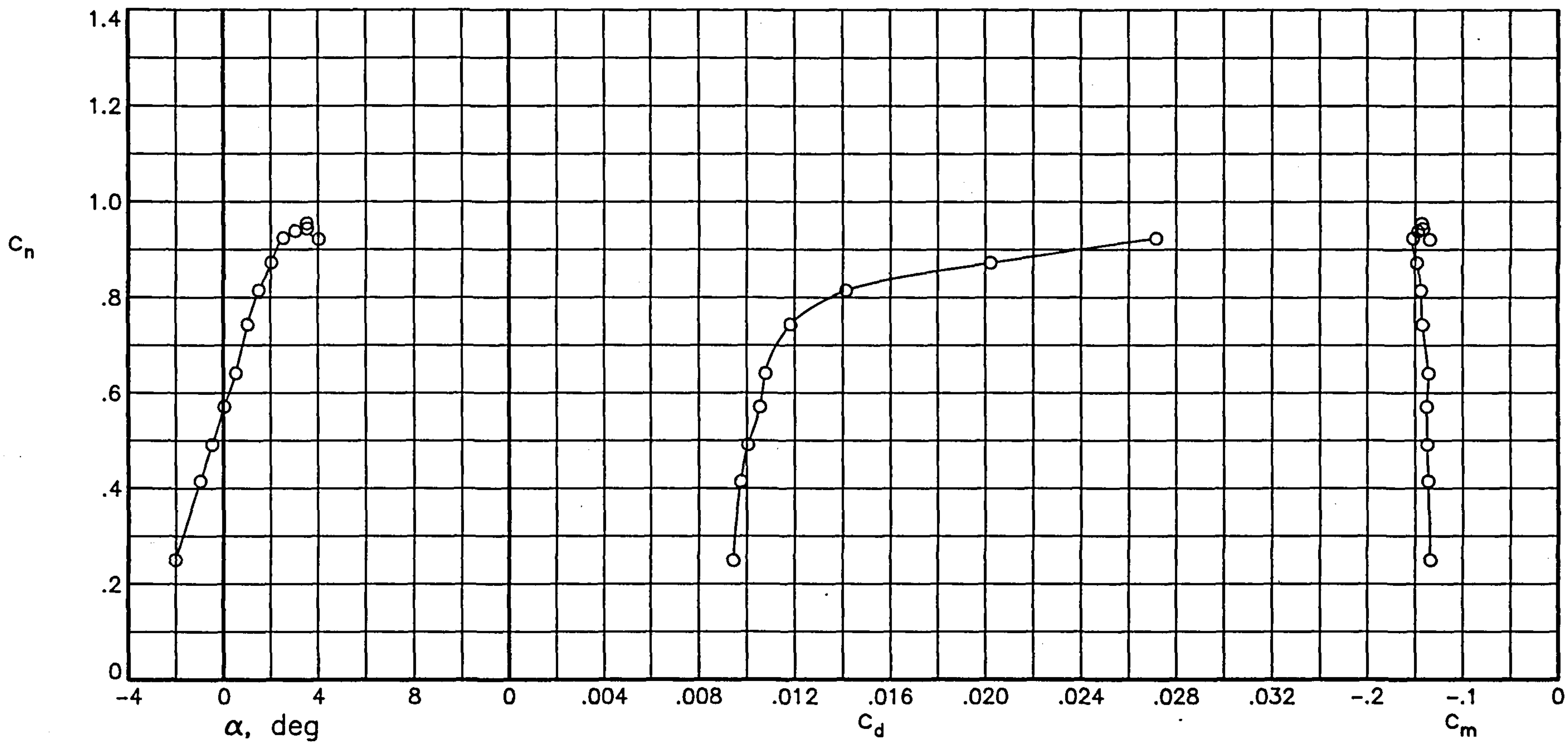

(f) $R = 15.10 \times 10^6$; $M = 0.7388$.

Figure 6.– Continued.

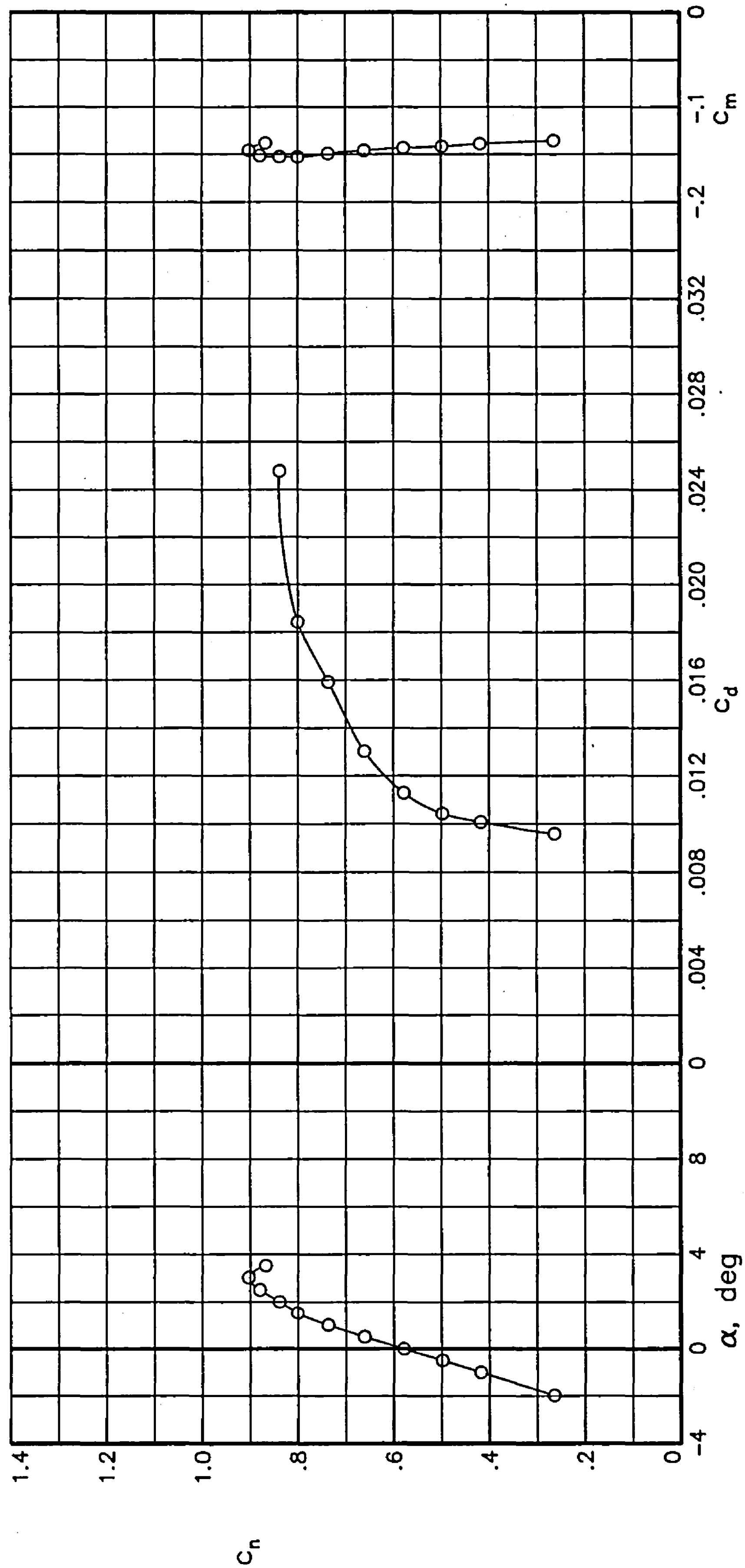

(g) R = 15.04 × 10^6; M = 0.7490.

Figure 6.– Continued.

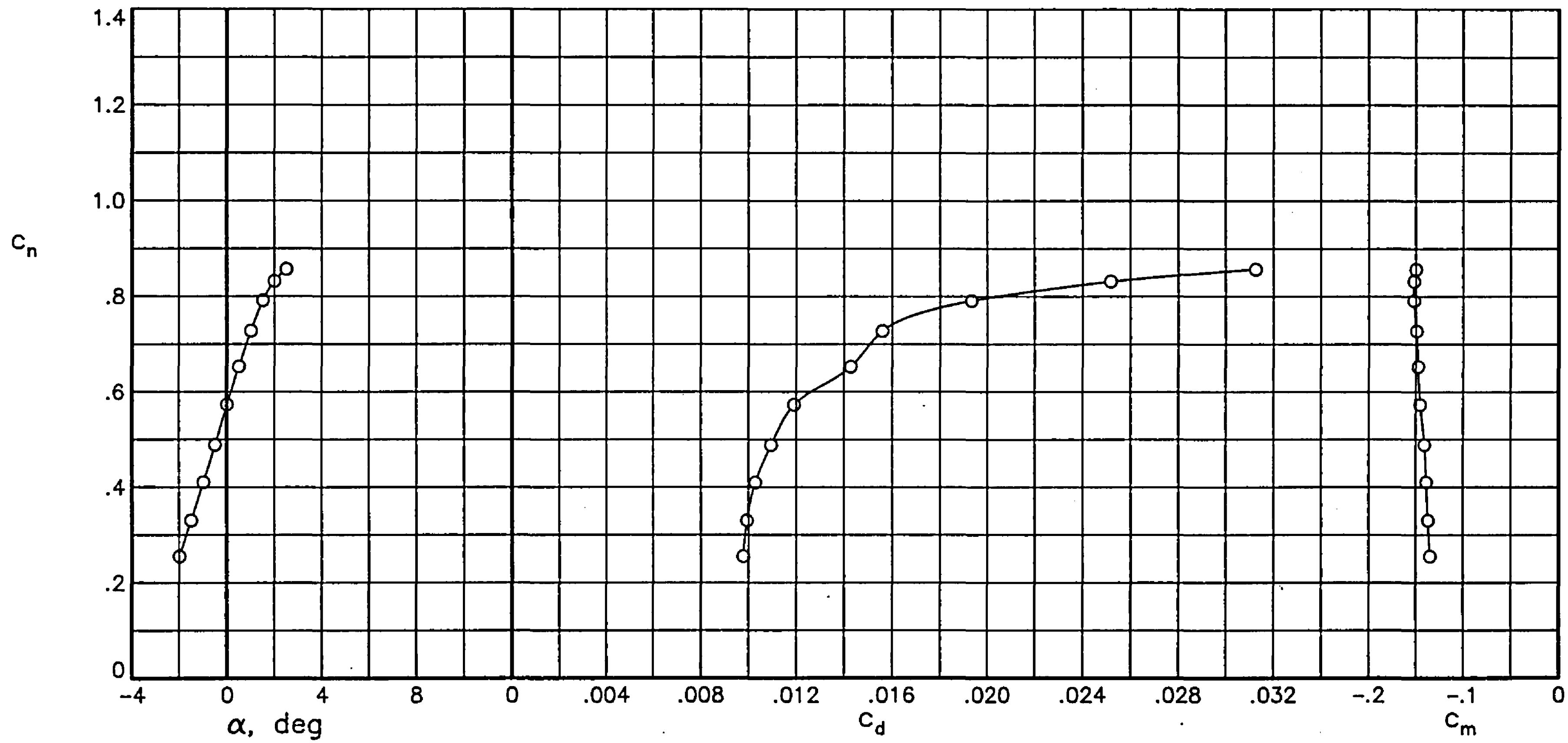

(h) $R = 15.01 \times 10^6$; $M = 0.7575$.

Figure 6.– Continued.

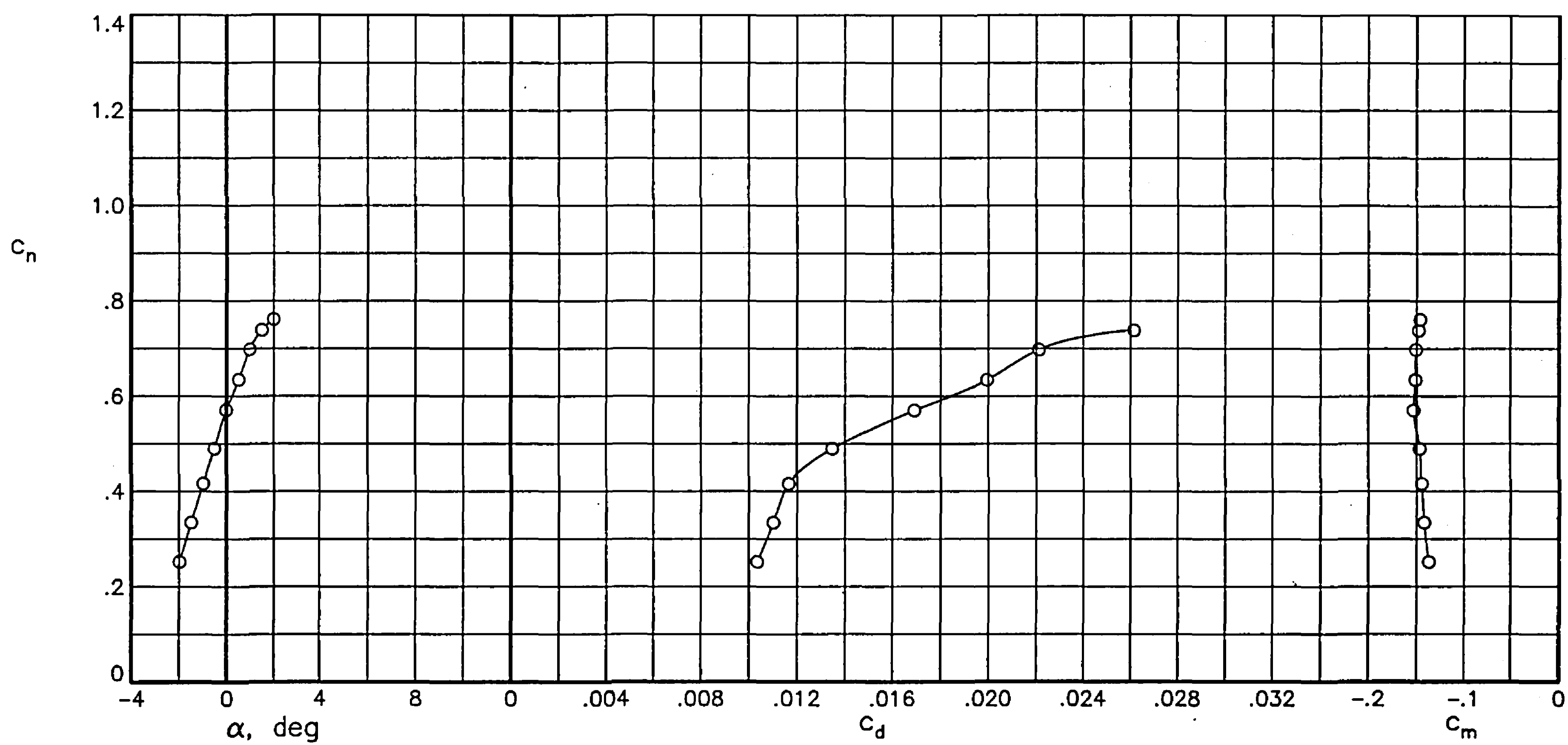

(i) $R = 14.89 \times 10^{6}$; $M = 0.7684$.

Figure 6.– Continued.

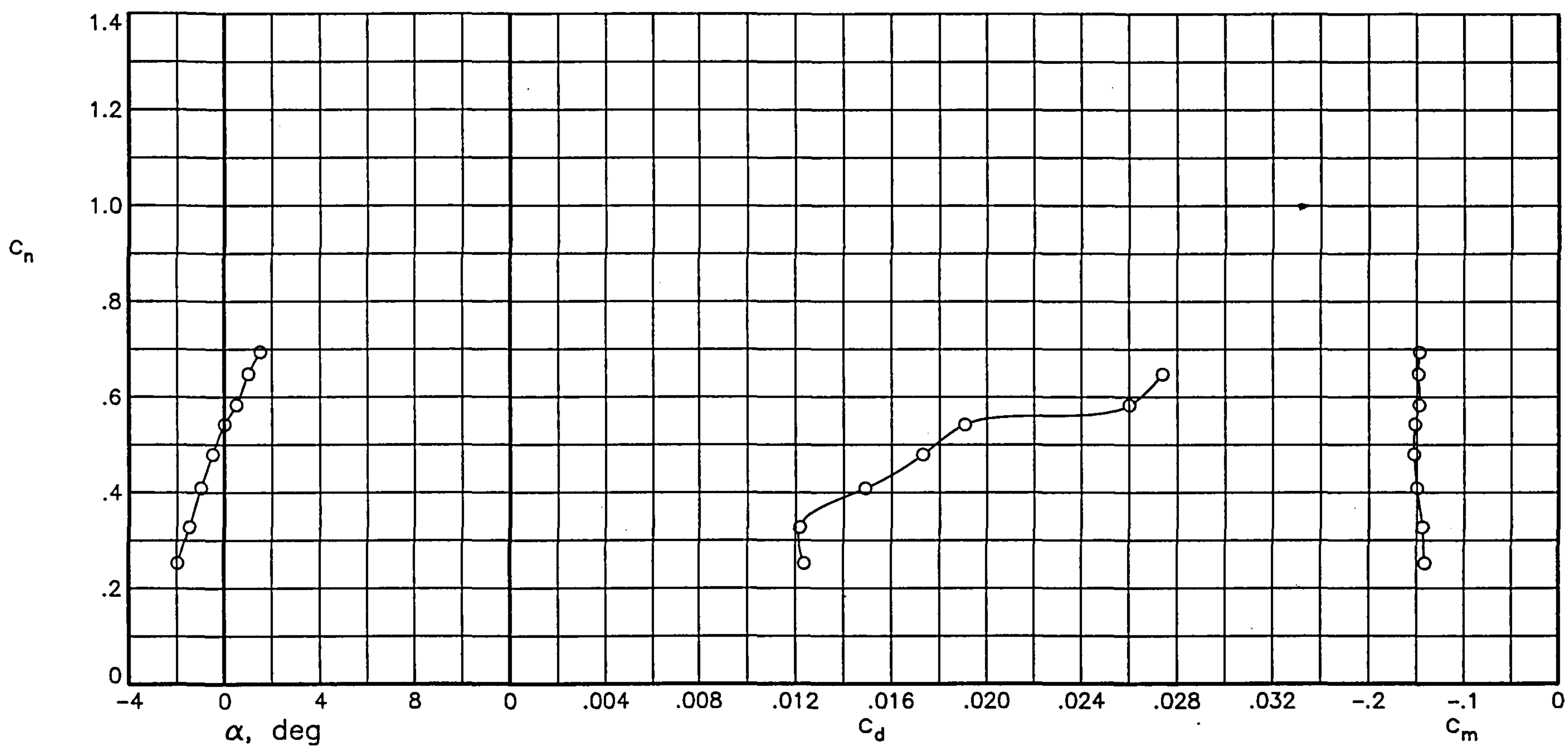

(j) $R = 14.91 \times 10^6$; $M = 0.7776$.

Figure 6.– Concluded.

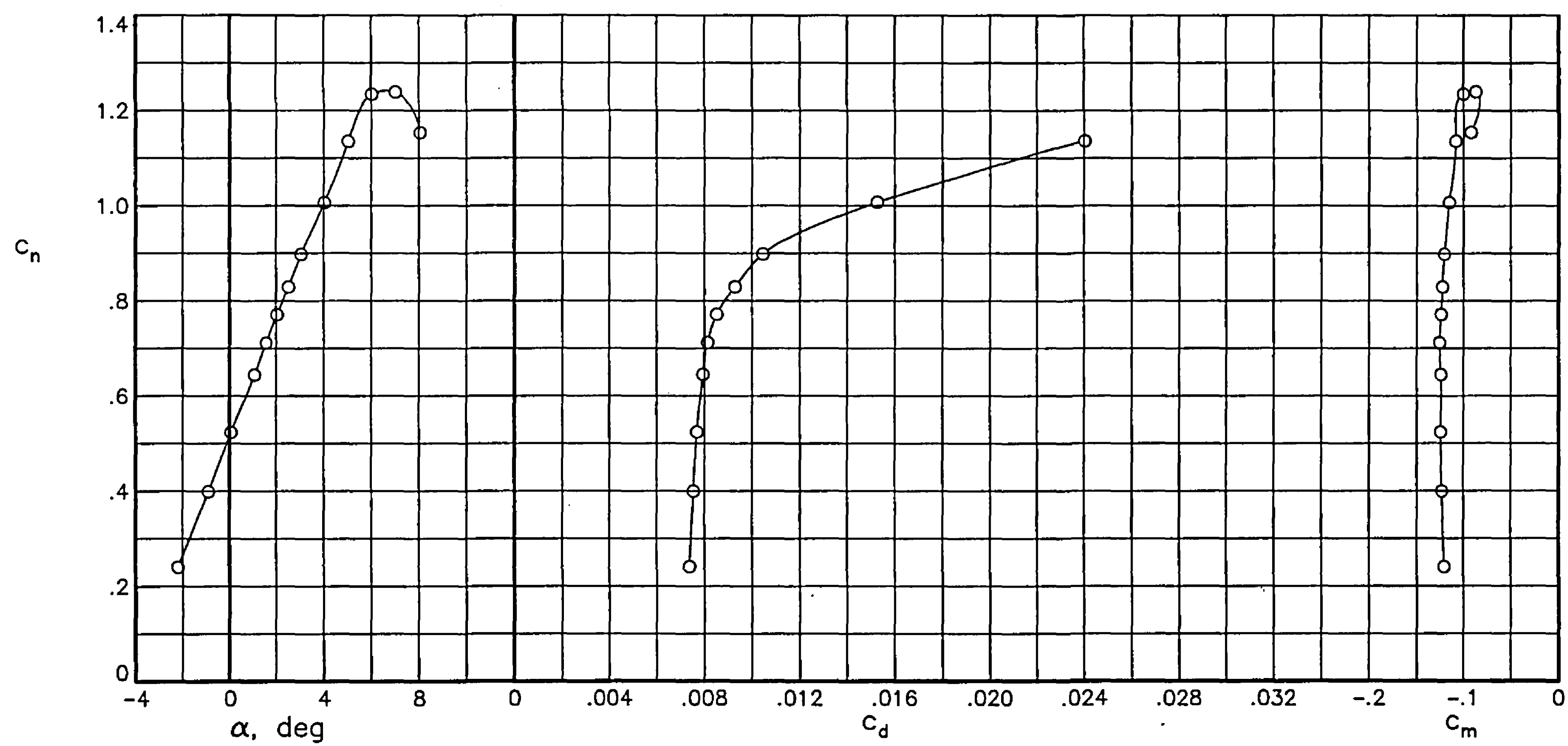

(a) $R = 30.17 \times 10^6$; $M = 0.6014$.

Figure 7.– Section characteristics at Reynolds numbers of 30×10^6.

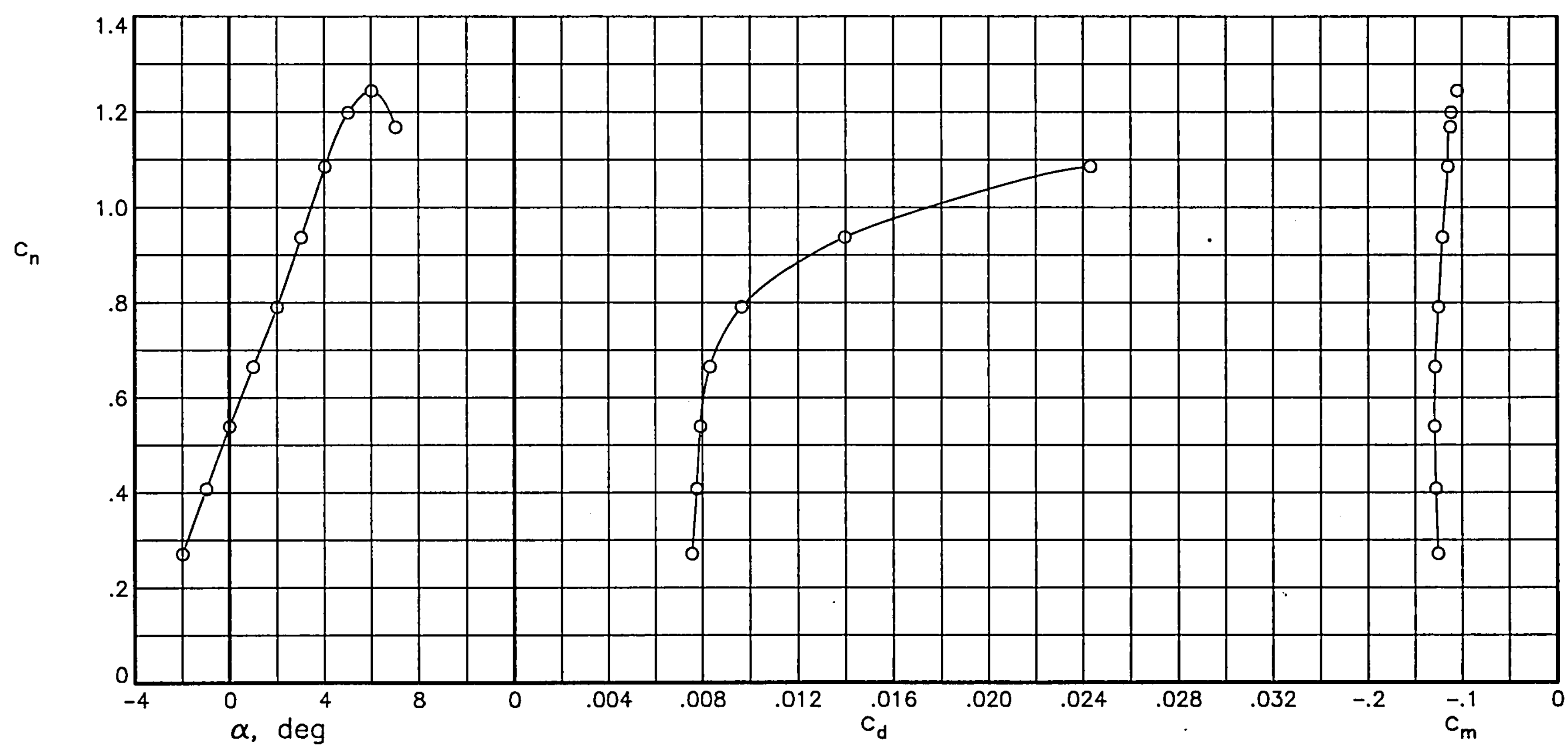

(b) R = 30.12 x 10^6; M = 0.6512.

Figure 7.– Continued.

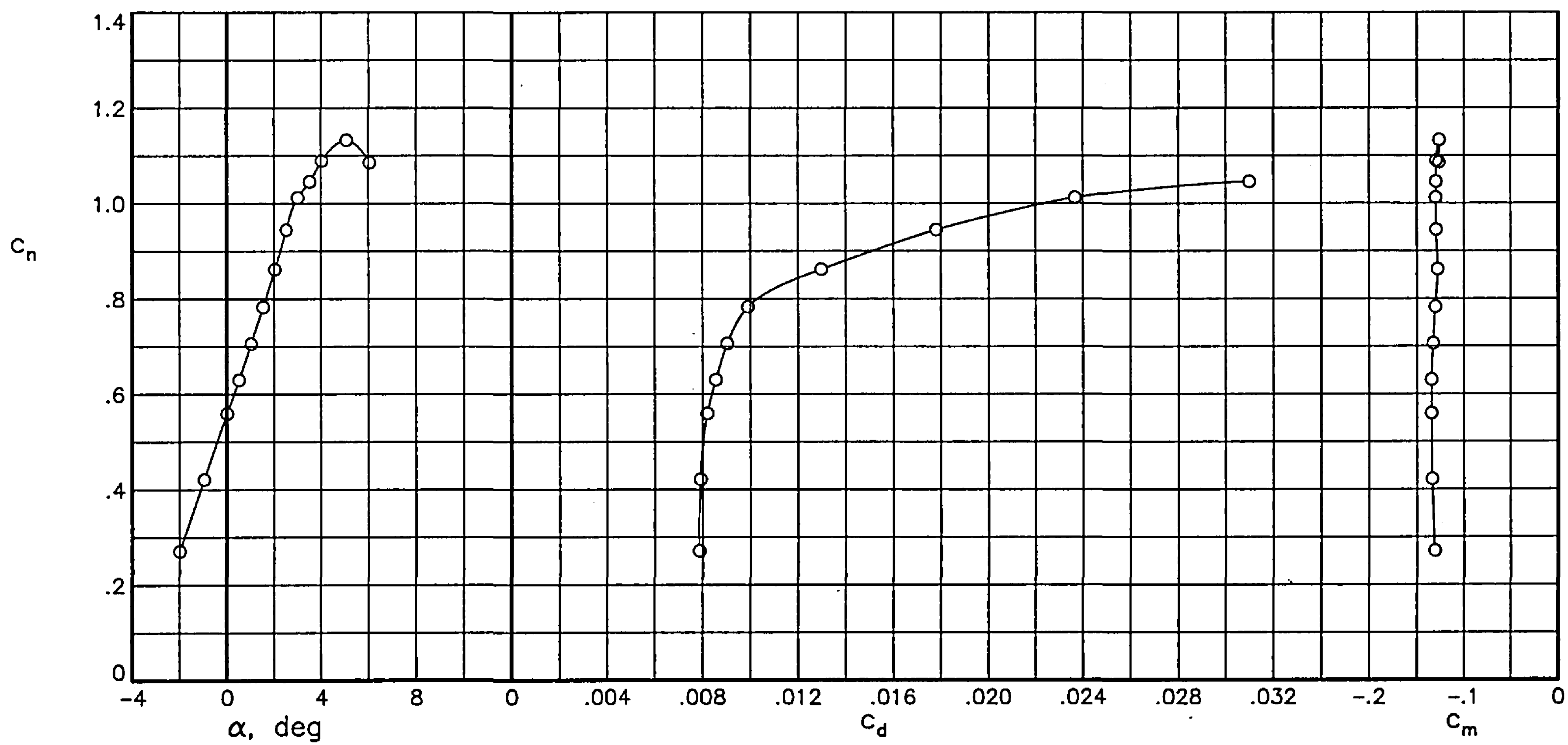

(c) $R = 30.16 \times 10^6$; $M = 0.7007$.

Figure 7.– Continued.

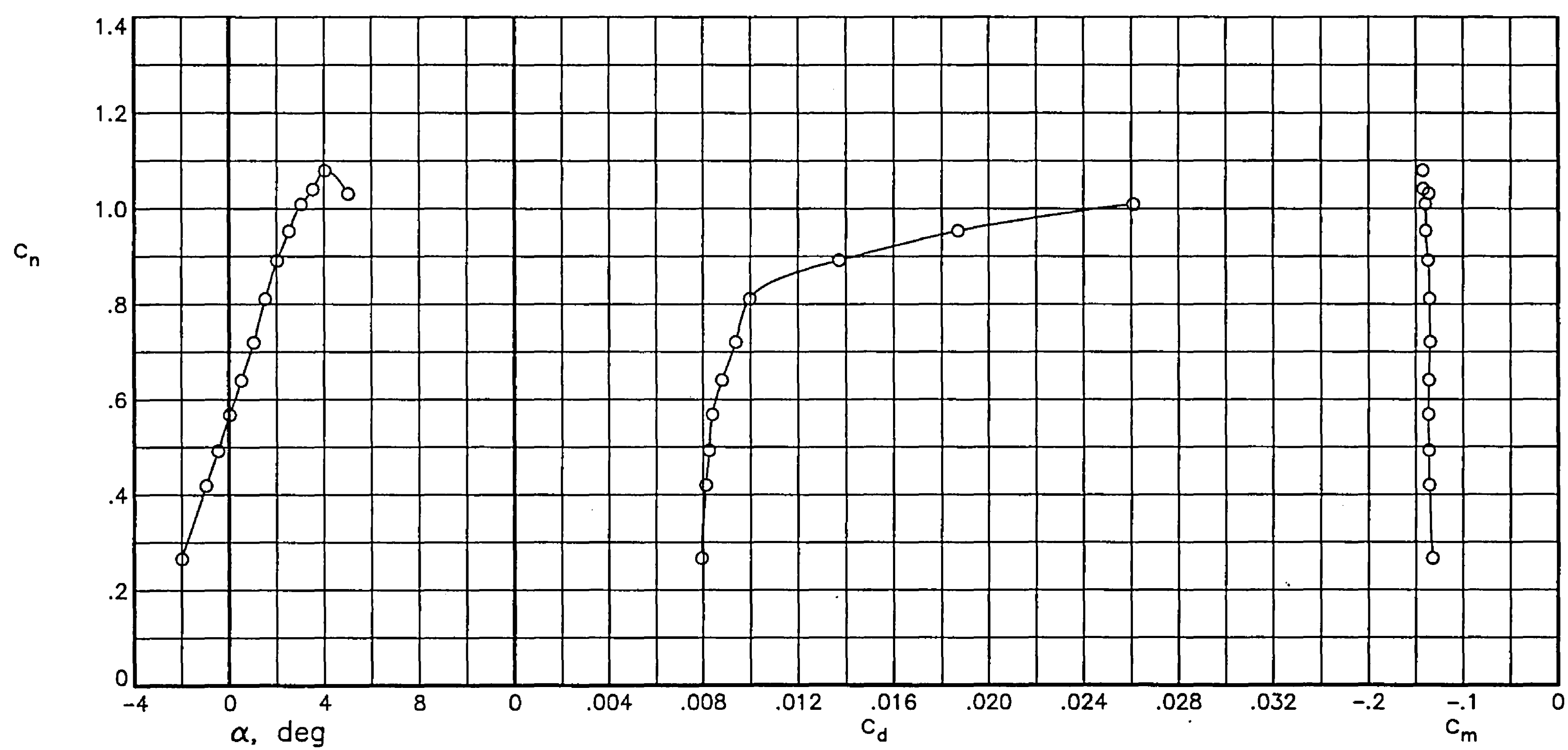

(d) $R = 30.20 \times 10^6$; $M = 0.7194$.

Figure 7.– Continued.

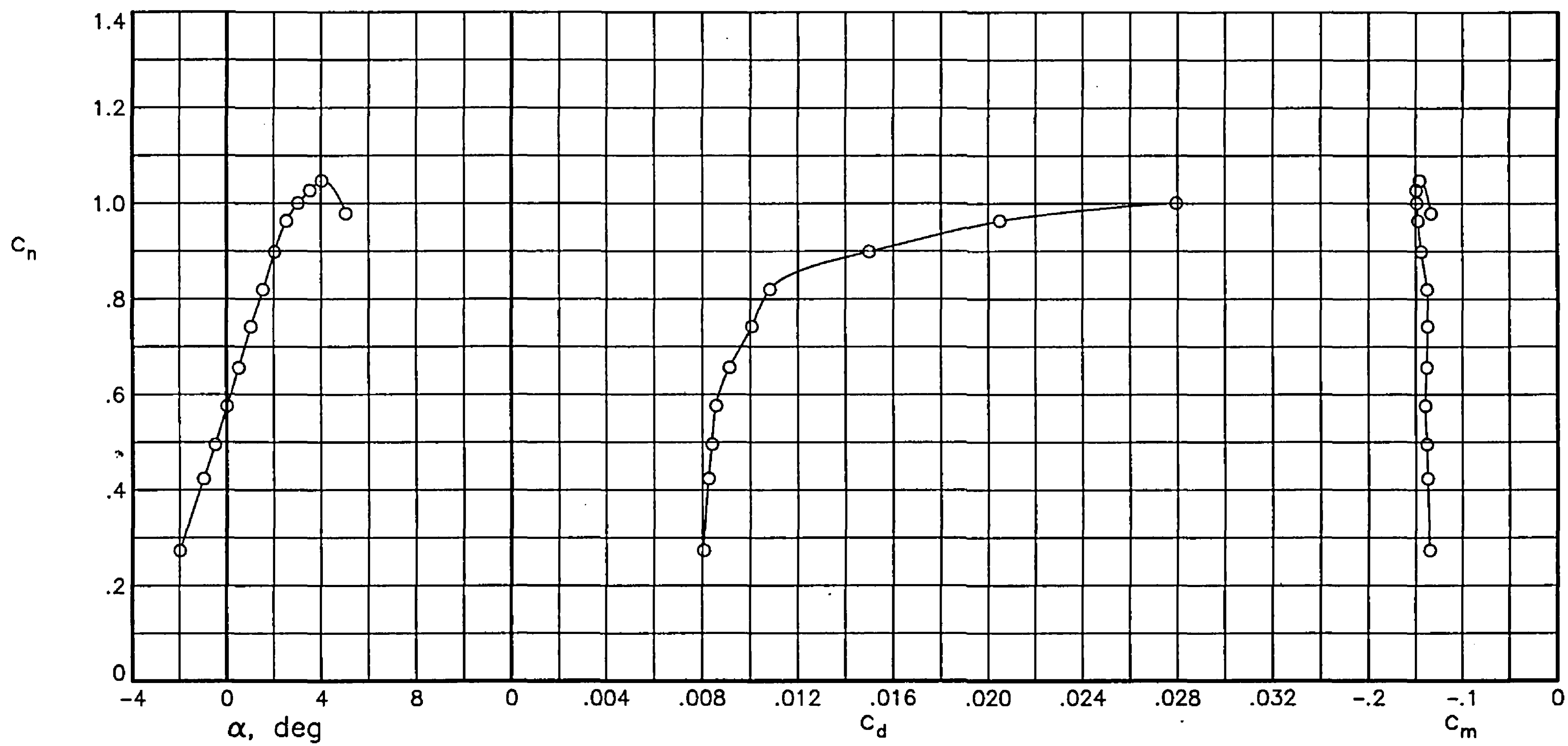

(e) $R = 30.02 \times 10^6$; $M = 0.7293$.

Figure 7.– Continued.

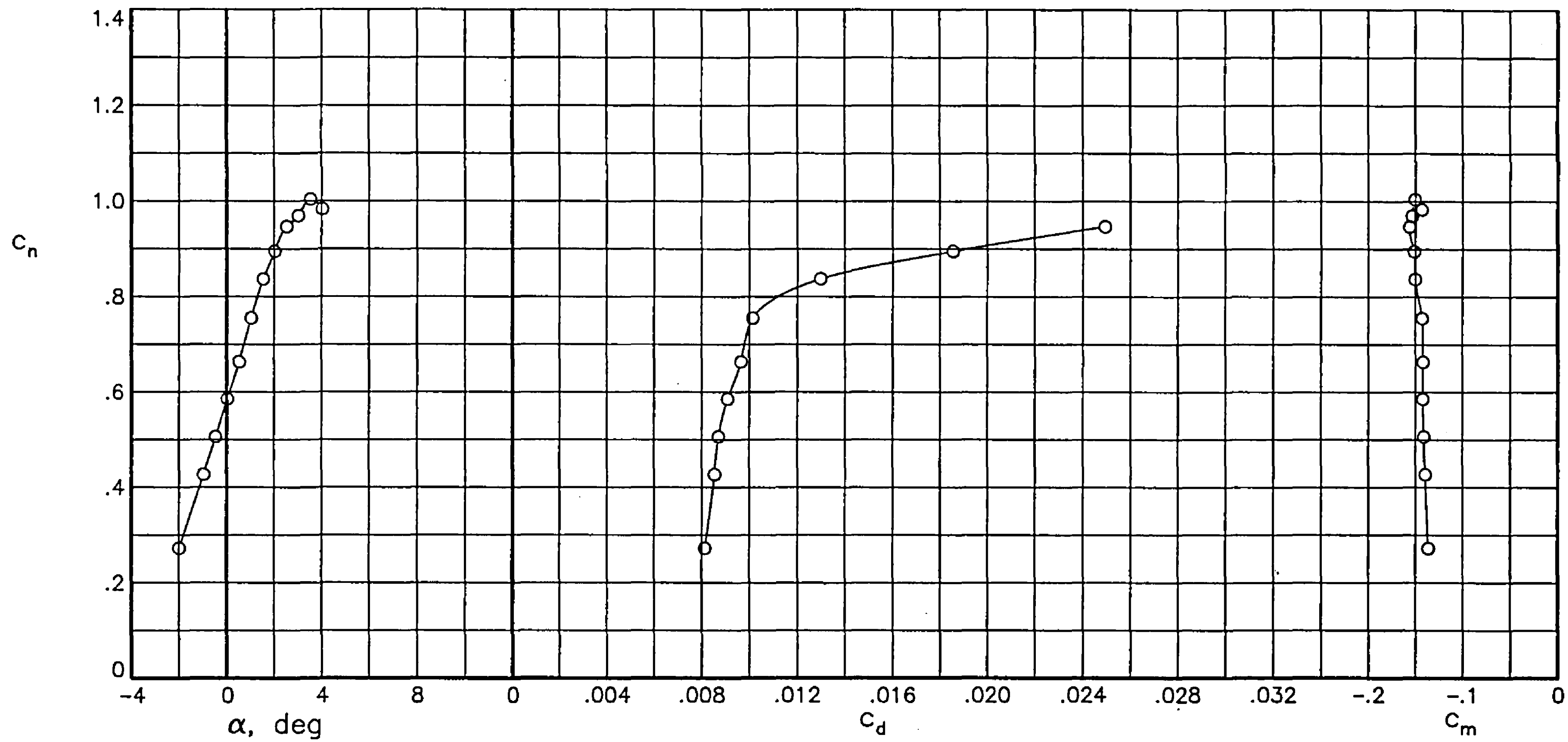

(f) $R = 30.04 \times 10^6$; $M = 0.7389$.

Figure 7.– Continued.

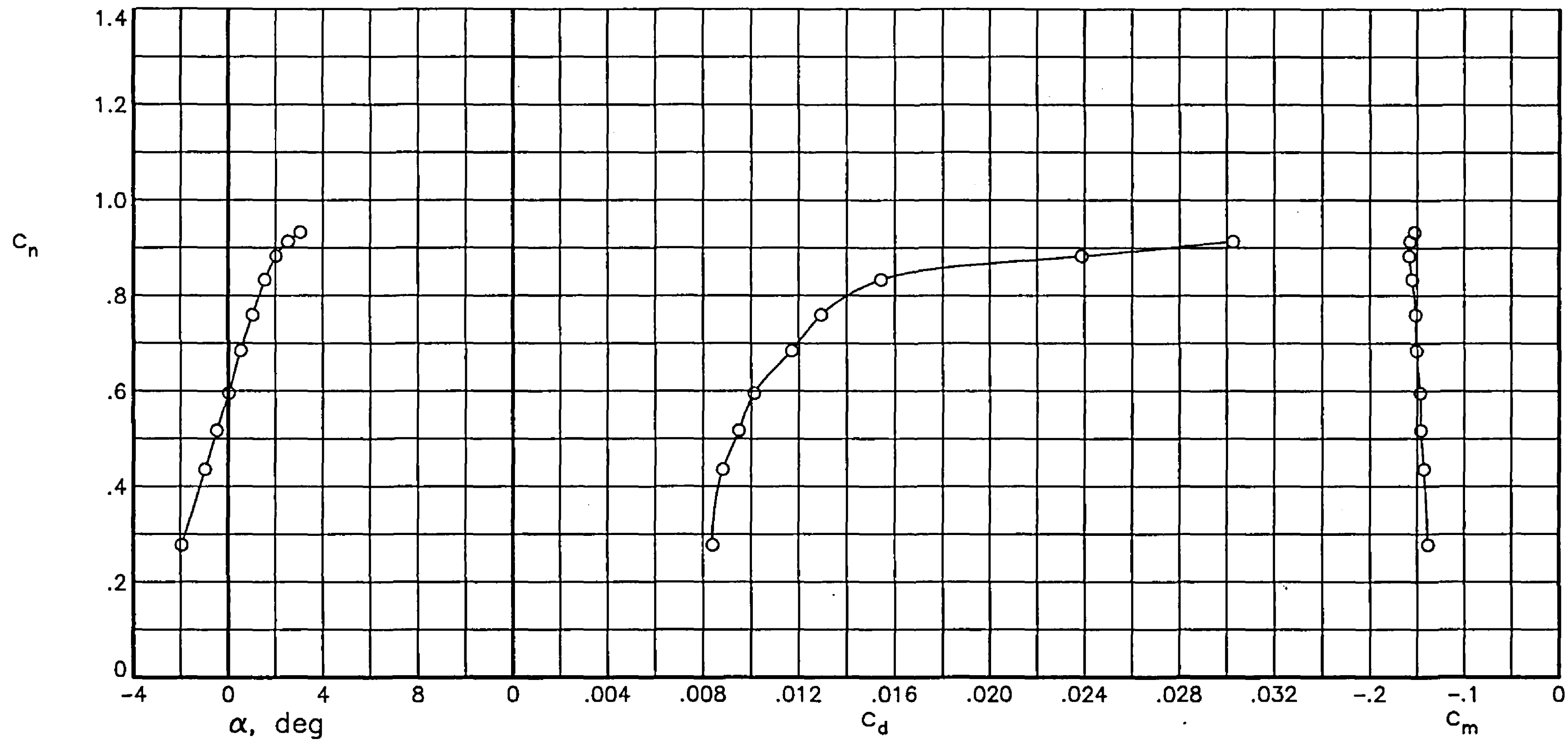

(g) $R = 30.09 \times 10^6$; $M = 0.7491$.

Figure 7.– Continued.

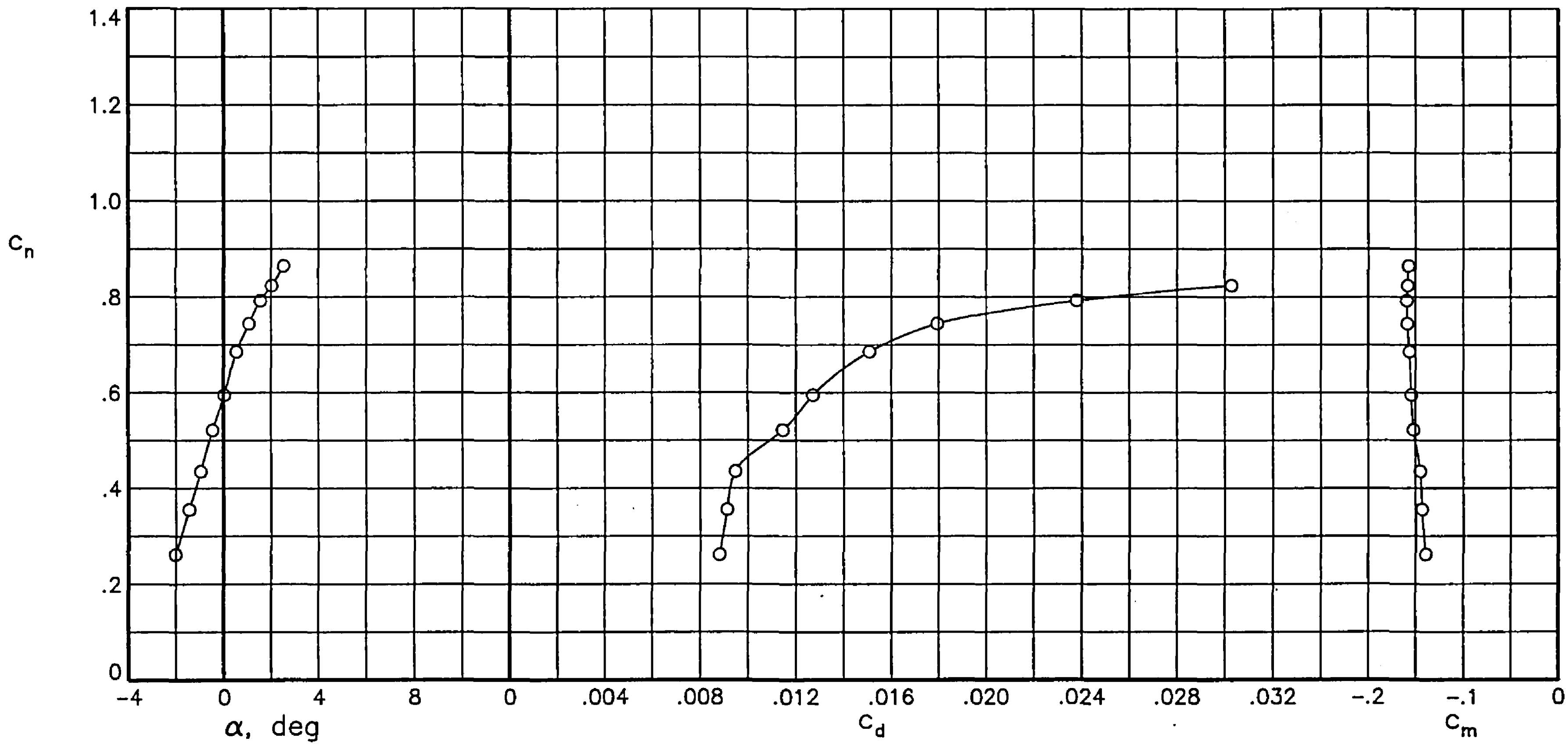

(h) $R = 30.02 \times 10^6$; $M = 0.7596$.

Figure 7.– Continued.

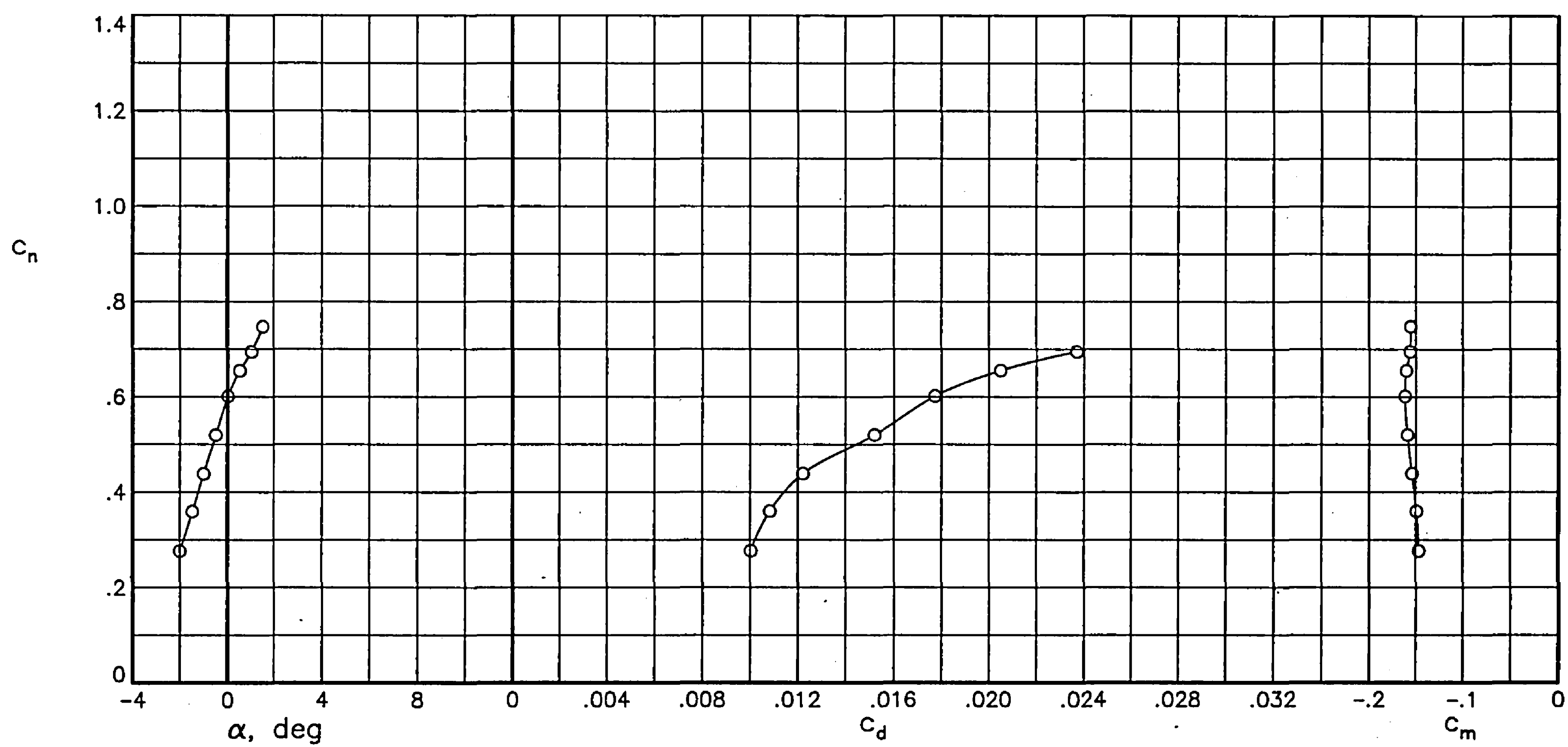

(i) $R = 30.24 \times 10^6$; $M = 0.7692$.

Figure 7.– Continued.

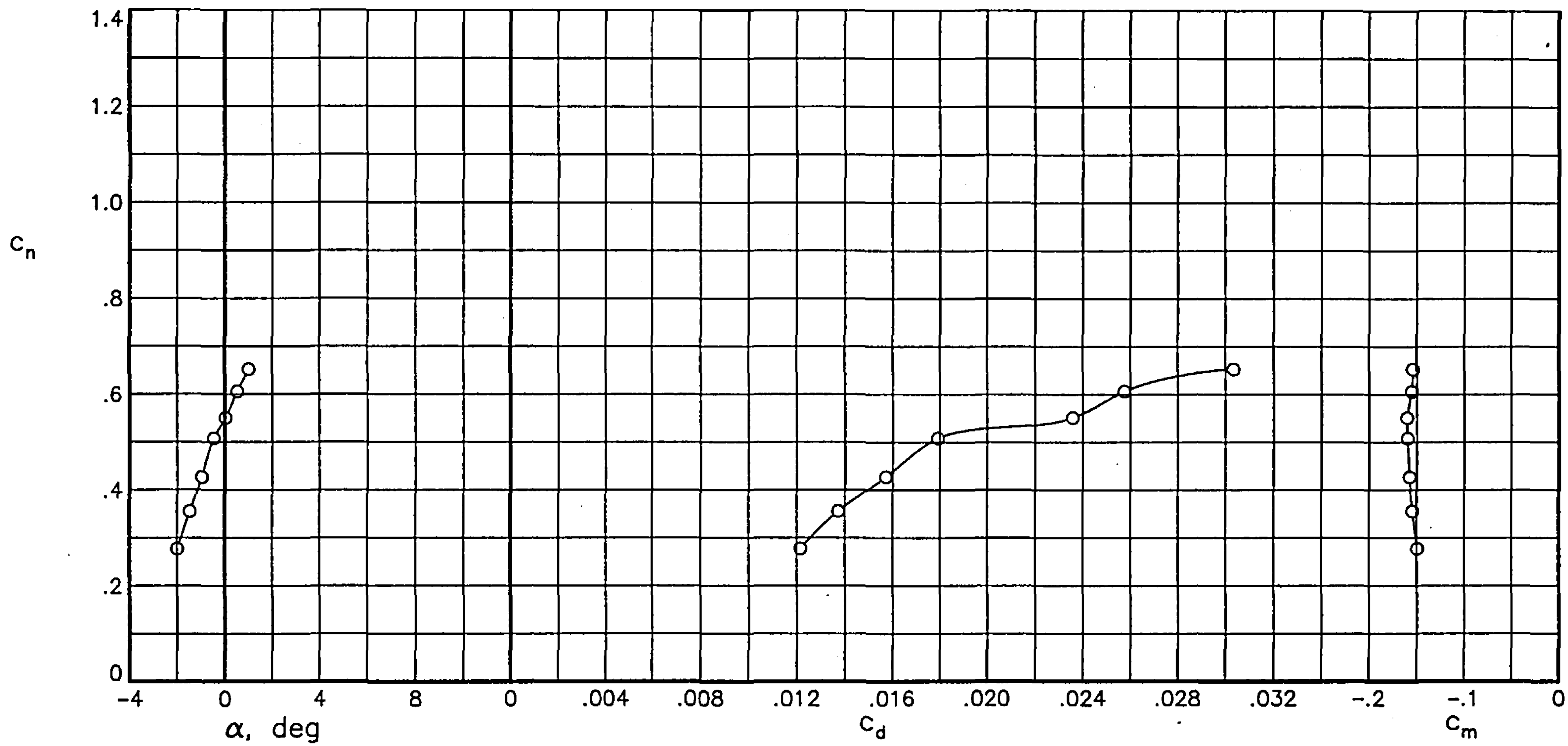

(j) $R = 30.07 \times 10^6$; $M = 0.7788$.

Figure 7.– Concluded.

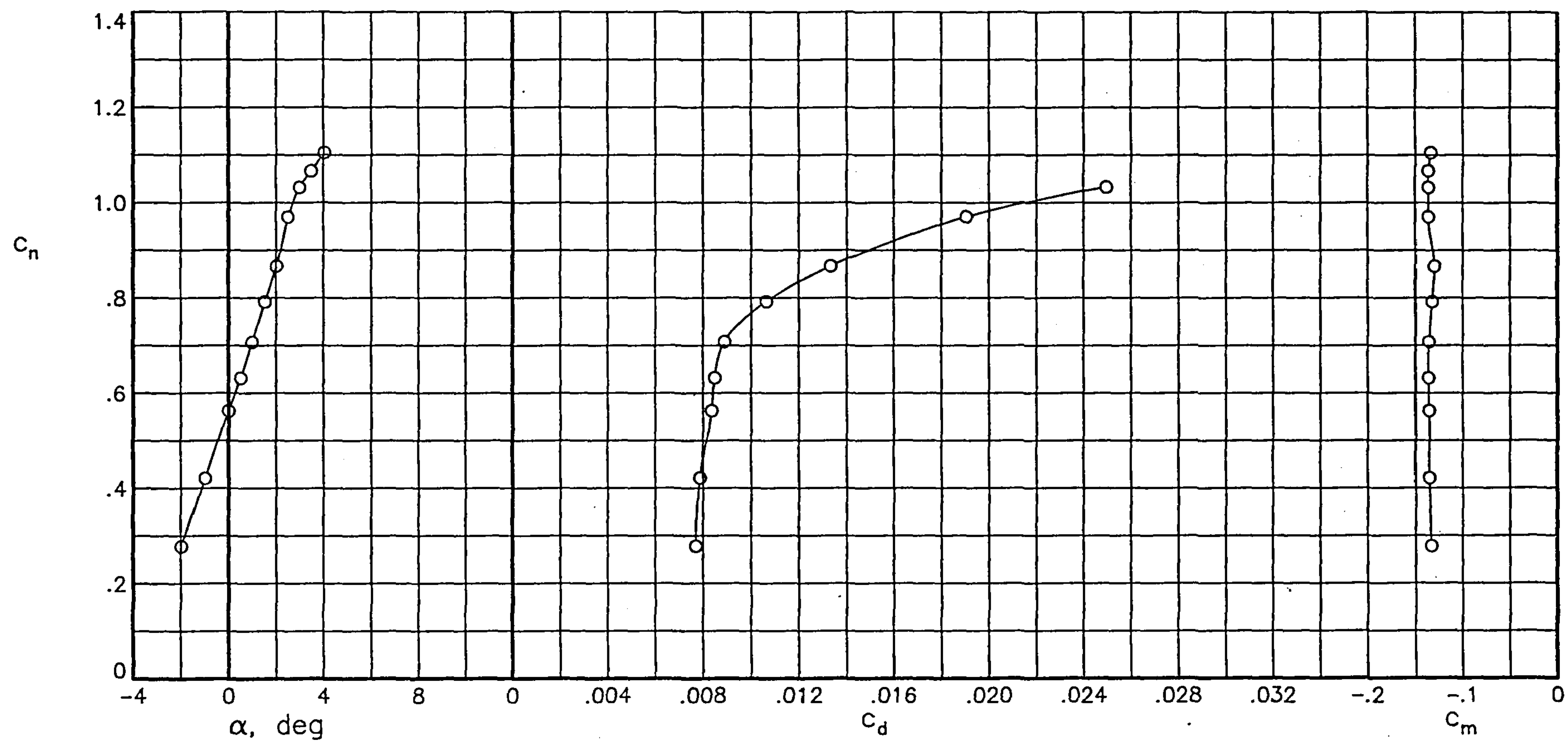

(a) $R = 40.11 \times 10^6$; $M = 0.7015$.

Figure 8.– Section characteristics at Reynolds numbers of 40×10^6.

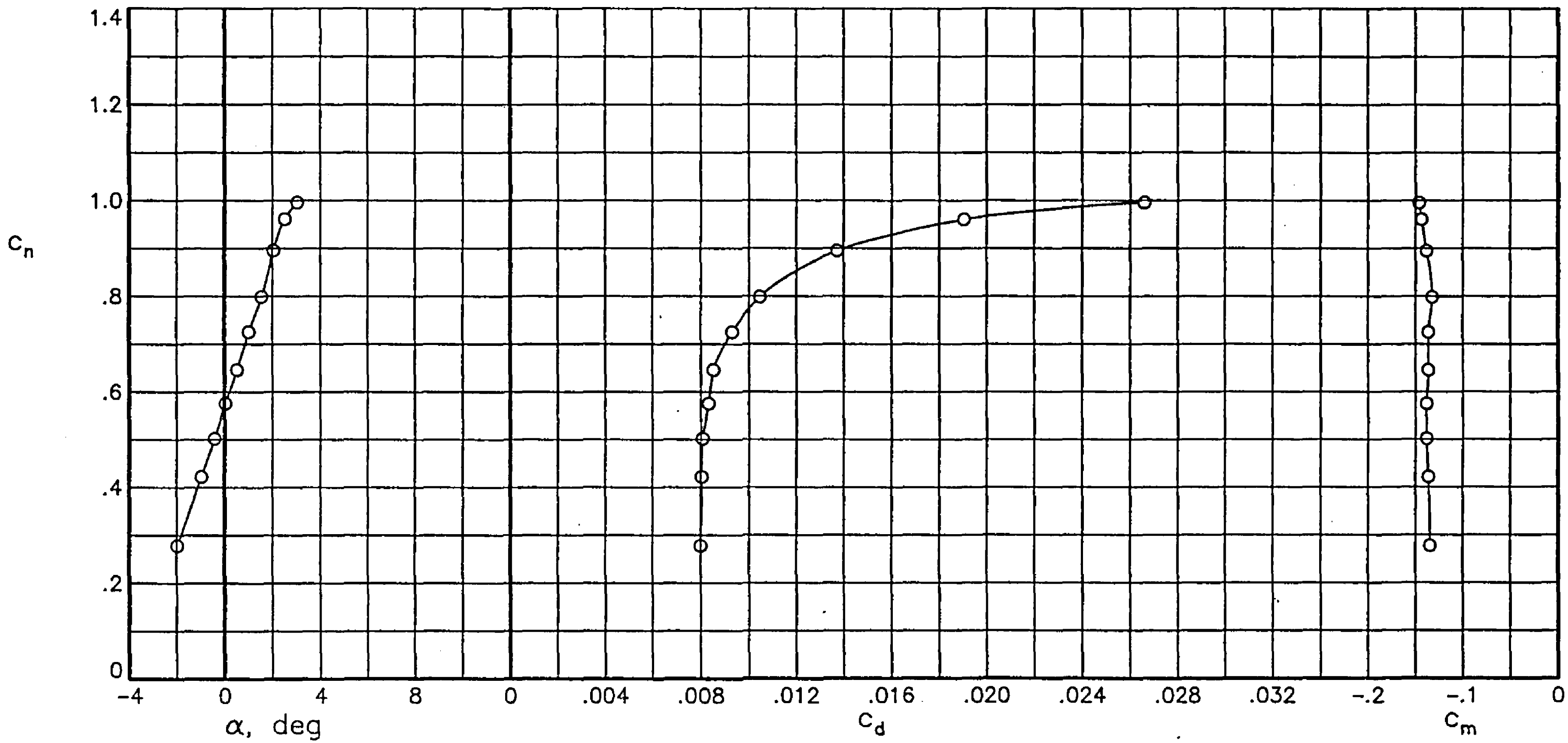

(b) $R = 40.10 \times 10^6$; $M = 0.7203$.

Figure 8.– Continued.

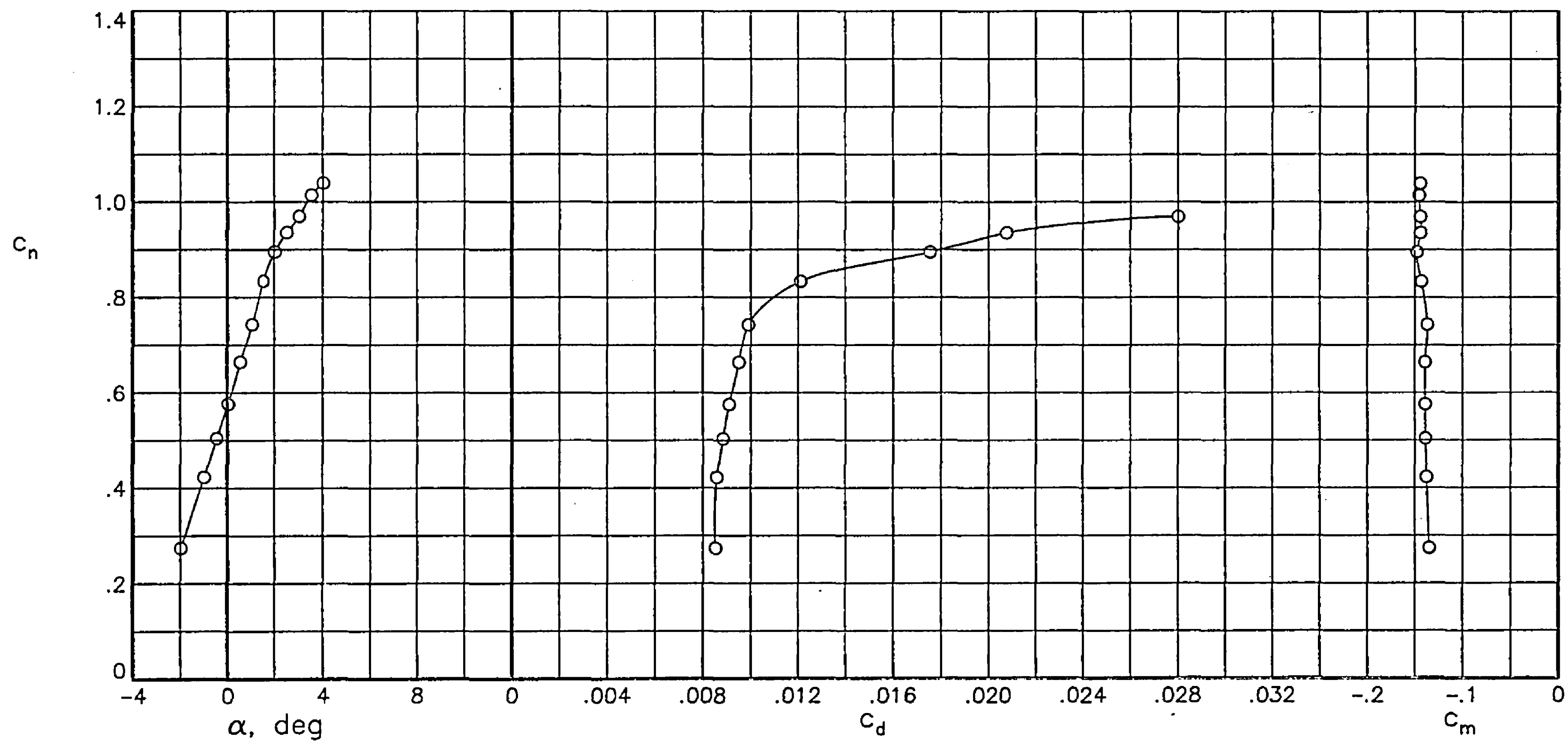

(c) $R = 40.10 \times 10^6$; $M = 0.7303$.

Figure 8.– Continued.

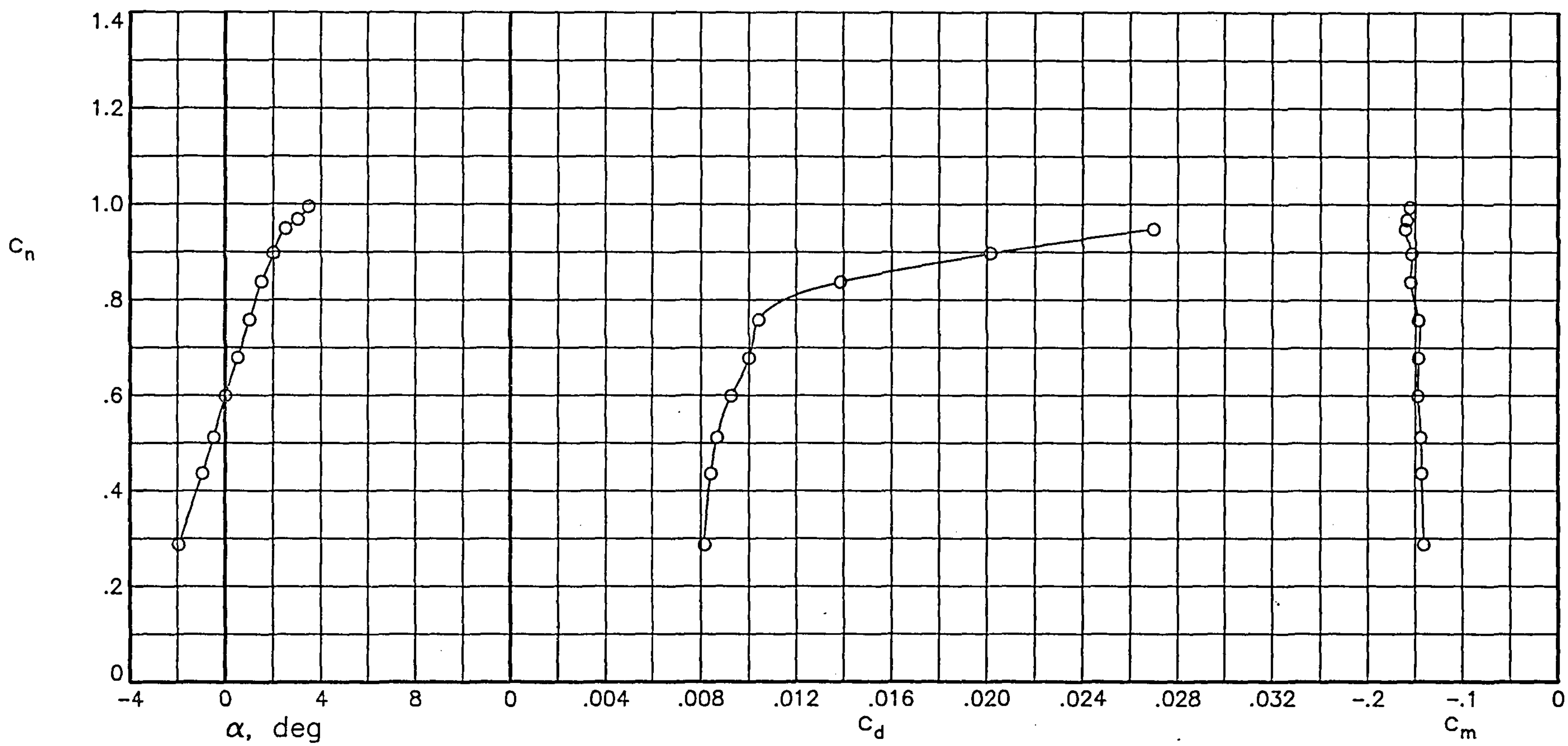

(d) $R = 39.92 \times 10^6$; $M = 0.7417$.

Figure 8.– Continued.

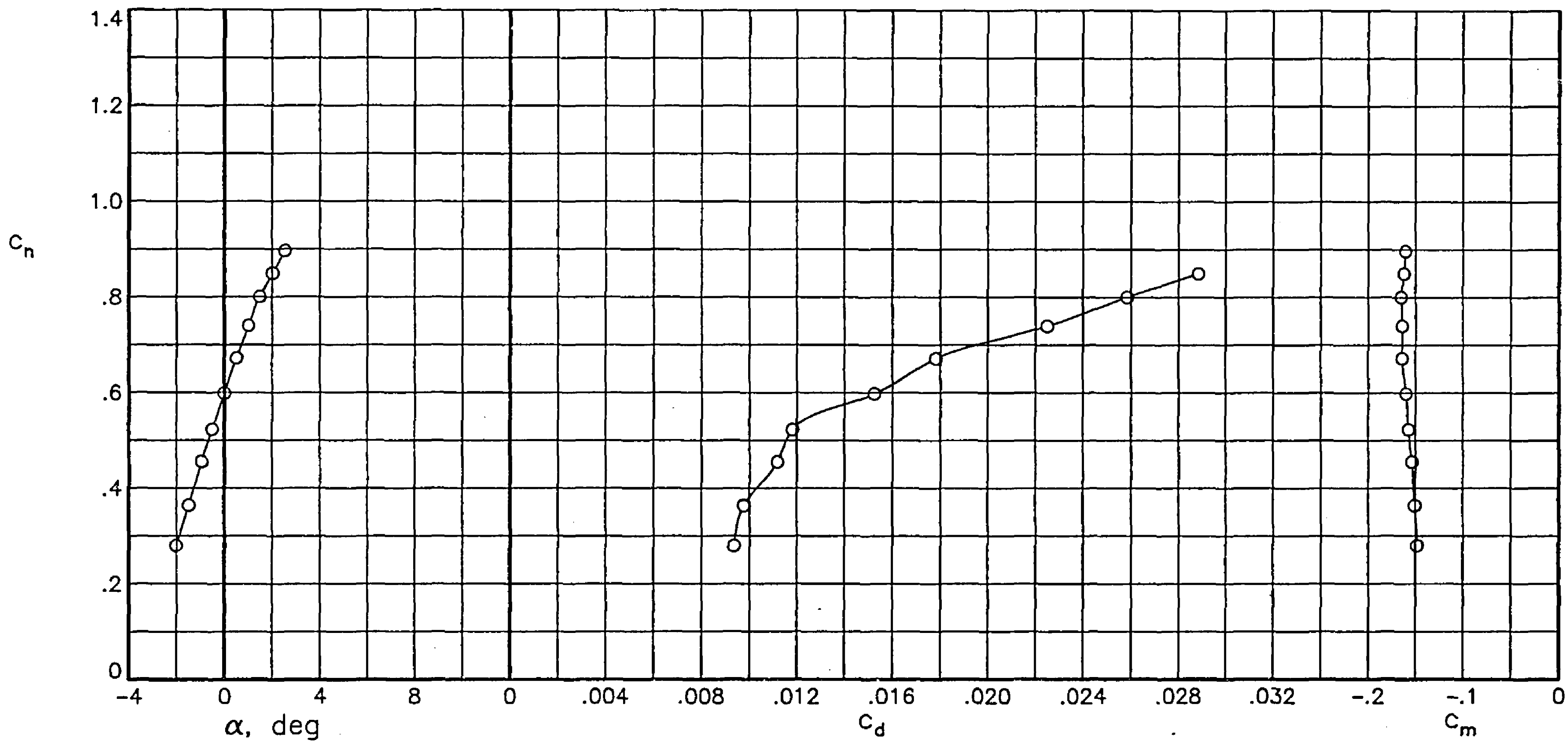

(e) $R = 39.75 \times 10^6$; $M = 0.7605$.

Figure 8.– Continued.

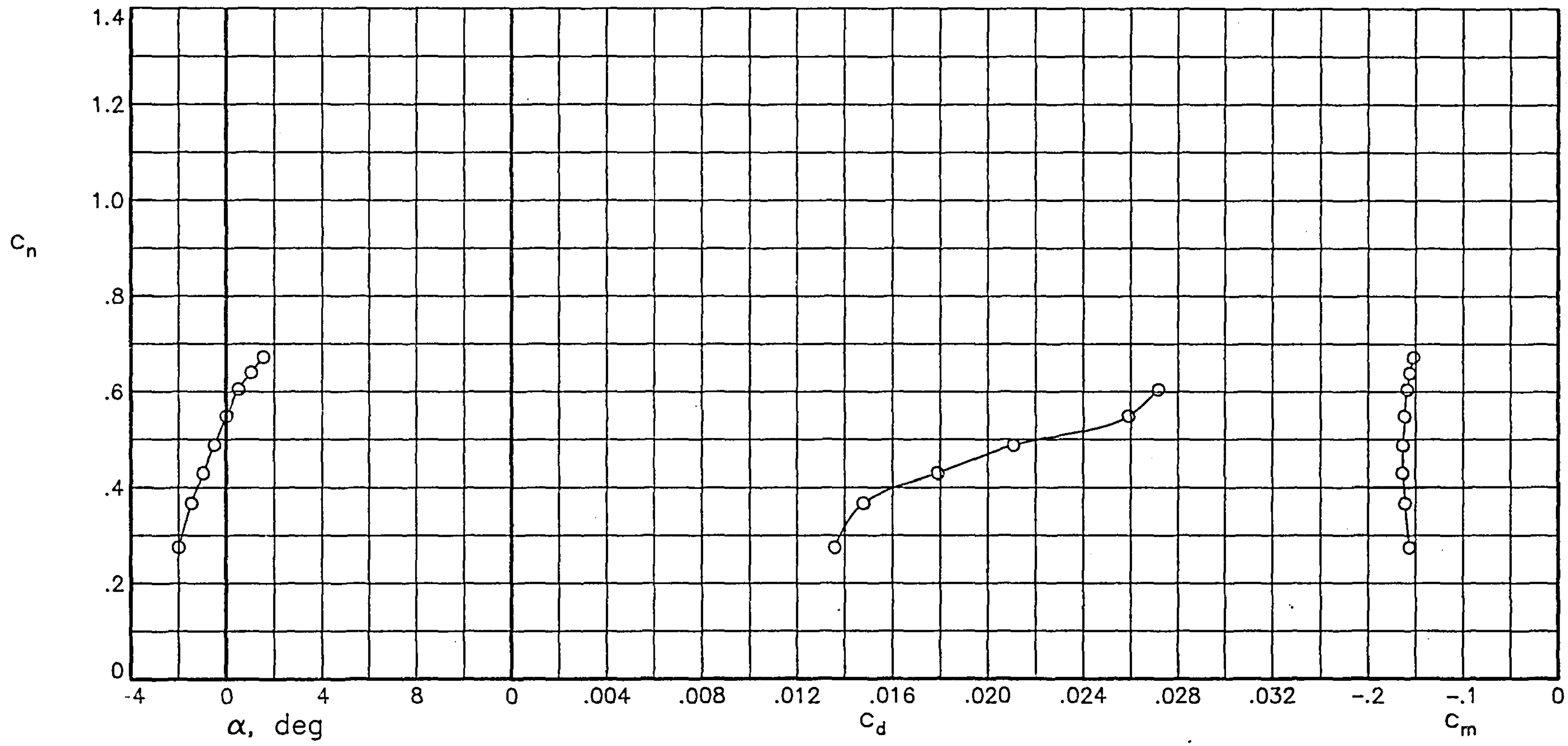

(f) $R = 39.91 \times 10^6$; $M = 0.7797$.

Figure 8.– Concluded.

NACA 65_1-213

tests conducted by NASA

Year	1984
Reference	NASA TM-85732
t/c	0,126
Transition	if fixed at 0,043c

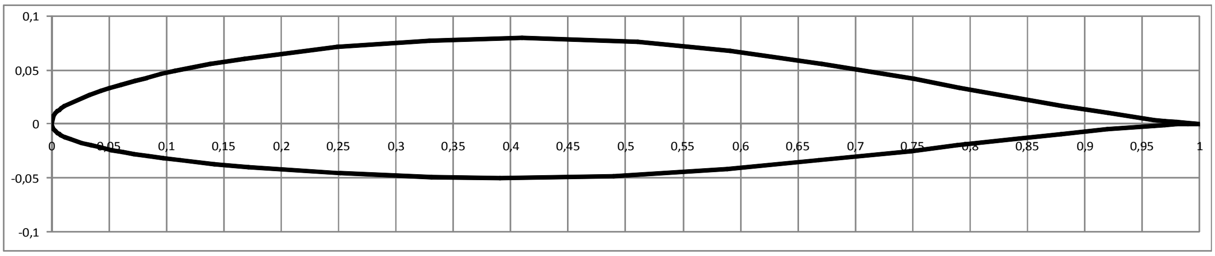

x/c	y_u/c	x/c	y_l/c
0	0	0	0
0,001678	0,007443	0,001838	-0,004839
0,00341	0,009994	0,003322	-0,006681
0,00503	0,011758	0,005031	-0,008288
0,0067	0,013252	0,00677	-0,009546
0,008386	0,014567	0,008257	-0,010597
0,011059	0,016381	0,01163	-0,012409
0,033239	0,027097	0,016498	-0,014435
0,043164	0,030862	0,026656	-0,017705
0,050622	0,033447	0,034238	-0,019749
0,060583	0,036629	0,041802	-0,021587
0,073052	0,040277	0,051865	-0,023792
0,083039	0,042983	0,061909	-0,025764
0,095534	0,046135	0,071938	-0,02756
0,108041	0,049058	0,084459	-0,029618
0,138096	0,055279	0,096966	-0,031501
0,16819	0,060579	0,111959	-0,03356
0,248574	0,071175	0,141904	-0,037127
0,329093	0,077504	0,17181	-0,040115
0,409721	0,079916	0,251426	-0,045921
0,510809	0,076324	0,330907	-0,049166
0,591318	0,067696	0,390446	-0,050093
0,671361	0,055594	0,489491	-0,048105
0,751123	0,041353	0,588682	-0,041596
0,790936	0,033806	0,668639	-0,0339
0,840669	0,024292	0,748877	-0,024841
0,88045	0,016869	0,789064	-0,020046
0,920247	0,00991	0,839331	-0,014024
0,960084	0,003893	0,87955	-0,009375
0,970053	0,002644	0,919753	-0,005108
0,980028	0,001537	0,959916	-0,001631
0,99001	0,000619	0,969947	-0,00098
1	0	0,979972	-0,000453
		0,98999	-0,000091
		1	0

NACA 65_1-213

free transition

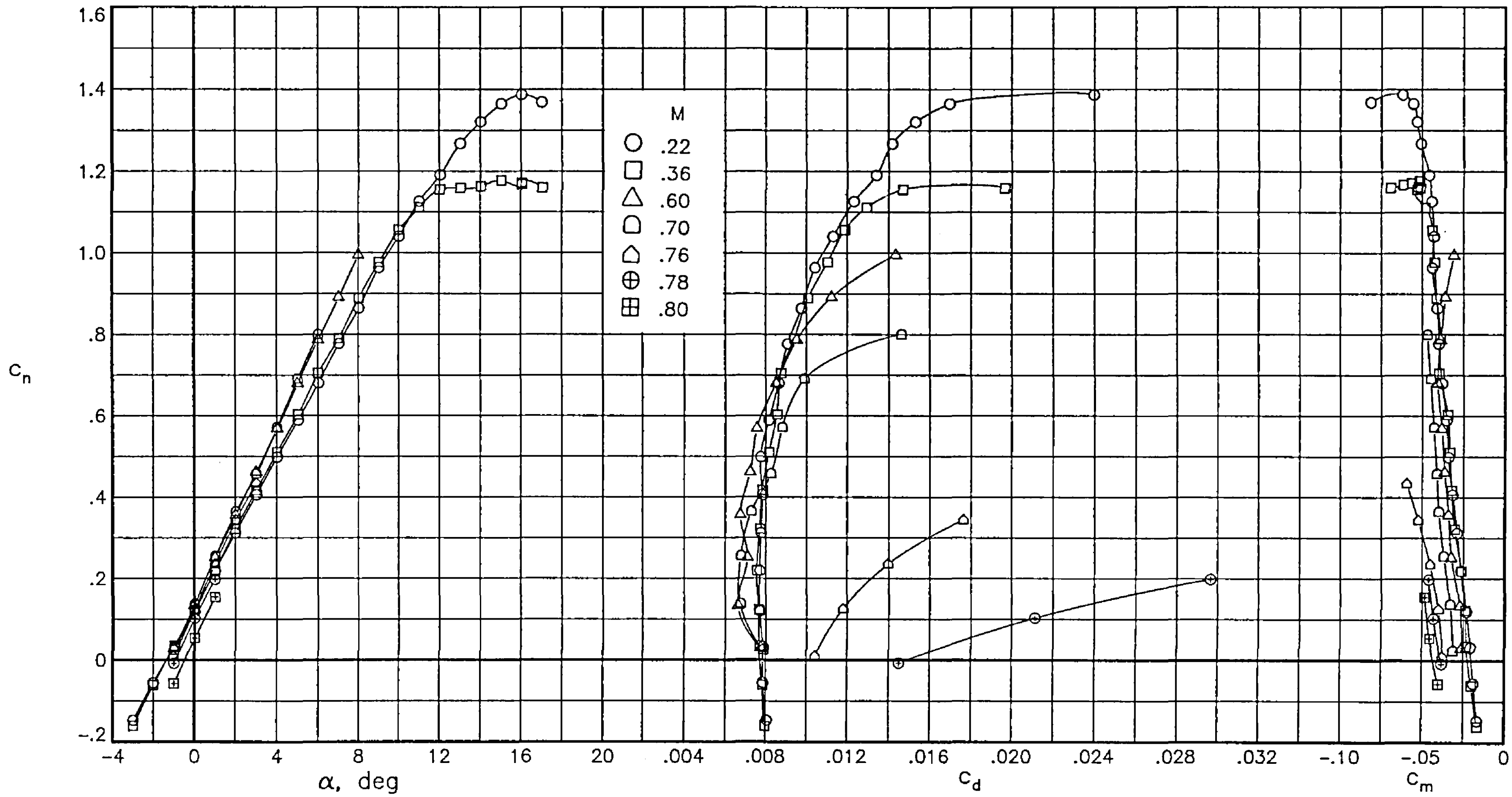

Figure 22.– Effect of Mach number on aerodynamic characteristics of airfoil with free transition at $R_c = 6 \times 10^6$.

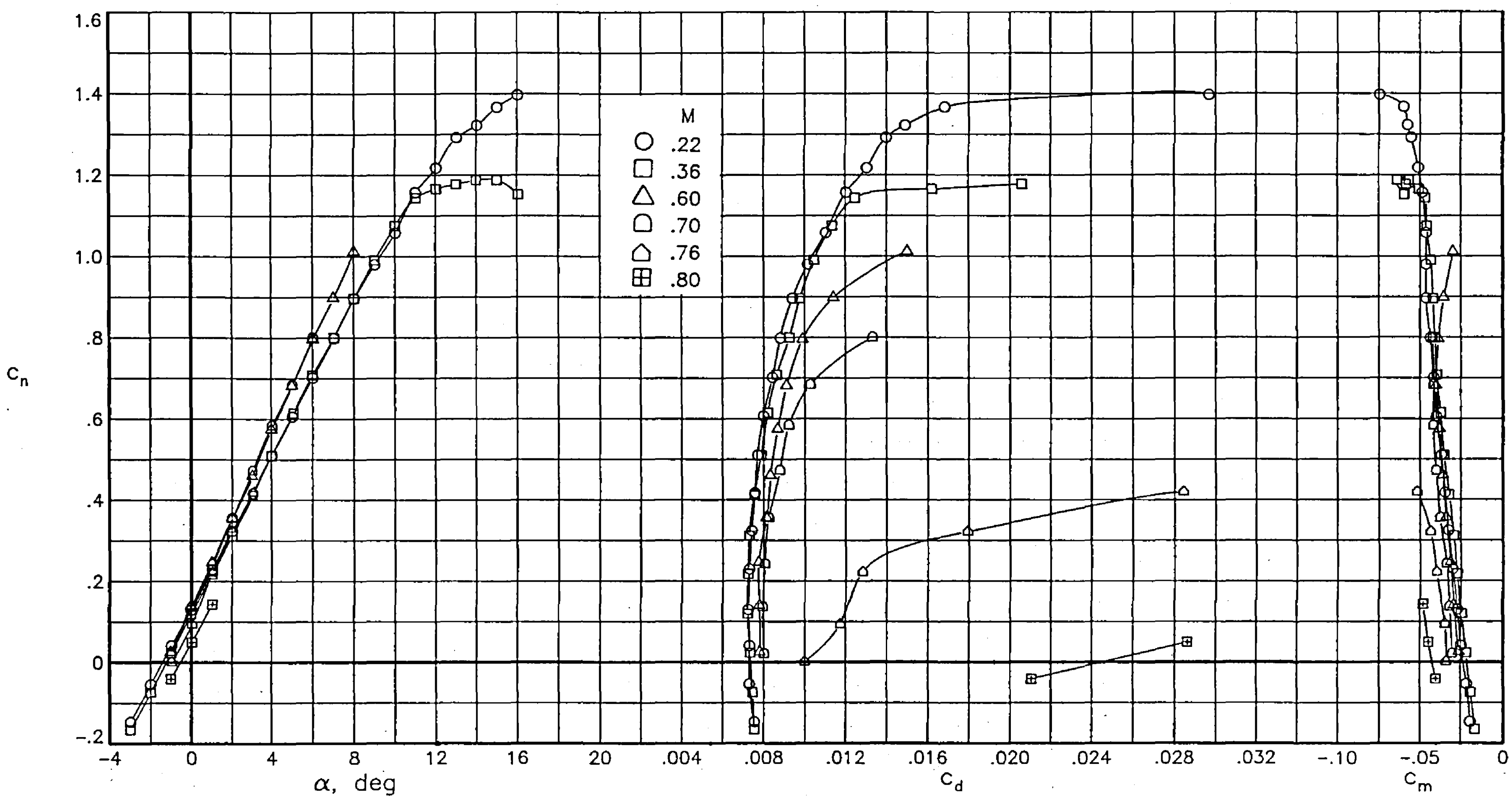

Figure 23.– Effect of Mach number on aerodynamic characteristics of airfoil with free transition at $R_c = 9 \times 10^6$.

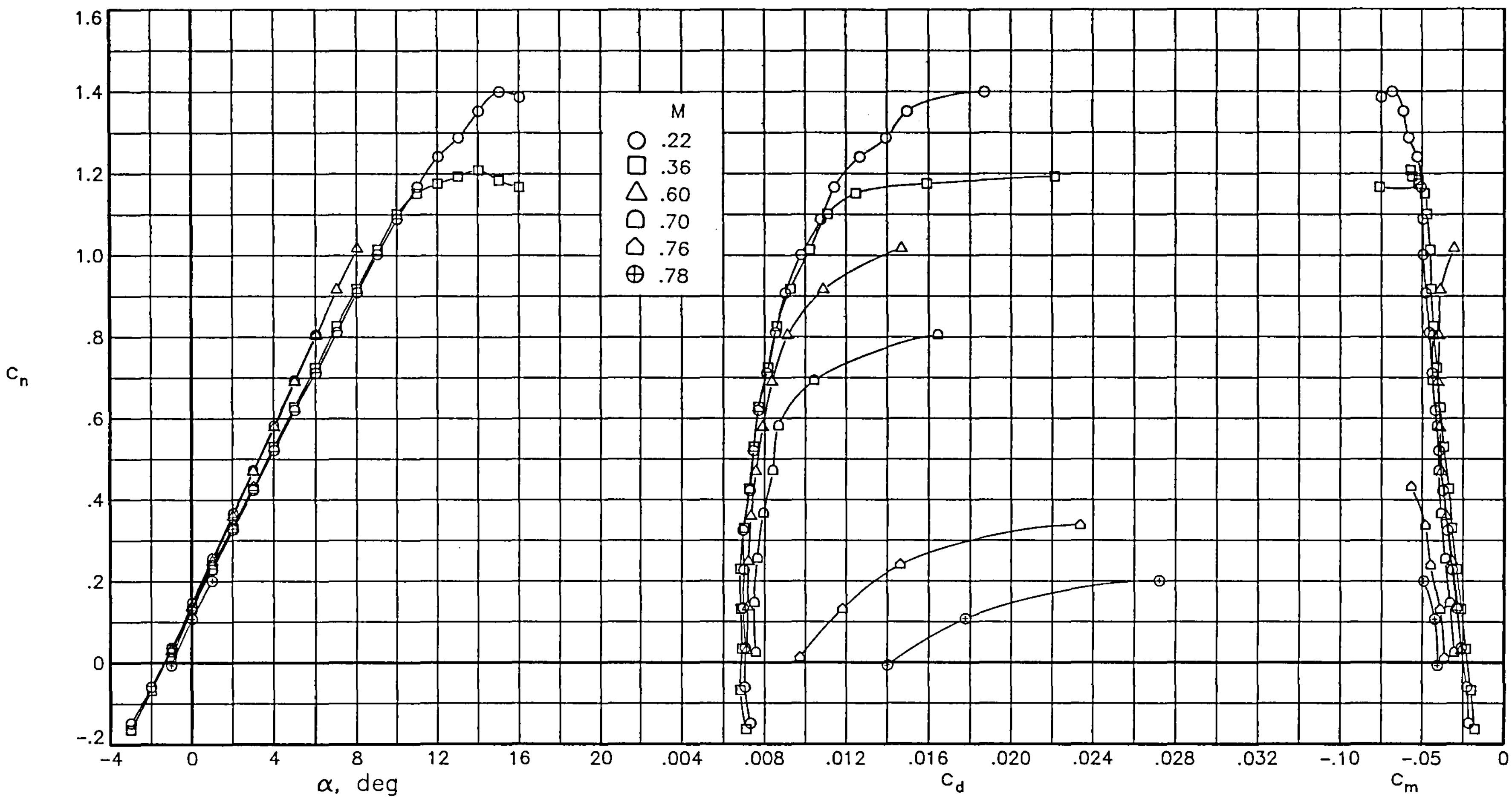

Figure 24.– Effect of Mach number on aerodynamic characteristics of airfoil with free transition at $R_c = 15 \times 10^6$.

NACA 65_1-213

fixed transition
at 0,043c

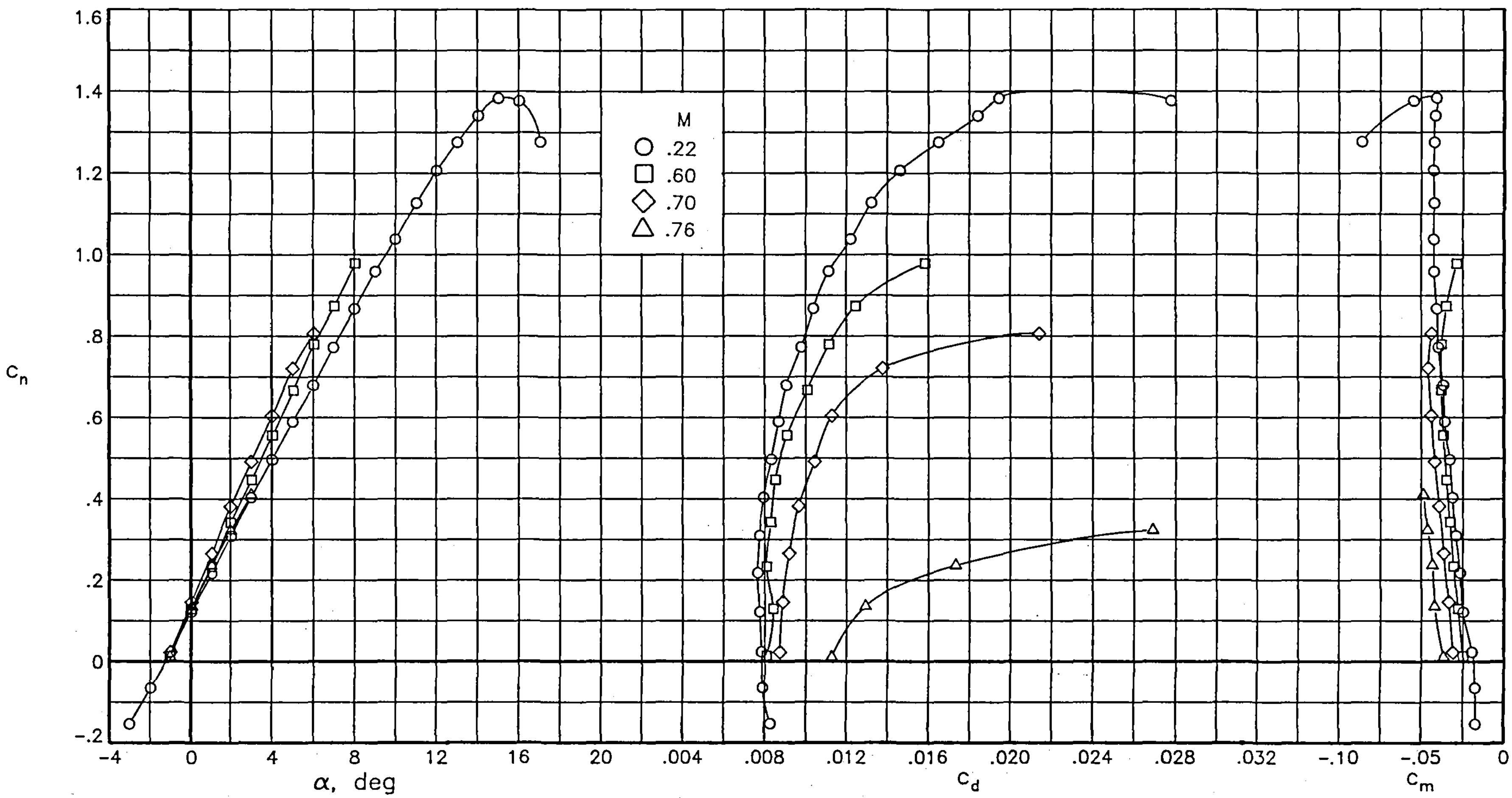

Figure 25.– Effect of Mach number on aerodynamic characteristics of airfoil with fixed transition at $R_c = 6 \times 10^6$.

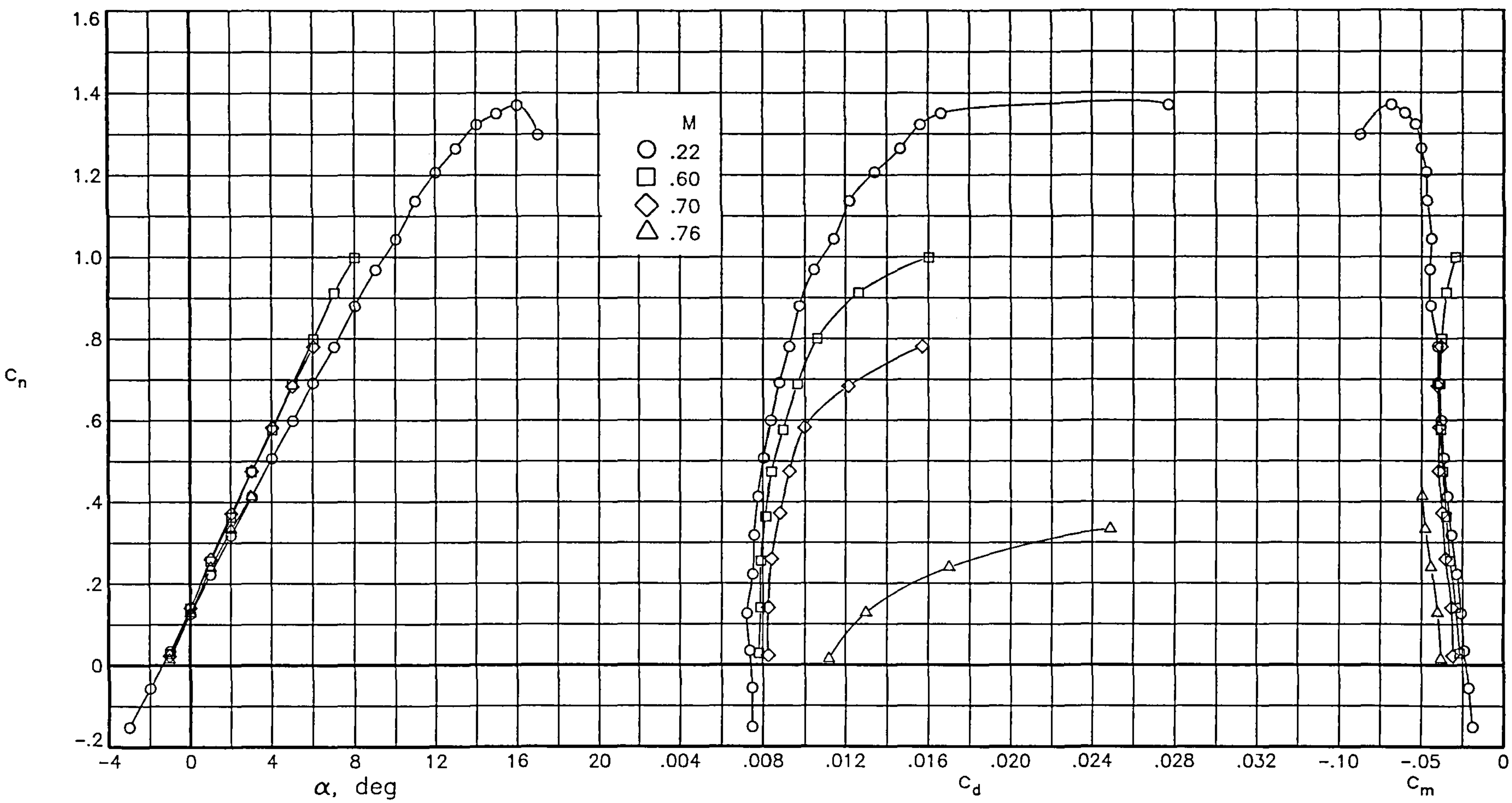

Figure 26.– Effect of Mach number on aerodynamic characteristics of airfoil with fixed transition at $R_c = 9 \times 10^6$.

NLR 7301
(NLR HT 73108210)

National Aerospace Laboratory NLR (The Netherlands)

Year	1979
Reference	AGARD-AR-138
t/c	0,163
$c_{l,design}$	0,6 (theory) 0,45 (exp)
M_{design}	0,721 (theory) 0,747 (exp)
Transition	if fixed at 0,3c

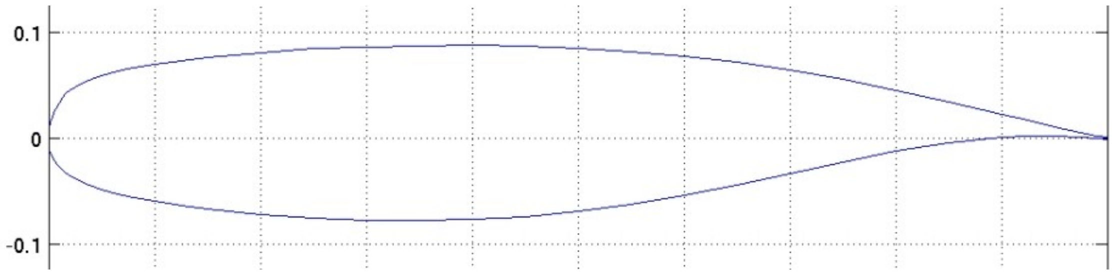

UIUC Airfoil Data Site

Coordinates from UIUC Airfoil Data Site

x/c	y_u/c	x/c	y_l/c
0	0	0	0
0,0005	0,0073	0,0005	-0,00748
0,001	0,01051	0,001	-0,0102
0,002	0,01518	0,002	-0,01373
0,0035	0,0203	0,0035	-0,01735
0,005	0,02424	0,005	-0,02016
0,0065	0,02756	0,0065	-0,02252
0,008	0,03043	0,008	-0,02455
0,01	0,03375	0,01	-0,02688
0,0125	0,03729	0,0125	-0,02935
0,016	0,0414	0,016	-0,03225
0,02	0,04514	0,02	-0,03502
0,025	0,04873	0,025	-0,03794
0,035	0,05372	0,035	-0,04264
0,05	0,0592	0,05	-0,04806
0,065	0,06321	0,065	-0,05229
0,08	0,06636	0,08	-0,05576
0,1	0,06985	0,1	-0,05962
0,125	0,07347	0,125	-0,06358
0,15	0,07648	0,15	-0,06689
0,2	0,08115	0,2	-0,07194
0,25	0,08441	0,25	-0,07527
0,3	0,08649	0,3	-0,07713
0,35	0,08755	0,35	-0,07763
0,4	0,08764	0,4	-0,07672
0,45	0,08678	0,45	-0,07412
0,5	0,08495	0,5	-0,06934
0,55	0,08206	0,55	-0,06237
0,6	0,07789	0,6	-0,05386
0,65	0,07212	0,65	-0,04397
0,7	0,06458	0,7	-0,03316
0,75	0,05551	0,75	-0,02227
0,8	0,04523	0,8	-0,01221
0,85	0,03415	0,85	-0,00409
0,9	0,02269	0,9	0,00108
0,925	0,01696	0,925	0,00228
0,95	0,01129	0,95	0,00246
0,975	0,00577	0,975	0,00153
0,99	0,00258	0,99	0,00042
1	0,00055	1	-0,00055

UPPER PART

X	Z
0.0000012	-.0004162
0.0002895	+.0052191
0.0005870	+.0076768
0.0008861	+.0095965
0.0011758	+.0112217
0.0014662	+.0126337
0.0017468	+.0138934
0.0020176	+.0150413
0.0022988	+.0160878
0.0025701	+.0170734
0.0028314	+.0179878
0.0042209	+.0220528
0.0056121	+.0254172
0.0069239	+.0281722
0.0081862	+.0305312
0.0094795	+.0326872
0.0107530	+.0346503
0.0119867	+.0363594
0.0131194	+.0378449
0.0141918	+.0391576
0.0153049	+.0404096
0.0164386	+.0416006
0.0175319	+.0476834
0.0185343	+.0436187
0.0194052	+.0443882
0.0202255	+.0450763
0.0211270	+.0457913
0.0223832	+.0467230
0.0240550	+.0478651
0.0255447	+.0488004
0.0265278	+.0493759
0.0274908	+.0499059
0.0276023	+.0499651
0.0276428	+.0499865
0.0279647	+.0501553
0.0281700	+.0502615
0.0285818	+.0504716
0.0291330	+.0507471
0.0296602	+.0510052
0.0300455	+.0511909
0.0304510	+.0513850
0.0310492	+.0516694
0.0316879	+.0519702
0.0331276	+.0526347
0.0378375	+.0546577
0.0425480	+.0564729
0.0472590	+.0581064
0.0519705	+.0595825
0.0566824	+.0609237
0.0613946	+.0621505
0.0661071	+.0632814
0.0708198	+.0643330
0.0764002	+.0654949
0.0808444	+.0663708
0.0848828	+.0671354
0.0888097	+.0678502
0.0926554	+.0685253
0.0967347	+.0692169
0.1028790	+.0702150
0.1090235	+.0711645
0.1174463	+.0723954
0.1225001	+.0730979
0.1298374	+.0740738
0.1371749	+.0750008
0.1451619	+.0759587
0.1531492	+.0768671
0.1620297	+.0778222
0.1709103	+.0787225
0.1757516	+.0791914
0.1830136	+.0798669
0.1902757	+.0805103
0.1956374	+.0809654
0.2009991	+.0814040
0.2063603	+.0818267
0.2117226	+.0822338
0.2175970	+.0826623
0.2234714	+.0830729
0.2293459	+.0834659
0.2352205	+.0838418
0.2417117	+.0842377
0.2482030	+.0846135
0.2546944	+.0849698
0.2611858	+.0853068
0.2683650	+.0856577
0.2755442	+.0859859
0.2827236	+.0862918
0.2899029	+.0865757
0.2977752	+.0868622
0.3056474	+.0871229
0.3135200	+.0873584
0.3213925	+.0875690
0.3300467	+.0877723
0.3387010	+.0879461
0.3473554	+.0880910
0.3560099	+.0882071
0.3651414	+.0882986
0.3742734	+.0883584
0.3834053	+.0883867
0.3925373	+.0883833
0.4018445	+.0883475
0.4111518	+.0882789
0.4204592	+.0881775
0.4297667	+.0880434
0.4386049	+.0878857
0.4474429	+.0876982
0.4562811	+.0874805
0.4651193	+.0872324
0.4728611	+.0869899
0.4806030	+.0867235
0.4883450	+.0864327
0.4960870	+.0861171
0.5026310	+.0858307
0.5091750	+.0855260
0.5157191	+.0852026
0.5222632	+.0848603
0.5302975	+.0844136
0.5383317	+.0839369
0.5436882	+.0836020
0.5525071	+.0830196
0.5613261	+.0823476
0.5686577	+.0818492
0.5759893	+.0812713
0.5822243	+.0807557
0.5884593	+.0802173
0.5938567	+.0797321
0.5992541	+.0792287
0.6040016	+.0787704
0.6087491	+.0782972
0.6130854	+.0778517
0.6174218	+.0773934
0.6254040	+.0765152
0.6329293	+.0755458
0.6401197	+.0747768
0.6470765	+.0739003
0.6539319	+.0730023
0.6606756	+.0720960
0.6674601	+.0711319
0.6742447	+.0701454
0.6811995	+.0691019
0.6881543	+.0680253
0.6951093	+.0669196
0.7020644	+.0657827
0.7093750	+.0645558
0.7166857	+.0632973
0.7239965	+.0620082
0.7313074	+.0606892
0.7390044	+.0592694
0.7467015	+.0578191
0.7543987	+.0563396
0.7620959	+.0548323
0.7703087	+.0531951
0.7785216	+.0515298
0.7867346	+.0498392
0.7949477	+.0481221
0.8038922	+.0462276
0.8128369	+.0443086
0.8217815	+.0423675
0.8307263	+.0404068
0.8406234	+.0382174
0.8505207	+.0360100
0.8604179	+.0337880
0.8703152	+.0315545
0.8804741	+.0292535
0.8906331	+.0269475
0.9007920	+.0246399
0.9137643	+.0216968
0.9239238	+.0193996
0.9340827	+.0171138
0.9442415	+.0148440
0.9588193	+.0116237
0.9636815	+.0105616
0.9685437	+.0095049
0.9734058	+.0084610
0.9782680	+.0074251
0.9831300	+.0064005
0.9879921	+.0053944
0.9928541	+.0043901
0.9977161	+.0034069
0.9999052	+.0029695
1.0020942	+.0025354
1.0042833	+.0021046
1.0064723	+.0016772
1.0086614	+.0012530
1.0108504	+.0008320
1.0130394	+.0004144
1.0152284	+.0000000

LOWER PART

X	Z
0.0000012	-.0004162
0.0002395	-.0056237
0.0004787	-.0076027
0.0007164	-.0090435
0.0009431	-.0102206
0.0011795	-.0112149
0.0014054	-.0121076
0.0016514	-.0129293
0.0017744	-.0133248
0.0018974	-.0137103
0.0021635	-.0144608
0.0024397	-.0151909
0.0031756	-.0169046
0.0039110	-.0184354
0.0046153	-.0197634
0.0052785	-.0209290
0.0059313	-.0219728
0.0066246	-.0230063
0.0073992	-.0240599
0.0082348	-.0251336
0.0091007	-.0261667
0.0099563	-.0271155
0.0104218	-.0280297
0.0117280	-.0289408
0.0127561	-.0298946
0.0139978	-.0309576
0.0154631	-.0321417
0.0170910	-.0333505
0.0179506	-.0339548
0.0184101	-.0345387
0.0197713	-.0351686
0.0207325	-.0357755
0.0219376	-.0365060
0.0231427	-.0372055
0.0245498	-.0379864
0.0259567	-.0387330
0.0268947	-.0392137
0.0296142	-.0405379
0.0323335	-.0417721
0.0341073	-.0425358
0.0358810	-.0432701
0.0376546	-.0439771
0.0394281	-.0446591
0.0423271	-.0457248
0.0452260	-.0467344
0.0481247	-.0476930
0.0510232	-.0486058
0.0565381	-.0502310
0.0620525	-.0517267
0.0675667	-.0531110
0.0730805	-.0544013
0.0771059	-.0552931
0.0811312	-.0561467
0.0851564	-.0569652
0.0891816	-.0577513
0.0929399	-.0584584
0.0966982	-.0591412
0.1004565	-.0598010
0.1042147	-.0604391
0.1078915	-.0610431
0.1115683	-.0616267
0.1152451	-.0621901
0.1189218	-.0627346
0.1264630	-.0638076
0.1340040	-.0648412
0.1417023	-.0658428
0.1494005	-.0667871
0.1581394	-.0677937
0.1668782	-.0687354
0.1756167	-.0696163
0.1843551	-.0704393
0.1895240	-.0708995
0.1946928	-.0713408
0.1998615	-.0717636
0.2050302	-.0721684
0.2110365	-.0726163
0.2170428	-.0730405
0.2230491	-.0734416
0.2290552	-.0738200
0.2363154	-.0742478
0.2435754	-.0746437
0.2508353	-.0750084
0.2580952	-.0753426
0.2673729	-.0757257
0.2766505	-.0760604
0.2859280	-.0763472
0.2952053	-.0765865
0.3053582	-.0767946
0.3155109	-.0769474
0.3256635	-.0770445
0.3358159	-.0770861
0.3460392	-.0770716
0.3561913	-.0770007
0.3663432	-.0768720
0.3764950	-.0766837
0.3866465	-.0764334
0.3967979	-.0761186
0.4069491	-.0757362
0.4171001	-.0752827
0.4272508	-.0747544
0.4374014	-.0741469
0.4475517	-.0734558
0.4594475	-.0725326
0.4688157	-.0717156
0.4745806	-.0711708
0.4856332	-.0700287
0.4933971	-.0691512
0.5001765	-.0683376
0.5067021	-.0675138
0.5133493	-.0666367
0.5202298	-.0656939
0.5274553	-.0646685
0.5351272	-.0635414
0.5431744	-.0623191
0.5516579	-.0609873
0.5545499	-.0605234
0.5636167	-.0590373
0.5726834	-.0575037
0.5821558	-.0558514
0.5916280	-.0541483
0.6011052	-.0523934
0.6105822	-.0505882
0.6197243	-.0487996
0.6288662	-.0469661
0.6376225	-.0451694
0.6463786	-.0433366
0.6550535	-.0414889
0.6637283	-.0396149
0.6727886	-.0376348
0.6818488	-.0356373
0.6915939	-.0334759
0.7013389	-.0313082
0.7118449	-.0289698
0.7223508	-.0266371
0.7279285	-.0254030
0.7335062	-.0241734
0.7390839	-.0229494
0.7446616	-.0217322
0.7506223	-.0204404
0.7565831	-.0191598
0.7625439	-.0178924
0.7685048	-.0166403
0.7752698	-.0152405
0.7820349	-.0138661
0.7888000	-.0125201
0.7955653	-.0112058
0.8040480	-.0096069
0.8125308	-.0080674
0.8210139	-.0065919
0.8294972	-.0051848
0.8396449	-.0035977
0.8497929	-.0021236
0.8599413	-.0007717
0.8700901	+.0004496
0.8763318	+.0011324
0.8864812	+.0021265
0.8966310	+.0029712
0.9067813	+.0036605
0.9169321	+.0041886
0.9270833	+.0045505
0.9372351	+.0047413
0.9473873	+.0047565
0.9575401	+.0045921
0.9676934	+.0042446
0.9748111	+.0038900
0.9839296	+.0032994
0.9884890	+.0029450
0.9930485	+.0025507
0.9971651	+.0021591
0.9999096	+.0018774
1.0026541	+.0015787
1.0040264	+.0014231
1.0073270	+.0010317
1.0106277	+.0006148
1.0143956	+.0001129
1.0152284	+.0000000

N.B.

redefined coordinate system for which $\alpha_{design} = -0.194^{\circ}$

TABLE 4.2 Co-ordinates of aerofoil NLR HT 7310810

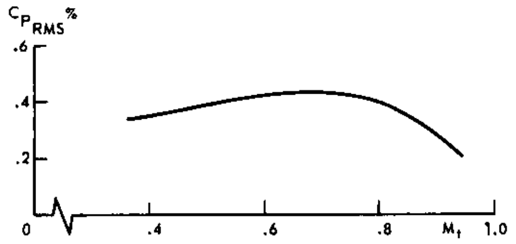

Fig. 4.5 Noise level in NLR pilot tunnel measured in stream

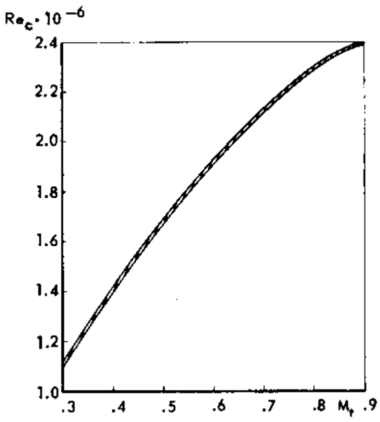

Fig. 4.6 Reynolds number based on chord lenght as function of Mach number

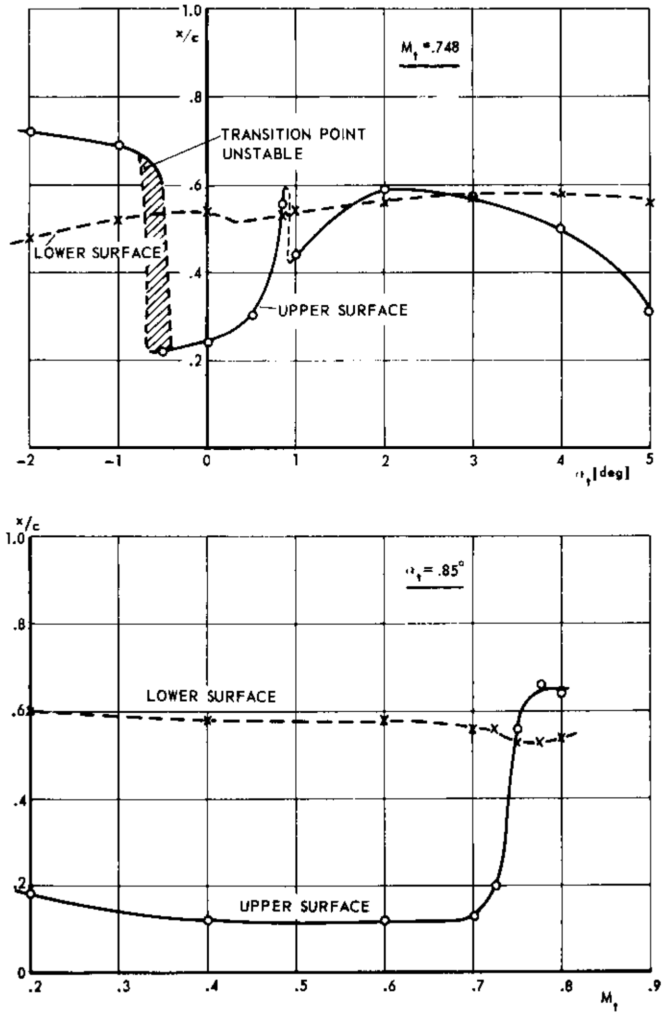

Fig. 4.7 Location of natural transition

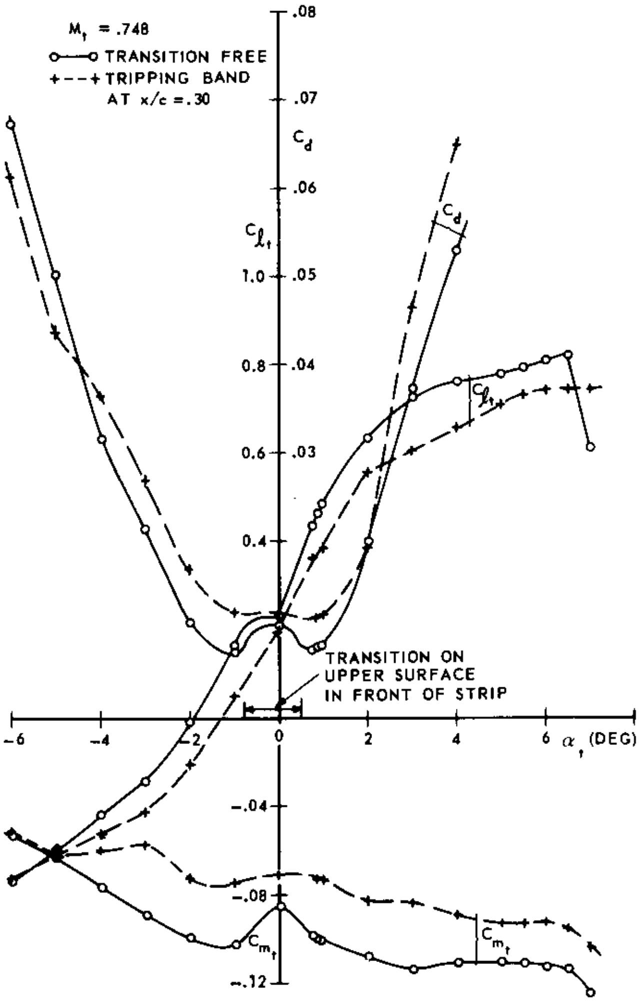

Fig. 4.8 Lift, drag and pitching moment as a funtion of angle of attack at M =.748

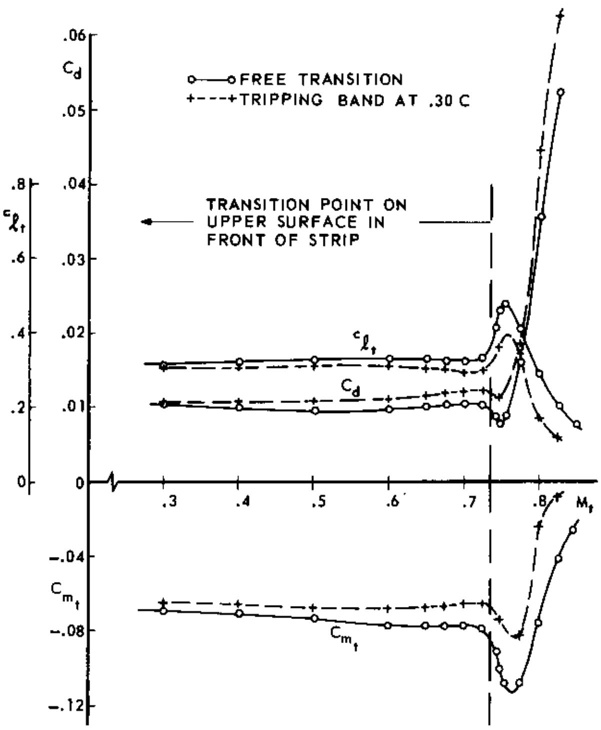

Fig. 4.9 Lift, drag and pitching moment as a funtion of Mach number at α_t =.85°

NPL 9510

British National Physics Laboratory

Year	1983
Reference	NASA TM-85663
t/c	0,11
$c_{l,design}$	0,6
M_{design}	0,75
Transition	if fixed: 0,04c upper surface 0,06c lower surface

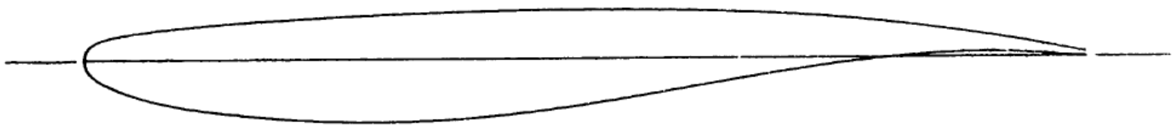

TABLE I.- AIRFOIL COORDINATES

Upper Surface

x/c	z/c
.0000	−.00002
.0004	.00392
.0016	.00760
.0025	.00942
.0050	.01277
.0100	.01670
.0150	.01922
.0200	.02100
.0250	.02238
.0300	.02357
.0400	.02553
.0500	.02722
.0600	.02871
.0700	.03007
.0800	.03129
.0900	.03241
.1000	.03343
.1200	.03530
.1400	.03694
.1600	.03839
.1800	.03970
.2000	.04090
.2200	.04205
.2400	.04315
.2600	.04417
.2800	.04507
.3000	.04592
.3200	.04669
.3400	.04741
.3600	.04806
.3800	.04867

x/c	z/c
.4000	.04917
.4200	.04959
.4400	.04990
.4600	.05013
.4800	.05027
.5000	.05031
.5200	.05028
.5400	.05016
.5600	.04995
.5800	.04970
.6000	.04930
.6200	.04879
.6400	.04818
.6600	.04741
.6800	.04655
.7000	.04543
.7200	.04415
.7400	.04263
.7600	.04093
.7800	.03902
.8000	.03688
.8200	.03459
.8400	.03205
.8600	.02933
.8800	.02642
.9000	.02337
.9200	.02009
.9400	.01655
.9600	.01278
.9800	.00888
1.0000	.00490

TABLE I.– AIRFOIL COORDINATES – Concluded

Lower Surface

x/c	z/c
.0000	–.00002
.0004	–.00397
.0016	–.00795
.0025	–.00976
.0050	–.01353
.0100	–.01846
.0150	–.02201
.0200	–.02498
.0250	–.02753
.0300	–.02984
.0400	–.03388
.0500	–.03738
.0600	–.04043
.0700	–.04310
.0800	–.04547
.0900	–.04753
.1000	–.04940
.1200	–.05265
.1600	–.05759
.2000	–.06114
.2400	–.06340
.2800	–.06438
.3200	–.06408
.3607	–.06247
.4000	–.05962
.4400	–.05553
.4800	–.05036
.5200	–.04428
.5600	–.03762
.6000	–.03067
.6400	–.02373
.6800	–.01705
.7199	–.01064
.7600	–.00503
.8000	–.00047
.8400	.00299
.8800	.00475
.9200	.00485
.9600	.00322
1.0000	.00002

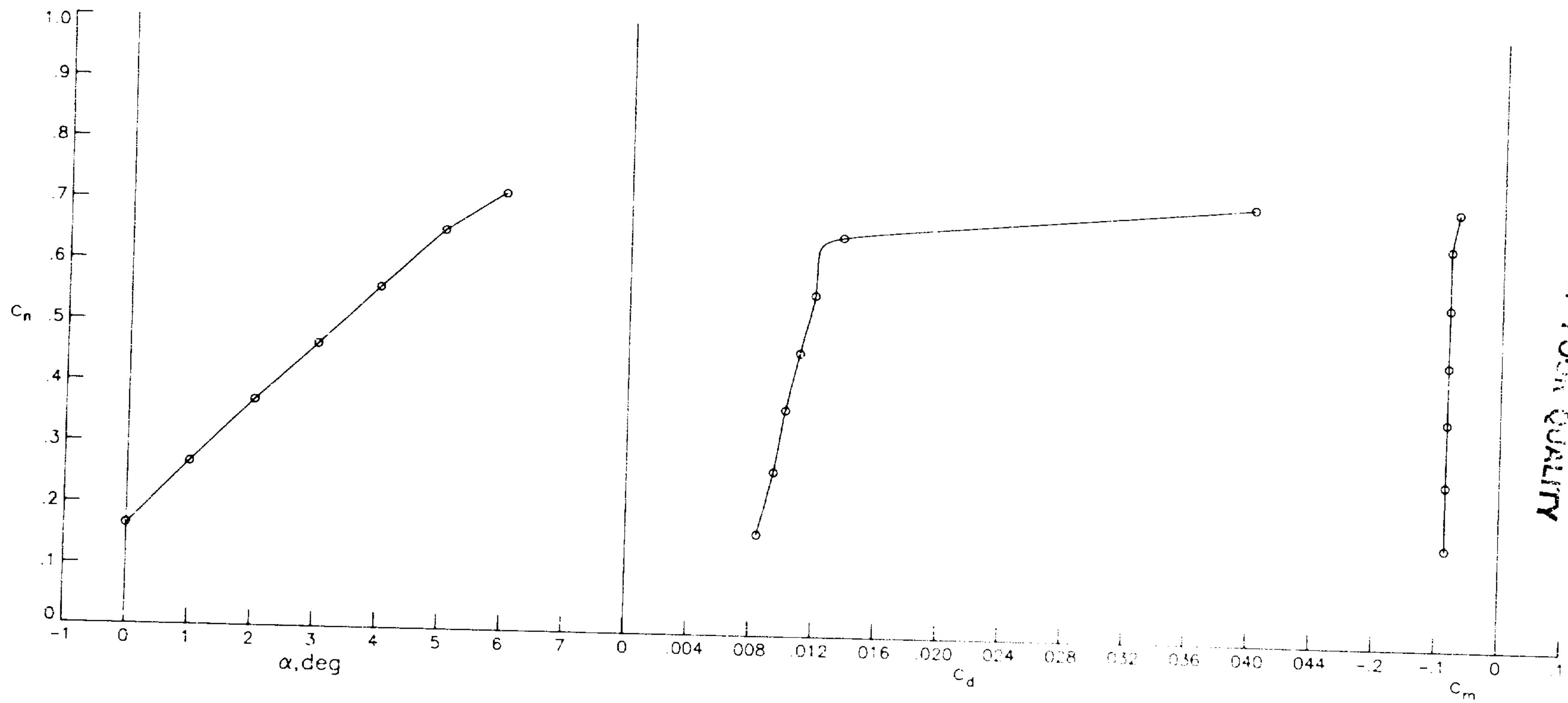

(a) $R = 1.36 \times 10^6$; $M = 0.3511$.

Figure 4.- Section characteristics for various Reynolds numbers and Mach numbers with $p_t = 1.20$ atm, $T_t = 300$ K, and fixed transition.

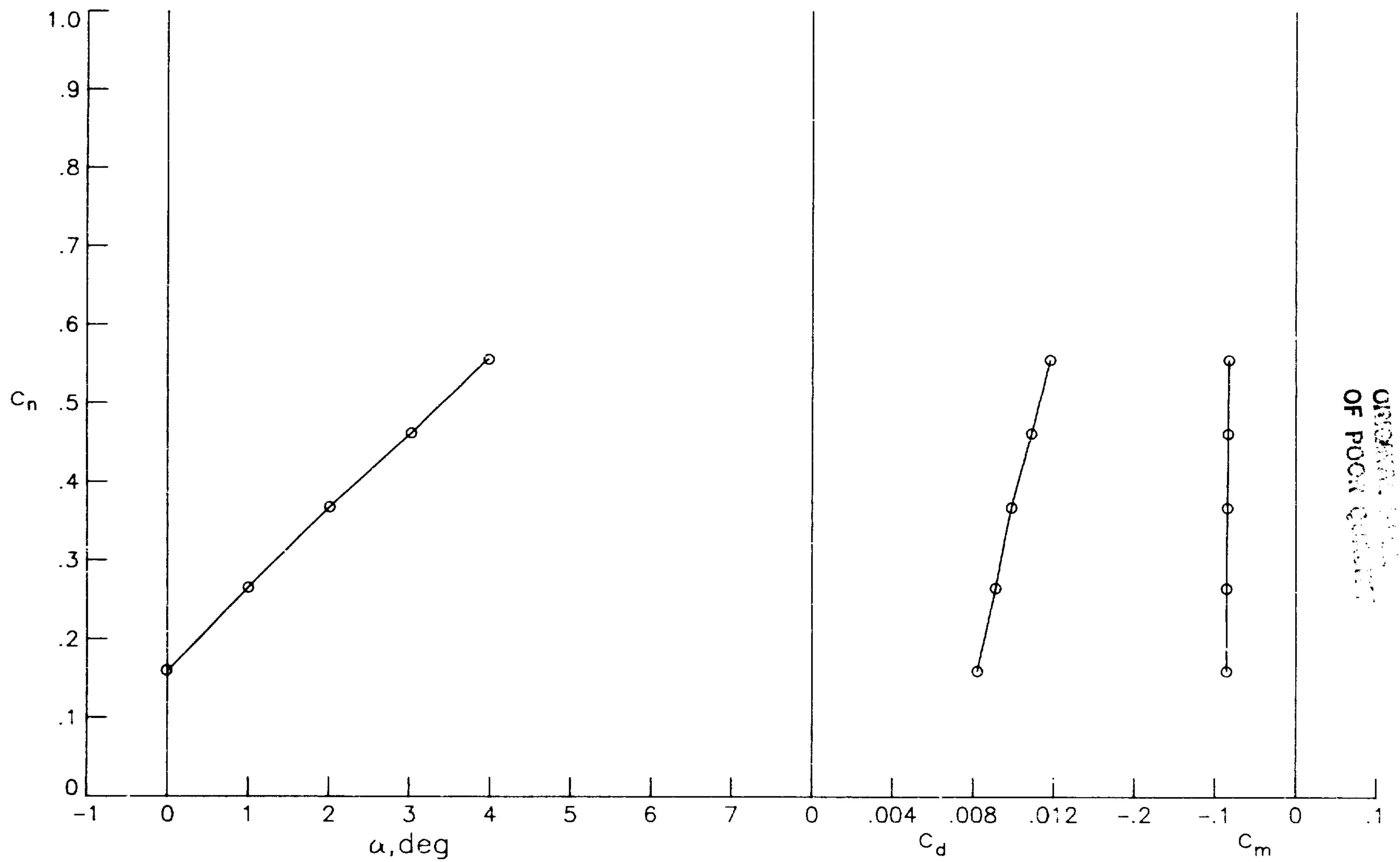

(b) $R = 1.49 \times 10^6$; $M = 0.3913$.

Figure 4.- Continued.

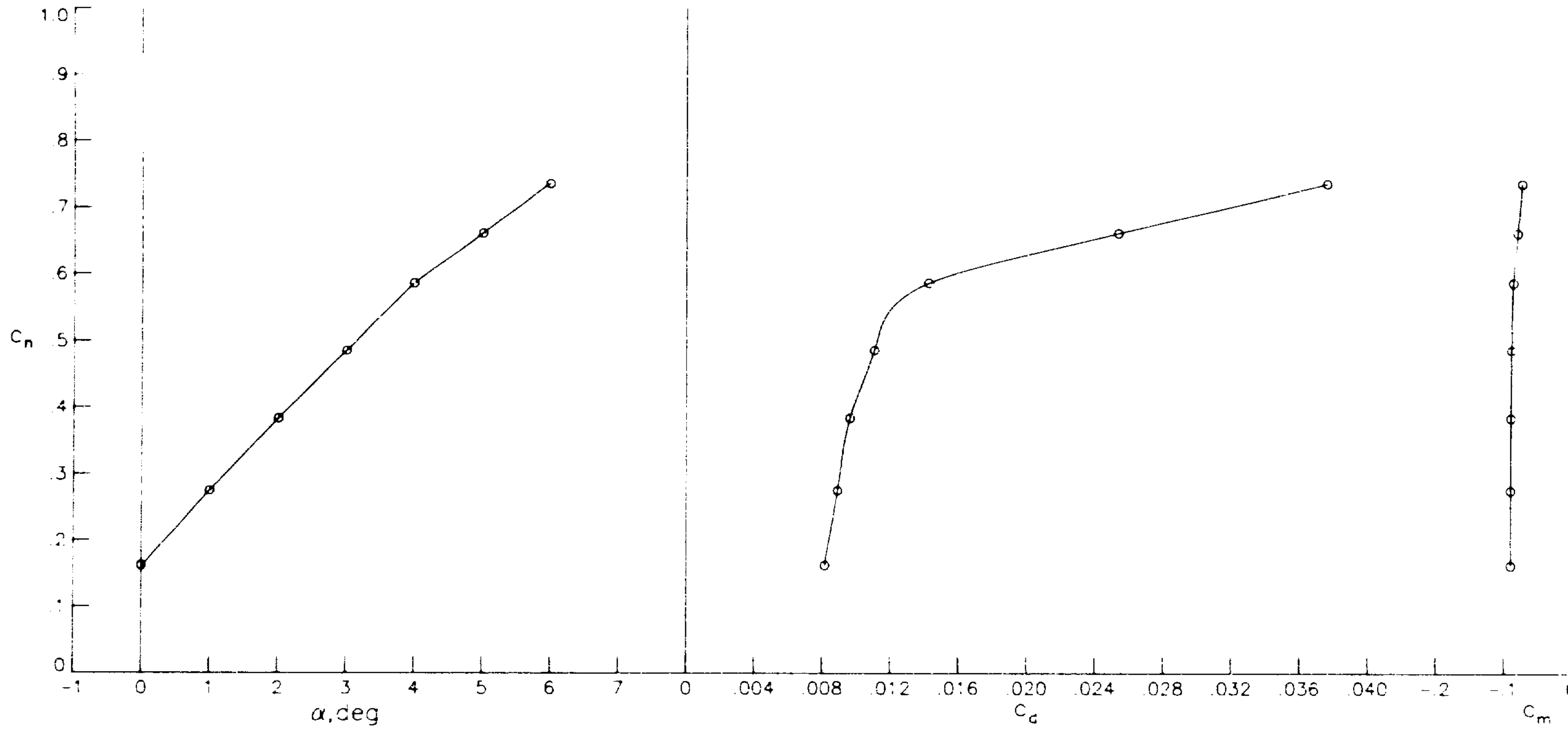

(c) $R = 1.86 \times 10^6$; $M = 0.5005$.

Figure 4.- Continued.

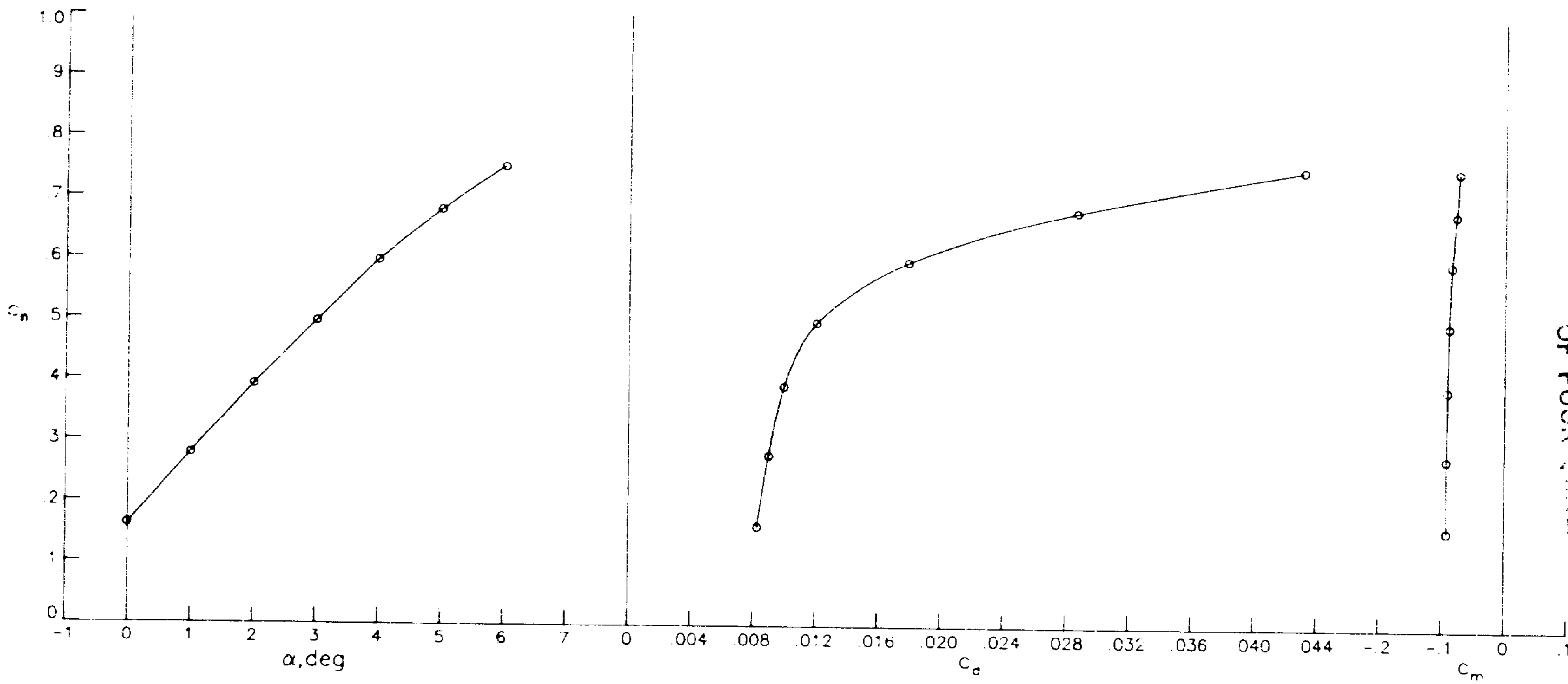

(d) $R = 1.99 \times 10^6$; $M = 0.5492$.

Figure 4.- Continued.

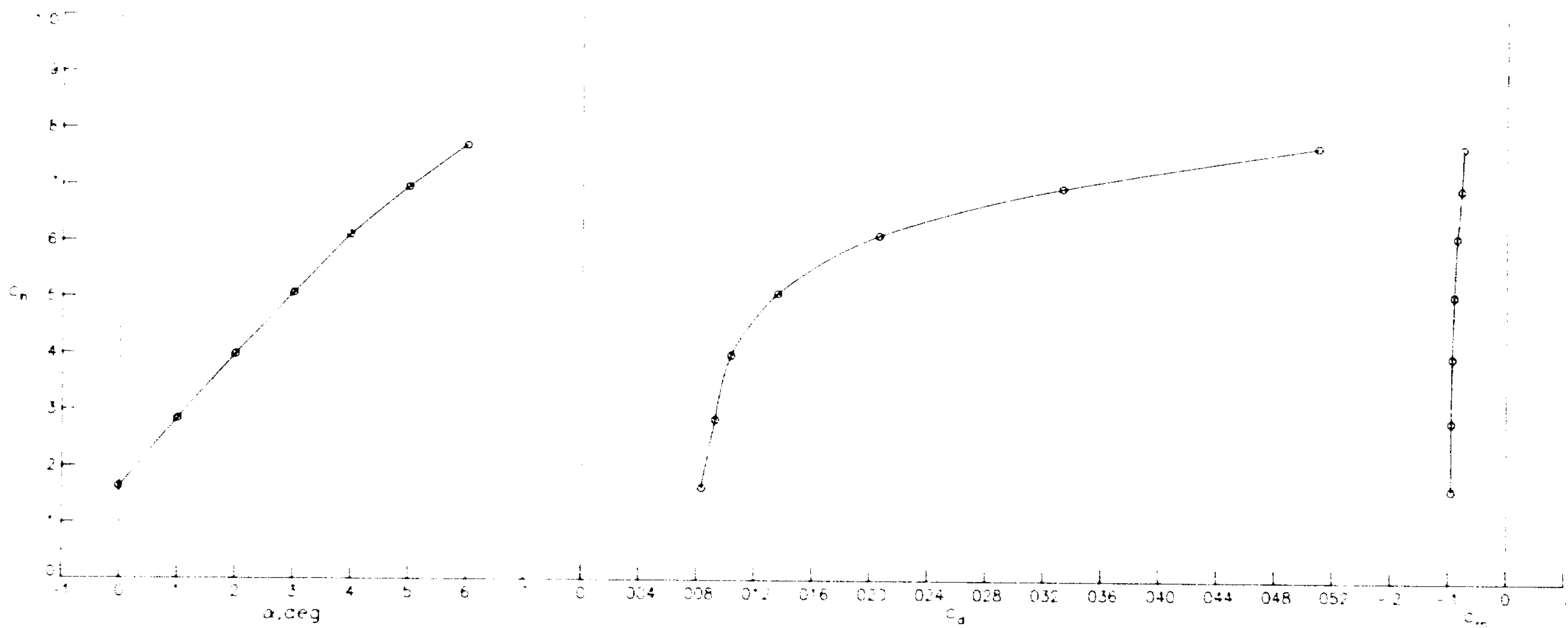

(e) $R = 2.11 \times 10^6$; $M = 0.5974$.

Figure 4.- Continued.

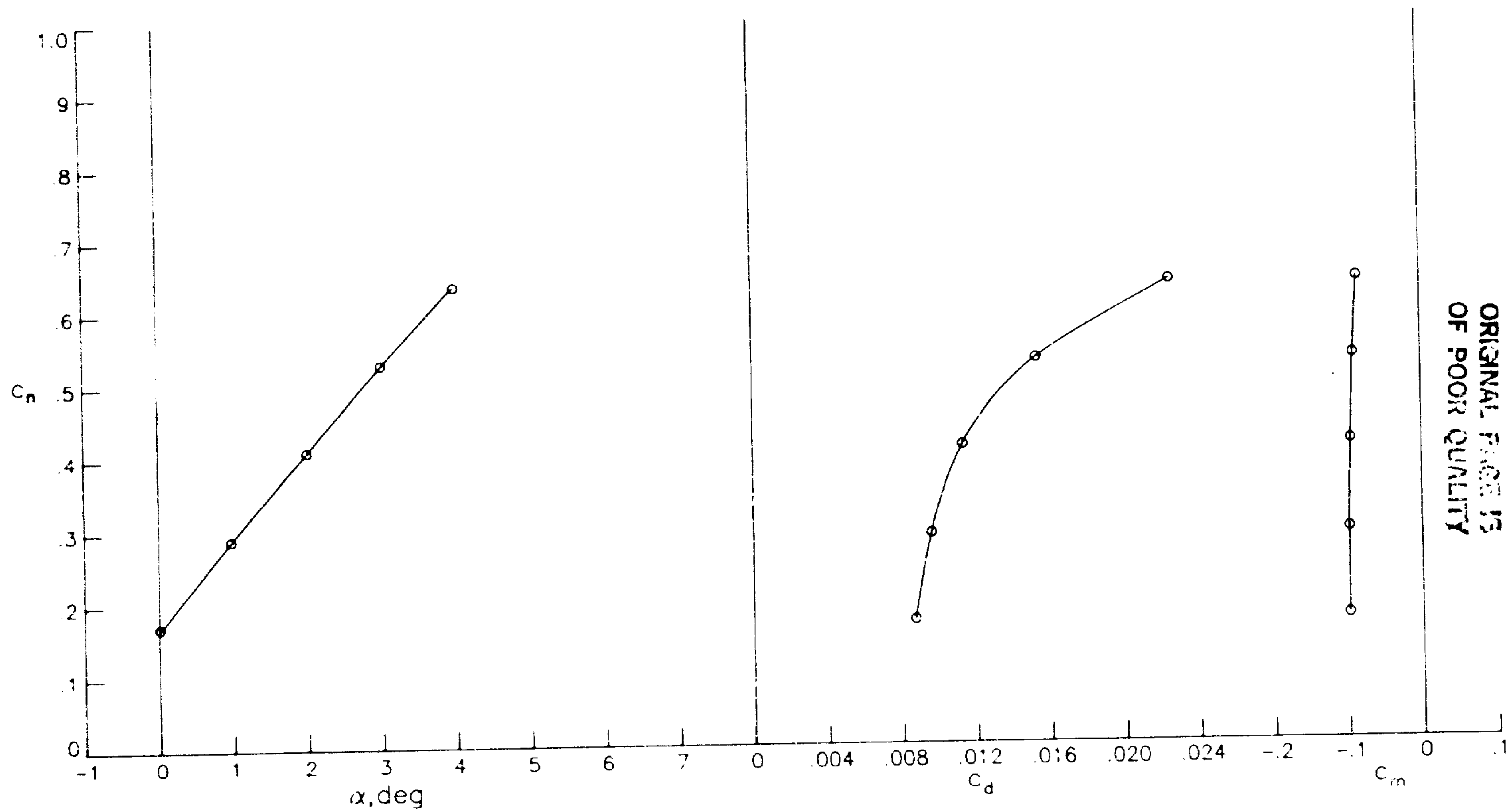

(f) R = 2.23 × 10^6; M = 0.6474.

Figure 4.- Concluded.

ORIGINAL PAGE IS
OF POOR QUALITY

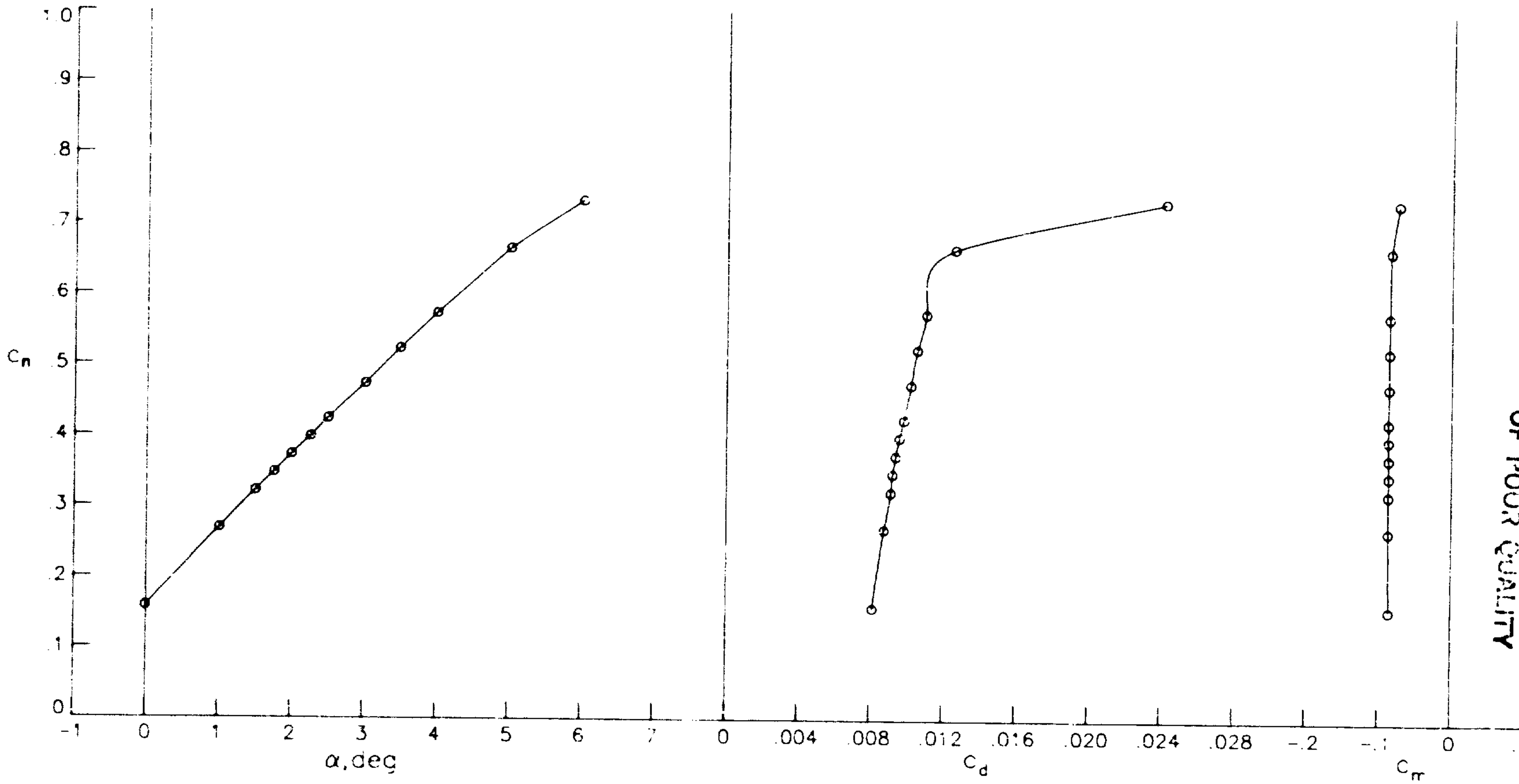

(a) $R = 2.20 \times 10^6$; $M = 0.4019$.

Figure 5.- Section characteristics for various Reynolds numbers and Mach numbers with $p_t = 1.20$ atm, $T_t = 227$ K, and fixed transition.

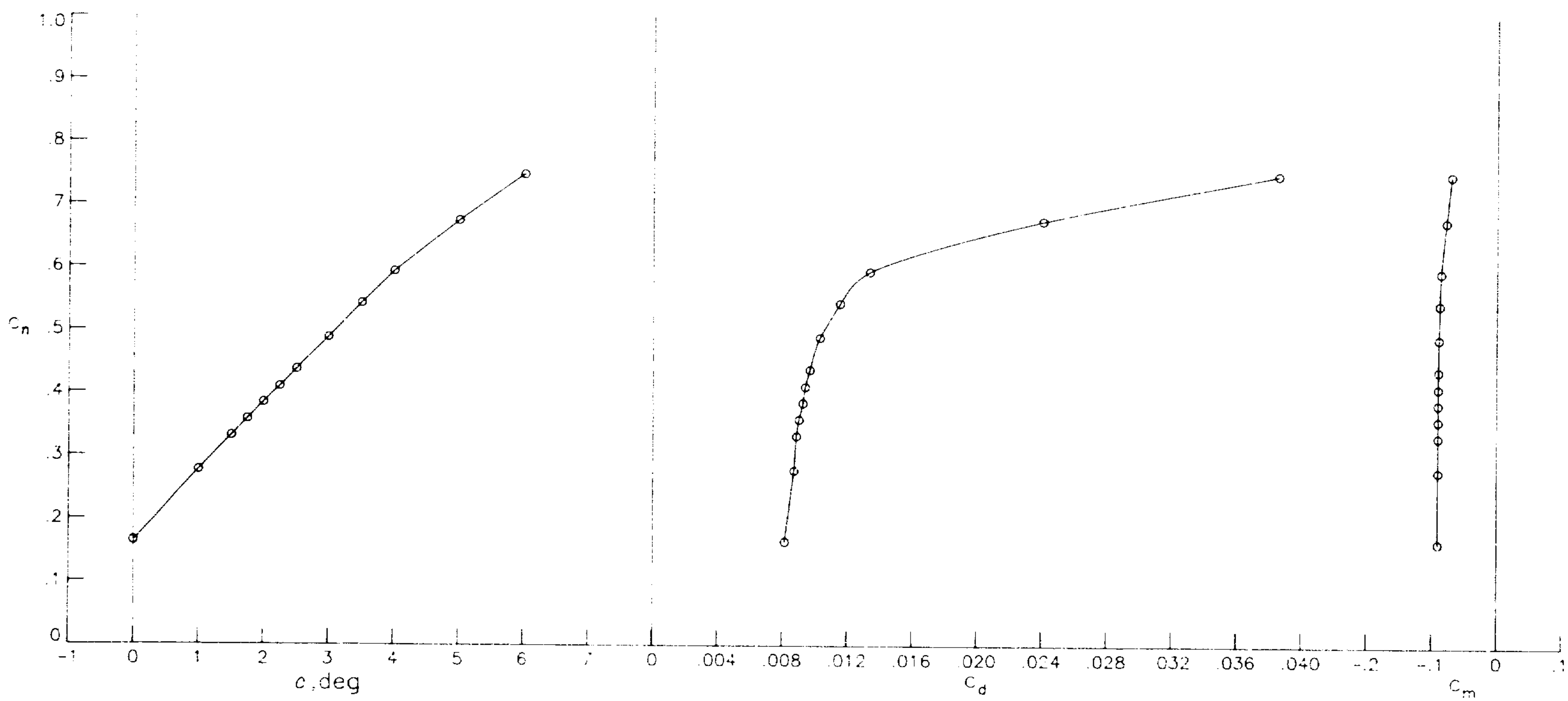

(b) $R = 2.66 \times 10^6$; $M = 0.4991$.

Figure 5.- Continued.

ORIGINAL PAGE IS
OF POOR QUALITY

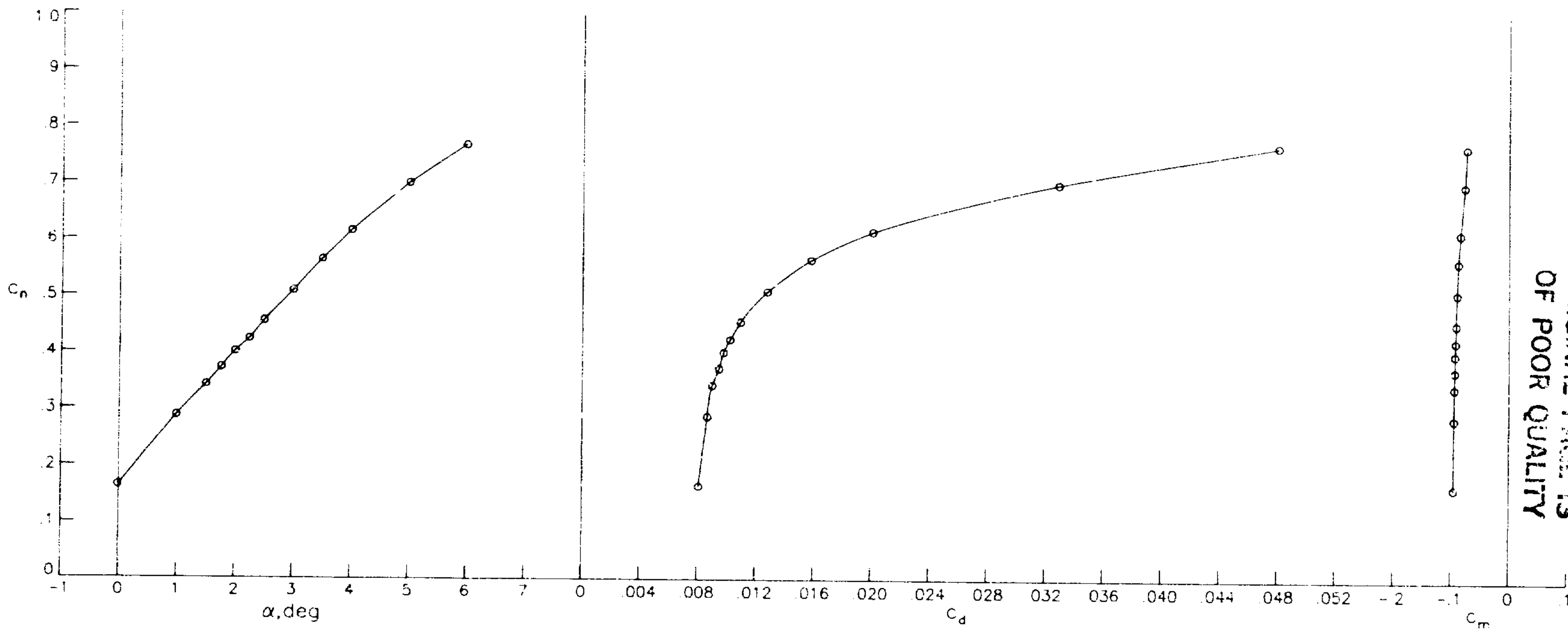

(c) $R = 3.06 \times 10^6$; $M = 0.5991$.

Figure 5.- Continued.

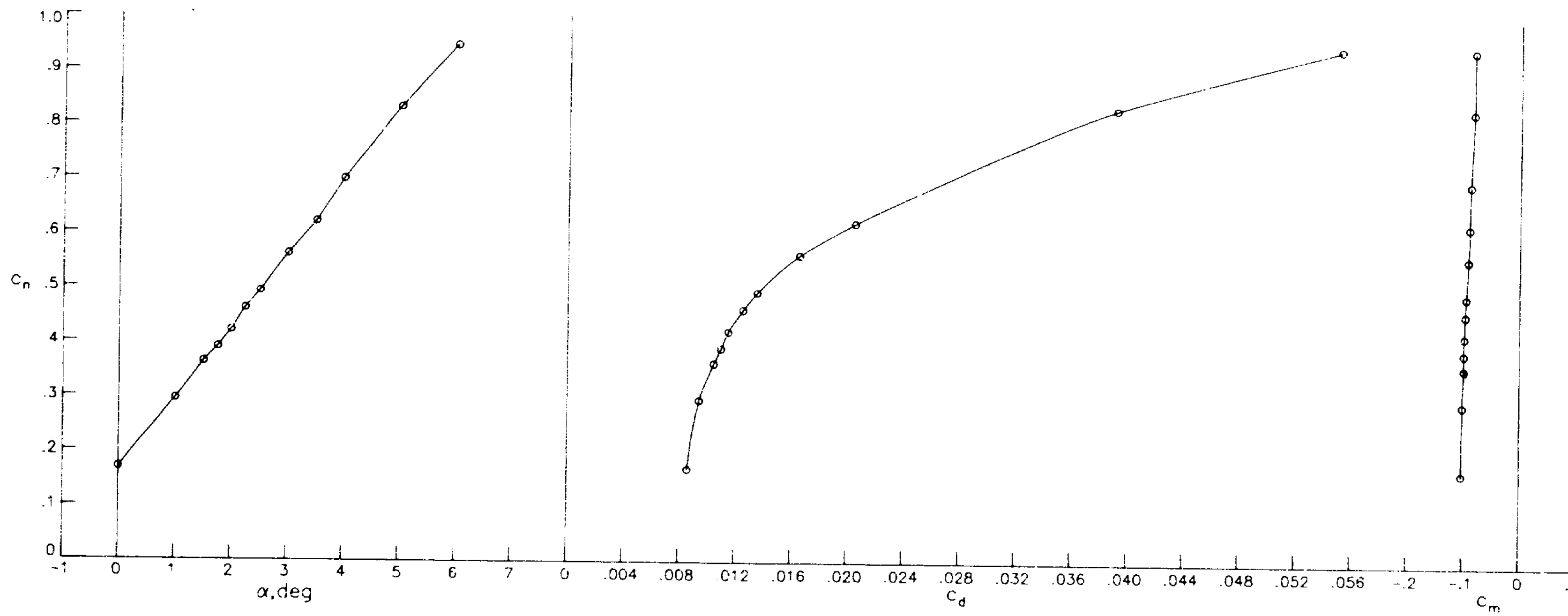

(d) $R = 3.38 \times 10^6$; $M = 0.6974$.

Figure 5.- Continued.

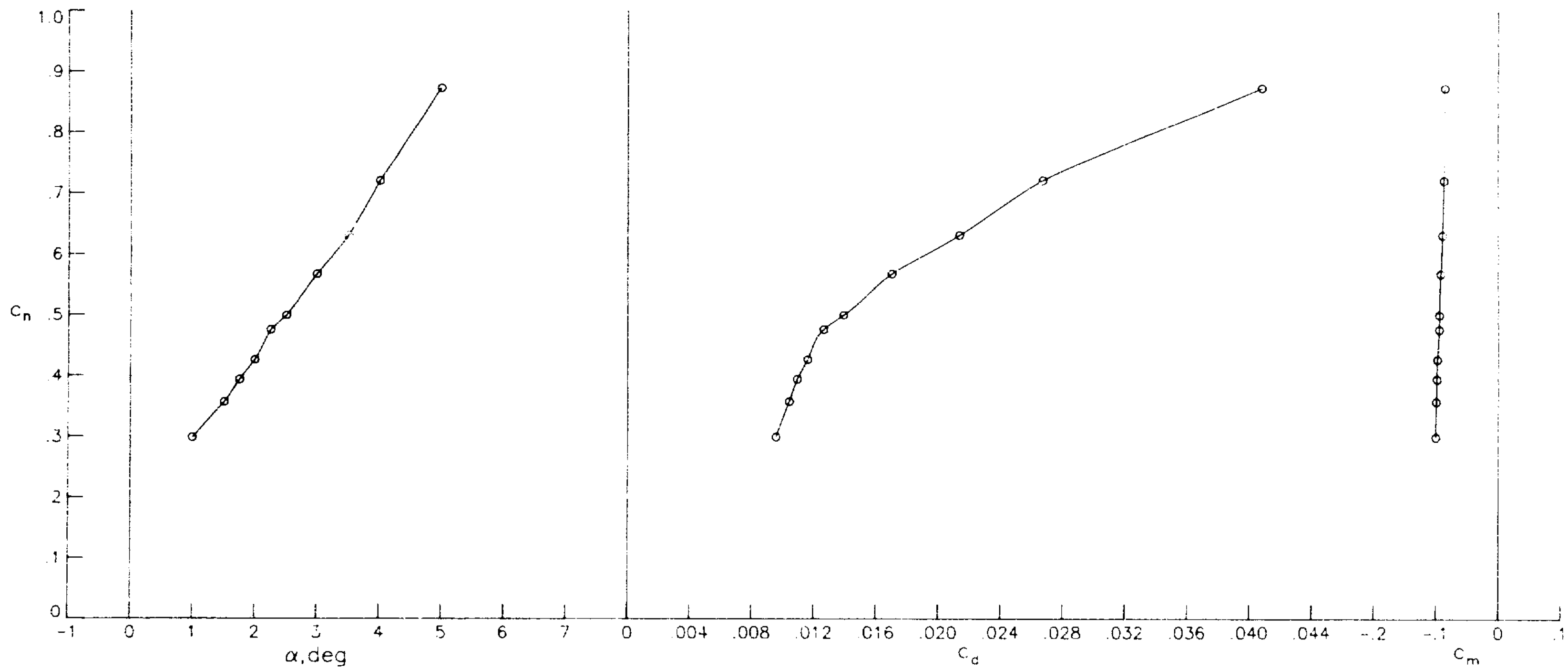

(e) $R = 3.44 \times 10^6$; $M = 0.7156$.

Figure 5.- Continued.

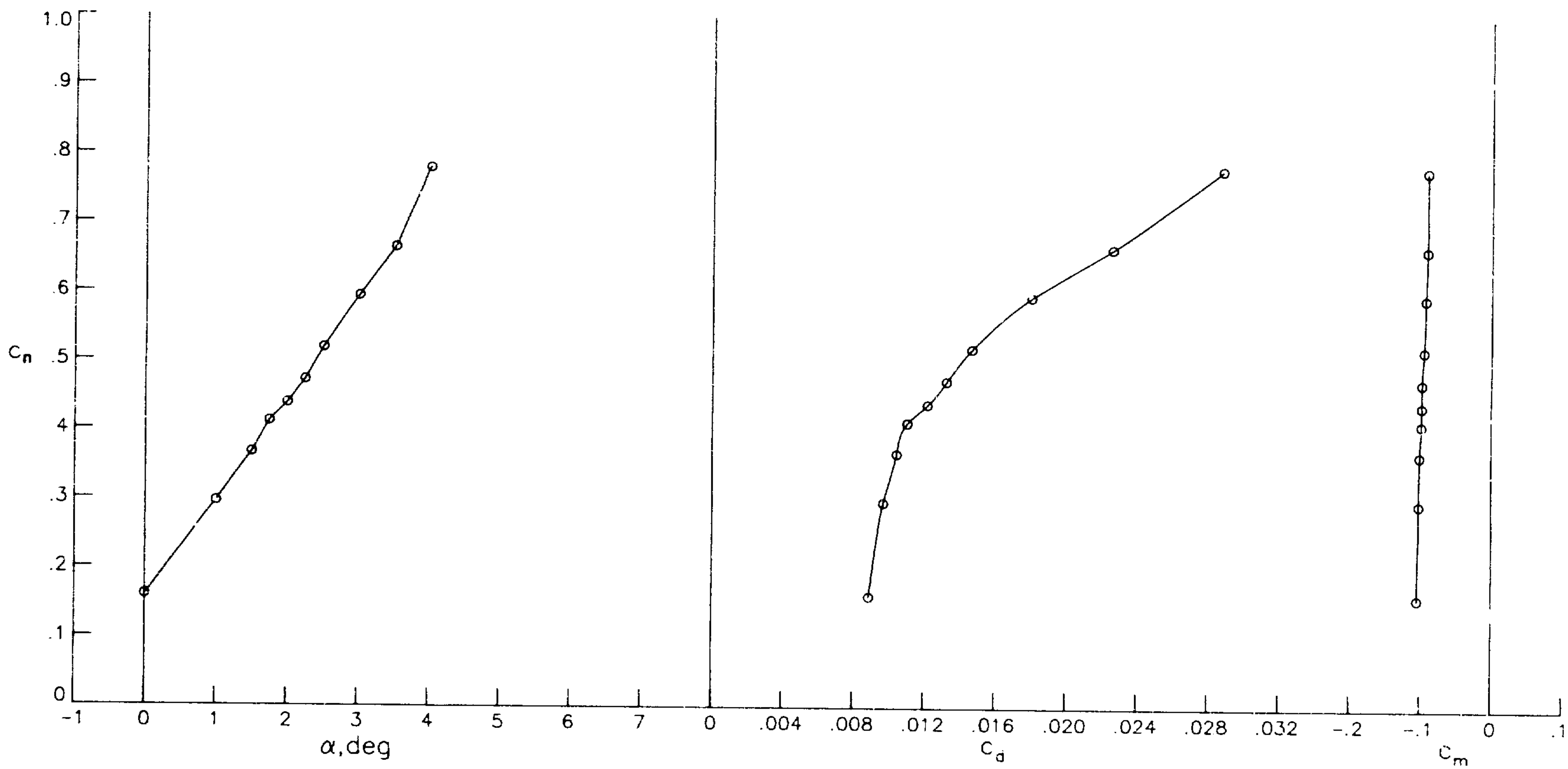

(f) $R = 3.49 \times 10^6$; $M = 0.7358$.

Figure 5.- Continued.

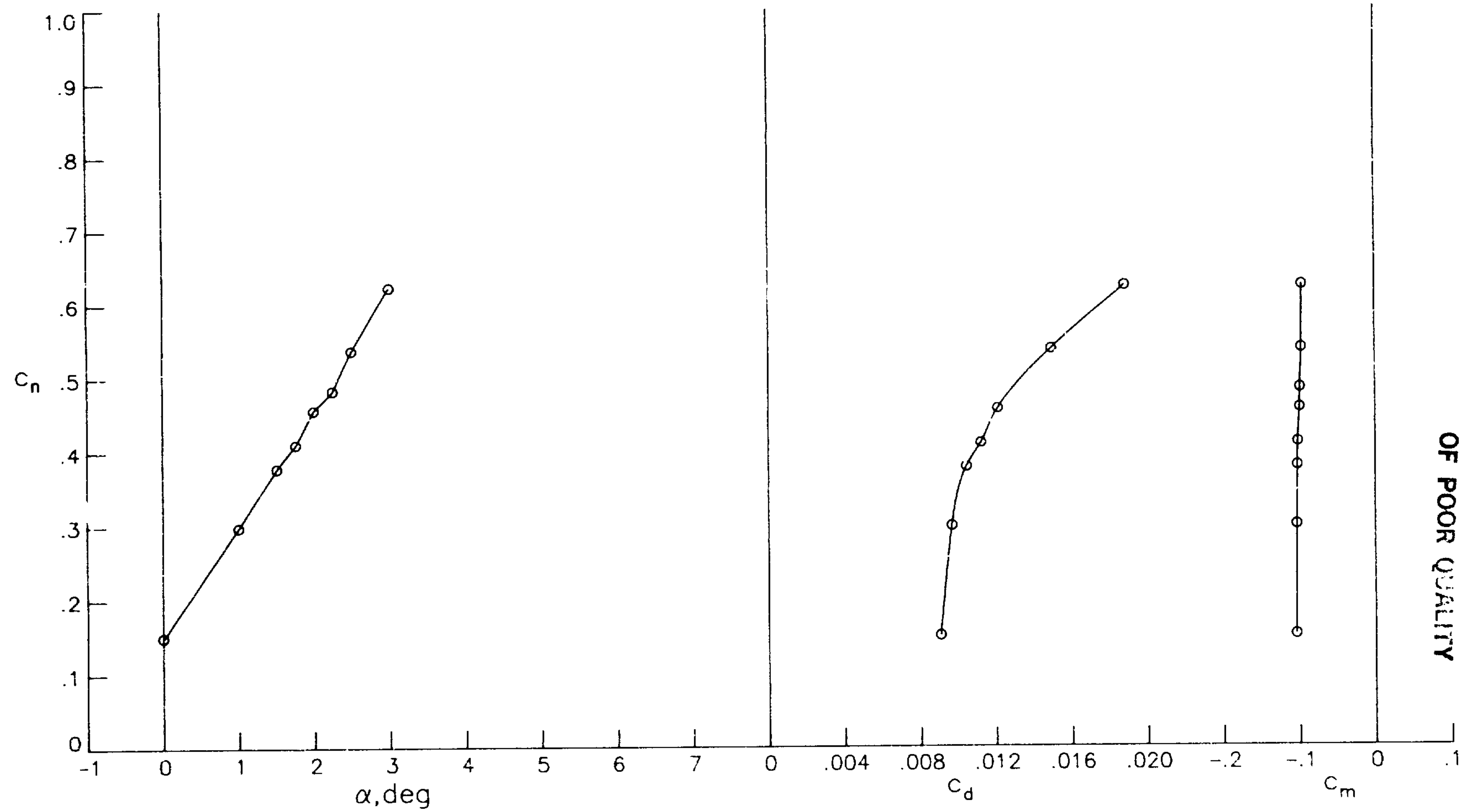

(g) $R = 3.55 \times 10^6$; $M = 0.7553$.

Figure 5.- Continued.

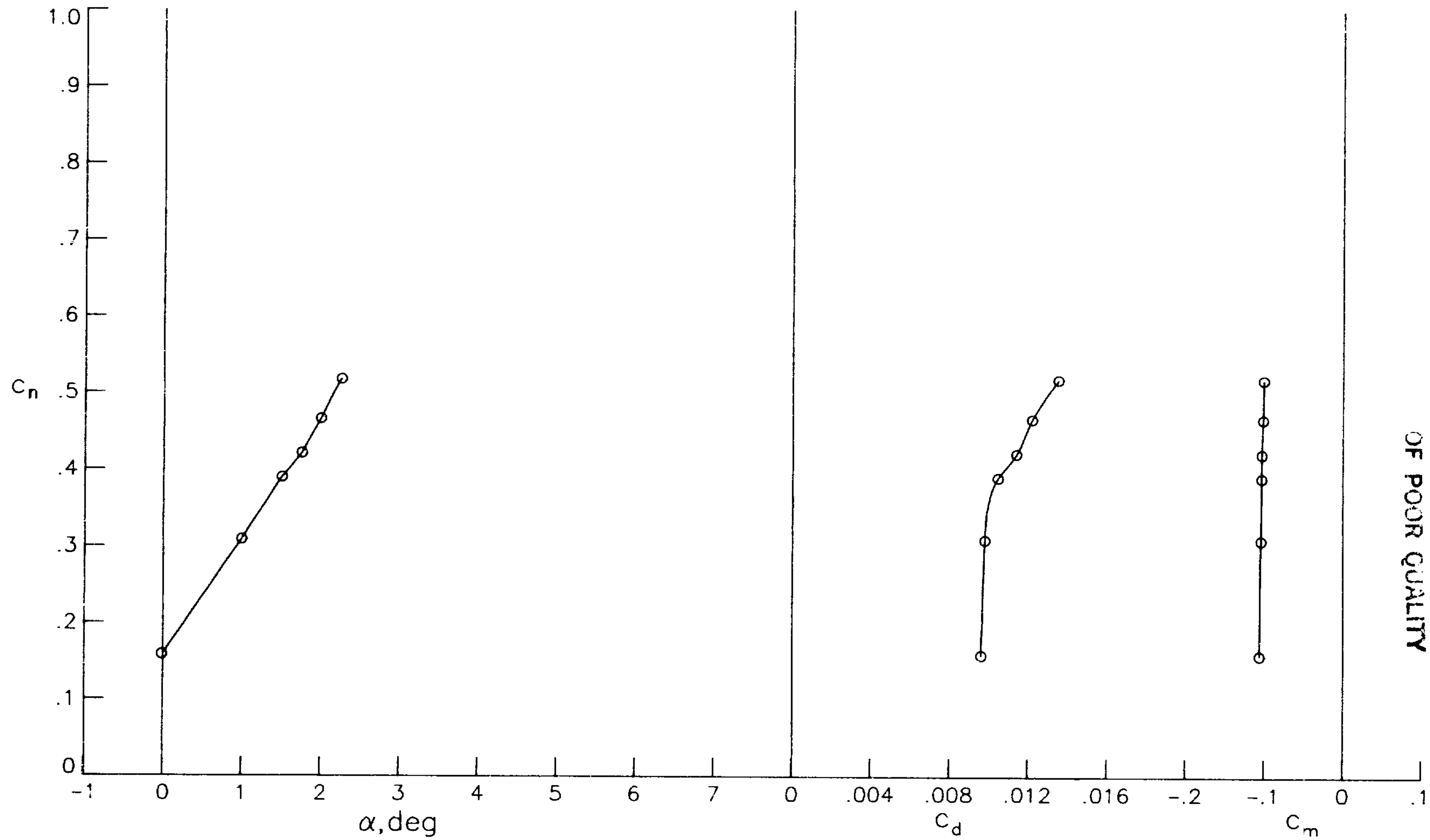

(h) $R = 3.60 \times 10^6$; $M = 0.7763$.

Figure 5.- Concluded.

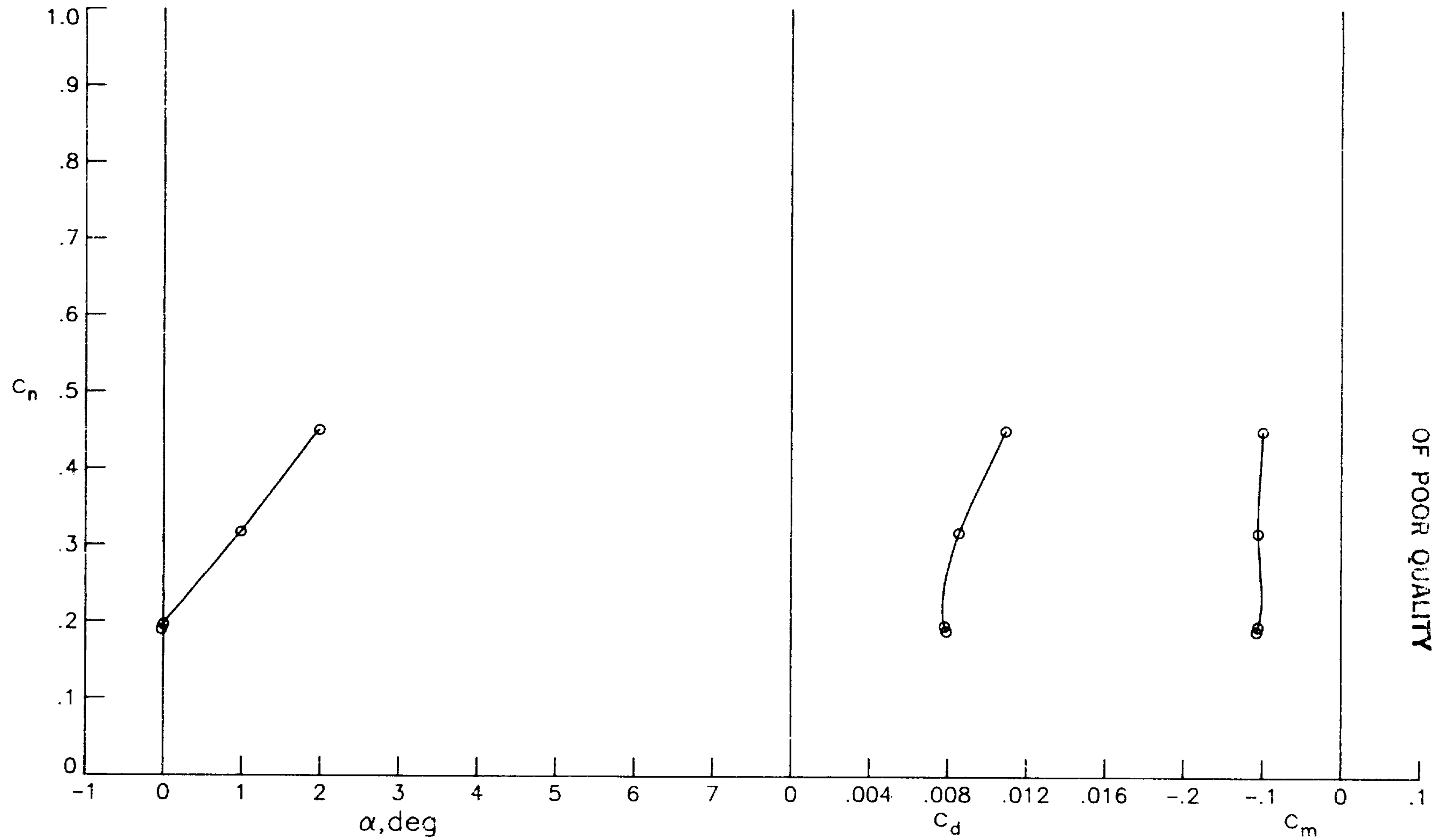

(a) $R = 3.60 \times 10^6$; $M = 0.6977$; $p_t = 1.69$ atm; $T_t = 280$ K.

Figure 6.- Section characteristics for two different values of Reynolds number, Mach number, total pressure, and total temperature with free transition.

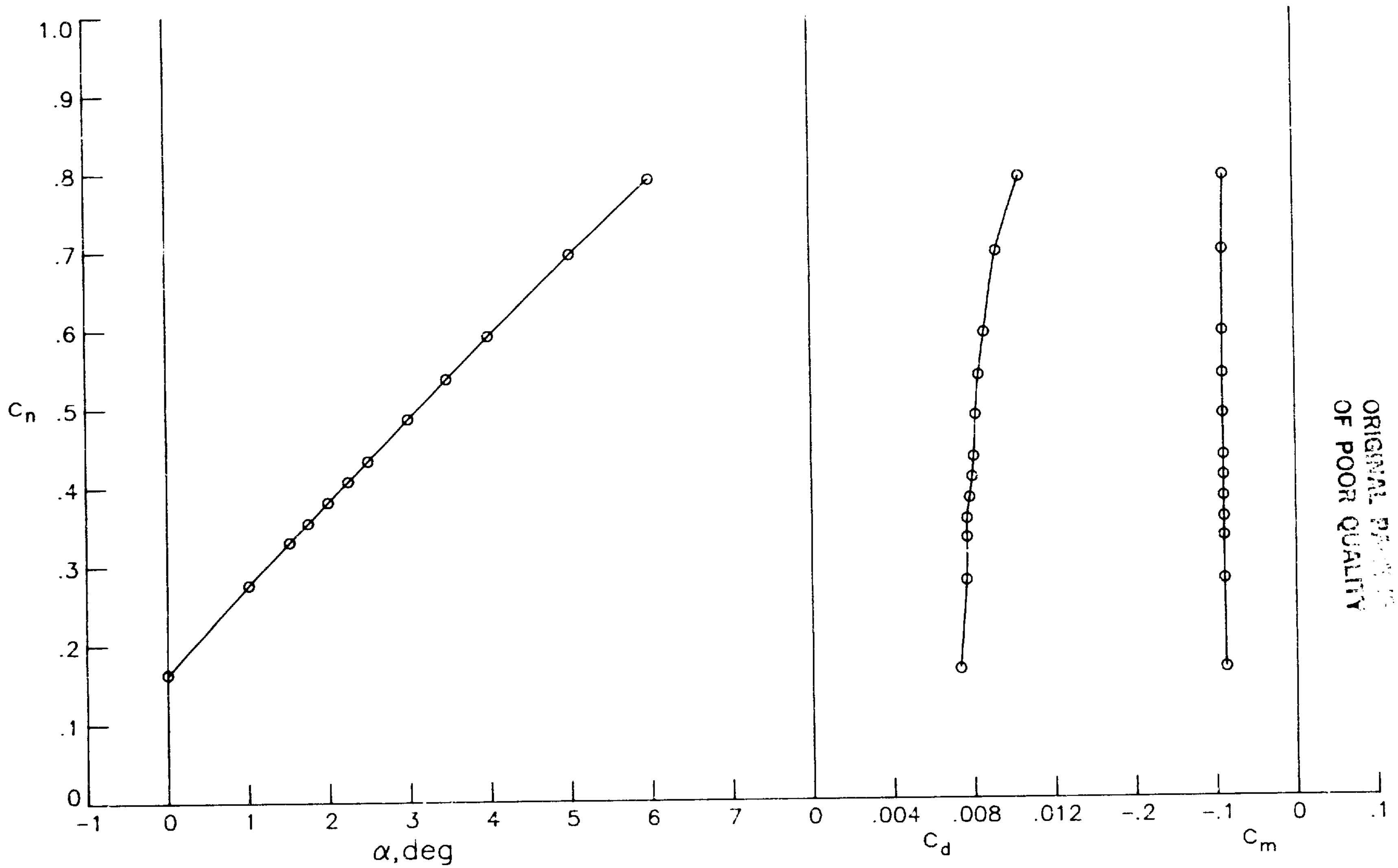

(b) $R = 6.27 \times 10^6$; $M = 0.3989$; $p_t = 3.47$; $T_t = 230$ K.

Figure 6.- Concluded.

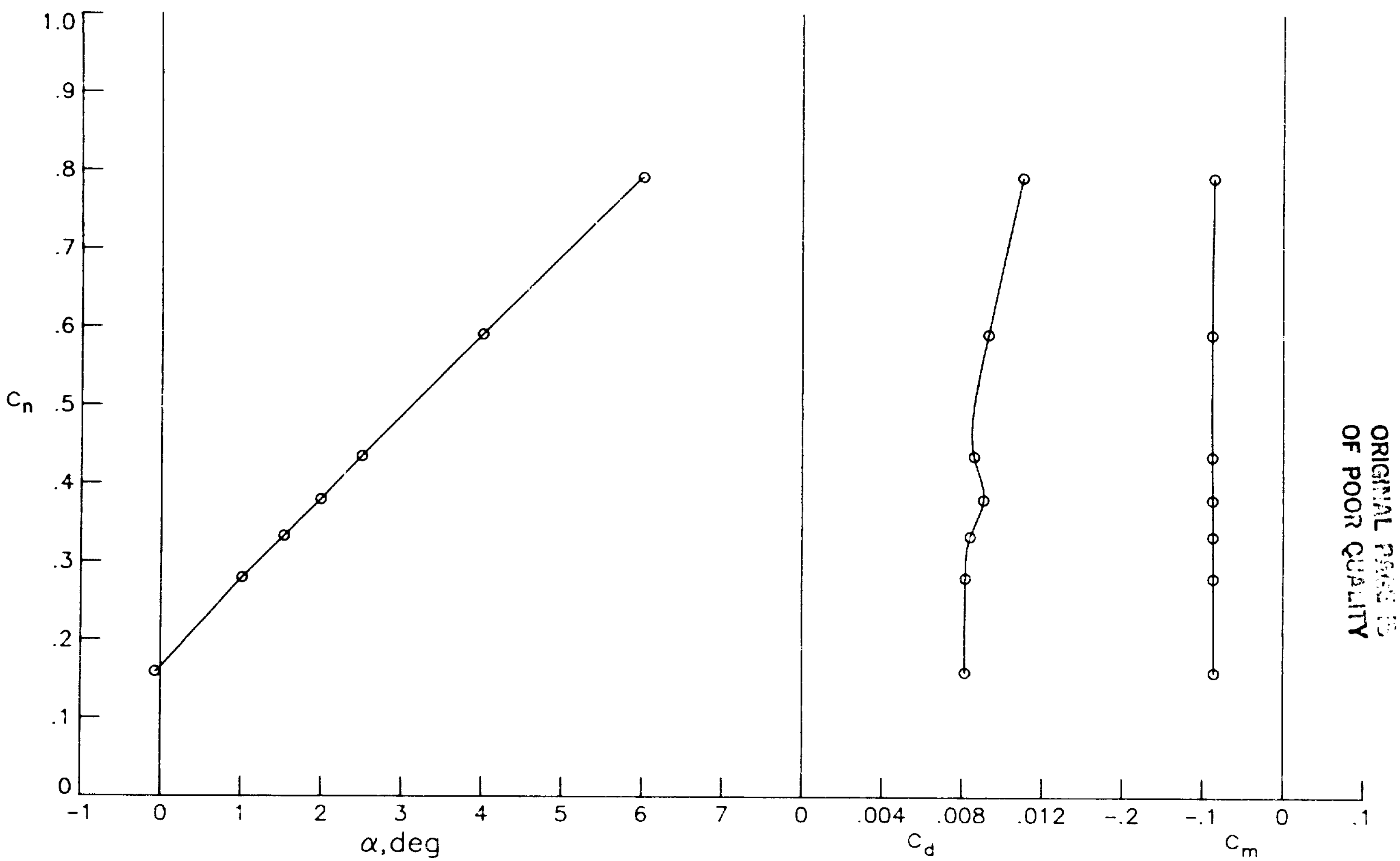

(a) R = 7.02 × 10^6; M = 0.3980.

Figure 7.- Section characteristics at Reynolds numbers of 7 × 10^6.

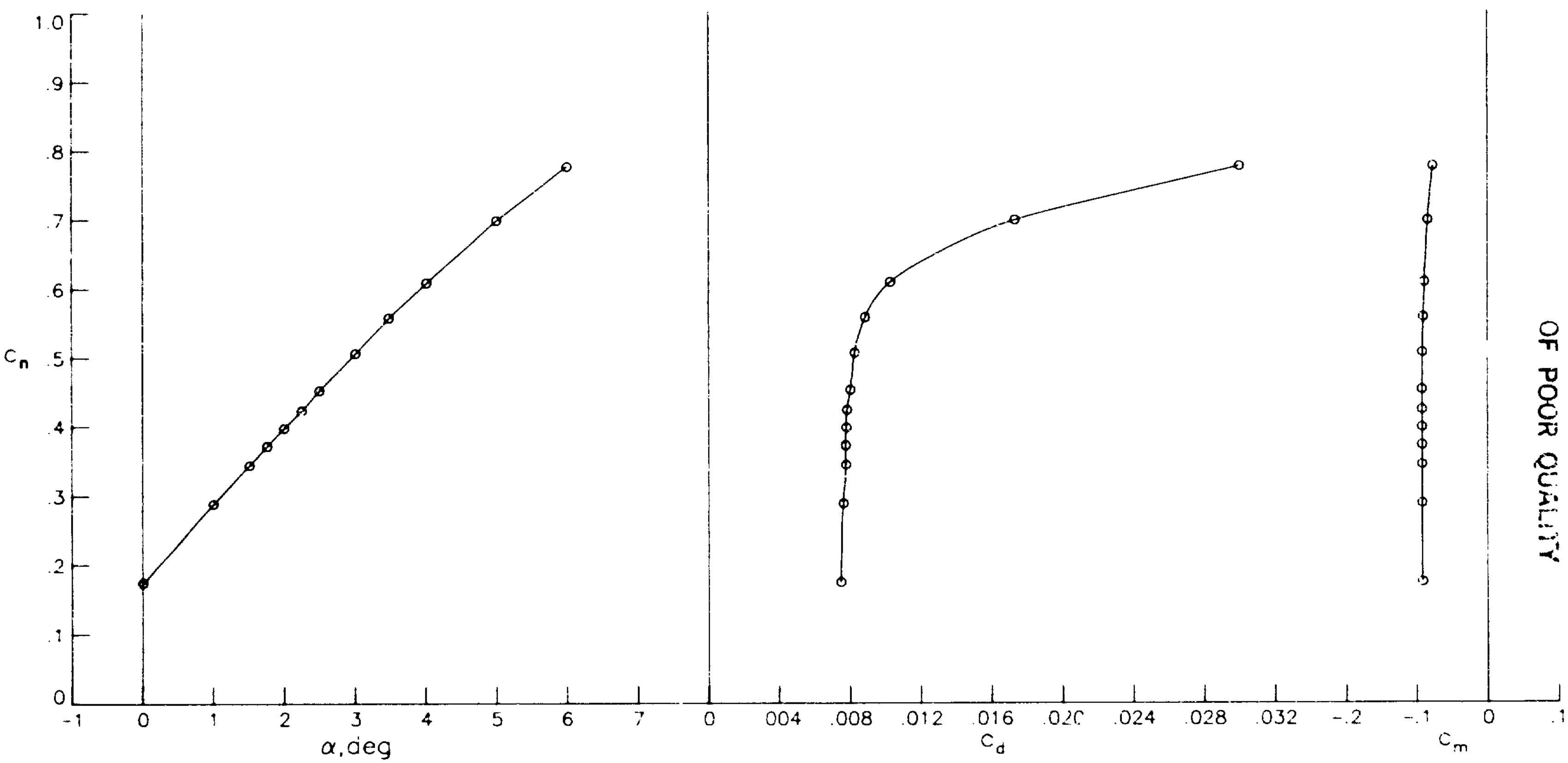

(b) $R = 7.07 \times 10^6$; $M = 0.4986$.

Figure 7.- Continued.

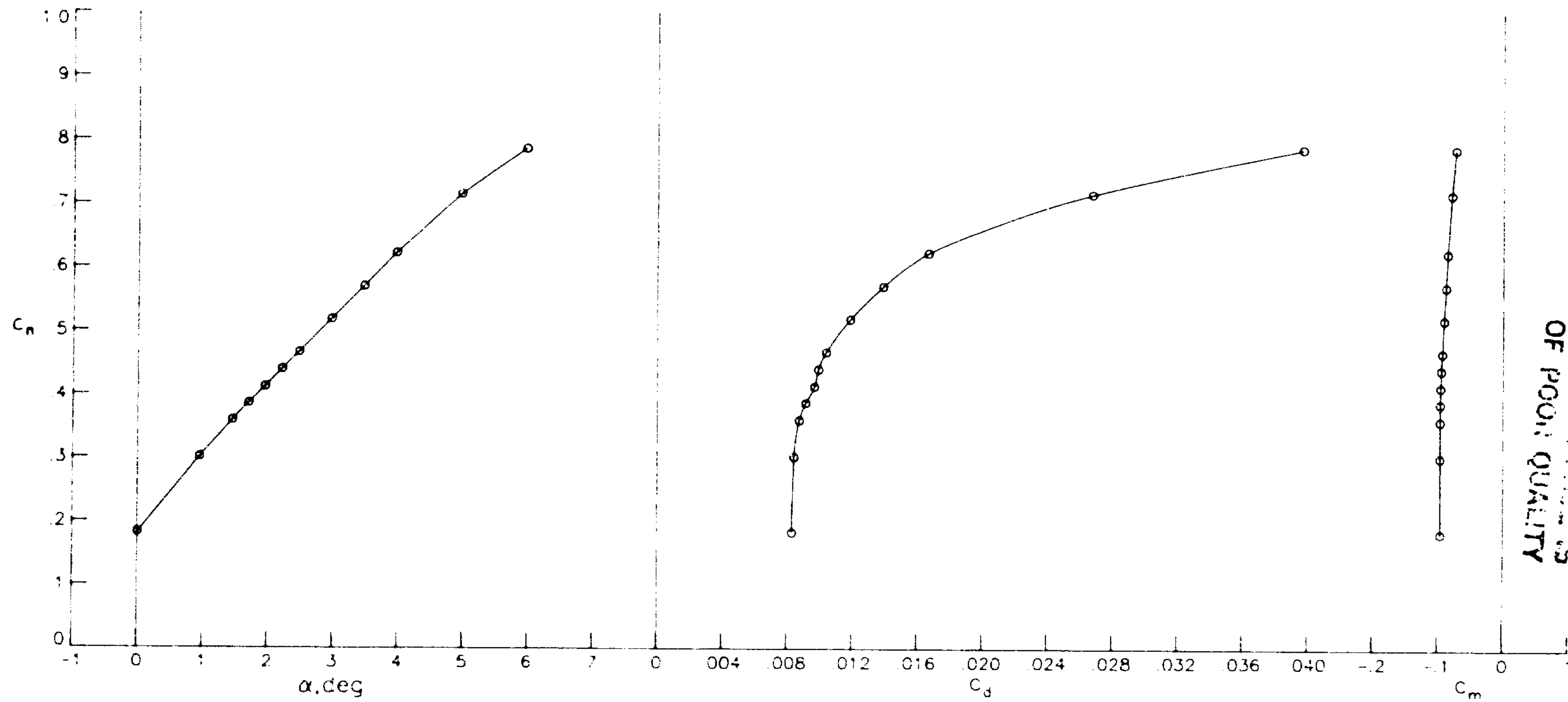

(c) $R = 6.99 \times 10^6$; $M = 0.5960$.

Figure 7.- Continued.

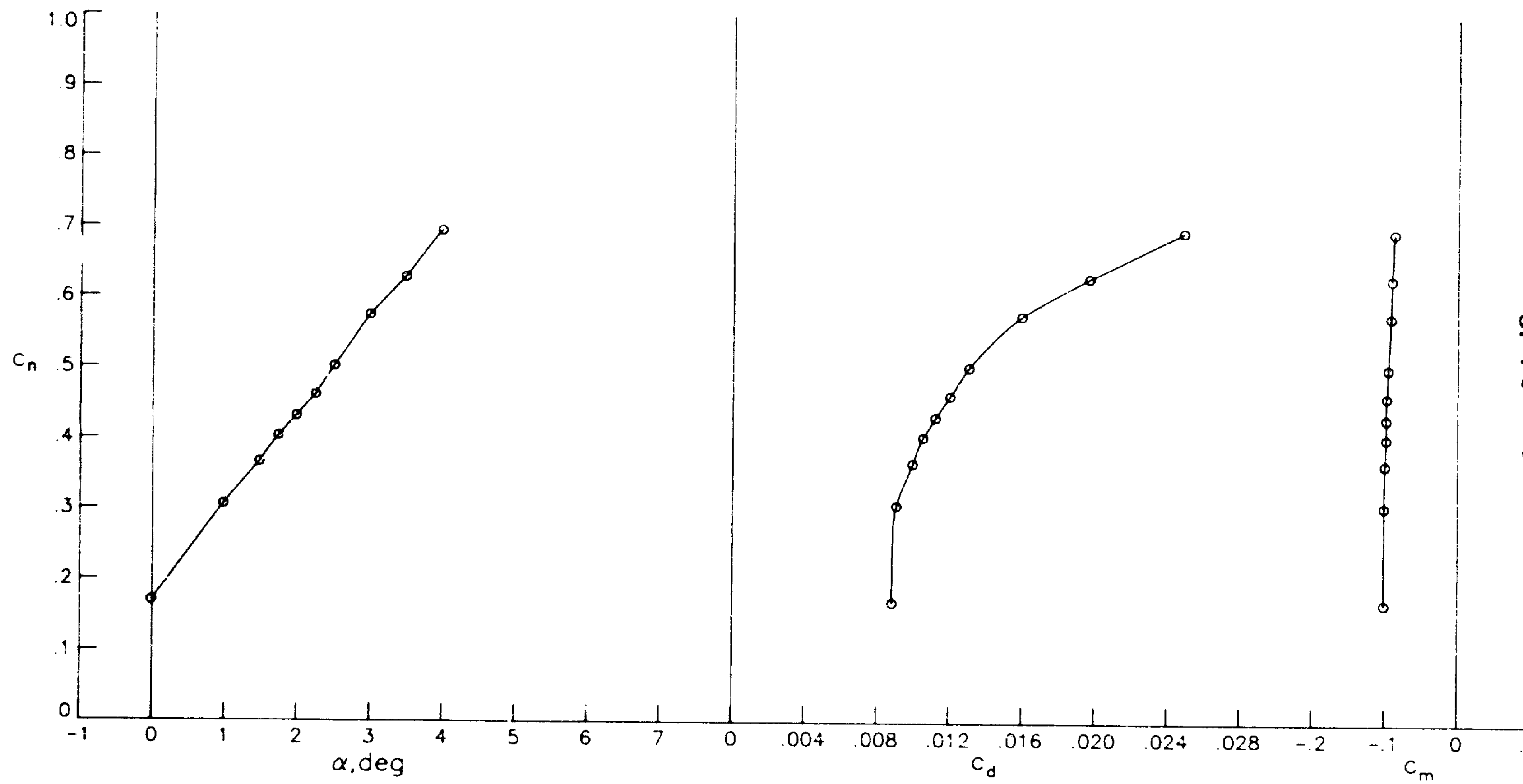

(d) $R = 7.04 \times 10^6$; $M = 0.6944$.

Figure 7.- Continued.

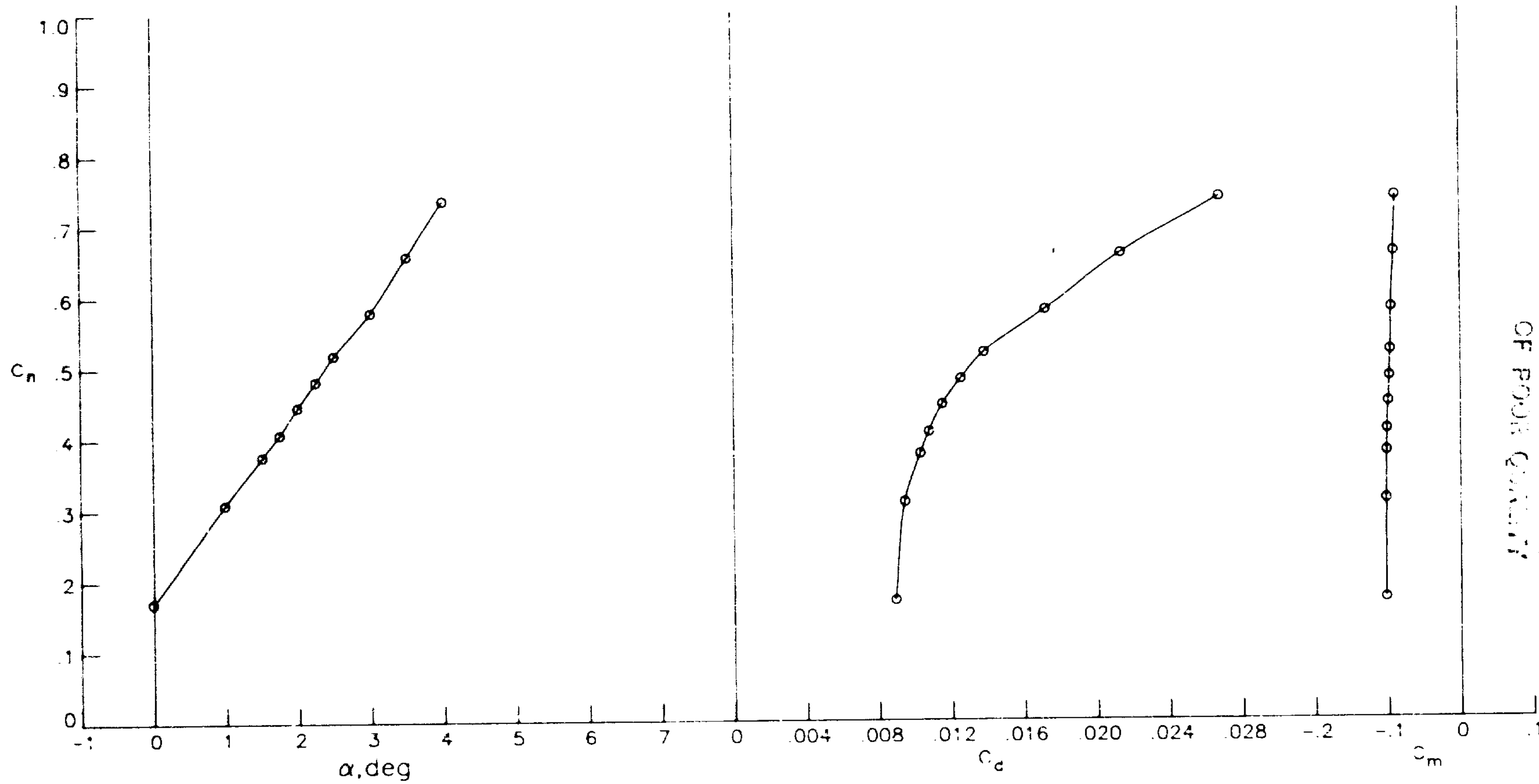

(e) $R = 7.03 \times 10^6$; $M = 0.7143$.

Figure 7.- Continued.

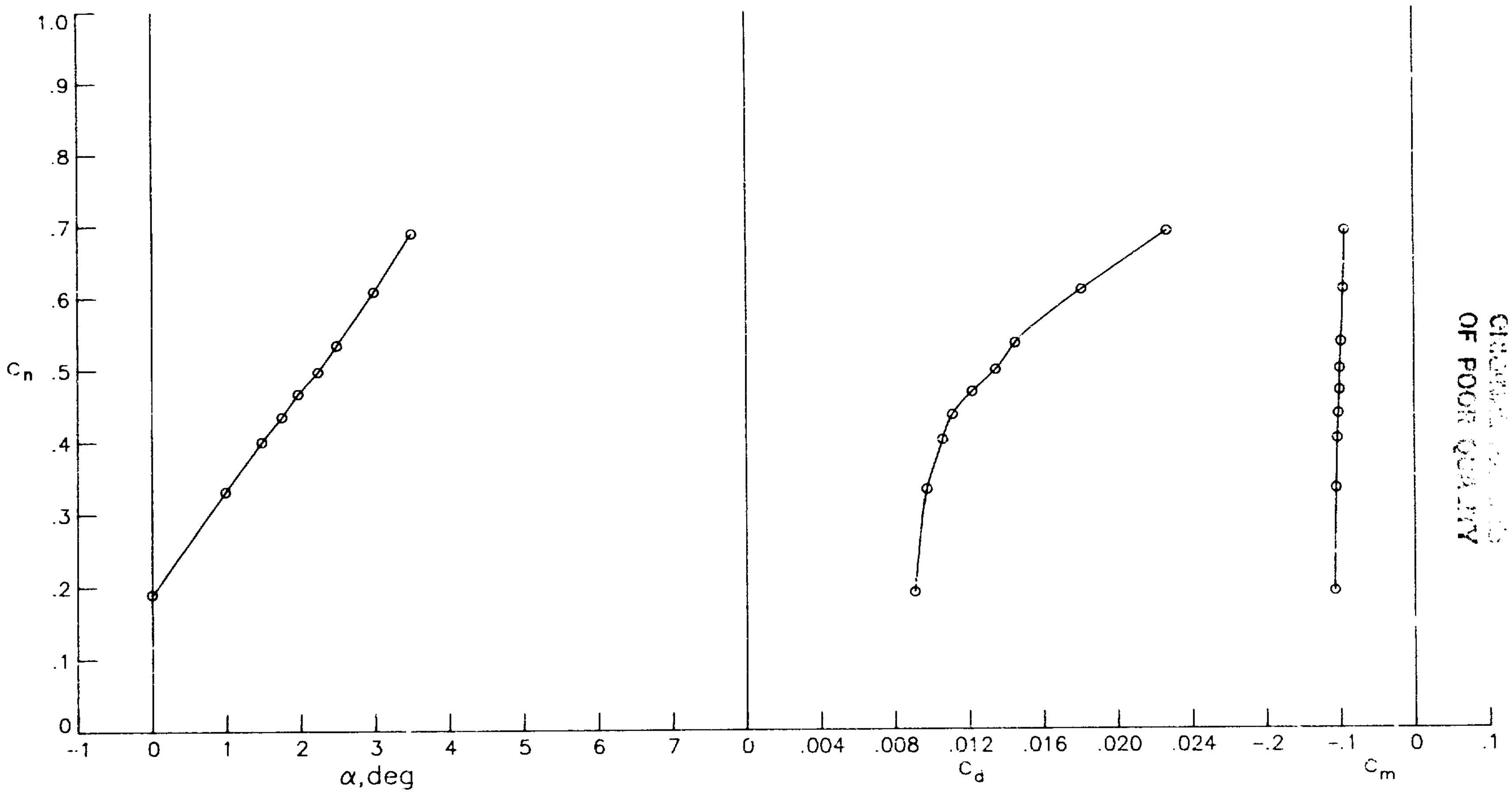

(f) $R = 7.02 \times 10^6$; $M = 0.7338$.

Figure 7.- Continued.

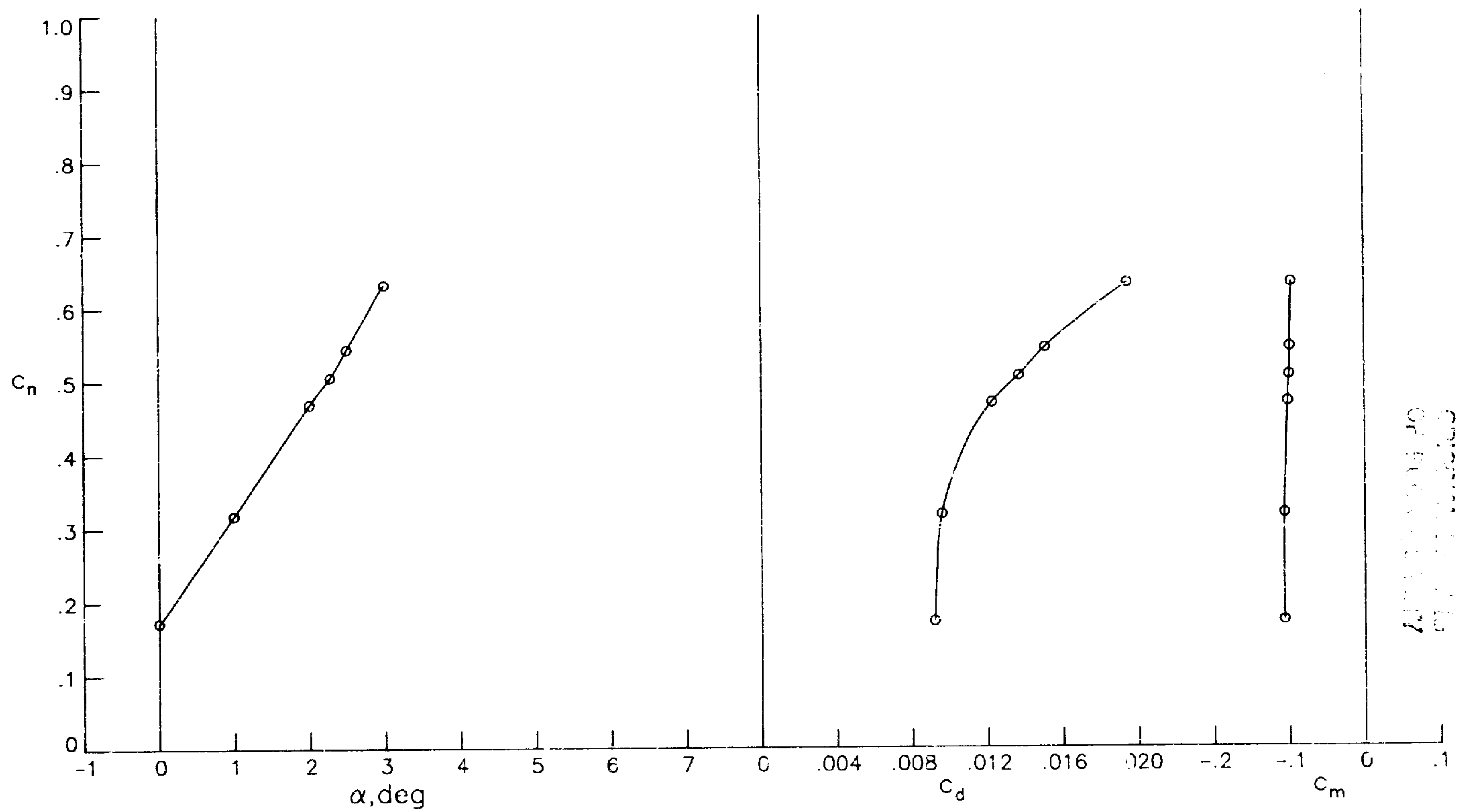

(g) $R = 7.02 \times 10^6$; $M = 0.7527$.

Figure 7.- Continued.

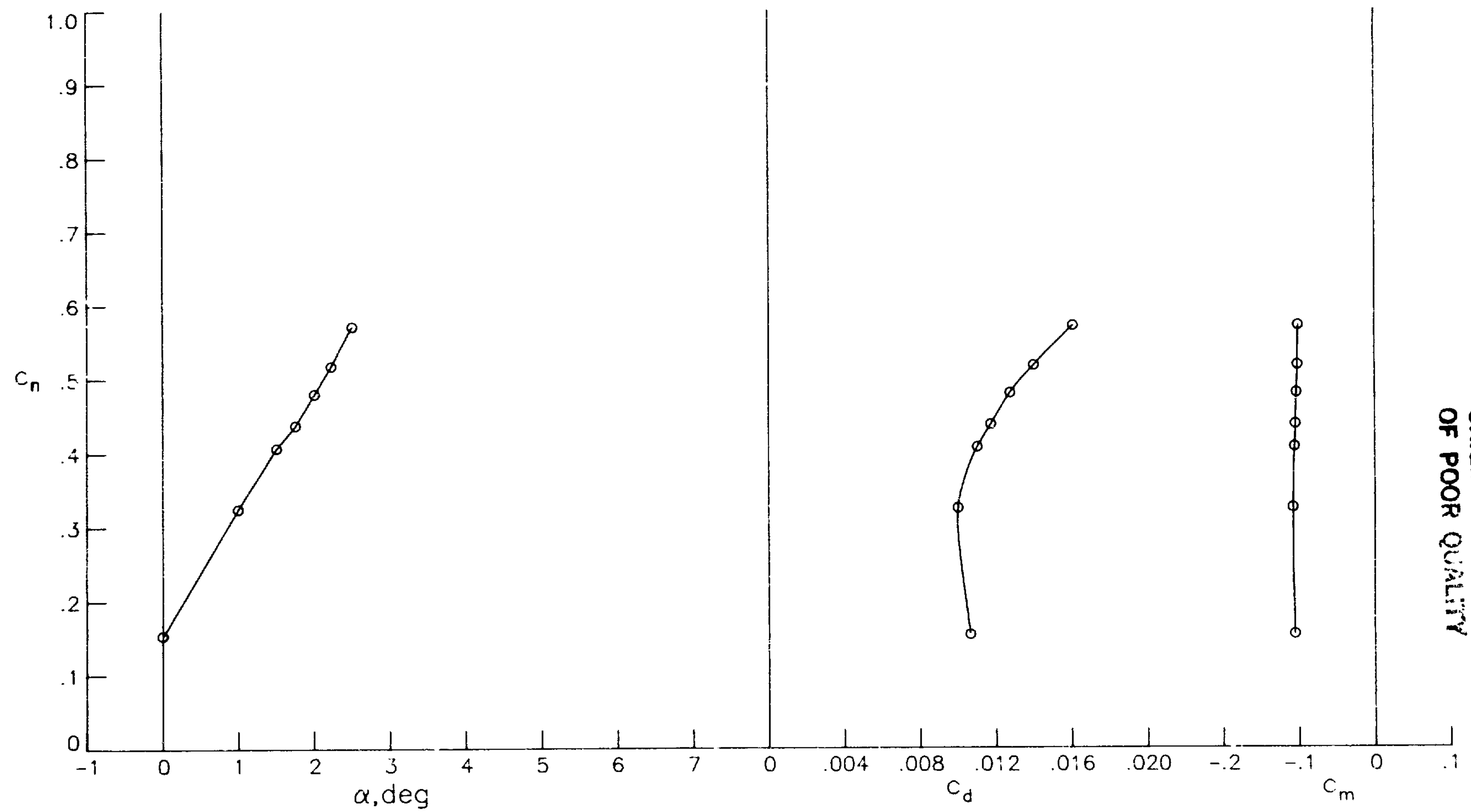

(h) $R = 7.04 \times 10^6$; $M = 0.7729$.

Figure 7.- Continued.

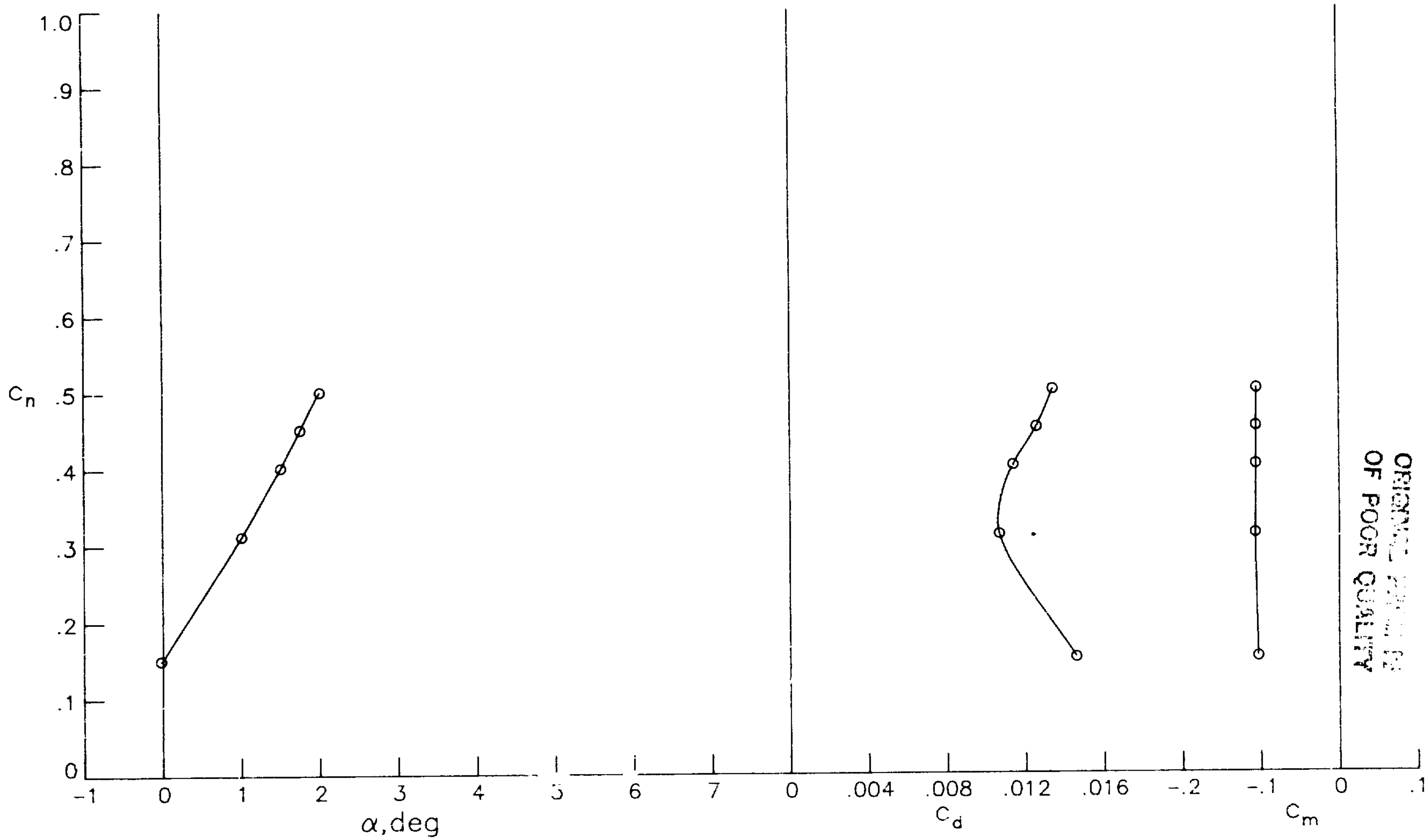

(i) R = 7.04 × 10^6; M = 0.7925.

Figure 7.- Continued.

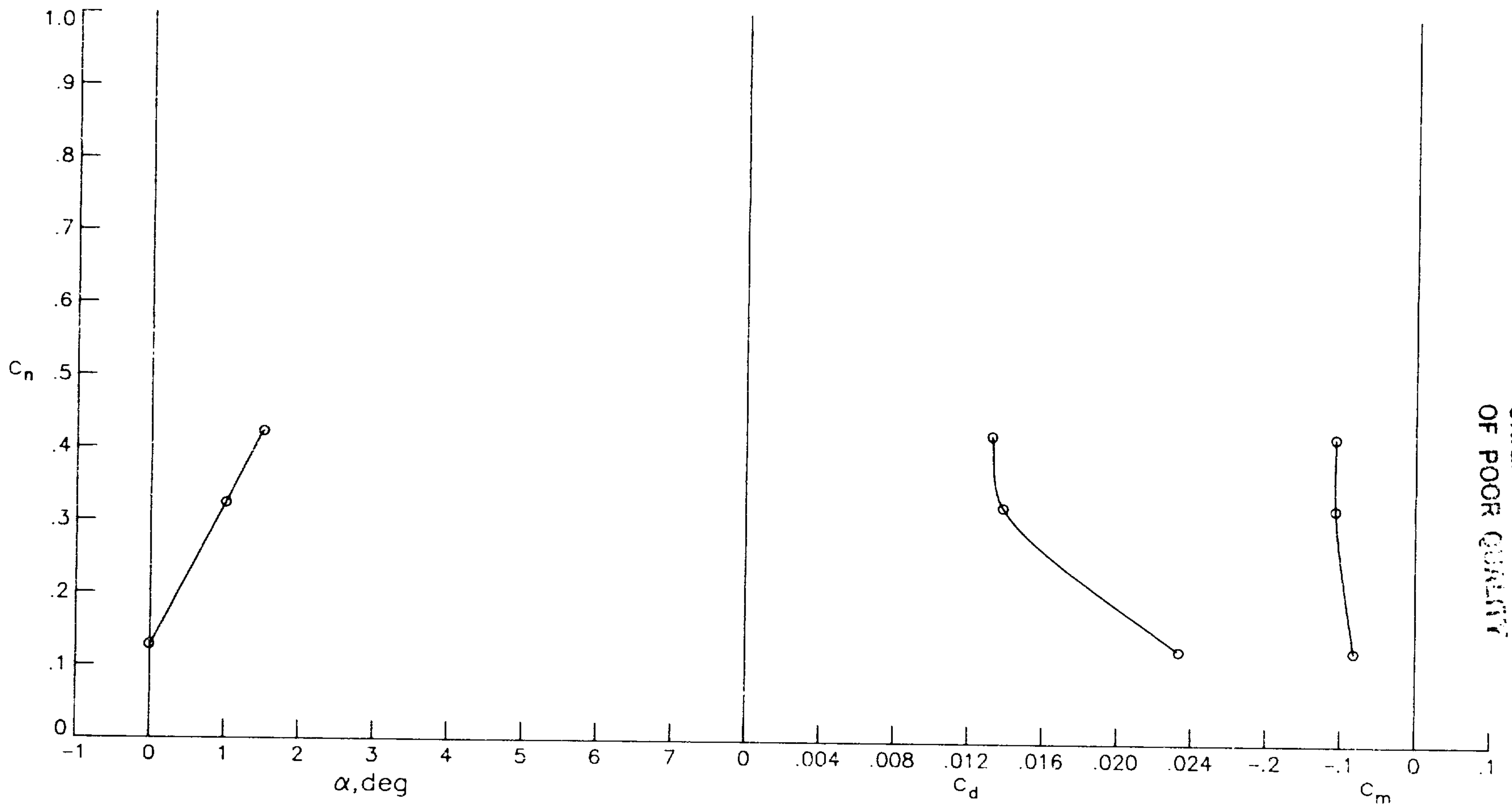

(j) $R = 7.06 \times 10^6$; $M = 0.8096$.

Figure 7.- Concluded.

ORIGINAL PAGE IS
OF POOR QUALITY

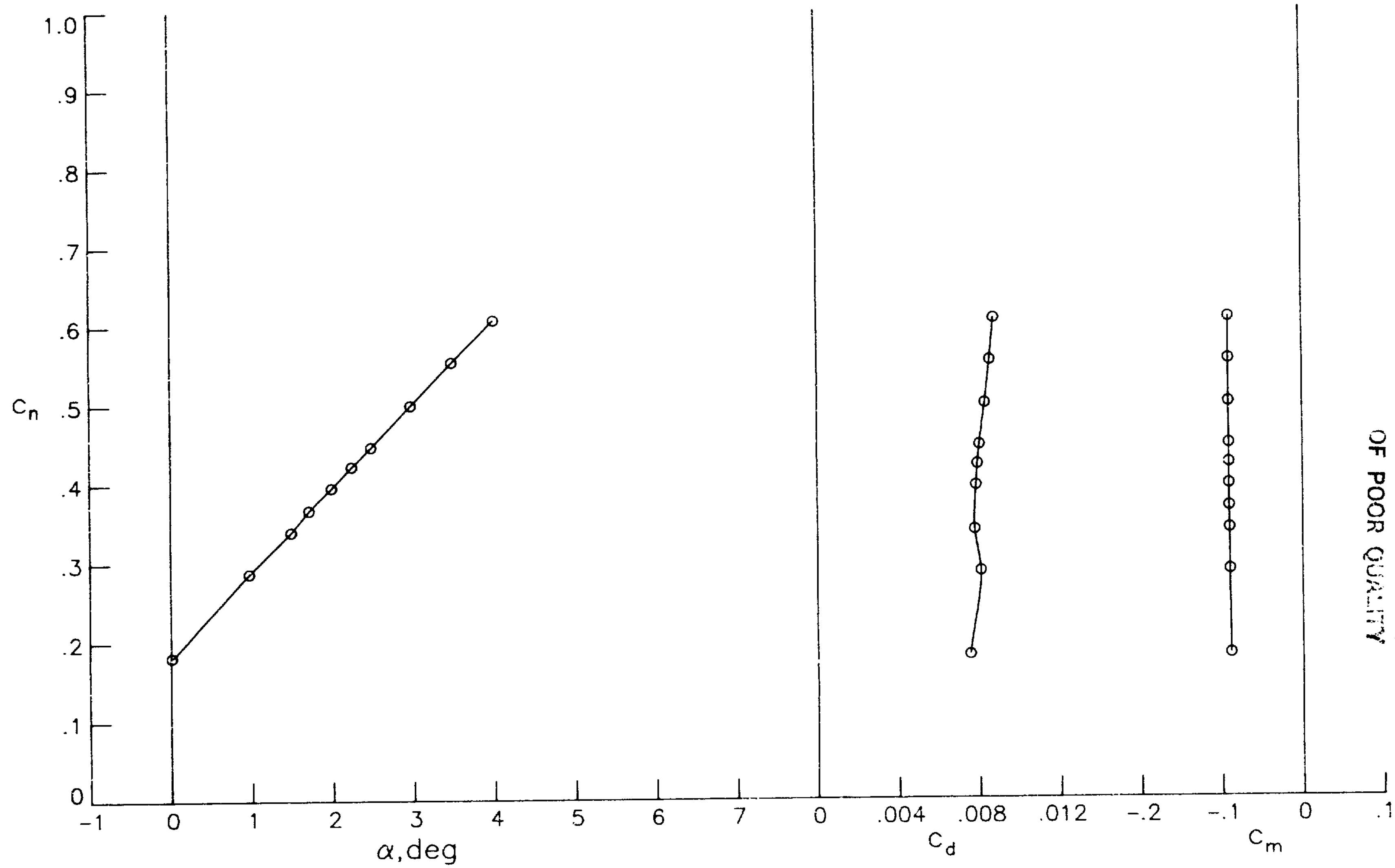

(a) $R = 15.02 \times 10^6$; $M = 0.3977$.

Figure 8.- Section characteristics at Reynolds numbers of 15×10^6.

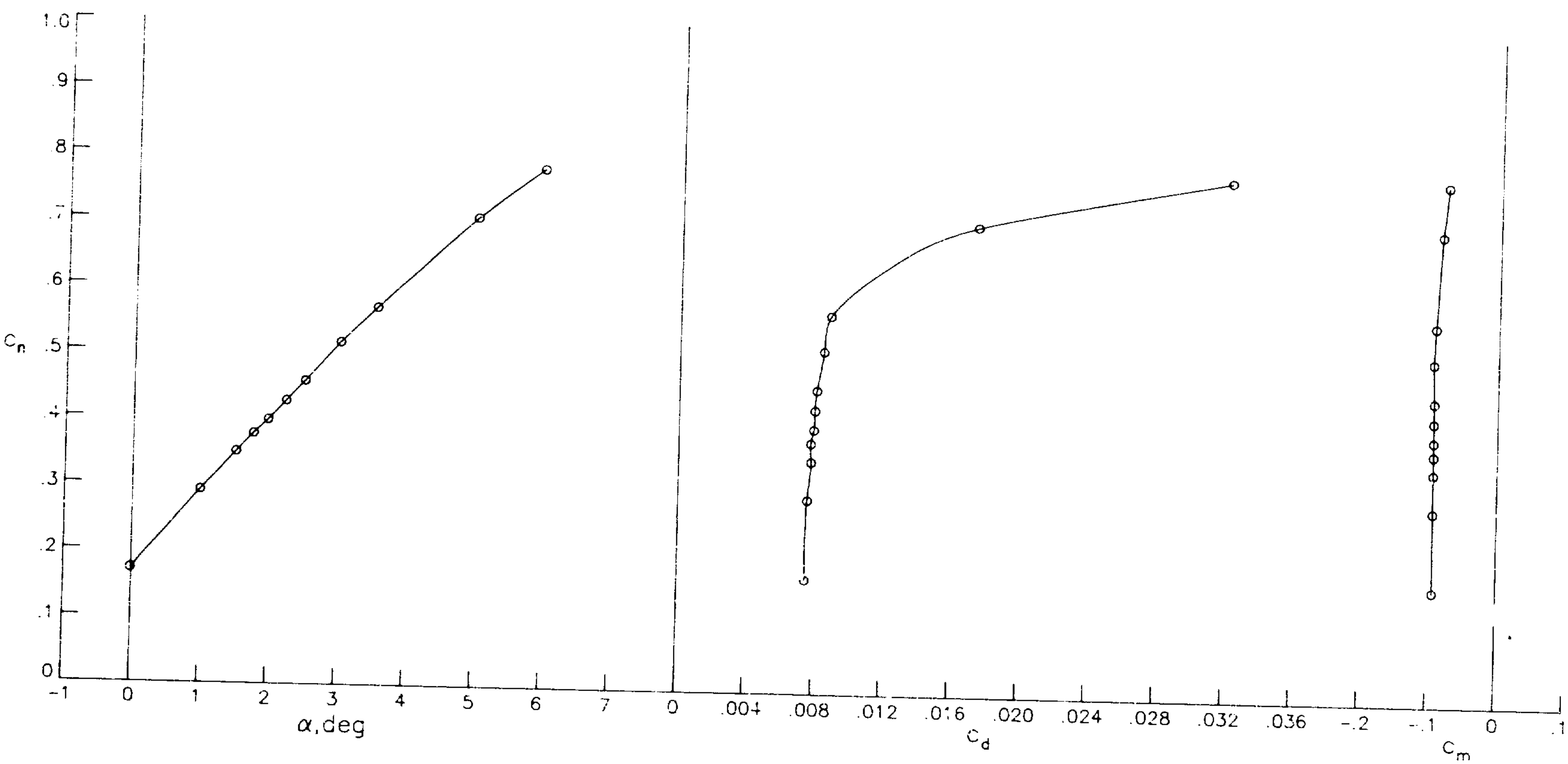

(b) R = 14.94 × 10^6; M = 0.4975.

Figure 8.- Continued.

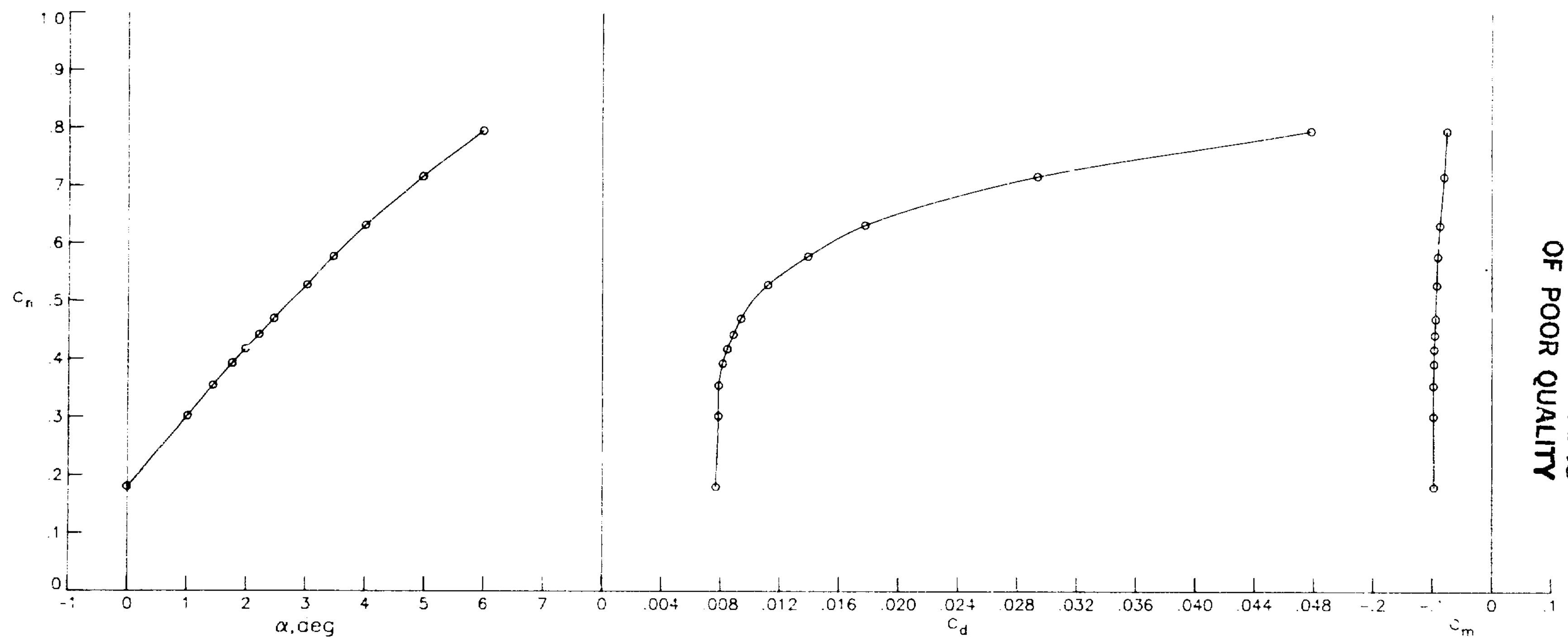

(c) $R = 14.89 \times 10^6$; $M = 0.5968$.

Figure 8.- Continued.

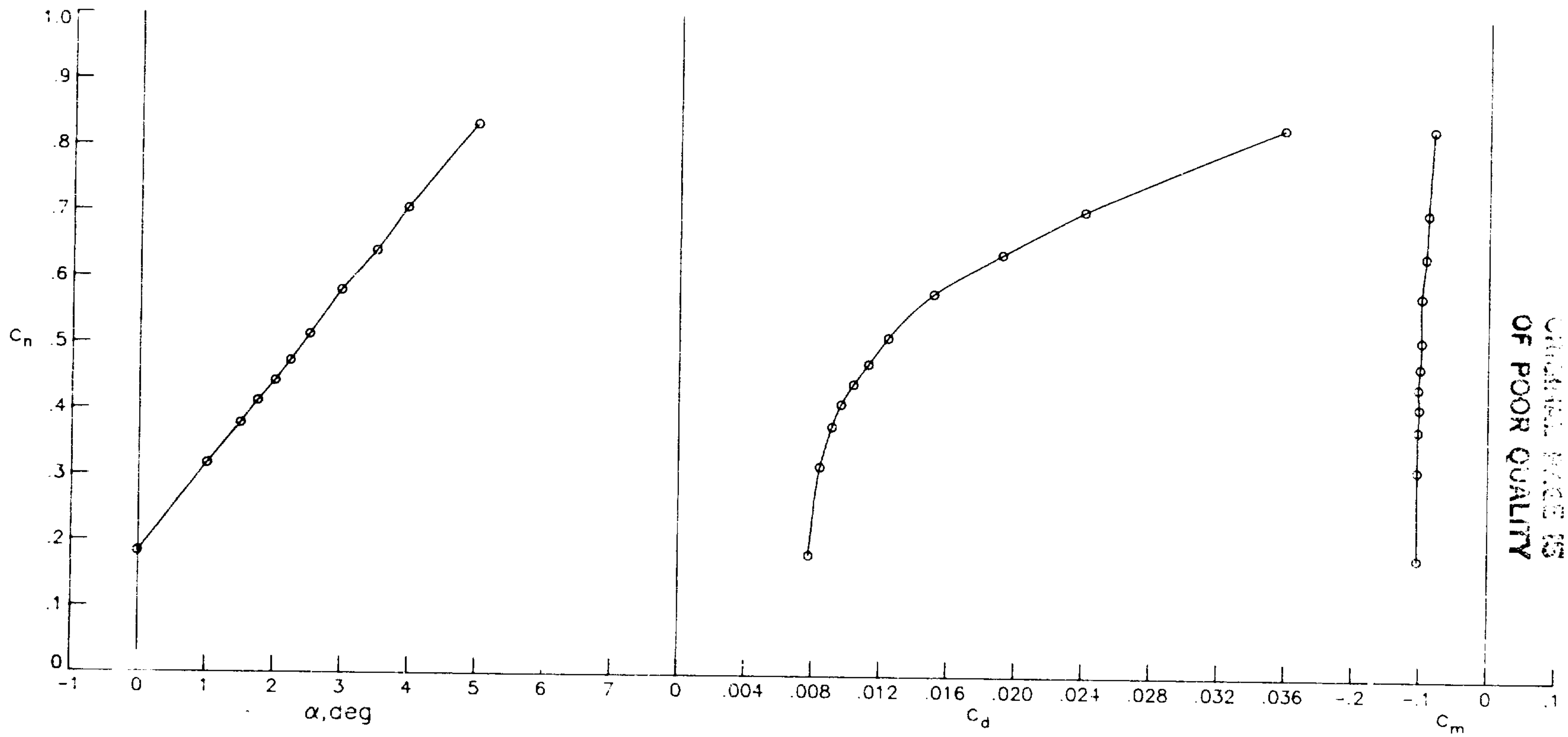

(d) $R = 14.88 \times 10^6$; $M = 0.6933$.

Figure 8.- Continued.

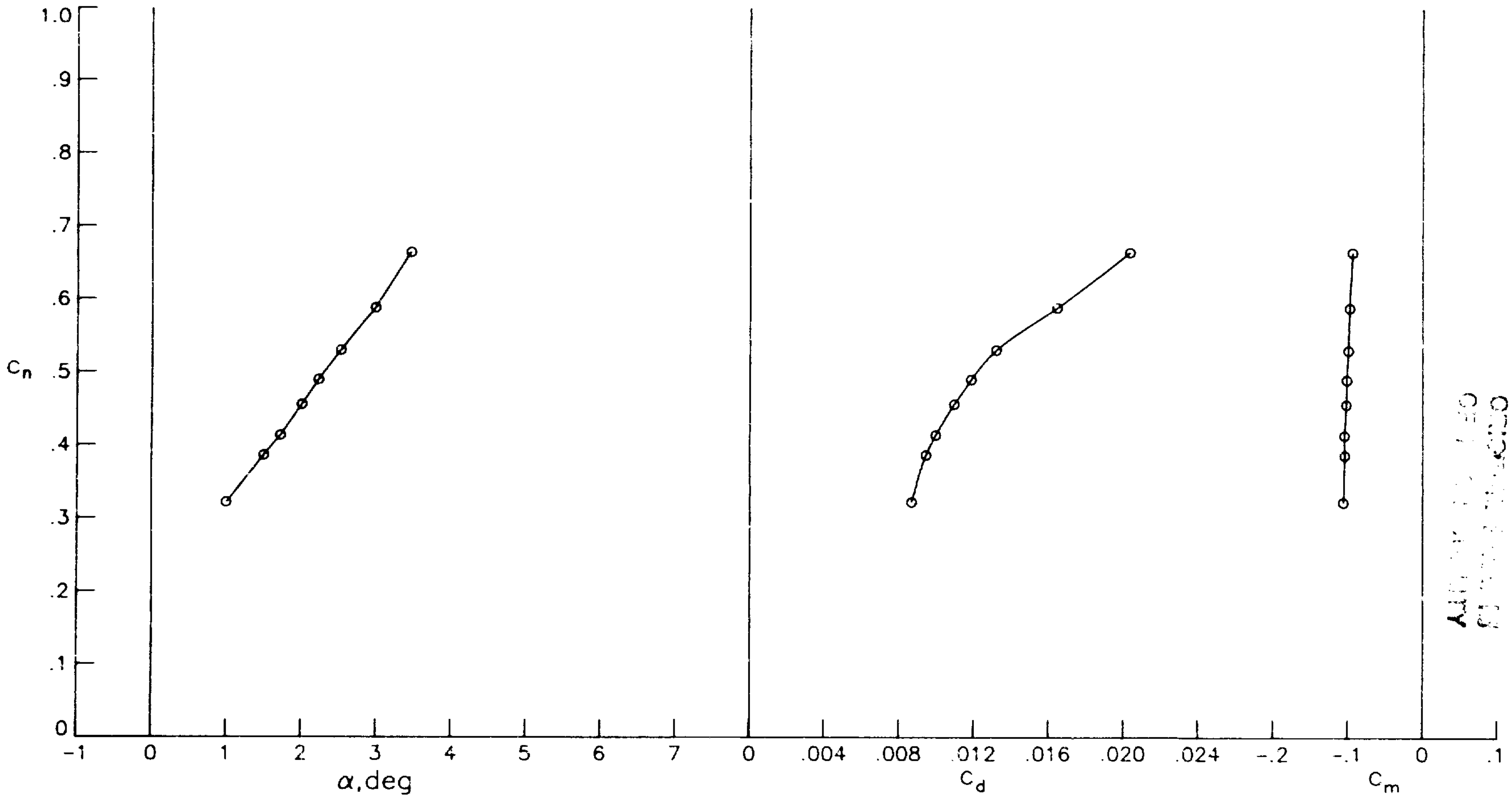

(e) $R = 14.94 \times 10^6$; $M = 0.7133$.

Figure 8.- Continued.

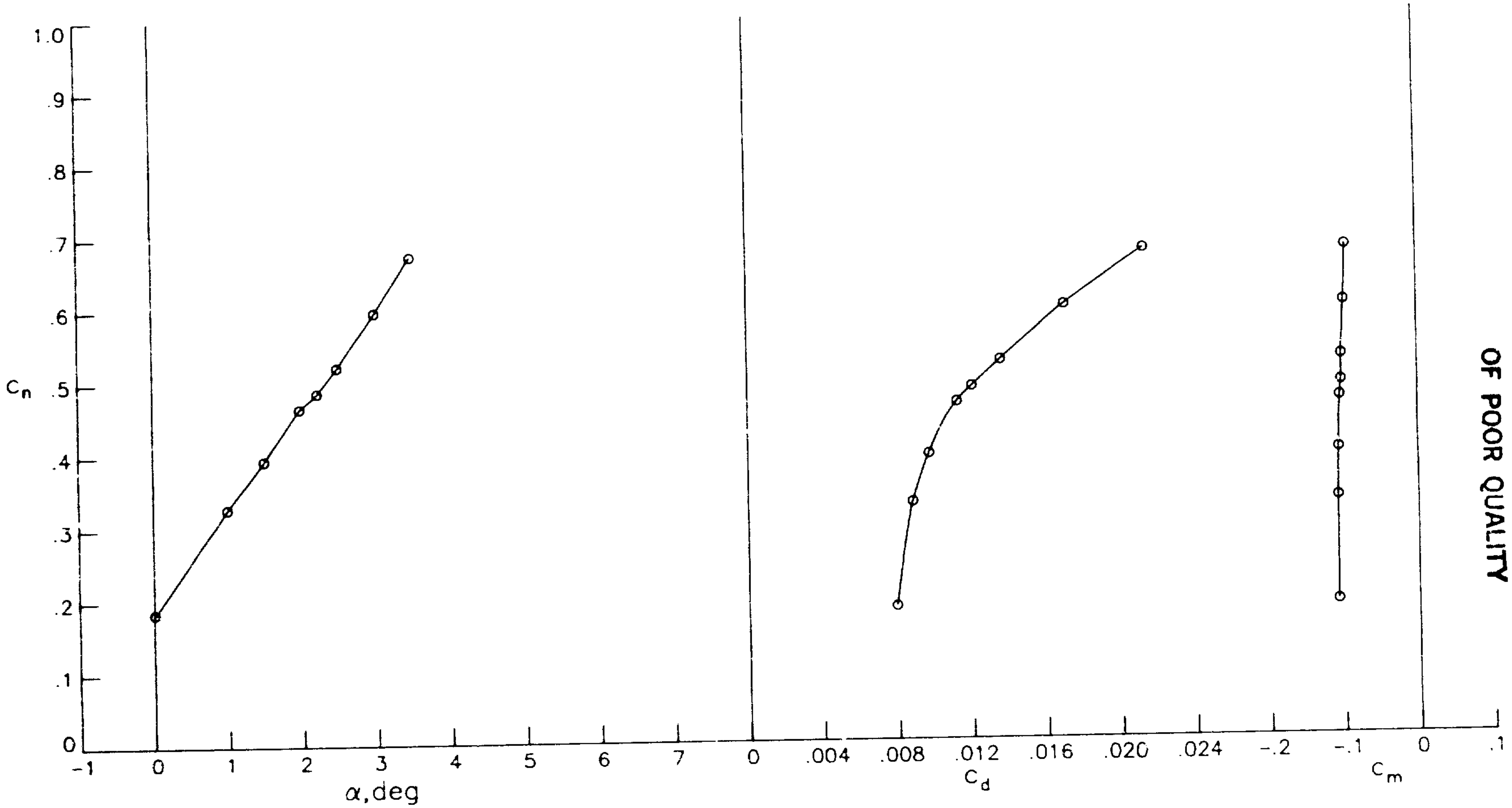

(f) $R = 14.98 \times 10^6$; $M = 0.7336$.

Figure 8.- Continued.

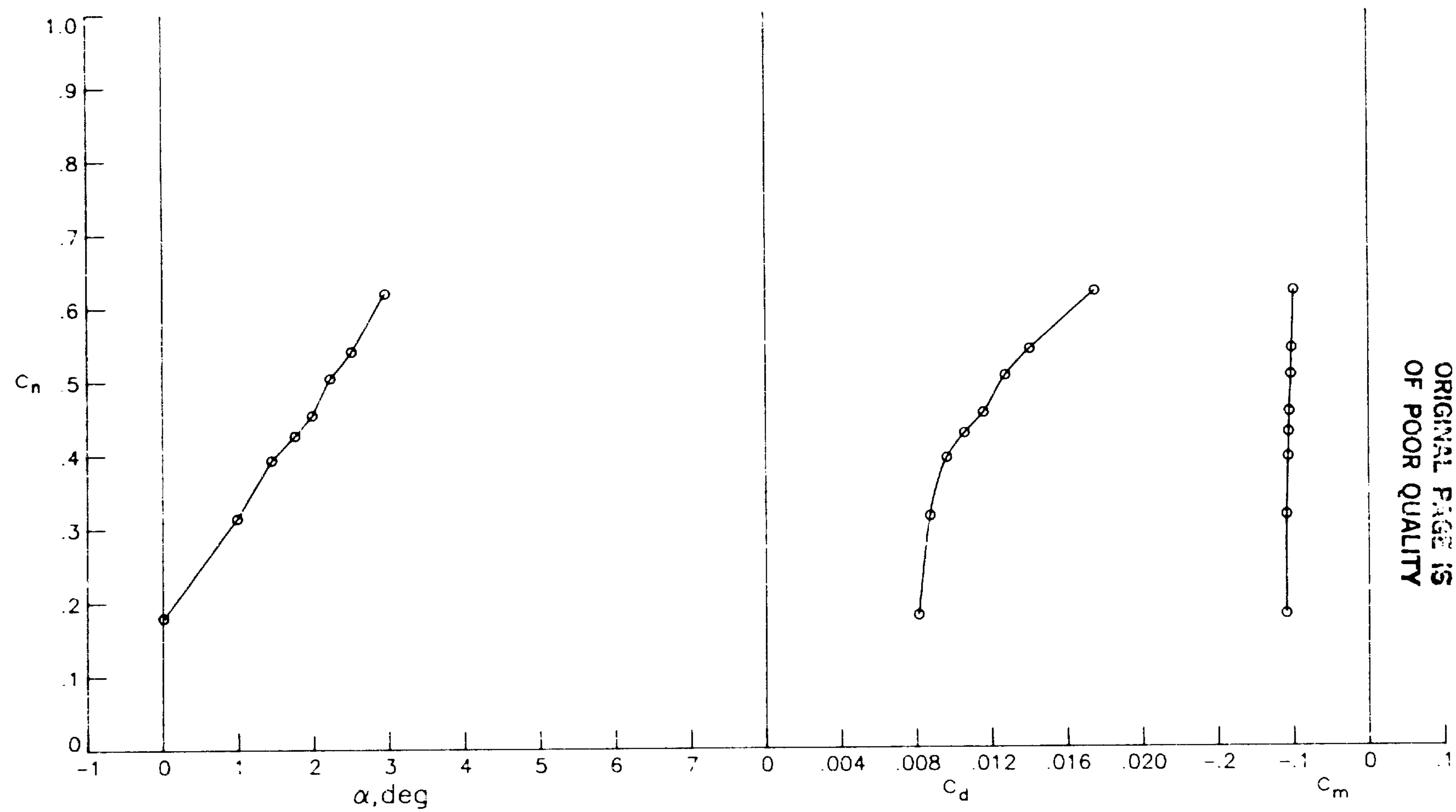

ORIGINAL PAGE IS
OF POOR QUALITY

(g) $R = 15.25 \times 10^6$; $M = 0.7536$.

Figure 8.- Continued.

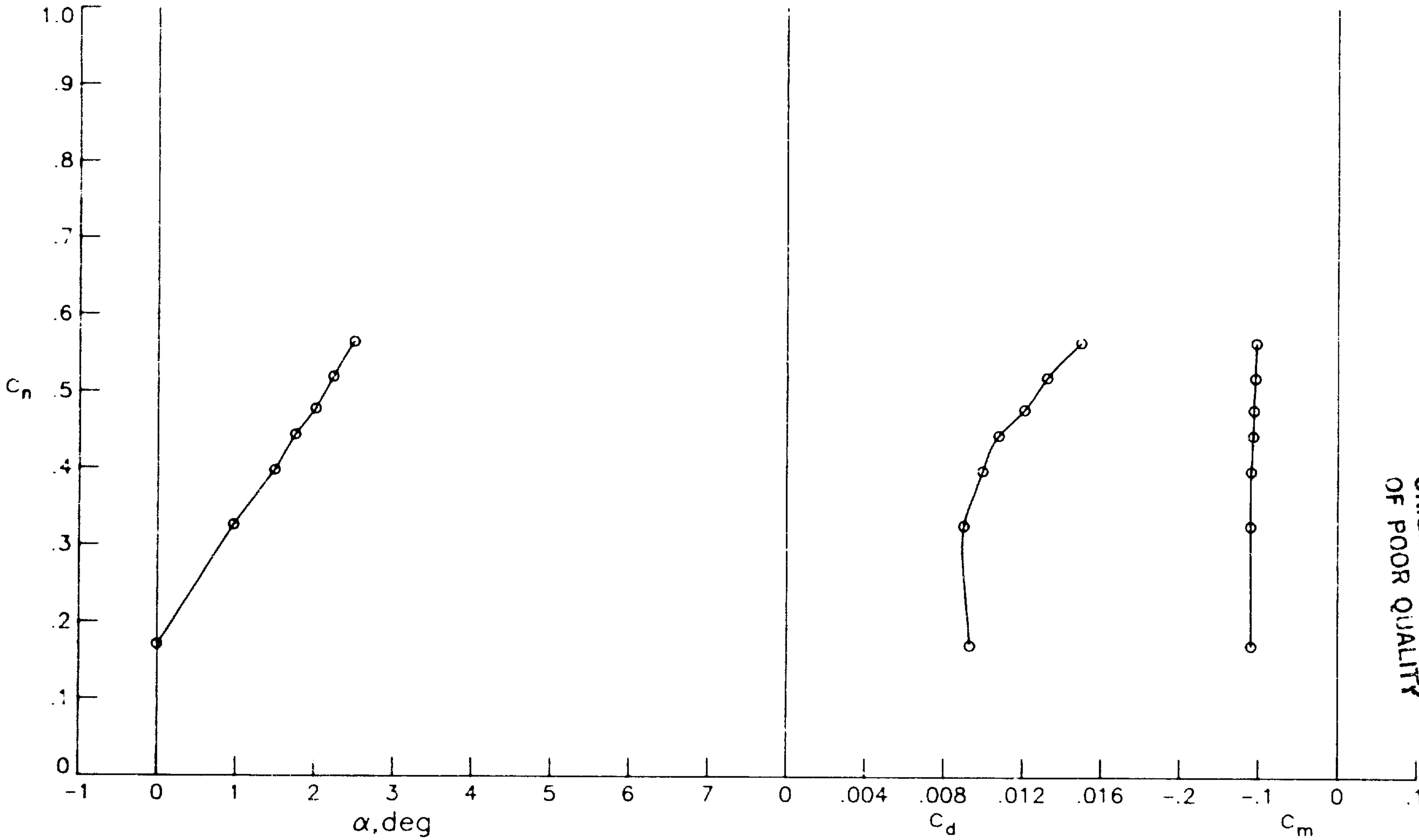

(h) $R = 14.88 \times 10^6$; $M = 0.7727$.

Figure 8.- Continued.

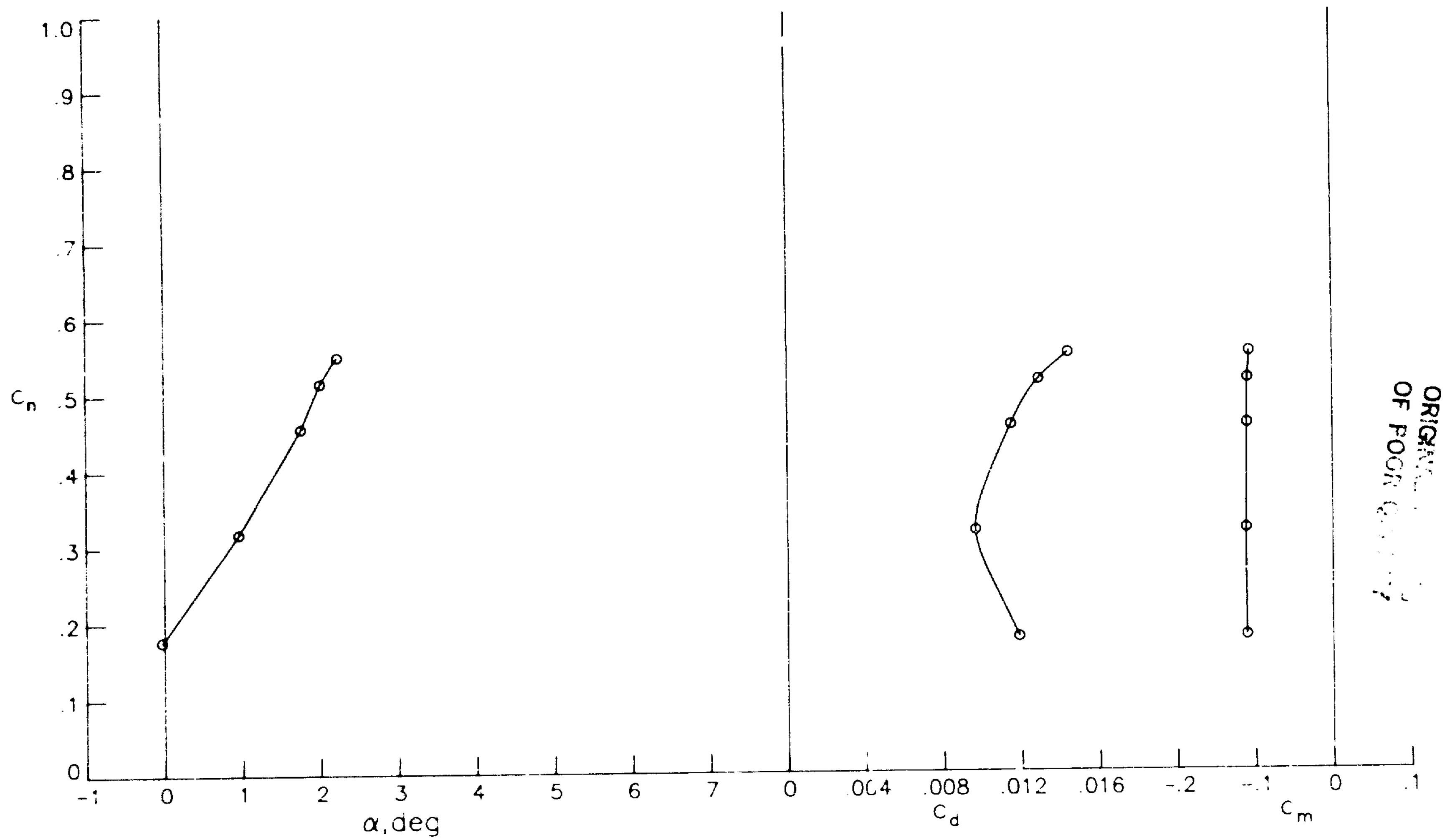

(i) $R = 14.94 \times 10^6$; $M = 0.7921$.

Figure 8.- Continued.

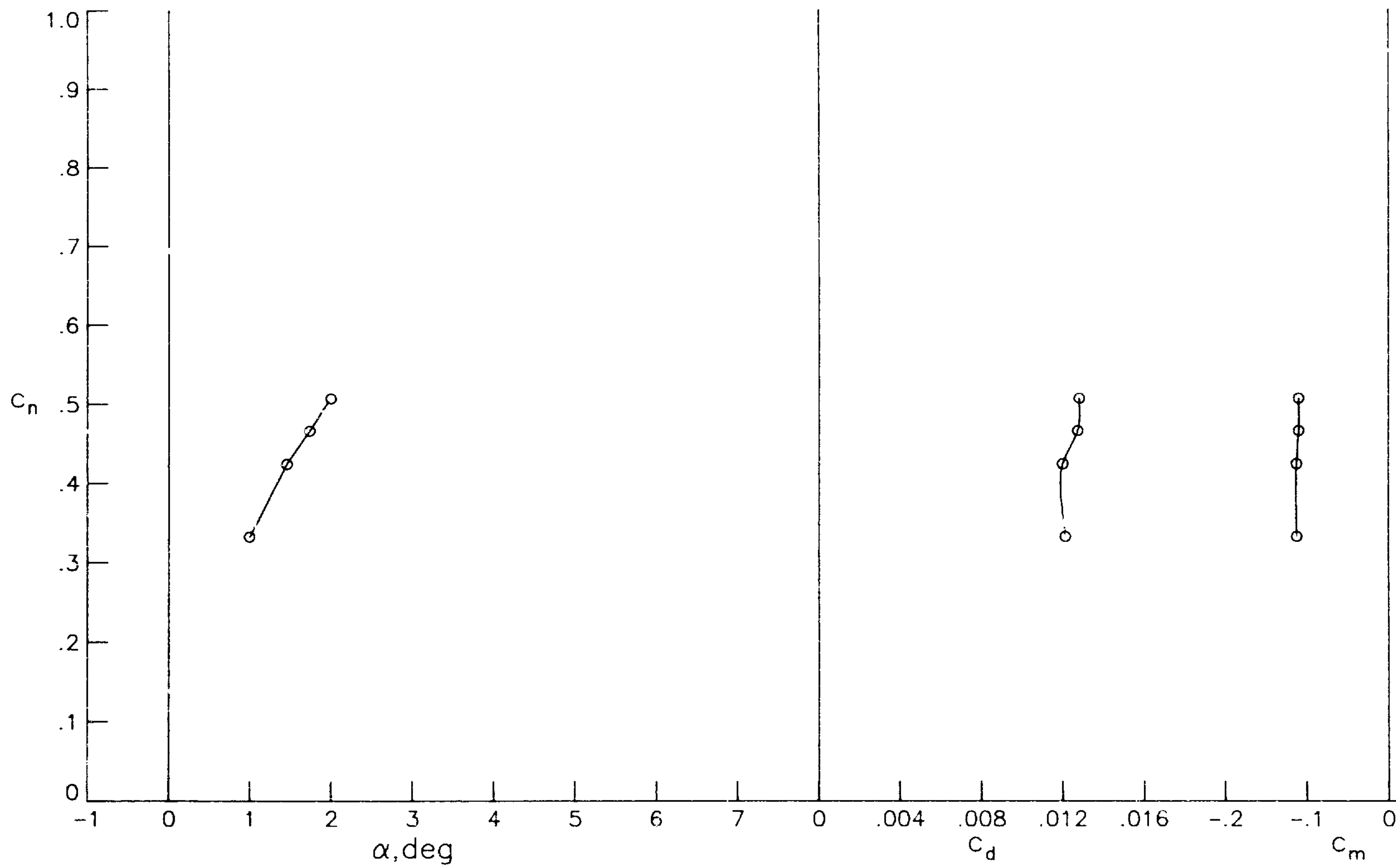

(j) $R = 14.90 \times 10^6$; $M = 0.8112$.

Figure 8.- Concluded.

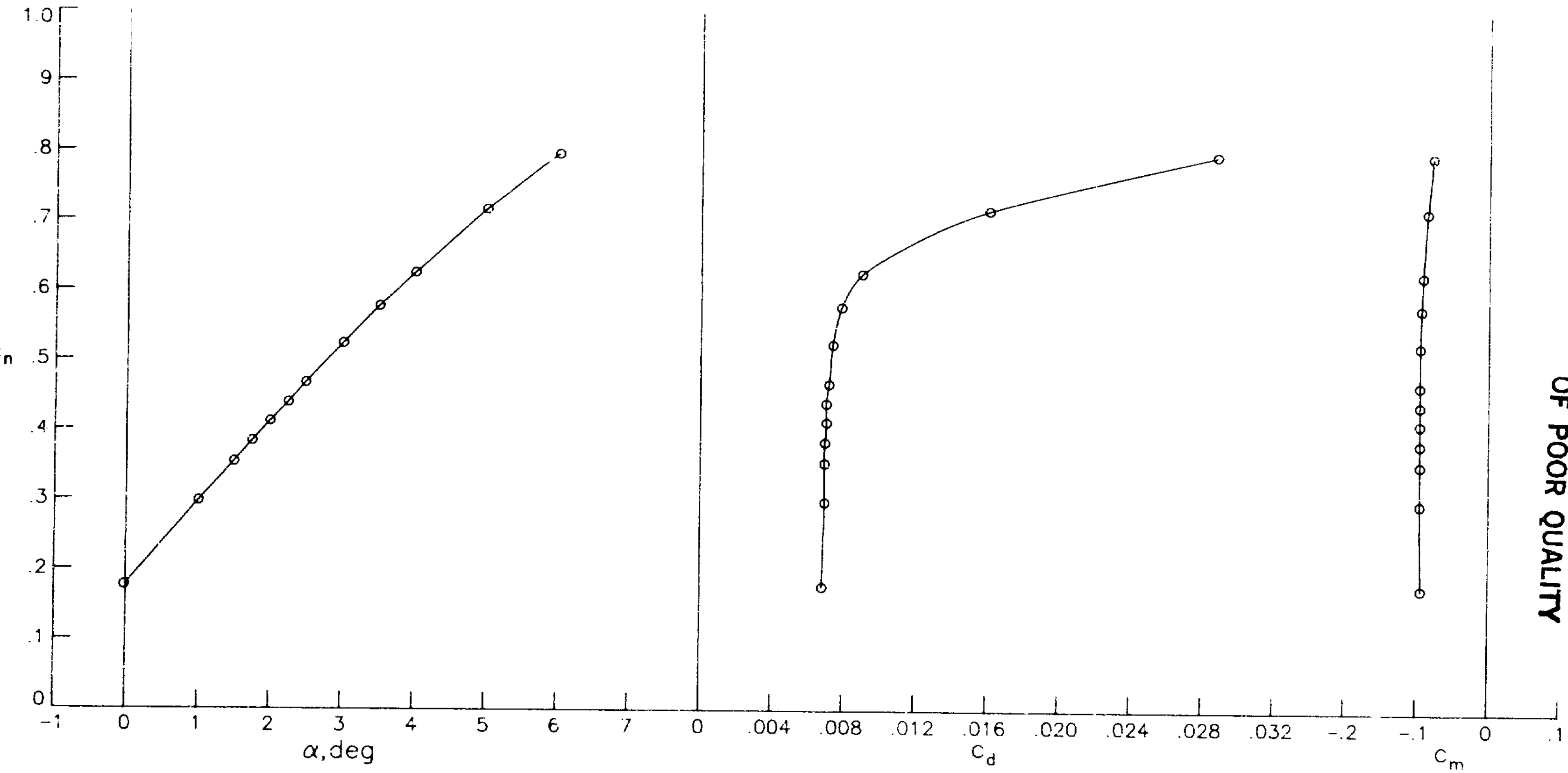

ORIGINAL PAGE IS OF POOR QUALITY

(a) $R = 30.03 \times 10^6$; $M = 0.4993$.

Figure 9.- Section characteristics at Reynolds numbers of 30×10^6.

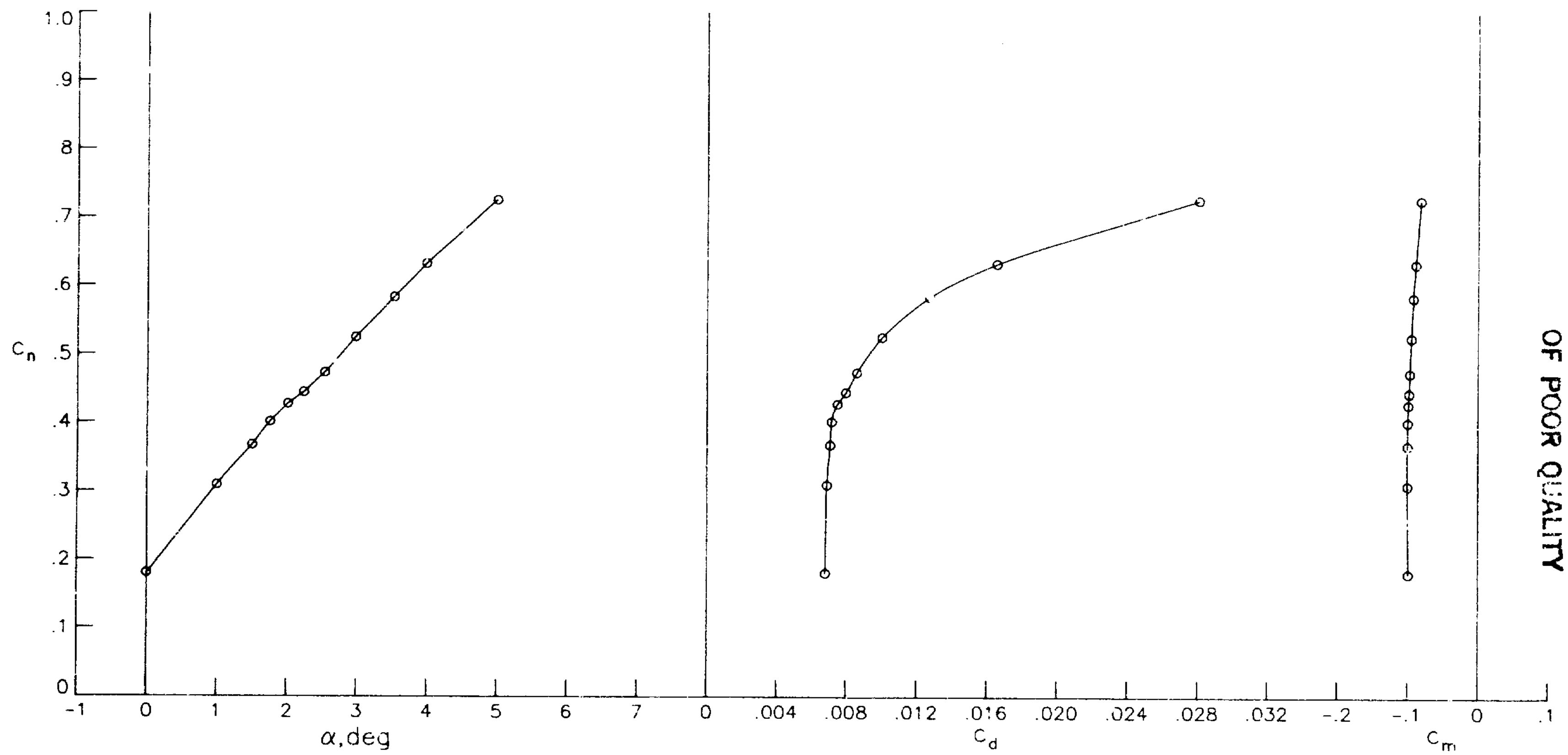

(b) $R = 30.13 \times 10^6$; $M = 0.5987$.

Figure 9.- Continued.

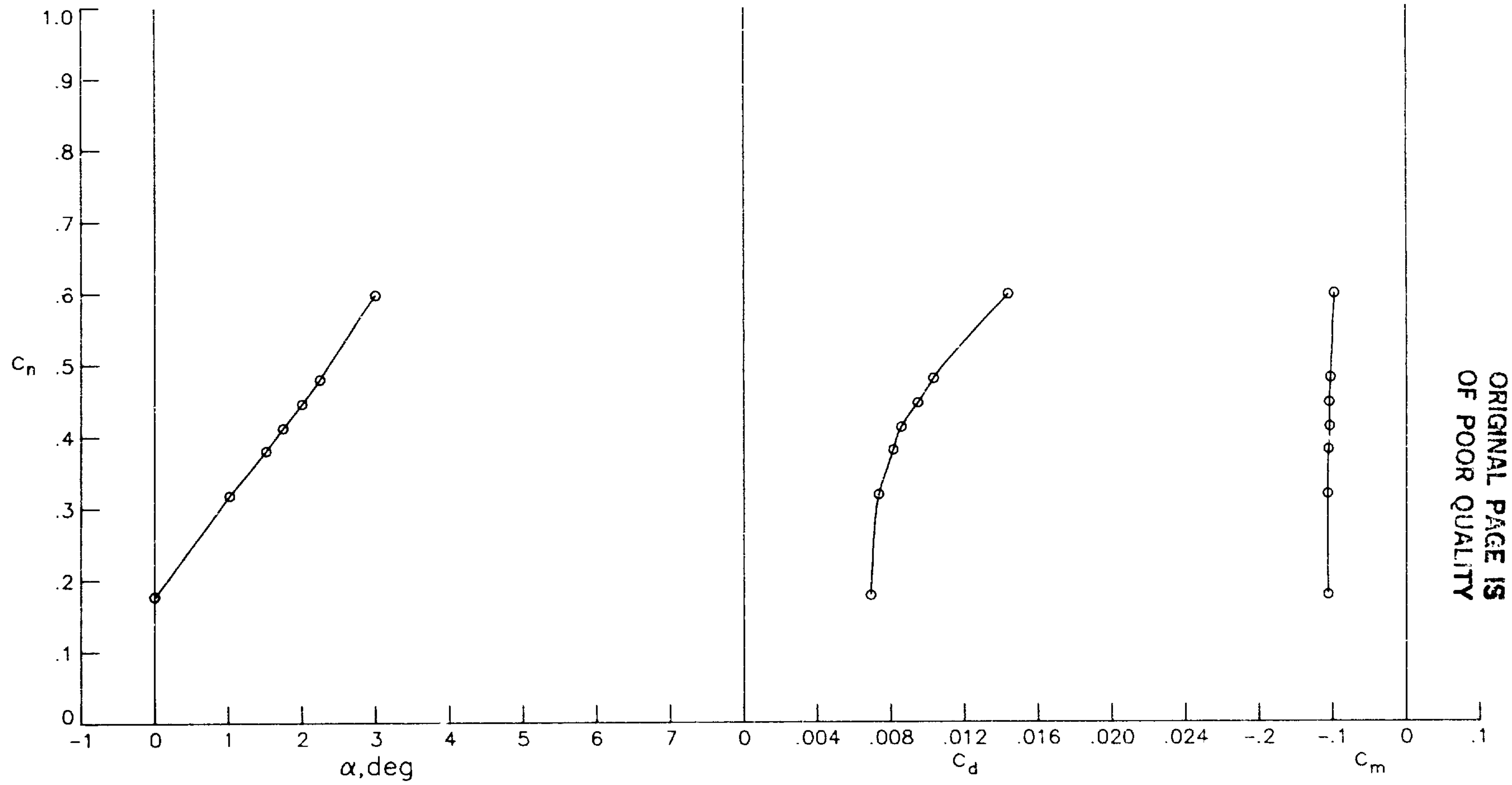

(c) $R = 30.20 \times 10^6$; $M = 0.6970$.

Figure 9.- Continued.

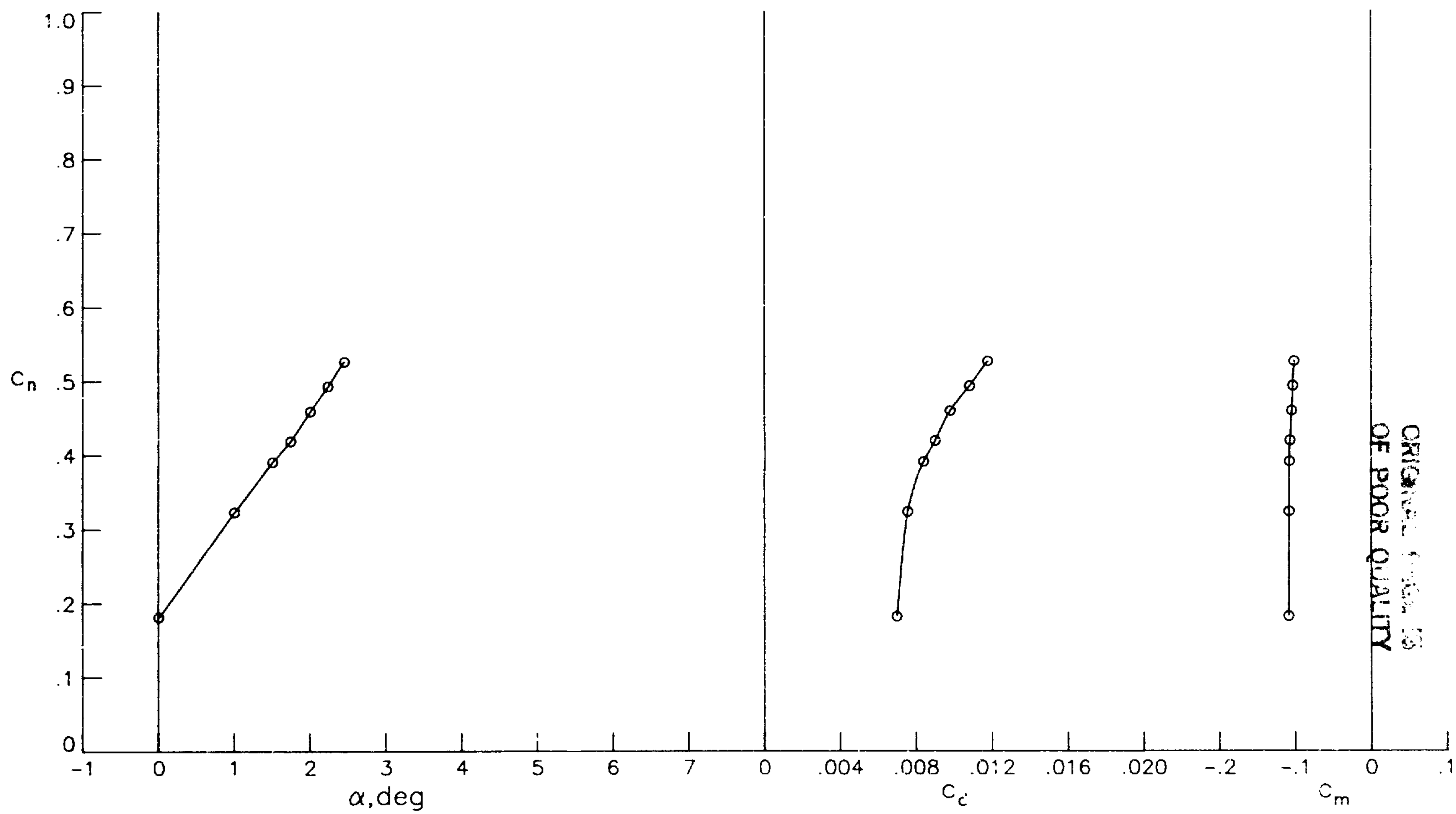

(d) $R = 30.09 \times 10^6$; $M = 0.7145$.

Figure 9.- Continued.

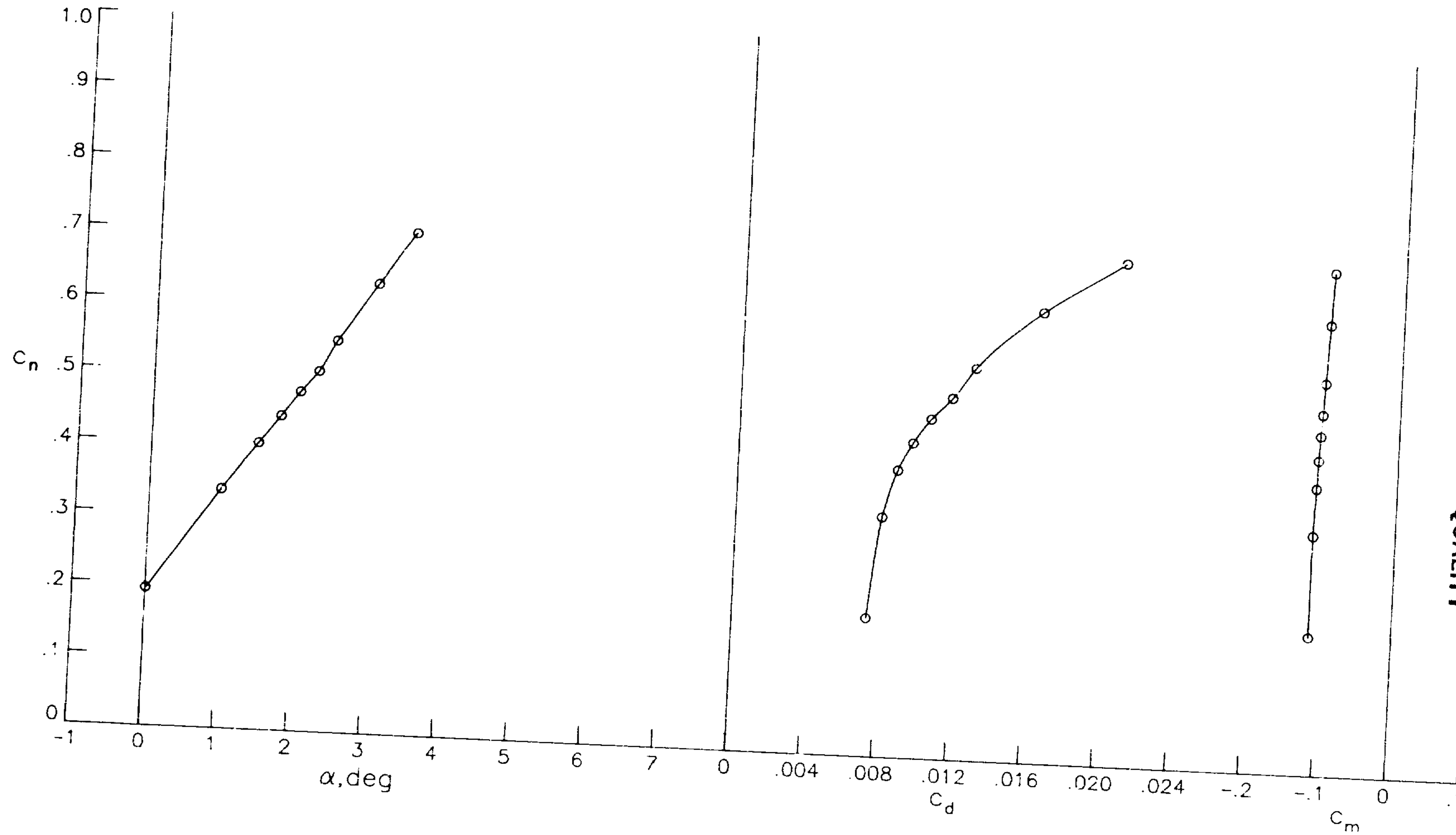

(e) $R = 30.04 \times 10^6$; $M = 0.7351$.

Figure 9.- Continued.

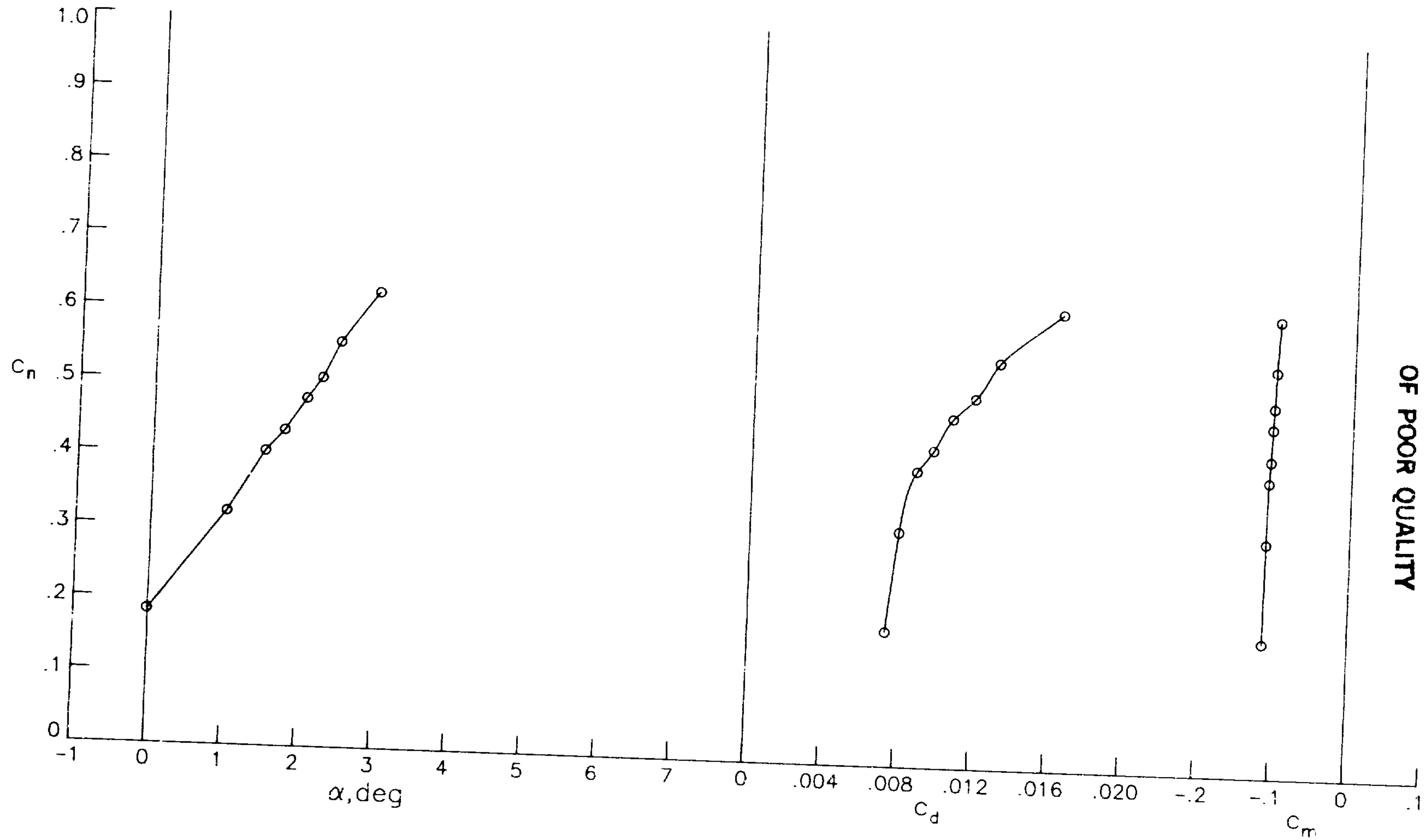

(f) $R = 29.62 \times 10^6$; $M = 0.7575$.

Figure 9.- Continued.

ORIGINAL PAGE IS OF POOR QUALITY

ORIGINAL PAGE IS
OF POOR QUALITY

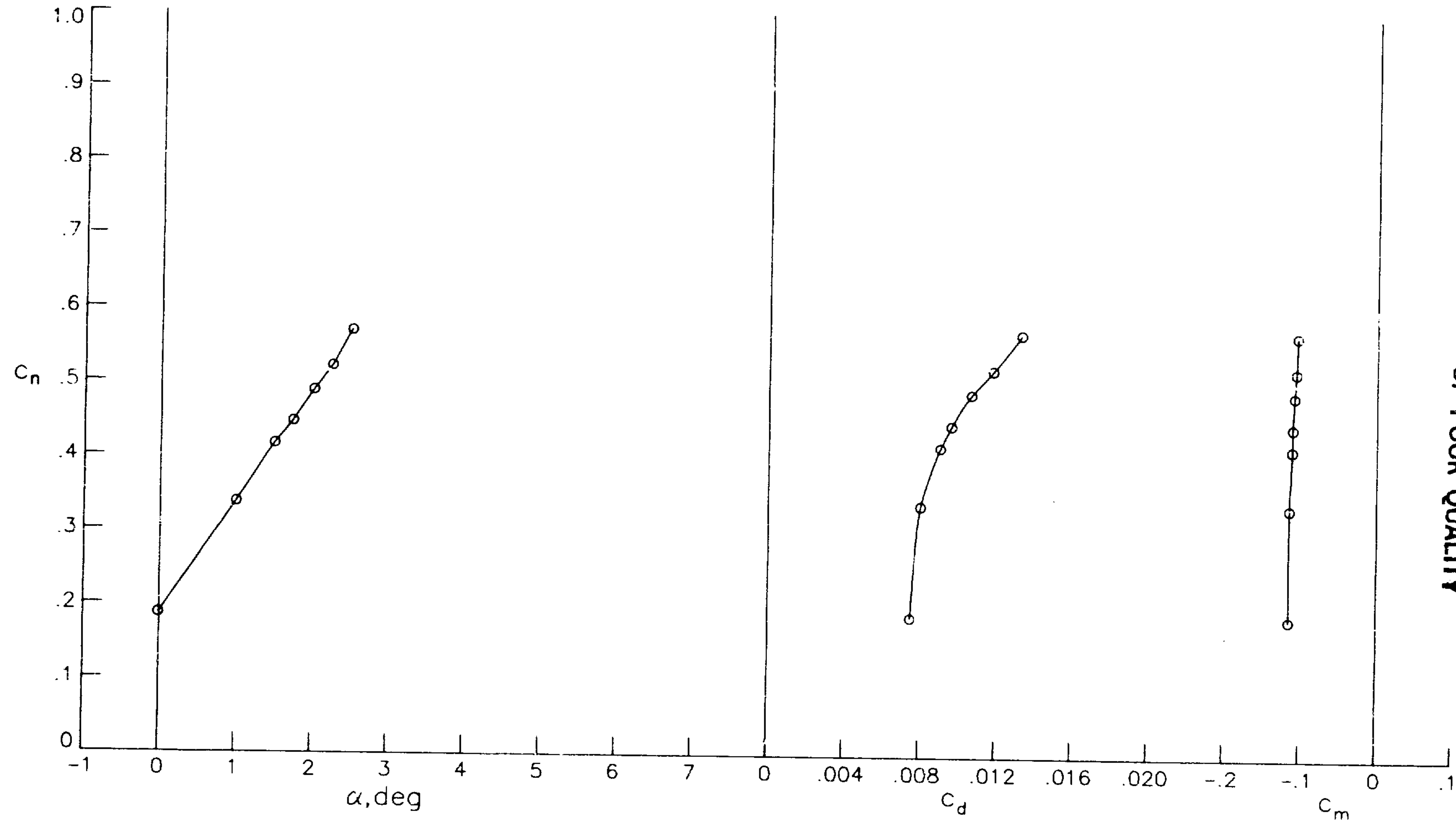

(g) $R = 30.07 \times 10^6$; $M = 0.7561$.

Figure 9.- Continued.

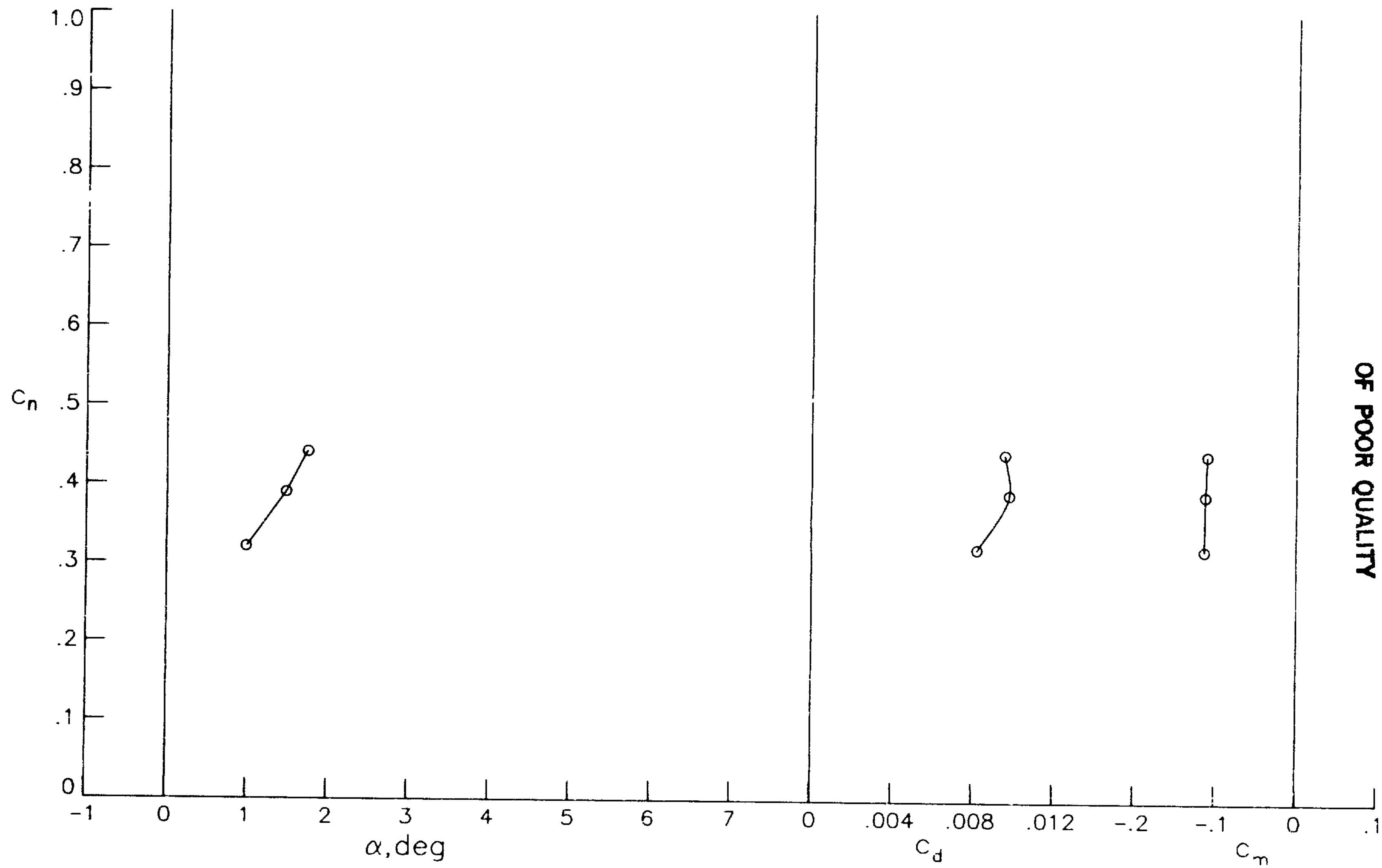

(h) $R = 29.88 \times 10^6$; $M = 0.7743$.

Figure 9.- Continued.

ORIGINAL PAGE IS
OF POOR QUALITY

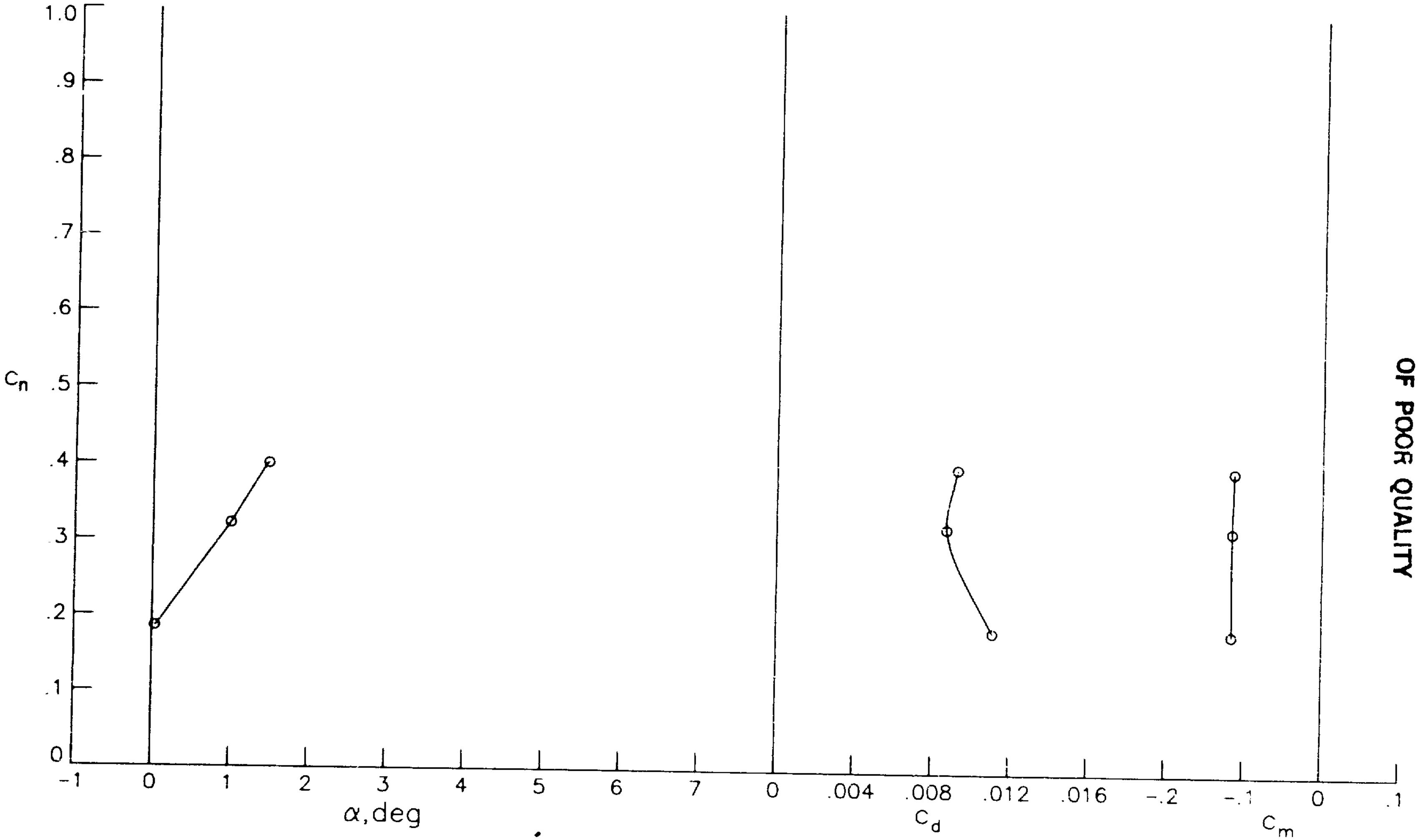

(i) $R = 30.03 \times 10^6$; $M = 0.7933$.

Figure 9.- Continued.

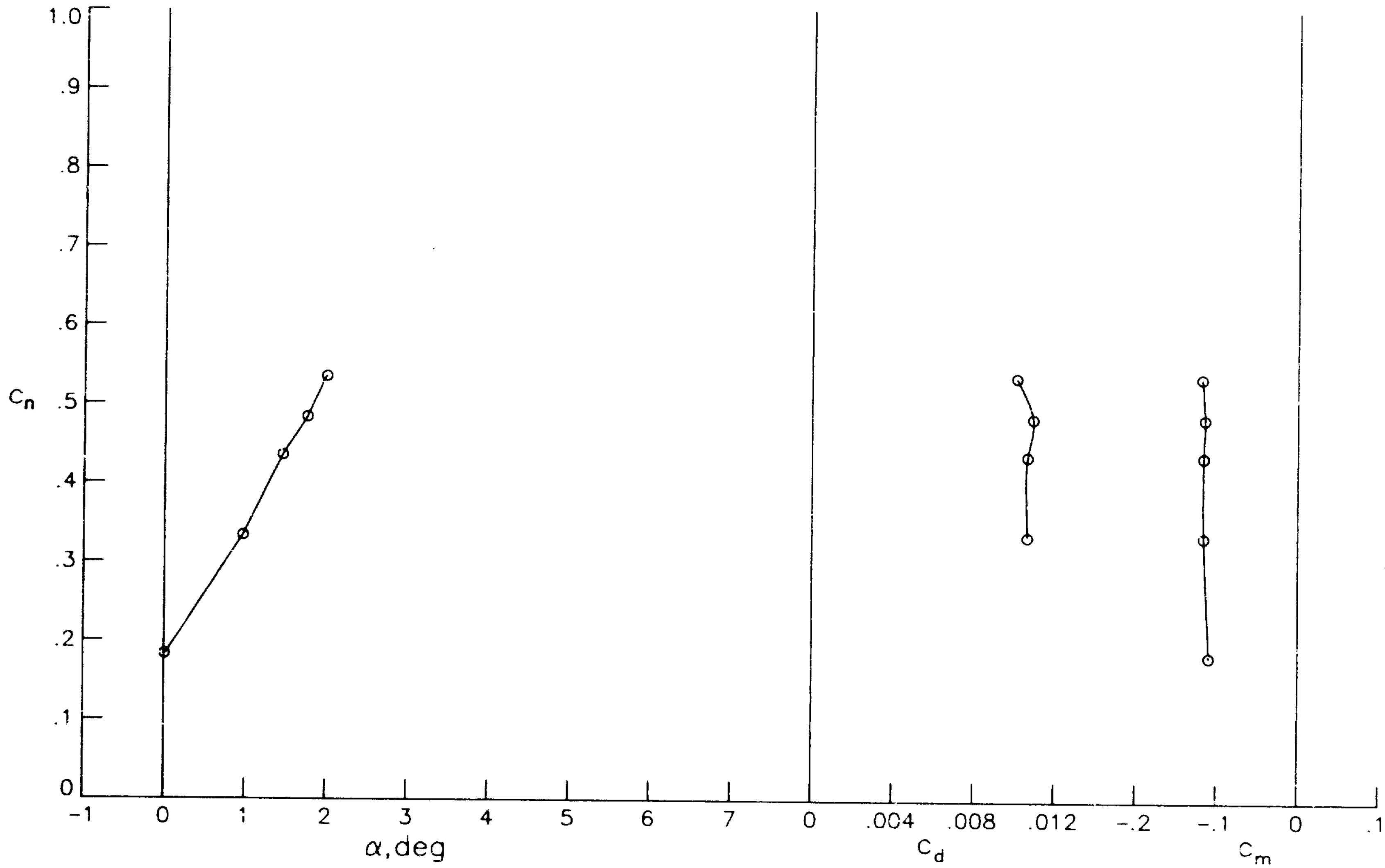

(j) $R = 30.04 \times 10^6$; $M = 0.8155$.

Figure 9.- Concluded.

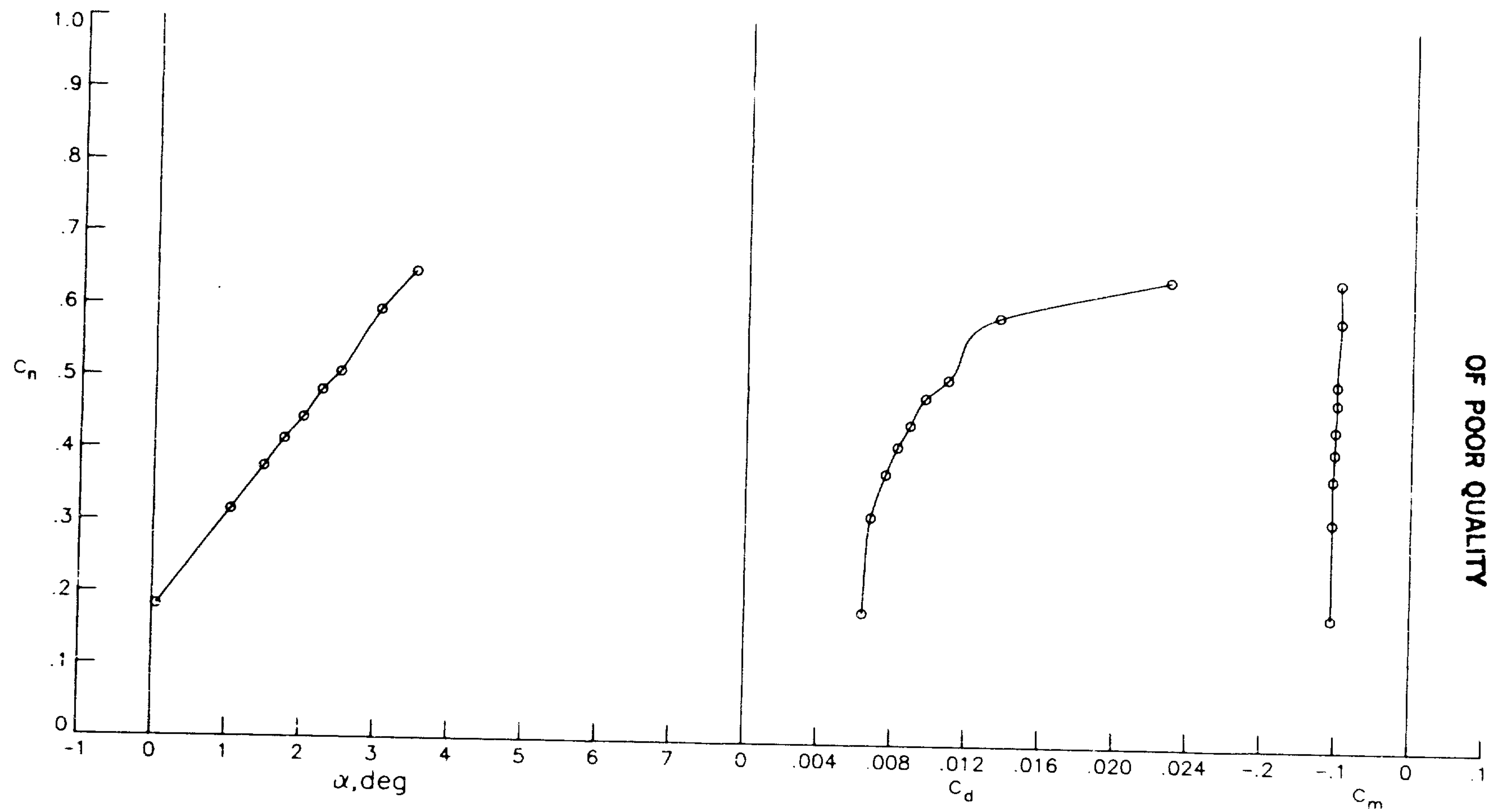

(a) $R = 47.63 \times 10^6$; $M = 0.6990$.

Figure 10.- Section characteristics at Reynolds numbers above 47×10^6.

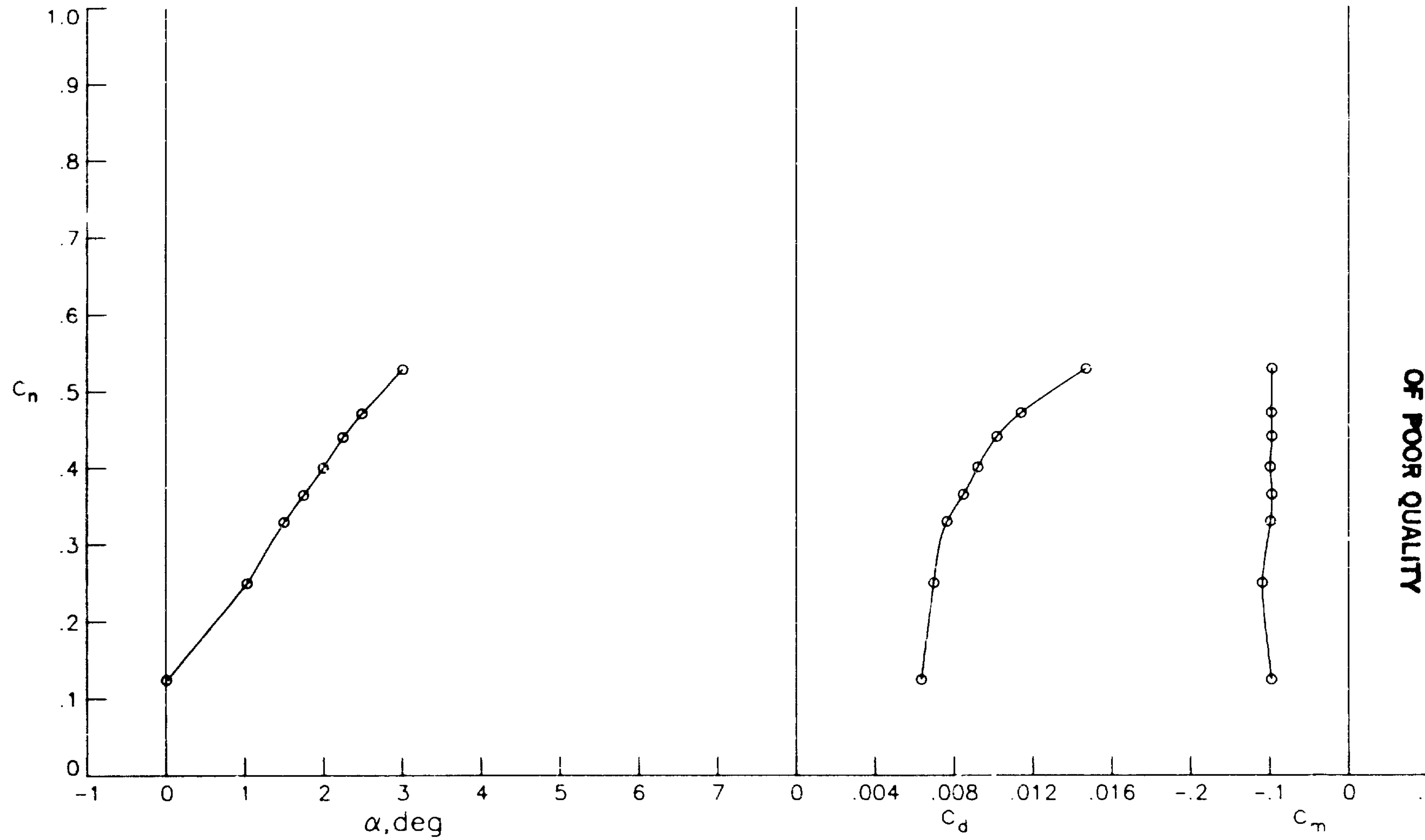

(b) $R = 47.72 \times 10^6$; $M = 0.7188$.

Figure 10.- Continued.

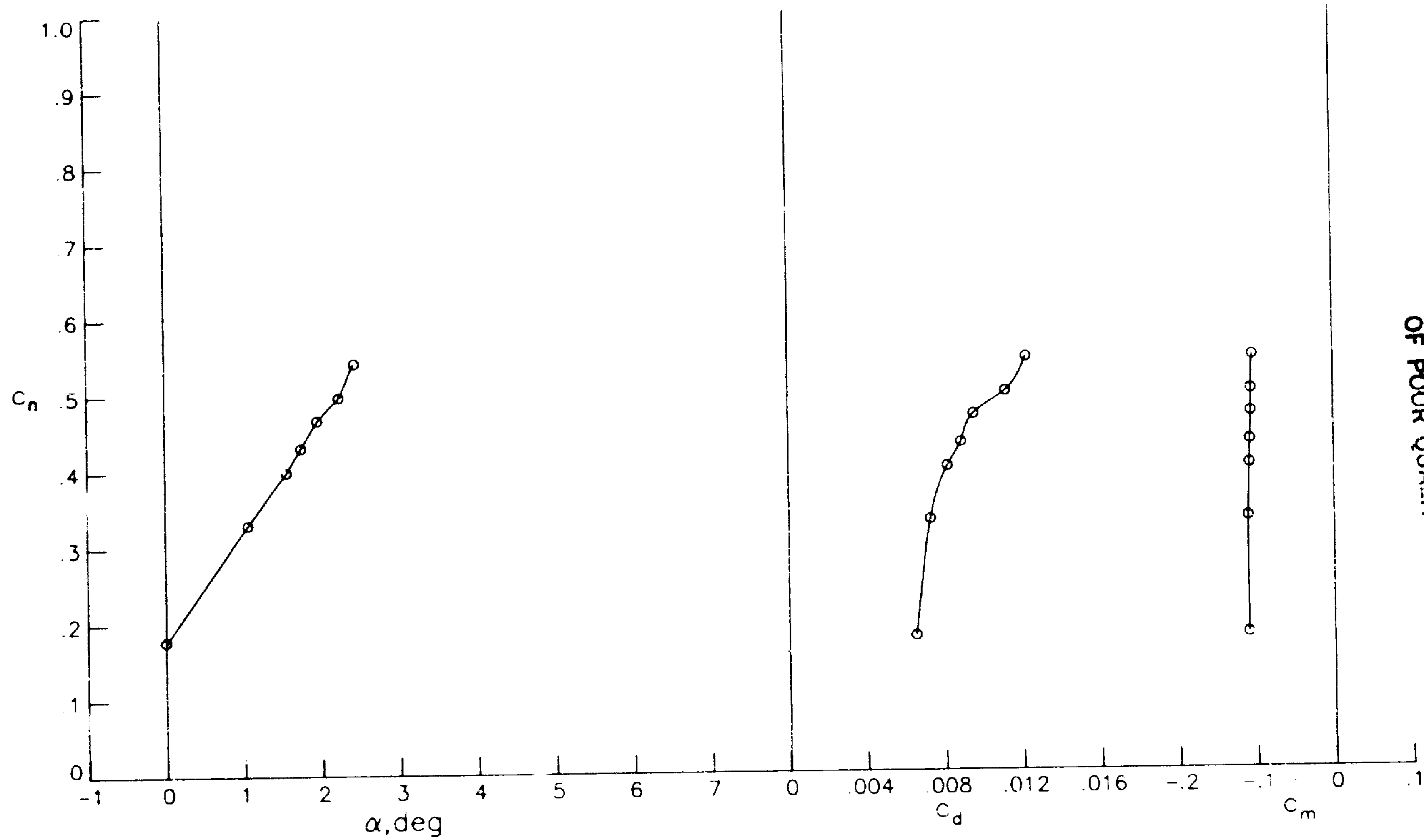

(c) R = 47.60 × 10^6; M = 0.7366.

Figure 10.- Continued.

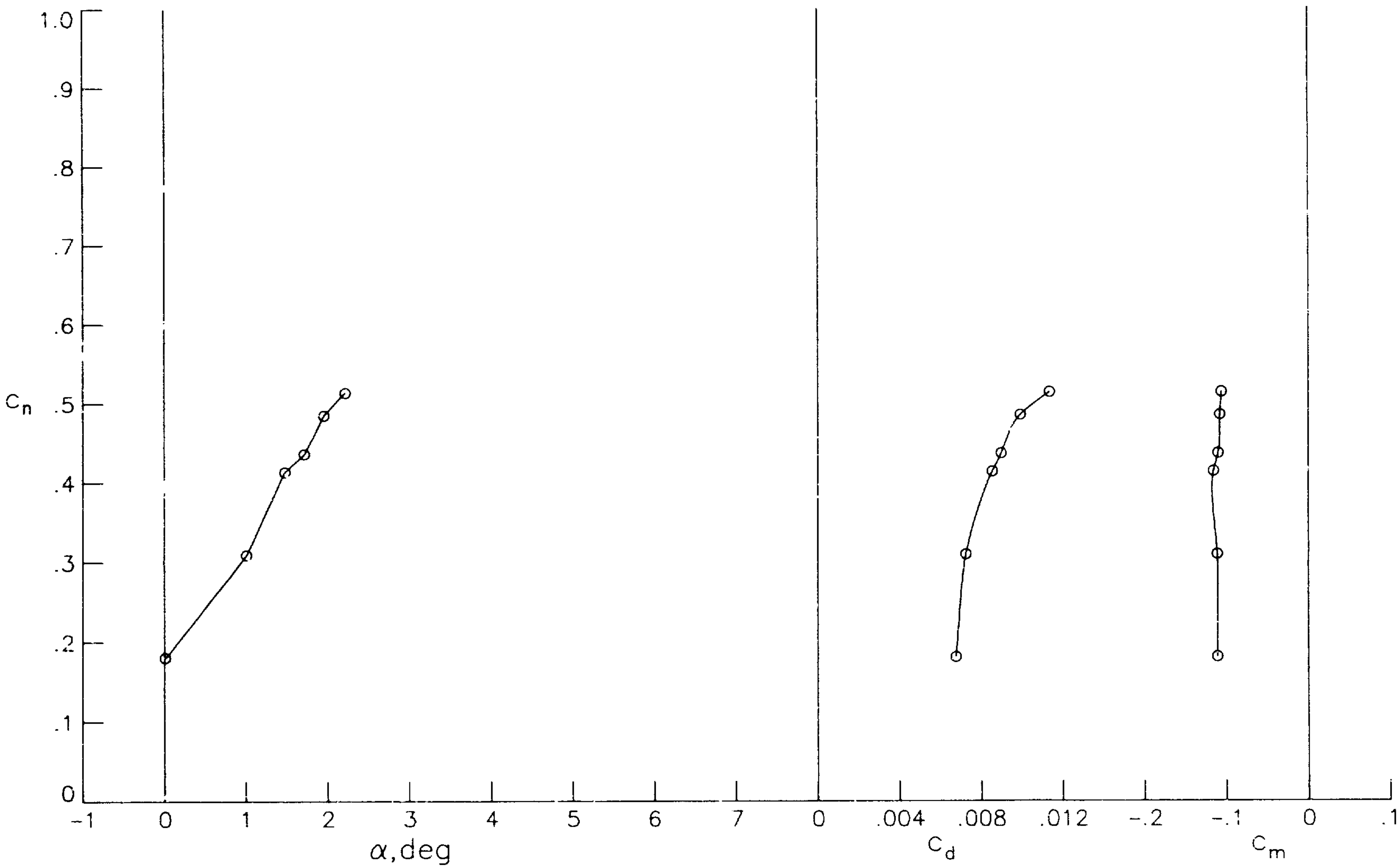

(d) $R = 47.55 \times 10^6$; $M = 0.7580$.

Figure 10.- Continued.

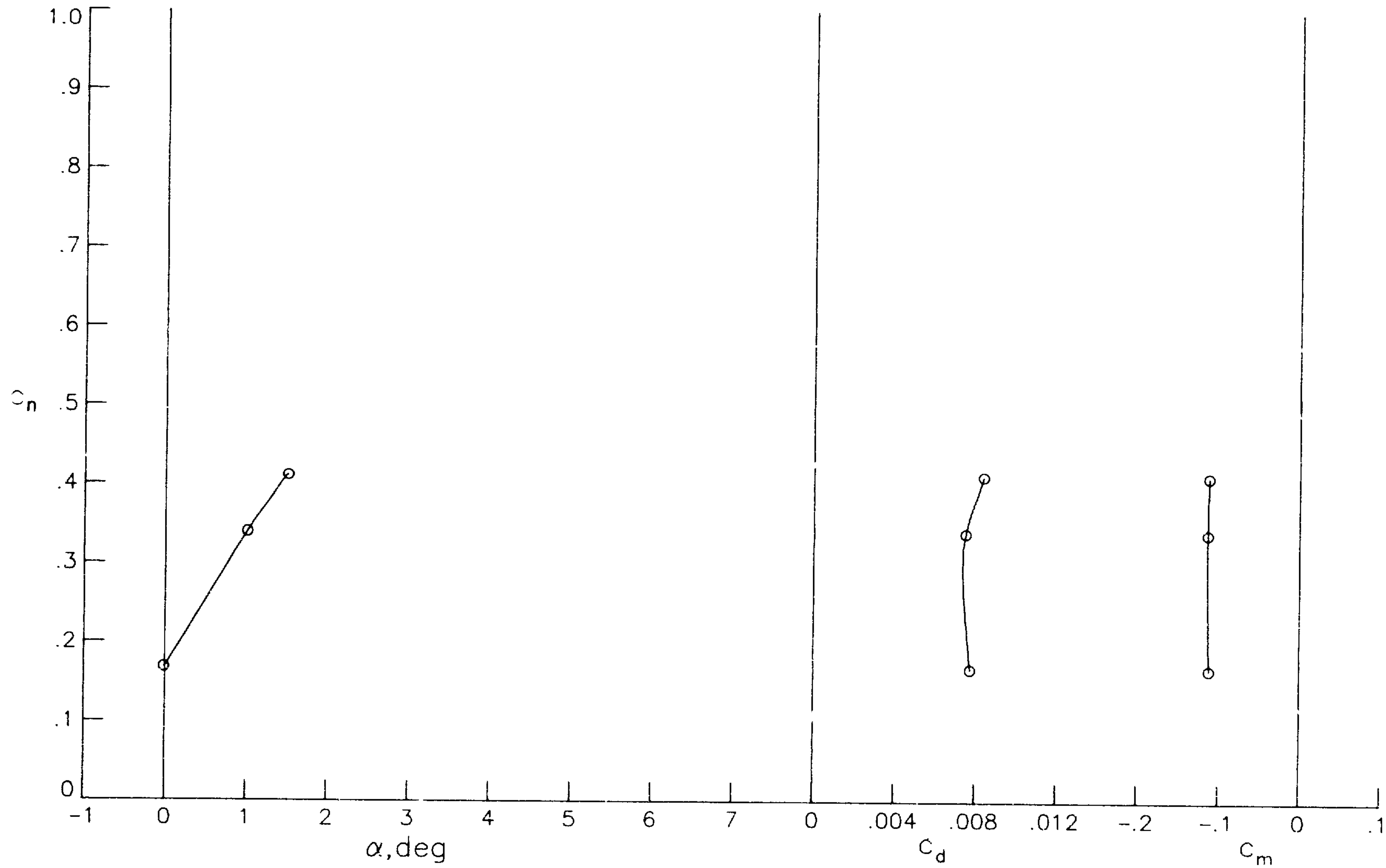

(e) $R = 47.47 \times 10^6$; $M = 0.7763$.

Figure 10.- Concluded.

SC(2)-0012

NASA

Year	1987
Reference	NASA TM-89102
t/c	0,12
Transition	free

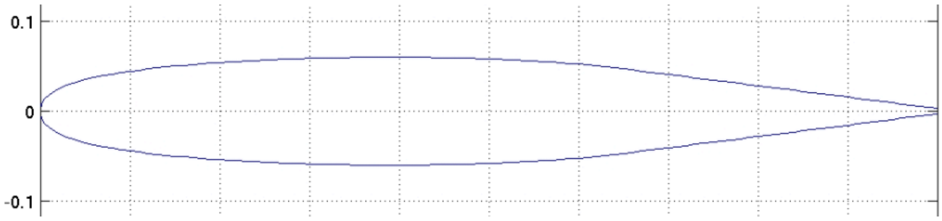

UIUC Airfoil Data Site

x/c	y_u/c	x/c	y_l/c
0	0	0	0
0,002	0,00912	0,002	-0,00912
0,005	0,01392	0,005	-0,01392
0,01	0,0186	0,01	-0,0186
0,02	0,02484	0,02	-0,02484
0,03	0,02916	0,03	-0,02916
0,04	0,0324	0,04	-0,0324
0,05	0,03504	0,05	-0,03504
0,06	0,03732	0,06	-0,03732
0,08	0,04119	0,08	-0,04119
0,1	0,04428	0,1	-0,04428
0,12	0,0468	0,12	-0,0468
0,14	0,04908	0,14	-0,04908
0,16	0,051	0,16	-0,051
0,18	0,05268	0,18	-0,05268
0,2	0,05412	0,2	-0,05412
0,22	0,05532	0,22	-0,05532
0,24	0,0564	0,24	-0,0564
0,26	0,05736	0,26	-0,05736
0,28	0,05808	0,28	-0,05808
0,3	0,0588	0,3	-0,0588
0,32	0,05928	0,32	-0,05928
0,34	0,05964	0,34	-0,05964
0,36	0,05988	0,36	-0,05988
0,38	0,06	0,38	-0,06
0,4	0,06	0,4	-0,06
0,42	0,05988	0,42	-0,05988
0,44	0,05964	0,44	-0,05964
0,46	0,05928	0,46	-0,05928
0,48	0,0588	0,48	-0,0588
0,5	0,05808	0,5	-0,05808
0,52	0,05736	0,52	-0,05736
0,54	0,0564	0,54	-0,0564
0,56	0,0552	1	-0,0552
1	0,05388	0,58	-0,05388
0,6	0,05232	0,6	-0,05232
0,62	0,0504	0,62	-0,0504
0,64	0,04824	0,64	-0,04824
0,66	0,04584	0,66	-0,04584
0,68	0,04332	0,68	-0,04332
0,7	0,0408	0,7	-0,0408
0,72	0,03828	0,72	-0,03828
0,74	0,03576	0,74	-0,03576
0,76	0,03324	0,76	-0,03324
0,78	0,03072	0,78	-0,03072
0,8	0,0282	0,8	-0,0282
0,82	0,02568	0,82	-0,02568
0,84	0,02316	0,84	-0,02316
0,86	0,02064	0,86	-0,02064
0,88	0,01812	0,88	-0,01812
0,9	0,0156	0,9	-0,0156
0,92	0,01308	0,92	-0,01308
0,94	0,01056	0,94	-0,01056
0,96	0,00804	0,96	-0,00804
0,983	0,0051	0,98	-0,00552
1	0,003	1	-0,003

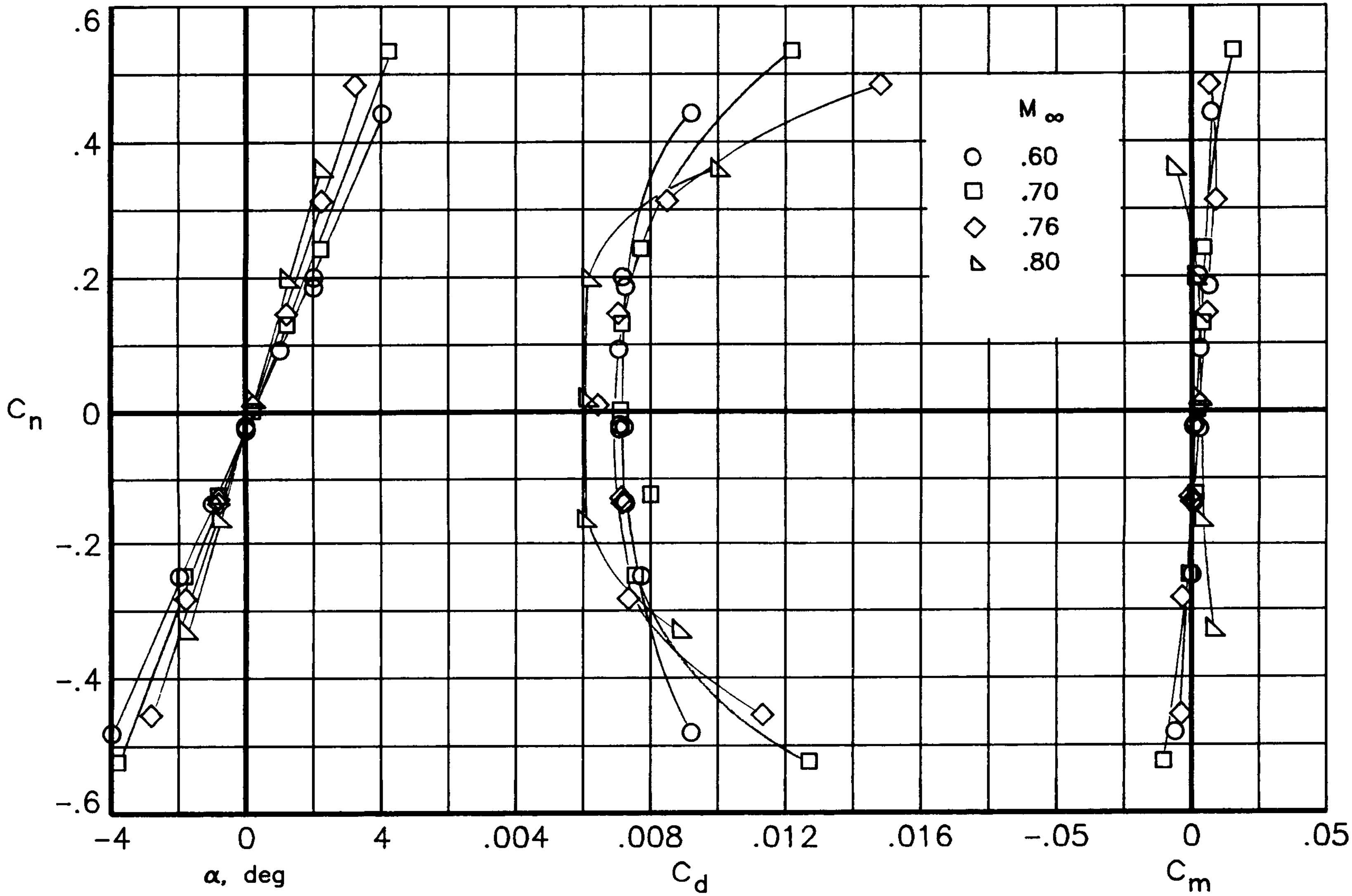

(a) $R_c = 6 \times 10^6$.

Figure 10.- Effect of Mach number on integrated force and moment coefficients.

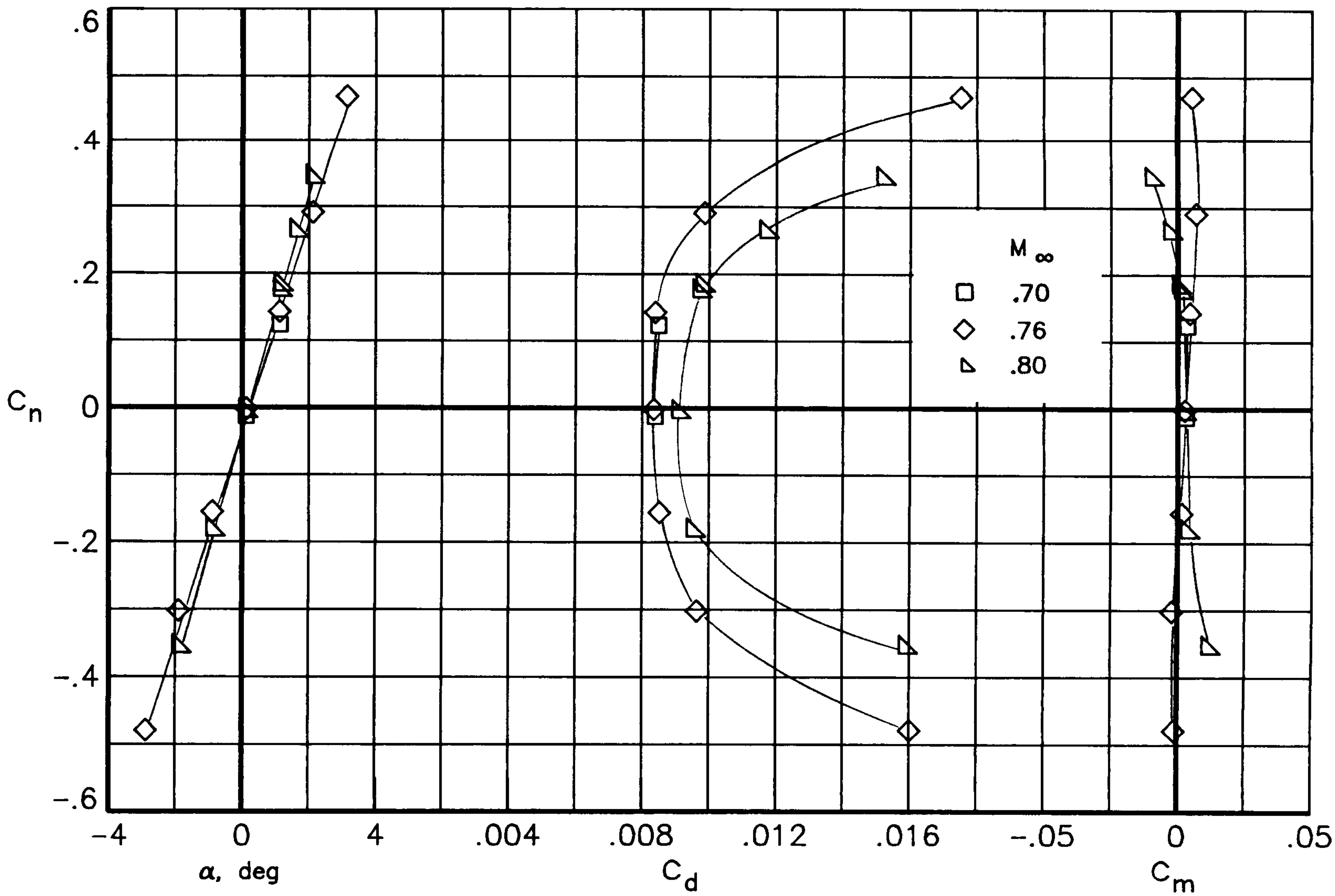

(b) $R_c = 9 \times 10^6$.

Figure 10.- Continued.

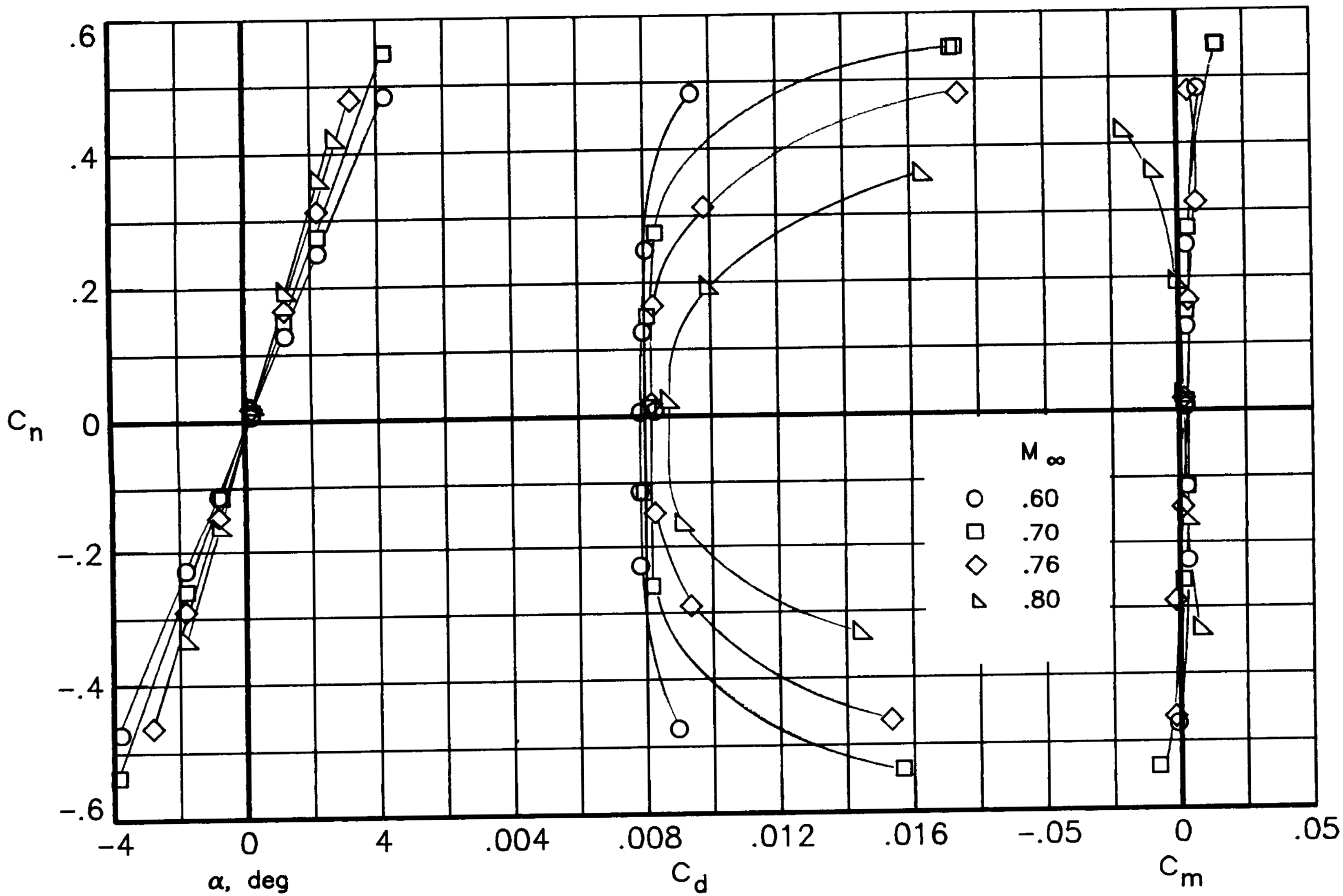

(c) $R_c = 15 \times 10^6$.

Figure 10.- Continued.

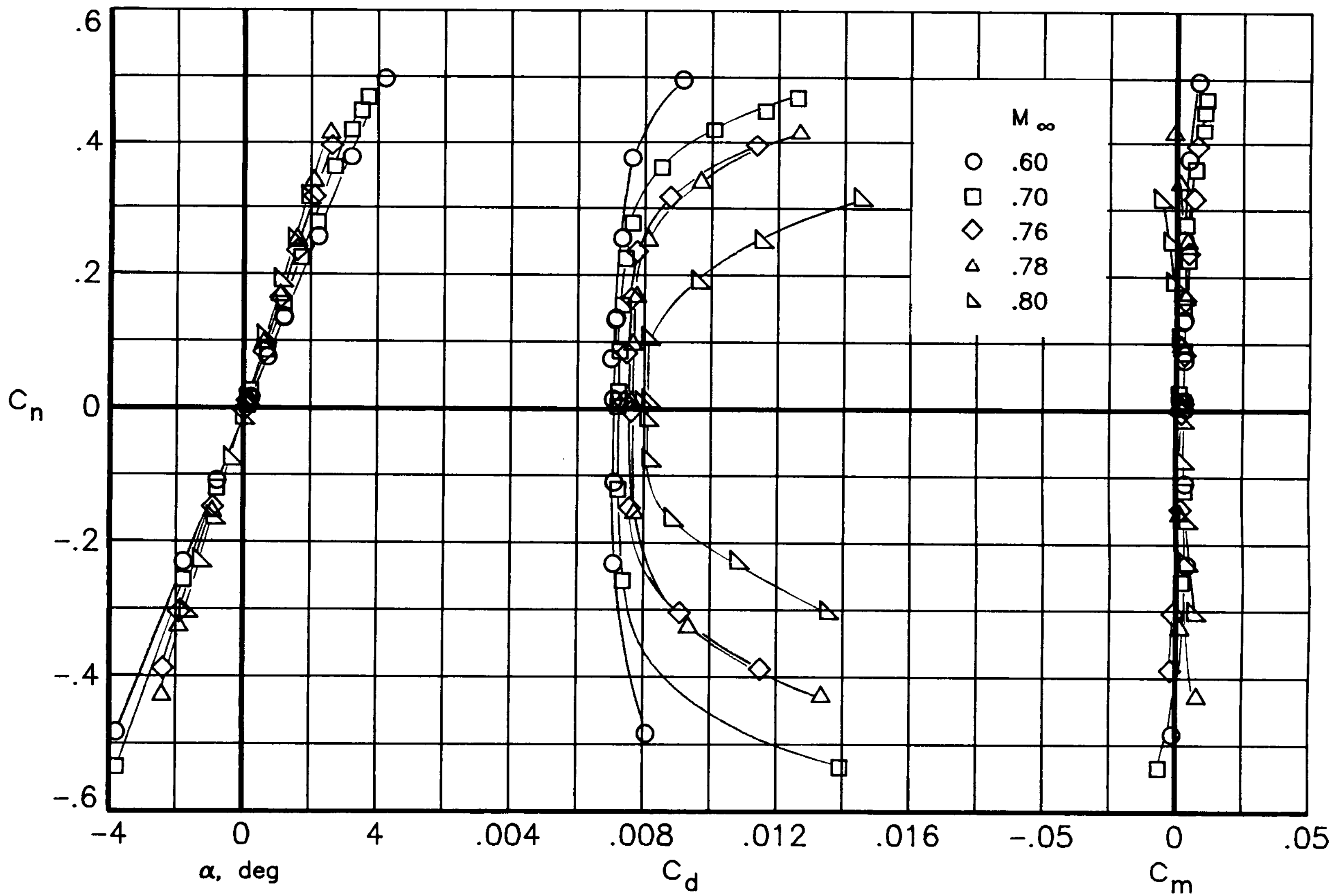

(d) $R_c = 30 \times 10^6$.

Figure 10.- Continued.

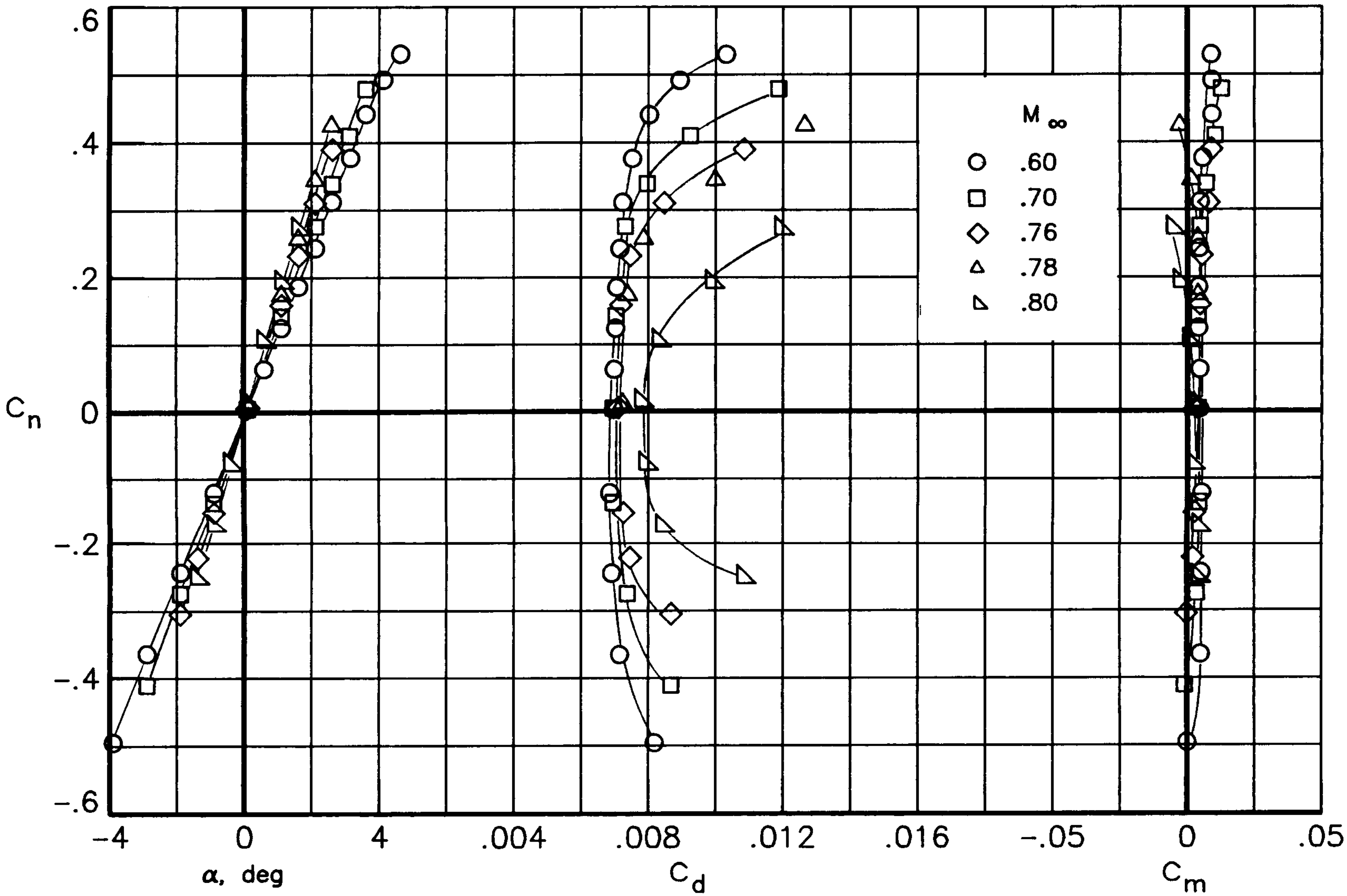

(e) $R_c = 40 \times 10^6$.

Figure 10.- Concluded.

SC(2)-0710
(Supercritical Airfoil 33)

NASA

Year	1975
Reference	NASA TM X-72711
t/c	0,10
$c_{l,design}$	0,7
M_{design}	0,78
Transition	fixed at 0,28c

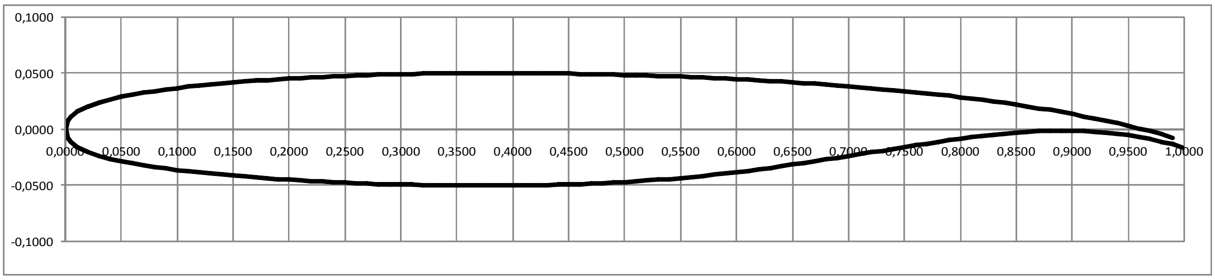

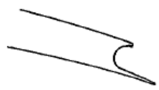

Sketch of T.E. at expanded scale

x/c	y_u/c	y_l/c
0,0000	0,0000	0,0000
0,0020	0,0075	-0,0075
0,0050	0,0116	-0,0116
0,0100	0,0156	-0,0156
0,0200	0,0206	-0,0203
0,0300	0,0240	-0,0235
0,0400	0,0267	-0,0262
0,0500	0,0289	-0,0284
0,0600	0,0308	-0,0303
0,0700	0,0325	-0,0320
0,0800	0,0340	-0,0335
0,0900	0,0354	-0,0349
0,1000	0,0367	-0,0362
0,1100	0,0379	-0,0374
0,1200	0,0389	-0,0385
0,1300	0,0399	-0,0395
0,1400	0,0408	-0,0405
0,1500	0,0417	-0,0414
0,1600	0,0425	-0,0422
0,1700	0,0432	-0,0430
0,1800	0,0439	-0,0437
0,1900	0,0446	-0,0444
0,2000	0,0452	-0,0450
0,2100	0,0457	-0,0456
0,2200	0,0462	-0,0462
0,2300	0,0467	-0,0467
0,2400	0,0472	-0,0472
0,2500	0,0476	-0,0476
0,2600	0,0480	-0,0480
0,2700	0,0483	-0,0484
0,2800	0,0486	-0,0487
0,2900	0,0489	-0,0490
0,3000	0,0491	-0,0493

0,3100	0,0493	-0,0495
0,3200	0,0495	-0,0497
0,3300	0,0496	-0,0499
0,3400	0,0497	-0,0500
0,3500	0,0498	-0,0501
0,3600	0,0499	-0,0502
0,3700	0,0500	-0,0502
0,3800	0,0500	-0,0502
0,3900	0,0500	-0,0502
0,4000	0,0500	-0,0501
0,4100	0,0499	-0,0500
0,4200	0,0498	-0,0499
0,4300	0,0497	-0,0497
0,4400	0,0496	-0,0495
0,4500	0,0495	-0,0492
0,4600	0,0493	-0,0488
0,4700	0,0491	-0,0484
0,4800	0,0489	-0,0480
0,4900	0,0487	-0,0475
0,5000	0,0484	-0,0470
0,5100	0,0481	-0,0464
0,5200	0,0478	-0,0457
0,5300	0,0475	-0,0450
0,5400	0,0472	-0,0442
0,5500	0,0468	-0,0434
0,5600	0,0464	-0,0425
0,5700	0,0460	-0,0415
0,5800	0,0456	-0,0405
0,5900	0,0451	-0,0394
0,6000	0,0446	-0,0382
0,6100	0,0441	-0,0370
0,6200	0,0436	-0,0357
0,6300	0,0430	-0,0343
0,6400	0,0424	-0,0329
0,6500	0,0418	-0,0315
0,6600	0,0412	-0,0300
0,6700	0,0405	-0,0285
0,6800	0,0398	-0,0270
0,6900	0,0391	-0,0255
0,7000	0,0383	-0,0239
0,7100	0,0375	-0,0223
0,7200	0,0367	-0,0207
0,7300	0,0358	-0,0191
0,7400	0,0349	-0,0175
0,7500	0,0340	-0,0159
0,7600	0,0330	-0,0143
0,7700	0,0320	-0,0128
0,7800	0,0309	-0,0113
0,7900	0,0298	-0,0099
0,8000	0,0287	-0,0085
0,8100	0,0275	-0,0072
0,8200	0,0262	-0,0060
0,8300	0,0248	-0,0049
0,8400	0,0234	-0,0038
0,8500	0,0219	-0,0029
0,8600	0,0204	-0,0022
0,8700	0,0188	-0,0017
0,8800	0,0171	-0,0014
0,8900	0,0153	-0,0013
0,9000	0,0135	-0,0013
0,9100	0,0116	-0,0016
0,9200	0,0096	-0,0021
0,9300	0,0075	-0,0028
0,9400	0,0054	-0,0039
0,9500	0,0032	-0,0053
0,9600	0,0008	-0,0069
0,9700	-0,0017	-0,0088
0,9800	-0,0044	-0,0110
0,9900	-0,0074	-0,0135
1,0000		-0,0163

[redacted]

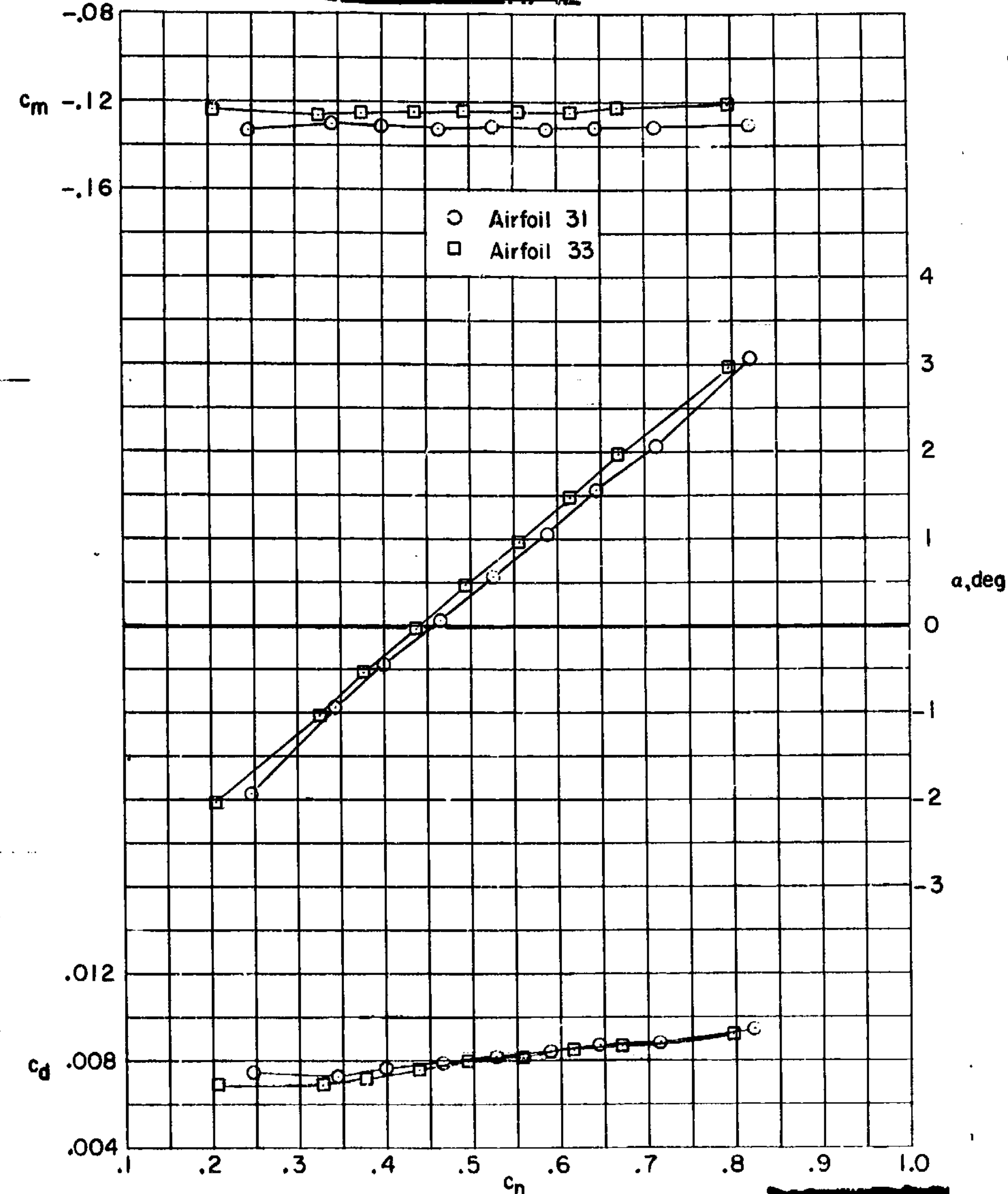

[redacted]

(a) M = 0.50.

Figure 7.- Comparison of force and moment characteristics of 10-percent-thick supercritical airfoils 31 and 33.

[redacted]

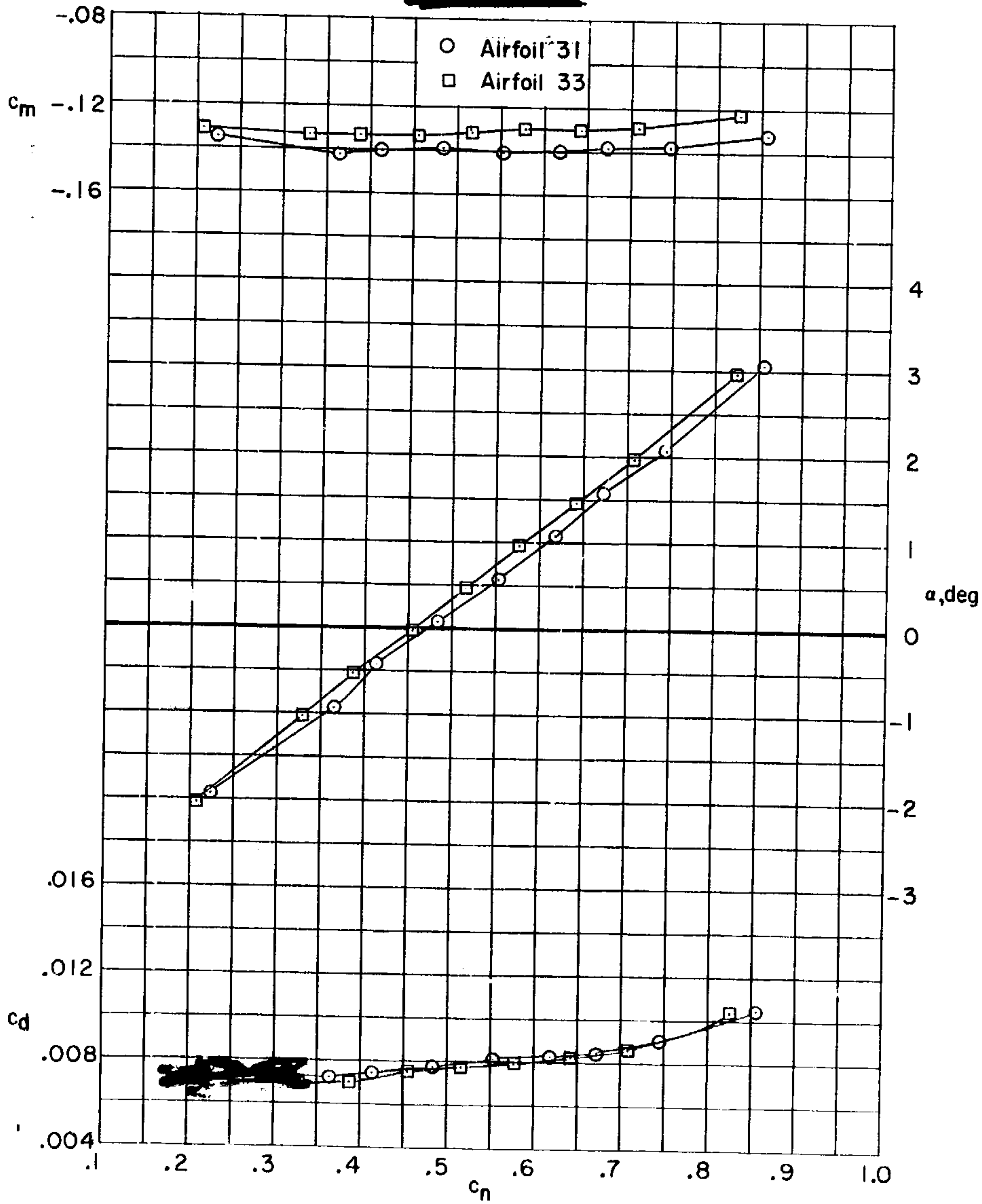

(b) M = 0.60.

Figure 7.- Continued.

[redacted]

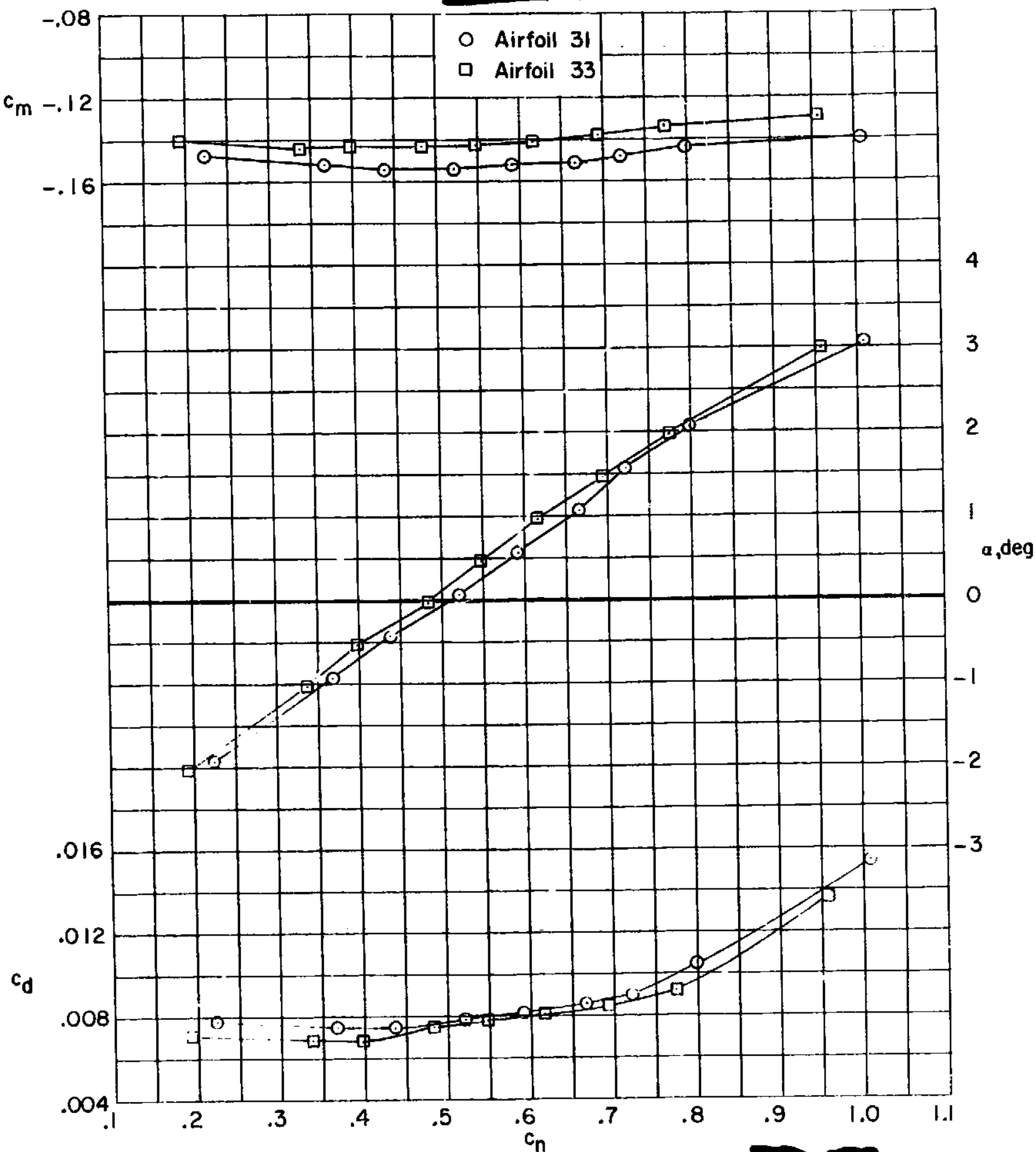

[redacted]

(c) M = 0.70.

Figure 7.- Continued.

[redacted]

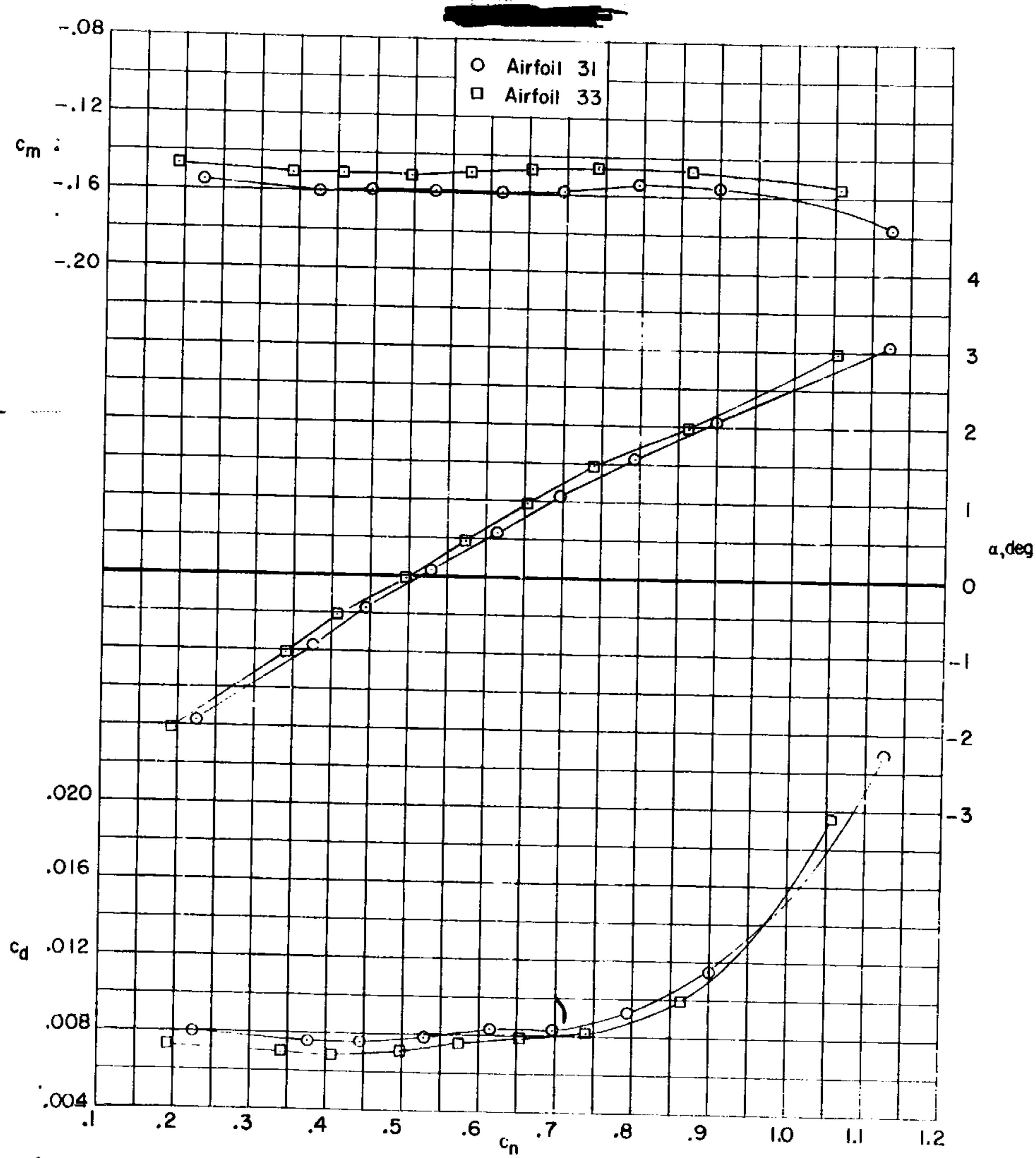

(d) M = 0.74.

[redacted]

Figure 7.- Continued.

[redacted]

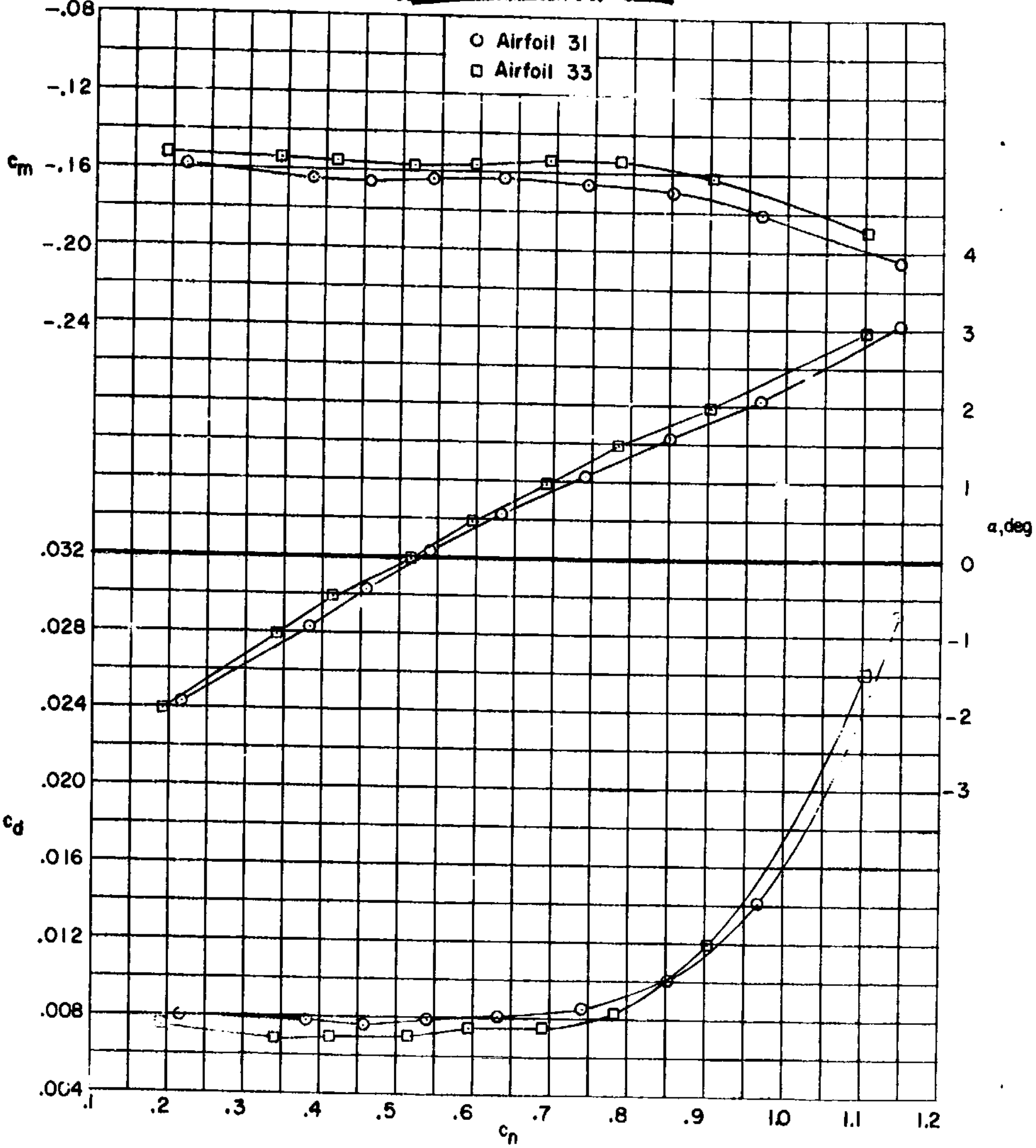

[redacted]

(e) M = 0.76.

Figure 7.- Continued.

[redacted]

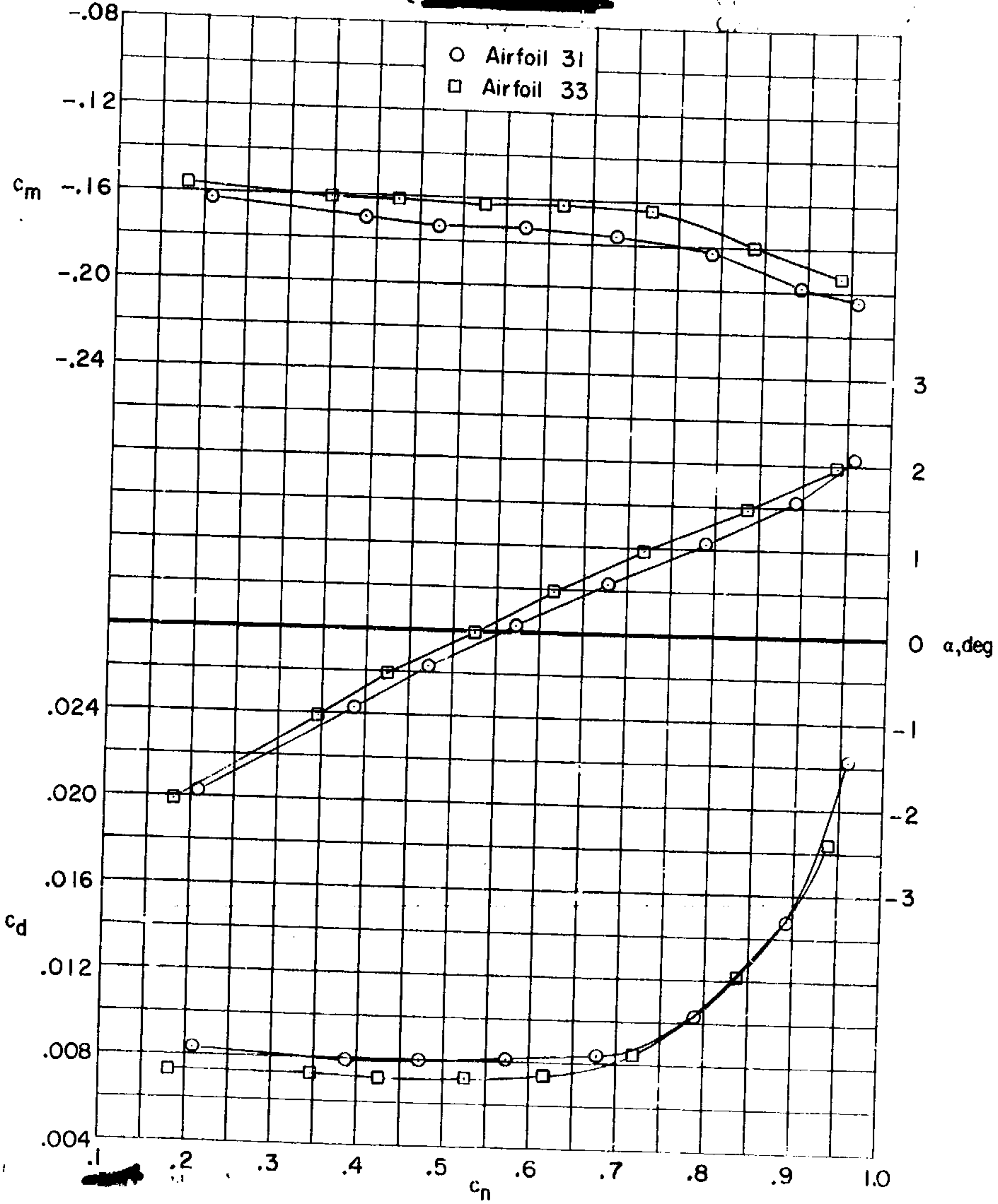

[redacted]

(g) M = 0.78.

Figure 7.- Continued.

[redacted]

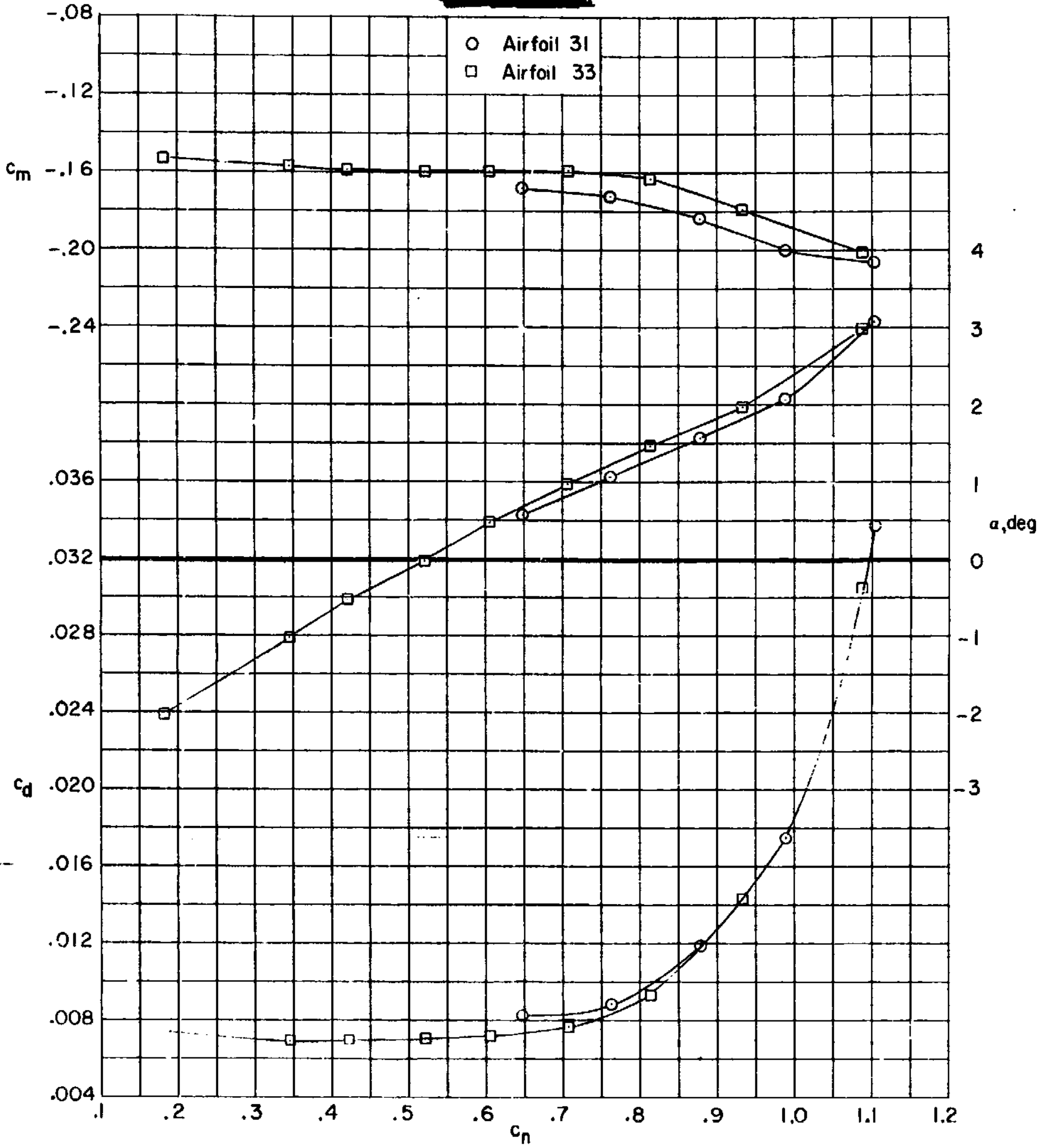

[redacted]

(f) M = 0.77.

Figure 7.- Continued.

[redacted]

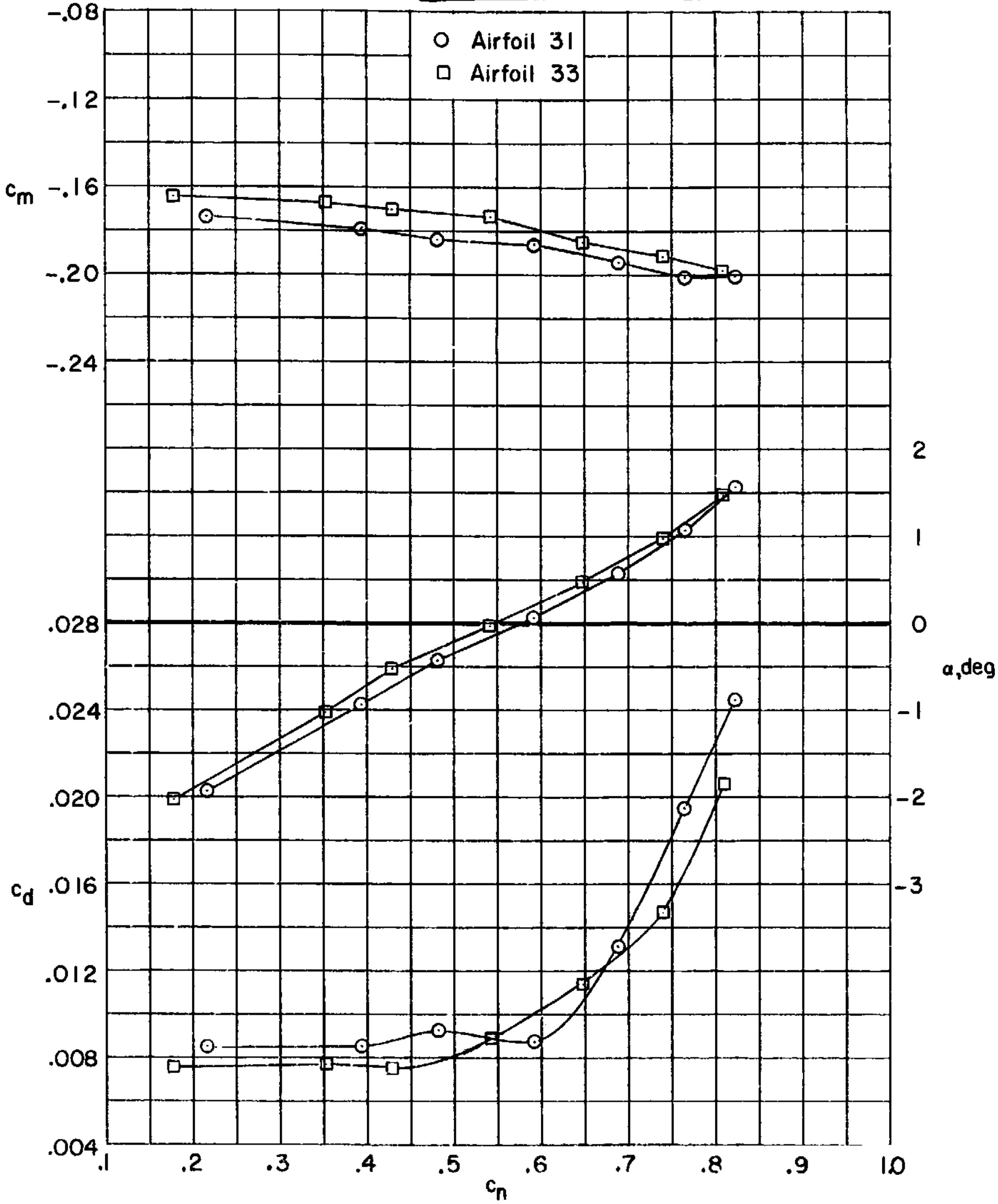

[redacted]

(l) M = 0.80.

Figure 7.- Continued.

[redacted]

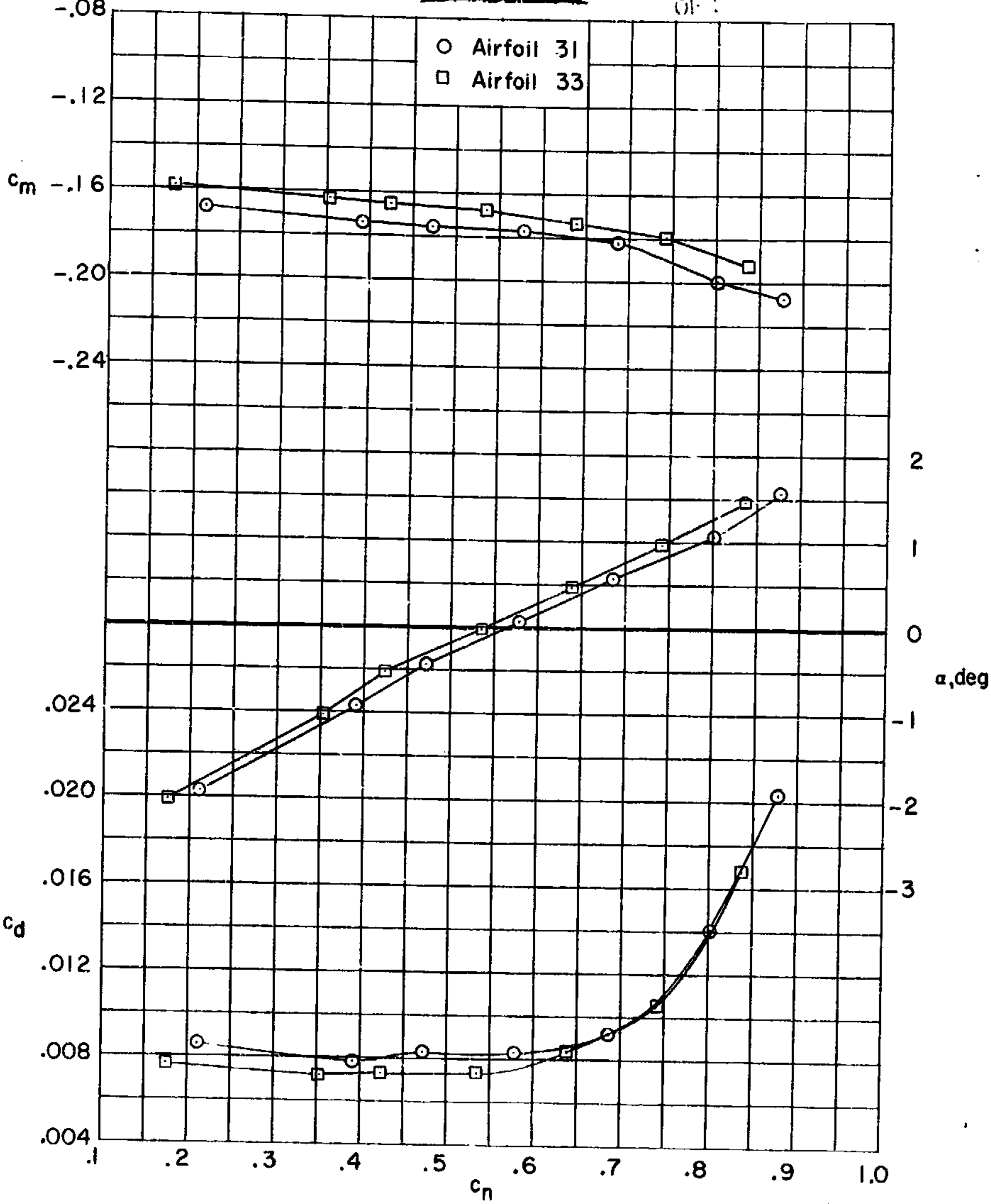

[redacted]

(h) M = 0.79.

Figure 7.- Continued.

[redacted]

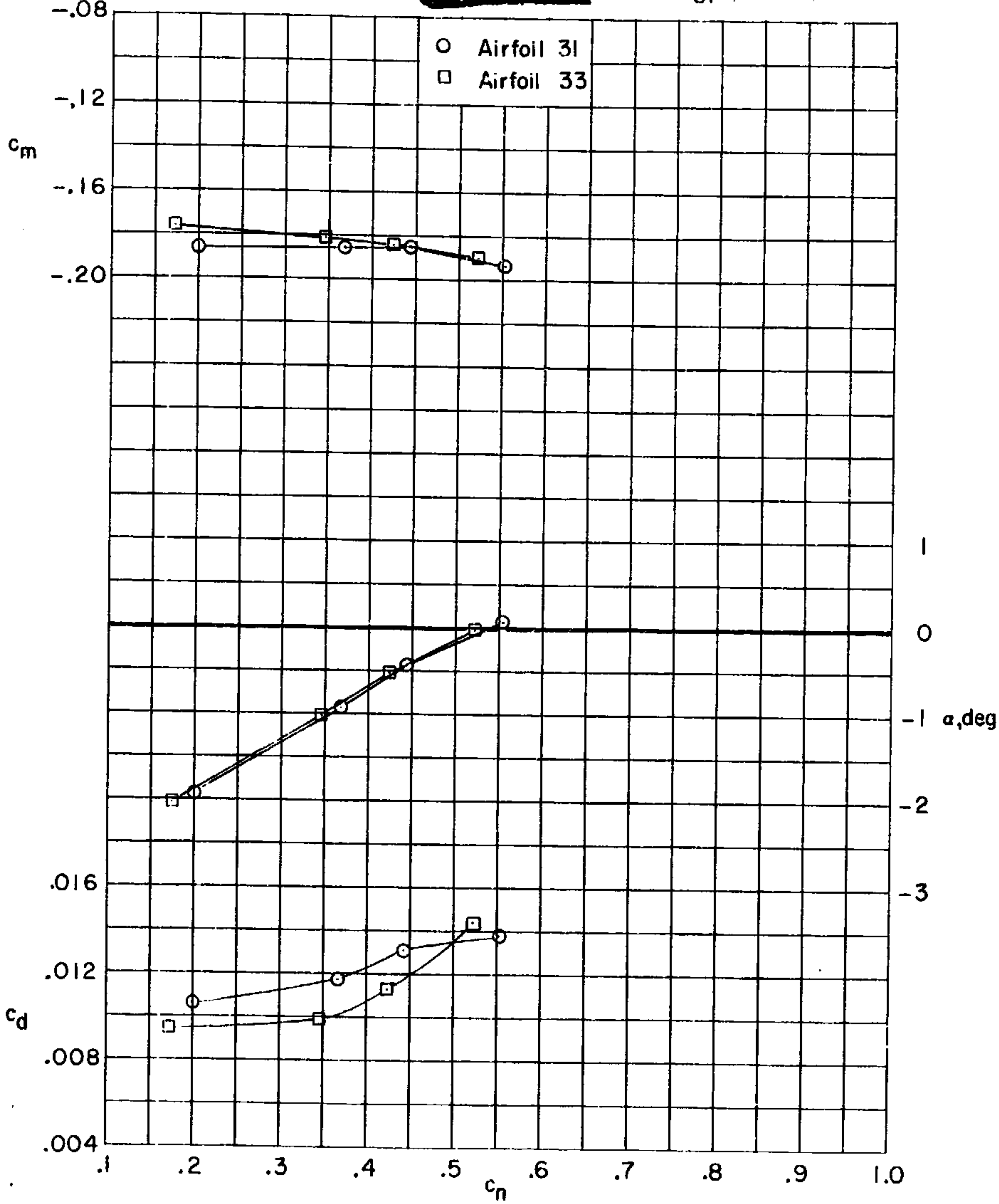

[redacted]

(k) M = 0.82.

Figure 7.- Concluded.

[redacted]

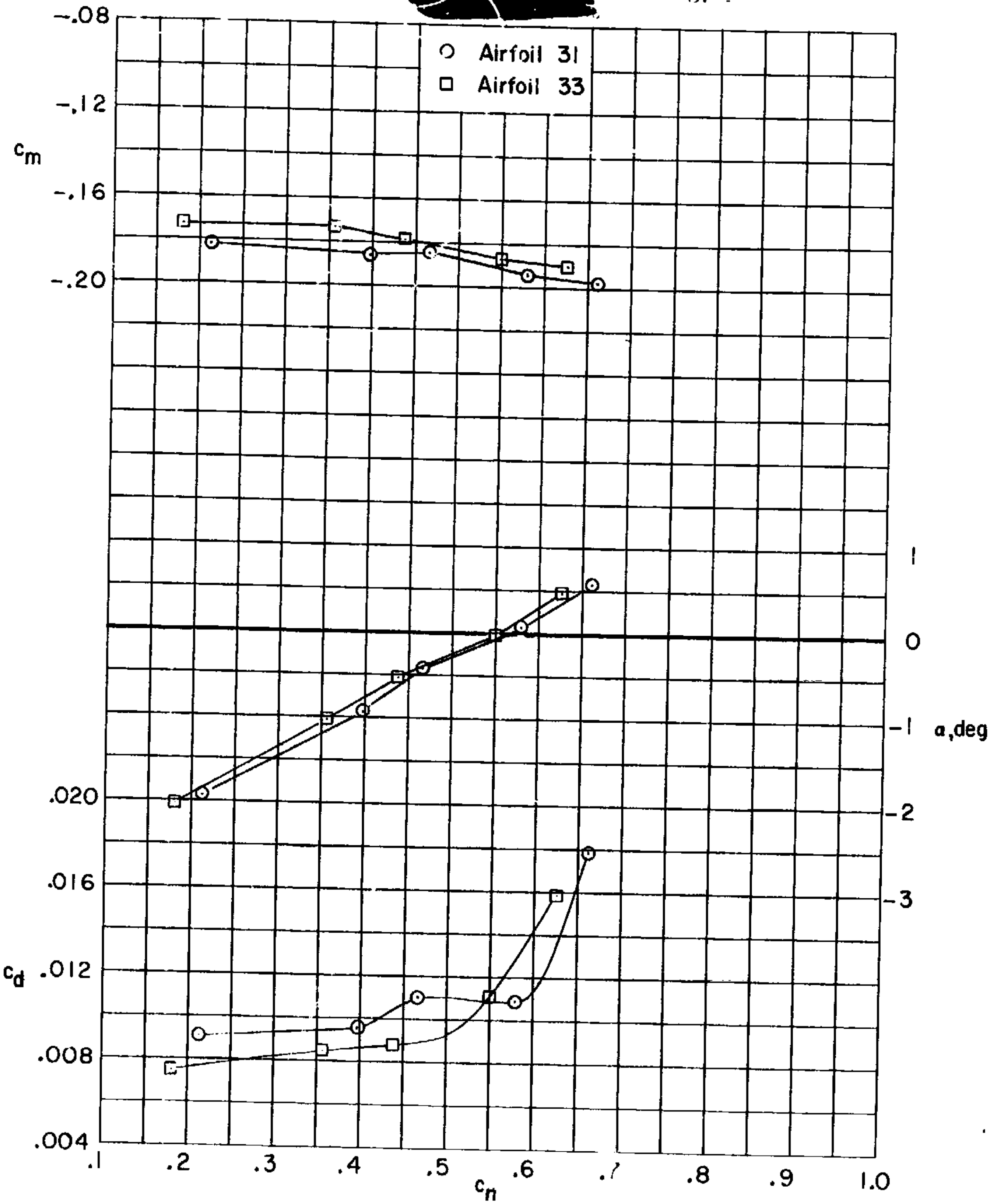

[redacted]

(j) M = 0.81.

Figure 7.- Continued.

[redacted]

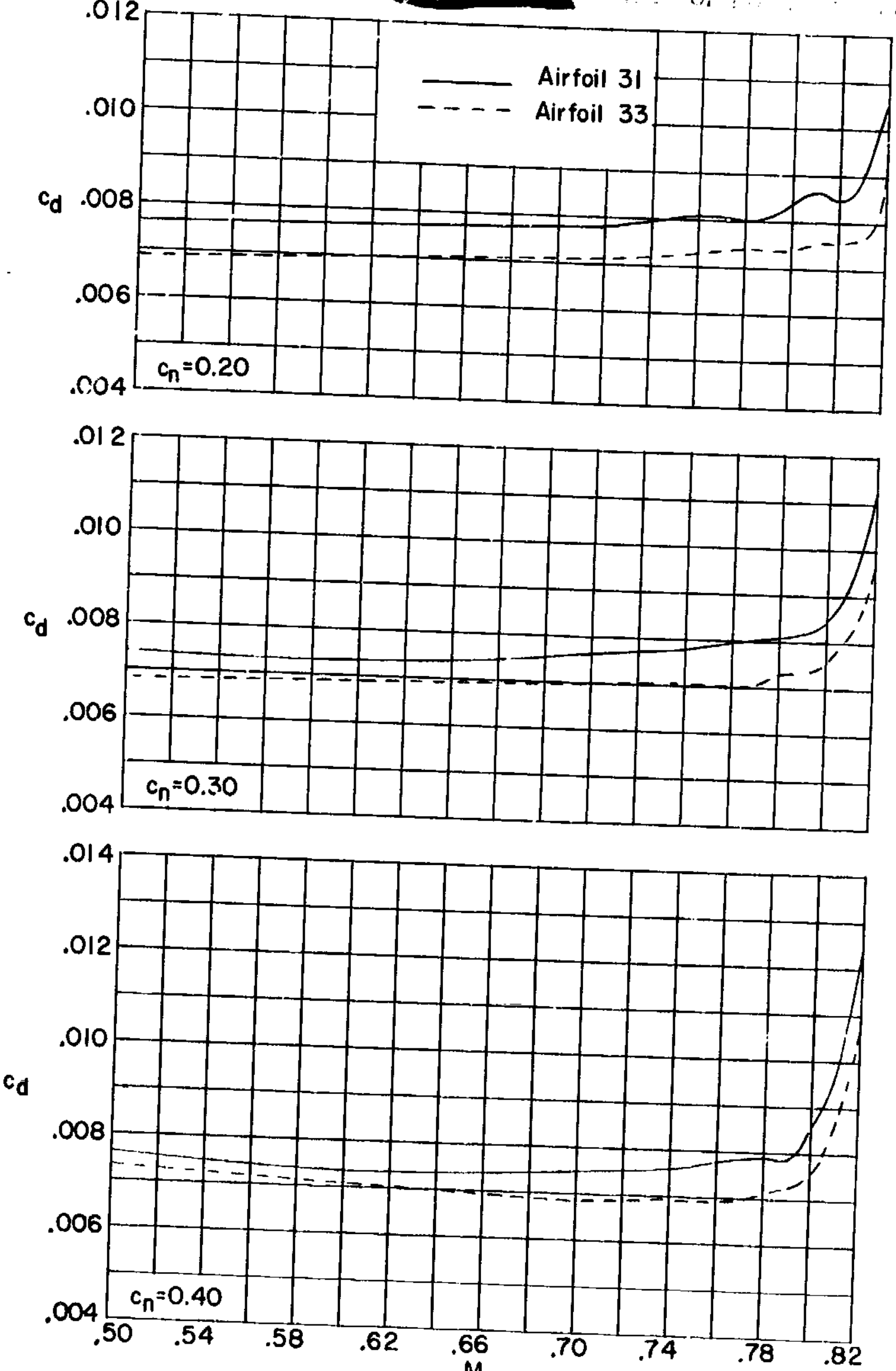

[redacted]

(a) c_n = 0.20, 0.30 and 0.40.

Figure 8. - Variation of measured section drag coefficient with Mach number of 10-percent-thick supercritical airfoils 31 and 33.

[redacted]

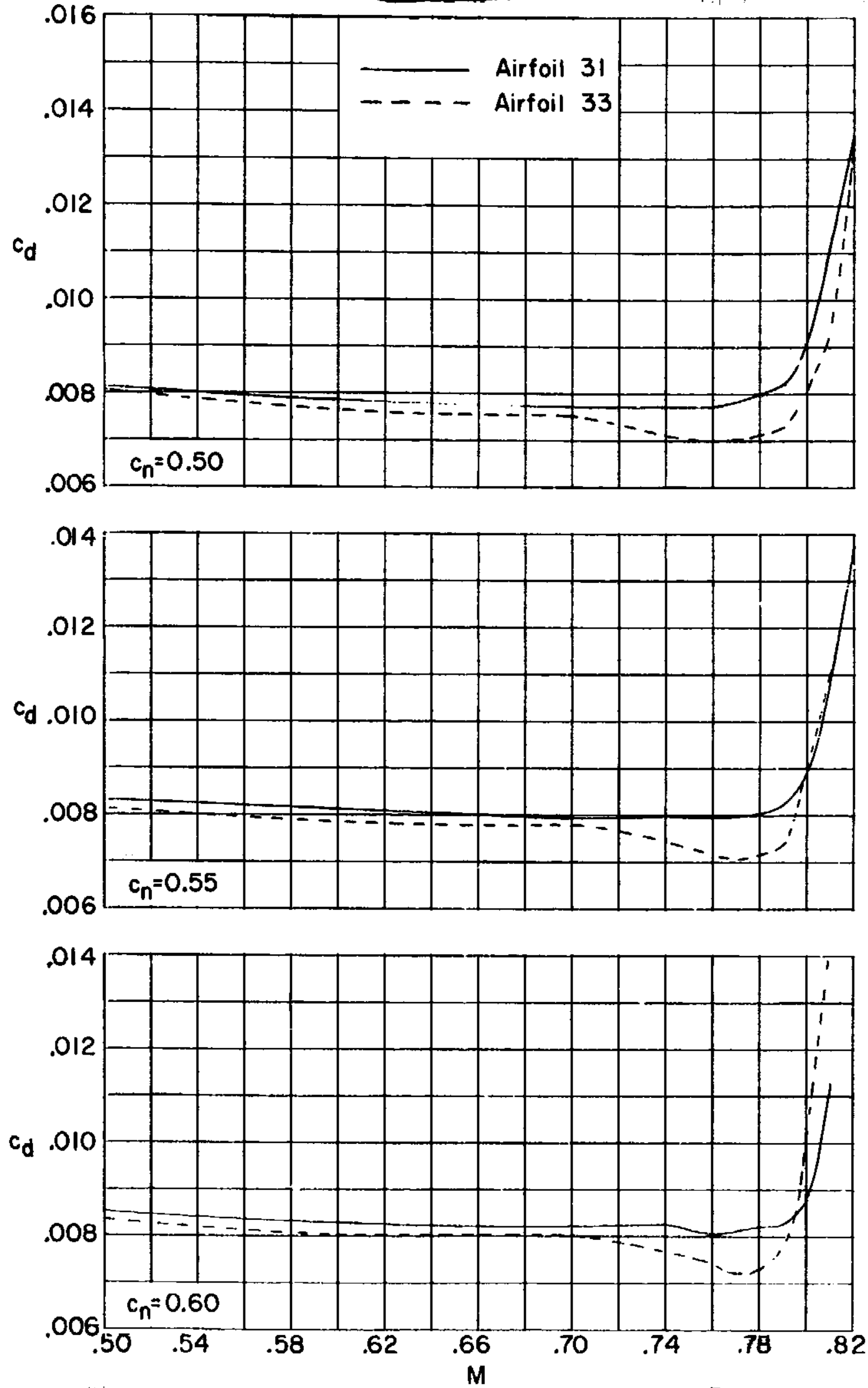

[redacted]

(b) c_n = 0.50, 0.55 and 0.60.

Figure 8. - Continued.

[redacted]

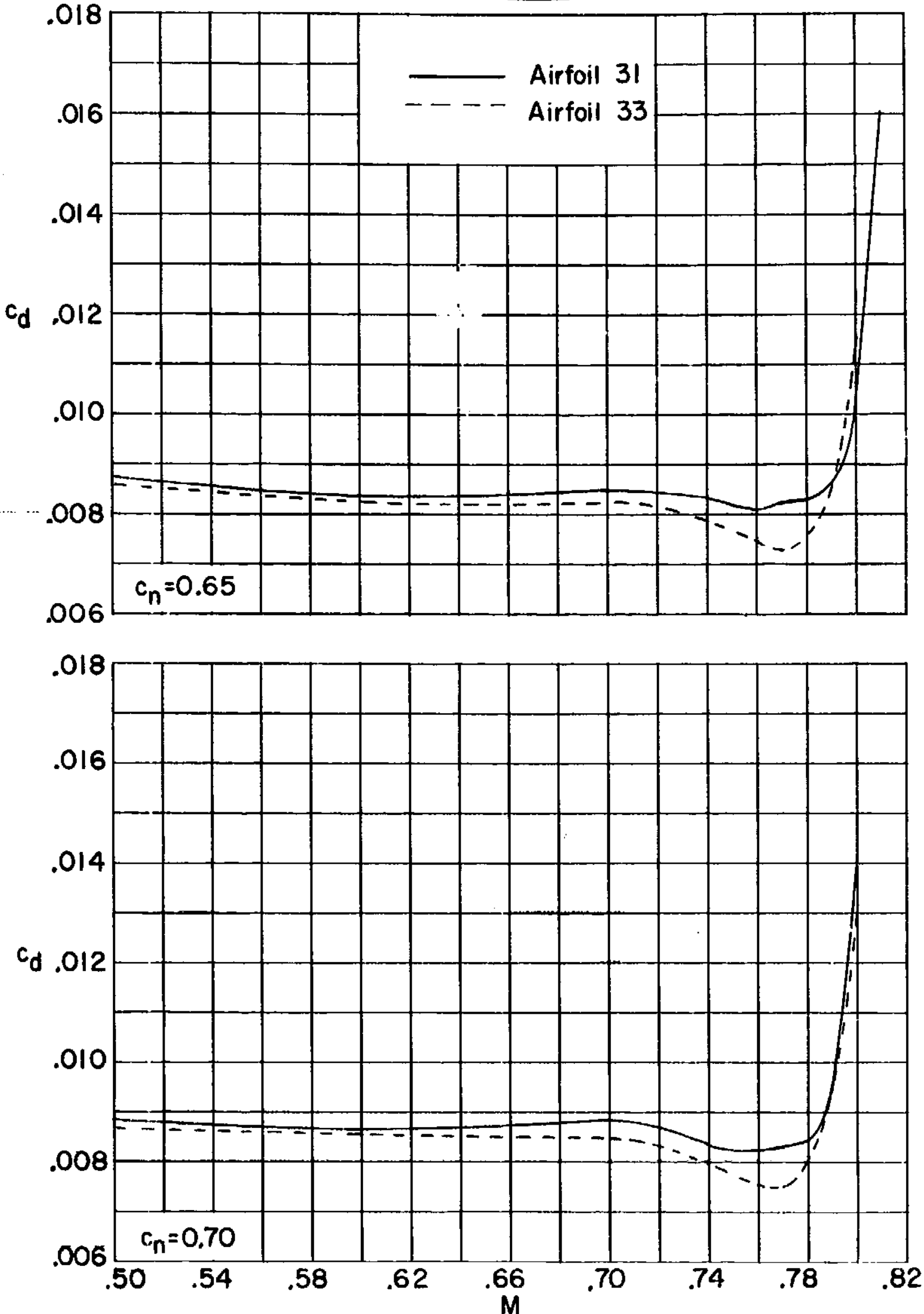

[redacted]

(c) c_n = 0.65 and 0.70.

Figure 8.- Continued.

[redacted]

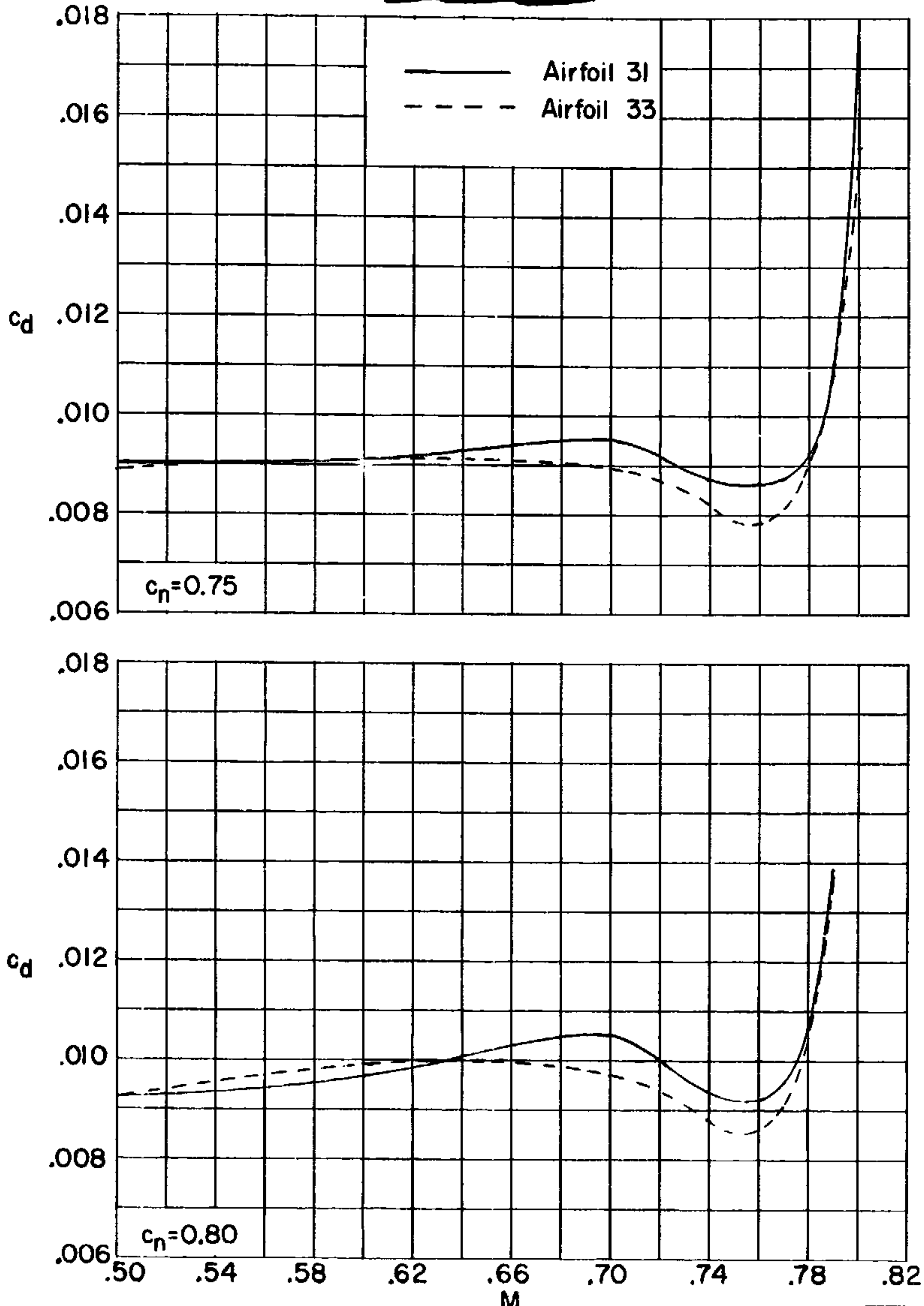

[redacted]

(d) c_n = 0.75 and 0.80.

Figure 8. - Continued.

[redacted]

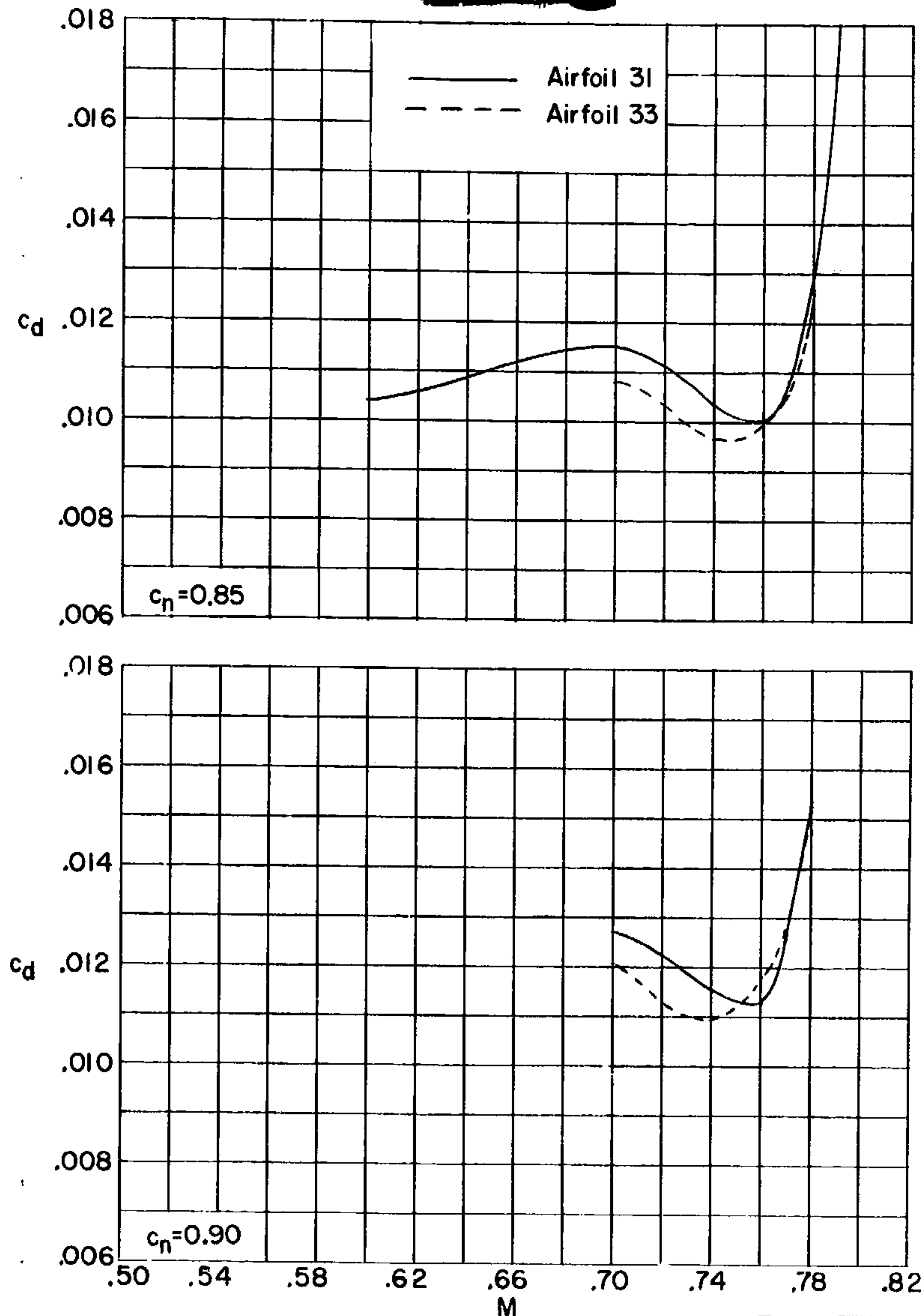

[redacted]

(e) c_n = 0.85 and 0.90.

Figure 8. - Concluded.

[redacted]

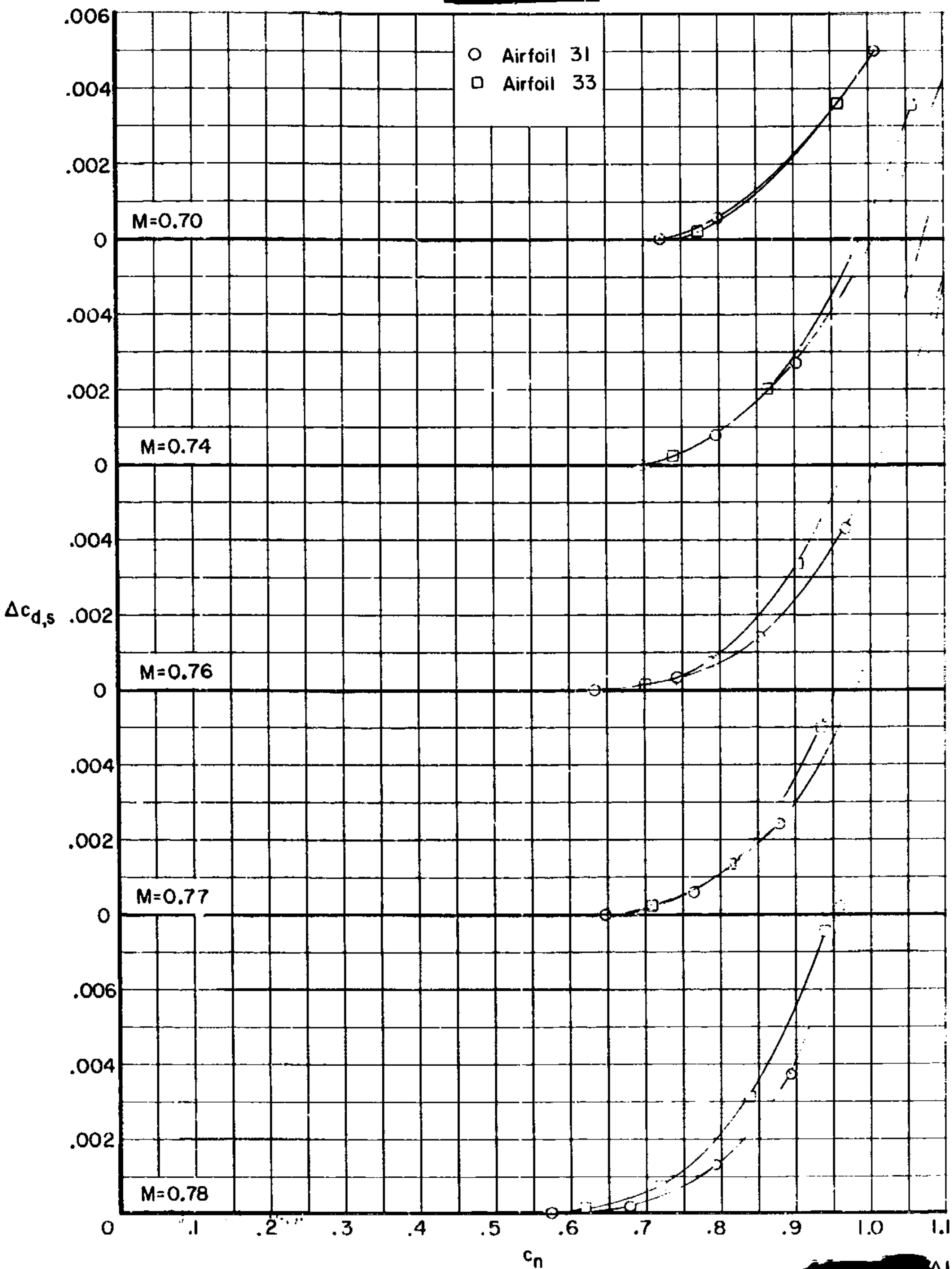

[redacted]AL

Figure 9. - Drag increment due to shock wave losses.

SC(2)-0714

NASA

Year	1975
Reference	high speed: NASA TM X-72712 low speed: NASA TM-81912
t/c	0,14
$c_{l,max}$	2,2
$c_{l,design}$	0,7
M_{design}	0,74
Transition	high speed: fixed at 0,28c low speed: fixed at 0,05c

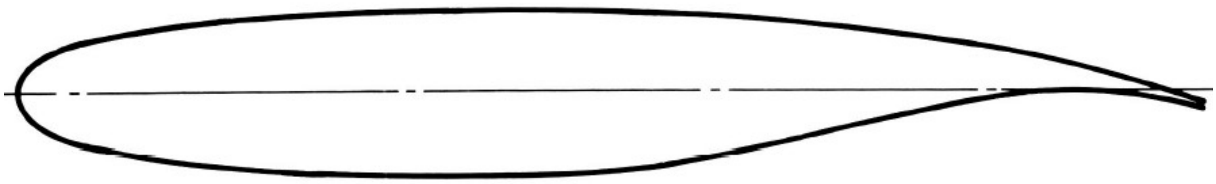

NASA TP 2890

[redacted]

ORIGINAL PAGE IS
OF POOR QUALITY

TABLE I.- SECTION COORDINATES FOR

14-PERCENT-THICK SUPERCRITICAL AIRFOIL

[c = 63.5 cm (25 in.); leading-edge radius = 0.030c]

x/c	$(y/c)_u$	$(y/c)_l$	x/c	$(y/c)_u$	$(y/c)_l$
0.0	0.0	0.0	.240	.0659	-.0661
.002	.0108	-.0108	.250	.0665	-.0667
.005	.0167	-.0165	.260	.0670	-.0672
.010	.0225	-.0223	.270	.0675	-.0677
.020	.0297	-.0295	.280	.0679	-.0681
.030	.0346	-.0343	.290	.0683	-.0685
.040	.0383	-.0381	.300	.0686	-.0688
.050	.0414	-.0411	.310	.0689	-.0691
.060	.0440	-.0438	.320	.0692	-.0693
.070	.0463	-.0461	.330	.0694	-.0695
.080	.0484	-.0481	.340	.0696	-.0696
.090	.0502	-.0500	.350	.0698	-.0697
.100	.0519	-.0517	.360	.0699	-.0697
.110	.0535	-.0533	.370	.0700	-.0697
.120	.0549	-.0547	.380	.0700	-.0696
.130	.0562	-.0561	.390	.0700	-.0695
.140	.0574	-.0574	.400	.0700	-.0693
.150	.0585	-.0585	.410	.0699	-.0691
.160	.0596	-.0596	.420	.0698	-.0689
.170	.0606	-.0606	.430	.0697	-.0686
.180	.0615	-.0616	.440	.0696	-.0682
.190	.0624	-.0625	.450	.0694	-.0678
.200	.0632	-.0633	.460	.0692	-.0673
.210	.0640	-.0641	.470	.0689	-.0667
.220	.0647	-.0648	.480	.0686	-.0661
.230	.0653	-.0655	.490	.0683	-.0654

[redacted]

[redacted]

TABLE I.- SECTION COORDINATES FOR

14-PERCENT-THICK SUPERCRITICAL AIRFOIL - Concluded

x/c	$(y/c)_u$	$(y/c)_l$	x/c	$(y/c)_u$	$(y/c)_l$
.500	.0680	-.0646	.760	.0457	-.0173
.510	.0676	-.0637	.770	.0442	-.0152
.520	.0672	-.0627	.780	.0426	-.0132
.530	.0668	-.0616	.790	.0409	-.0113
.540	.0663	-.0604	.800	.0392	-.0095
.550	.0658	-.0591	.810	.0374	-.0079
.560	.0652	-.0577	.820	.0356	-.0064
.570	.0646	-.0562	.830	.0337	-.0050
.580	.0640	-.0546	.840	.0317	-.0038
.590	.0634	-.0529	.850	.0297	-.0028
.600	.0627	-.0511	.860	.0276	-.0020
.610	.0620	-.0493	.870	.0255	-.0014
.620	.0613	-.0474	.880	.0233	-.0010
.630	.0605	-.0454	.890	.0210	-.0008
.640	.0596	-.0434	.900	.0186	-.0008
.650	.0587	-.0413	.910	.0162	-.0011
.660	.0578	-.0392	.920	.0137	-.0016
.670	.0568	-.0371	.930	.0111	-.0024
.680	.0558	-.0349	.940	.0084	-.0035
.690	.0547	-.0327	.950	.0057	-.0049
.700	.0536	-.0305	.960	.0029	-.0066
.710	.0524	-.0283	.970	0.0	-.0086
.720	.0512	-.0261	.980	-.0030	-.0109
.730	.0499	-.0239	.990	-.0062	-.0136
.740	.0486	-.0217	1.000	------	-.0165
.750	.0472	-.0195			

[redacted]

SC(2)-0714

High Mach Numbers
(M = 0,5 to M = 0,78)
- NASA TM X-72712 -

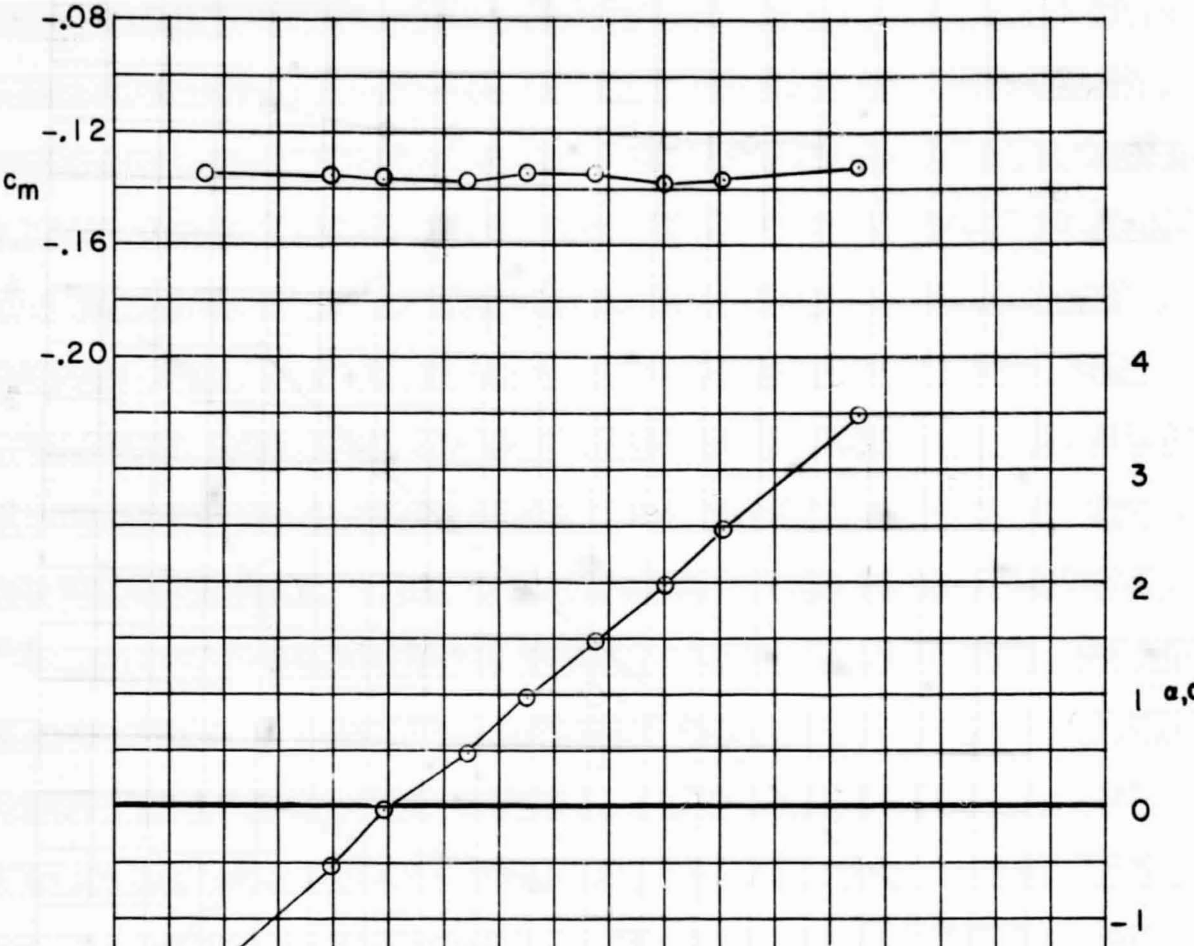

(a) M = 0.50.

Figure 7.- Force and moment characteristics of 14-percent-thick supercritical airfoil.

[redacted]

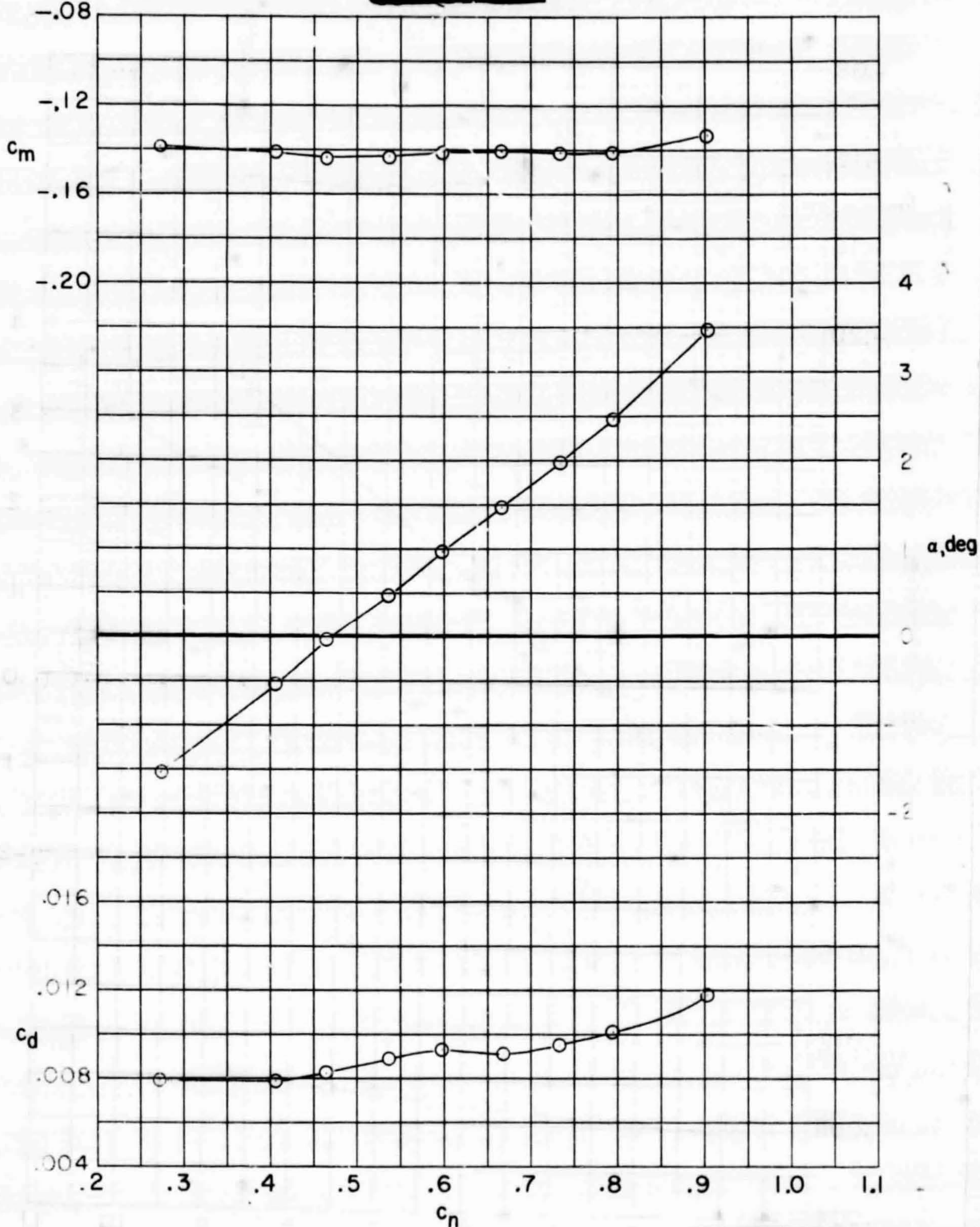

[redacted]

(b) M = 0.60.

Figure 7. - Continued.

ORIGINAL PAGE IS
OF POOR QUALITY

[redacted]

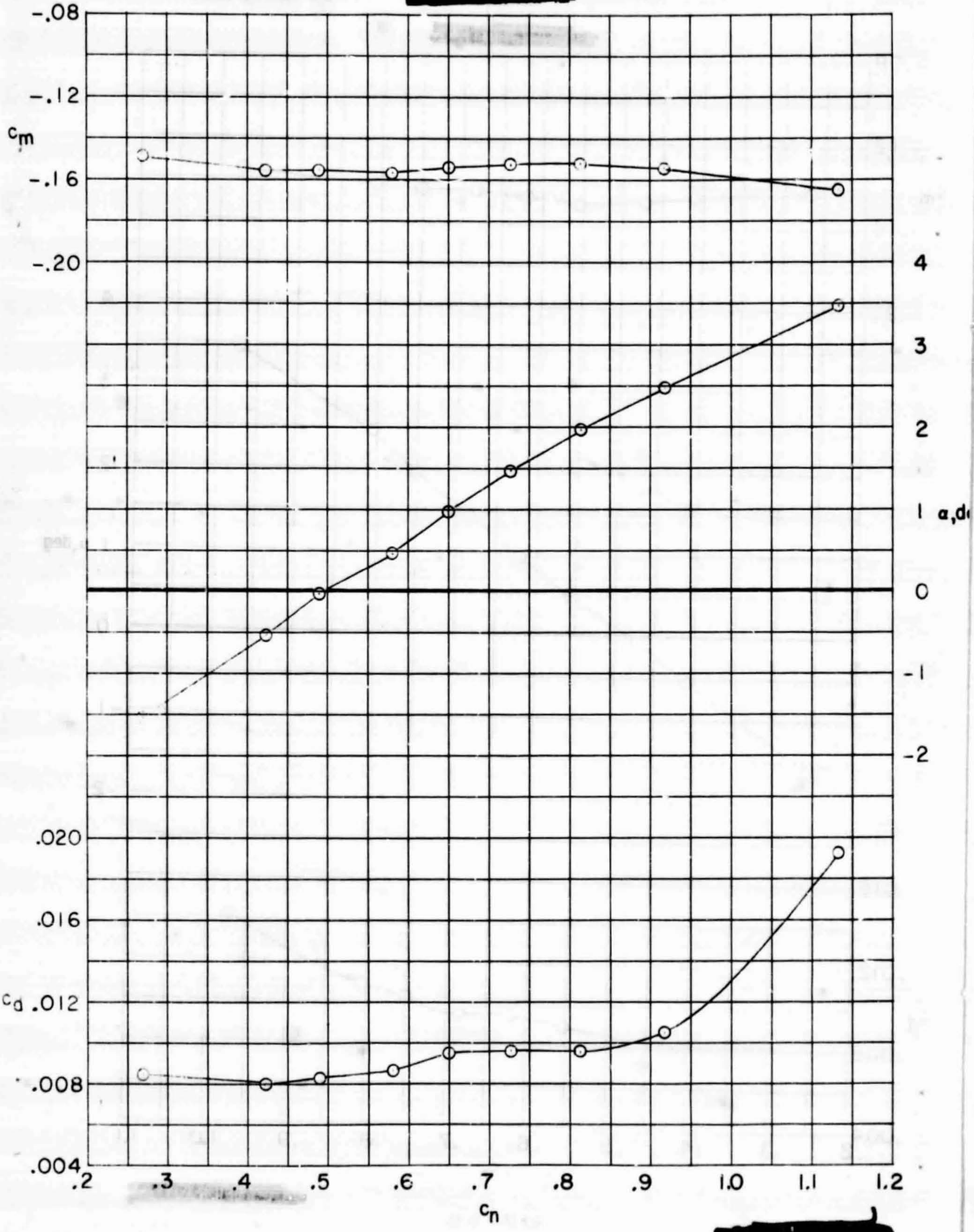

[redacted]

(d) M = 0.70.

Figure 72- Continued.

[redacted]

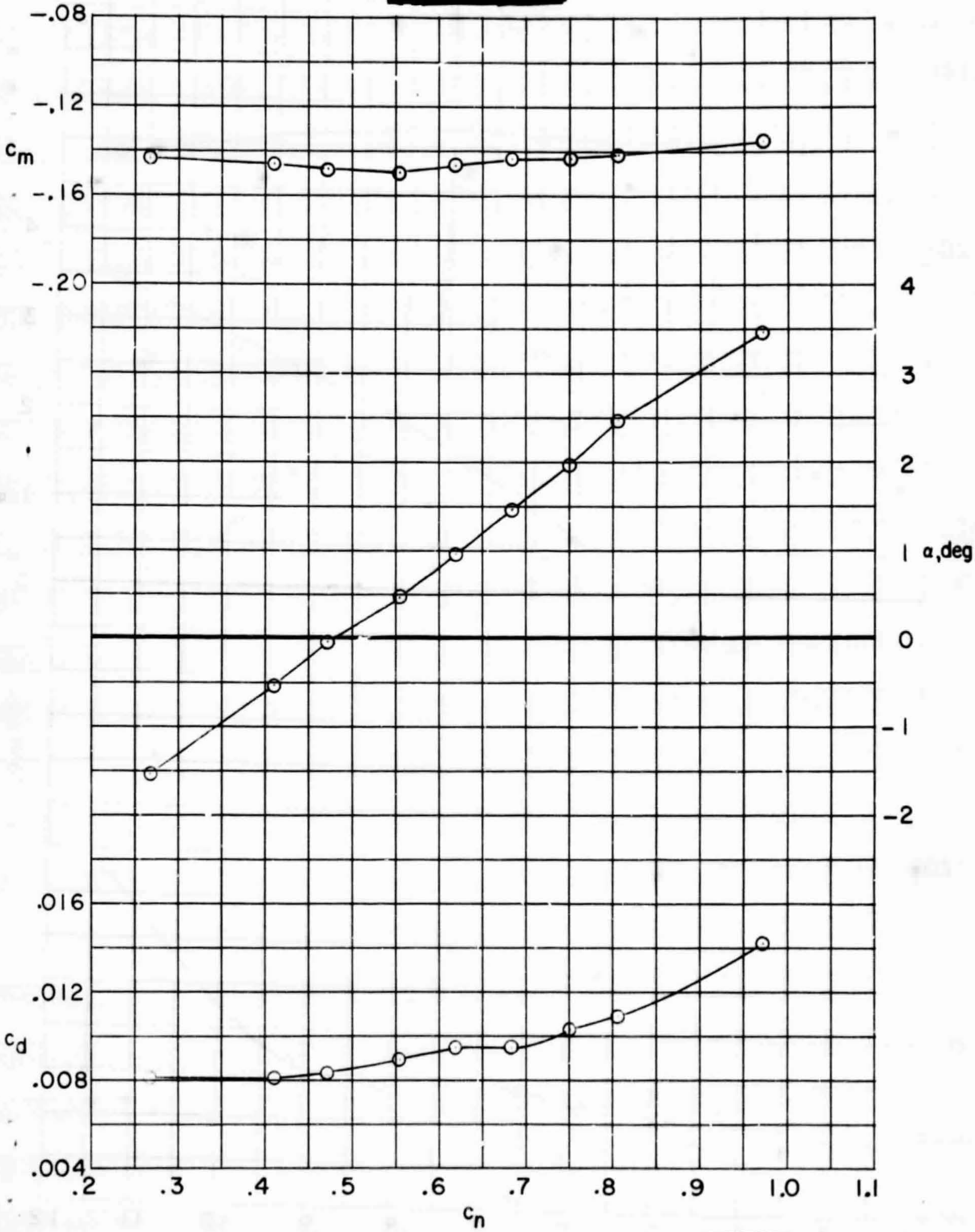

[redacted]

(c) M = 0.65.

Figure 7. - Continued.

[redacted]

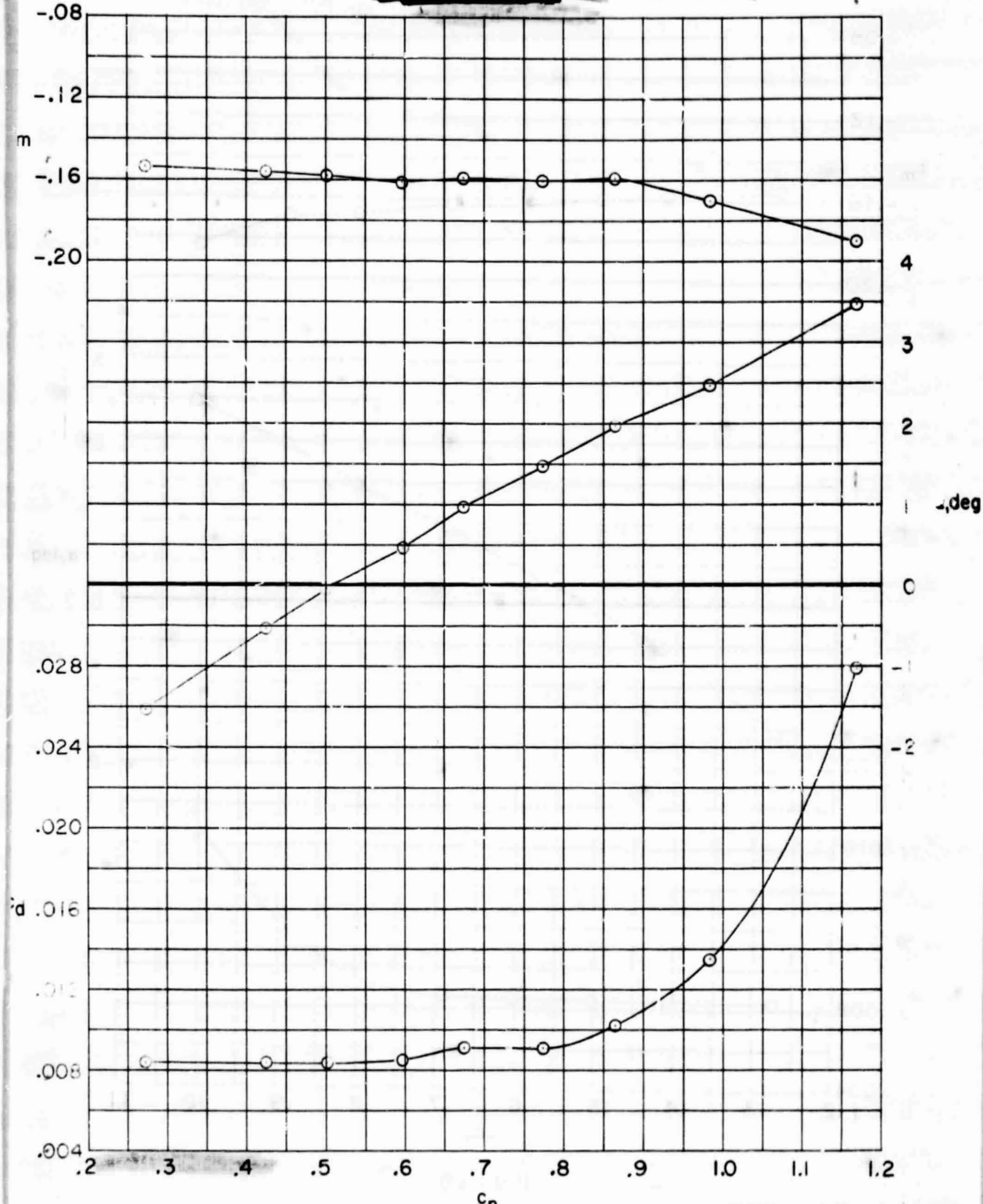

[redacted]

(e) M = 0.72.

Figure 7.- Continued.

[redacted]

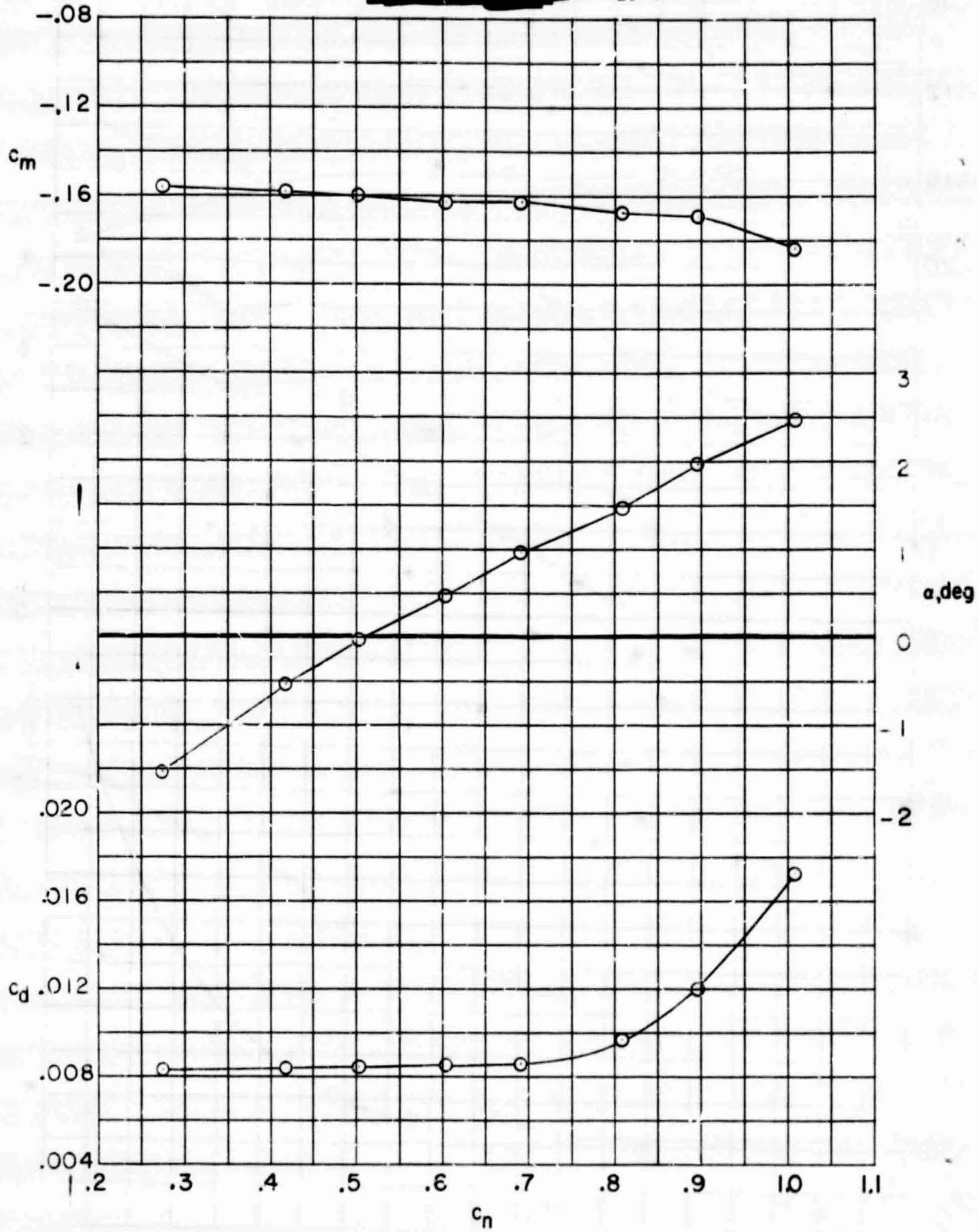

[redacted]

(f) M = 0.73.

Figure 7.- Continued.

[redacted]

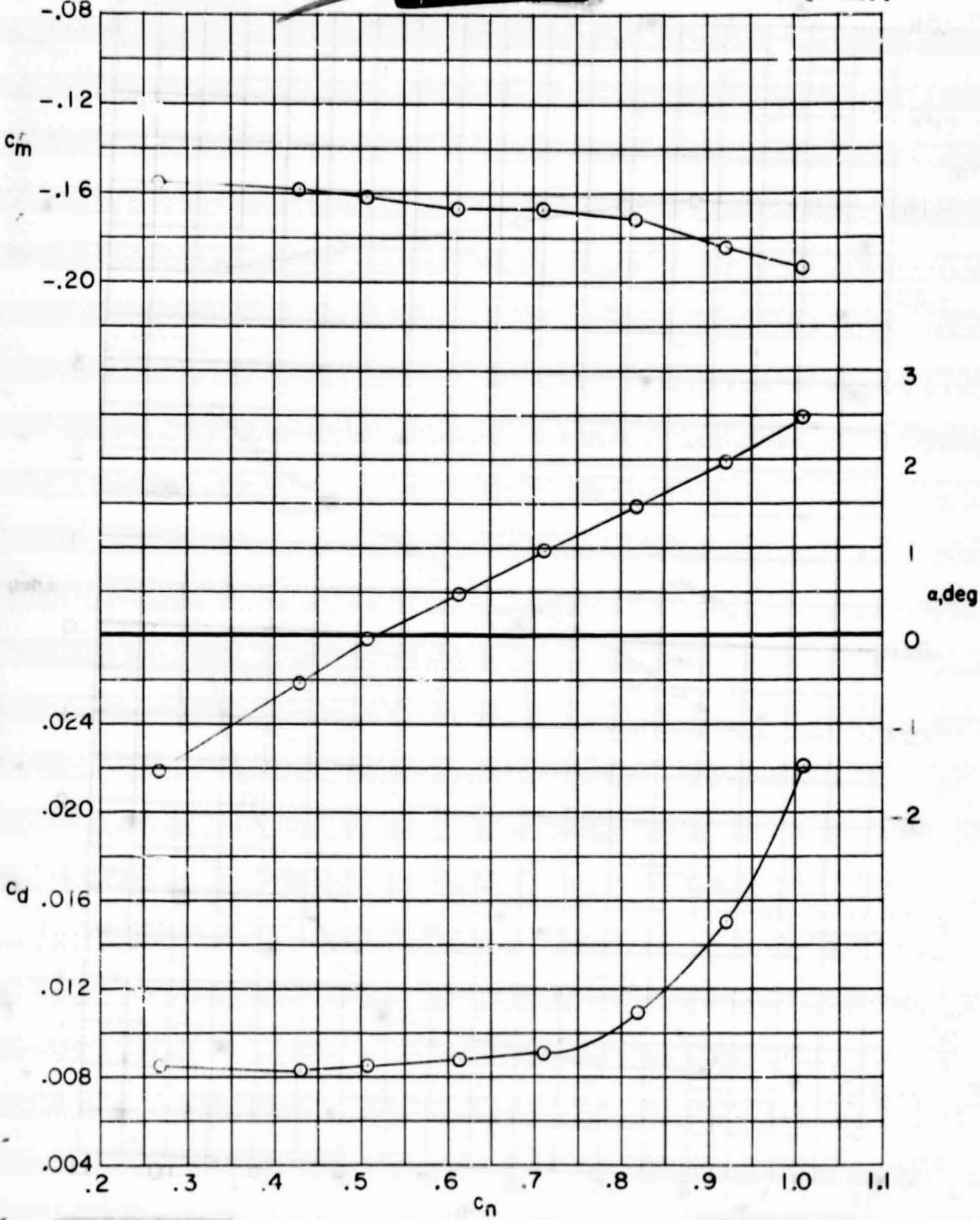

[redacted]

(g) M = 0.74.

Figure 7.- Continued.

[redacted]

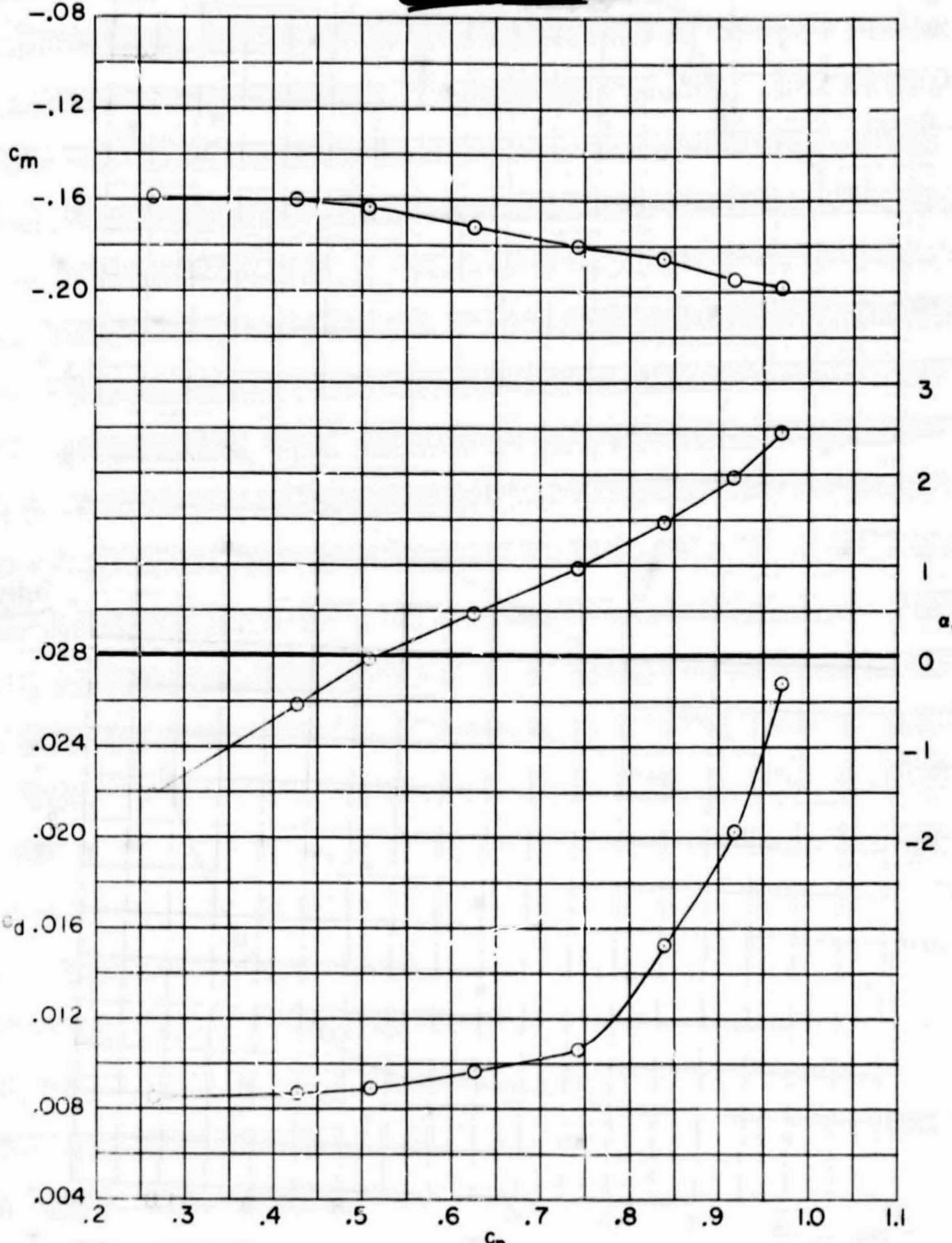

[redacted]

(h) M = 0.75.

Figure 7. - Continued.

ORIGINAL PAGE IS
OF POOR QUALITY

[redacted]

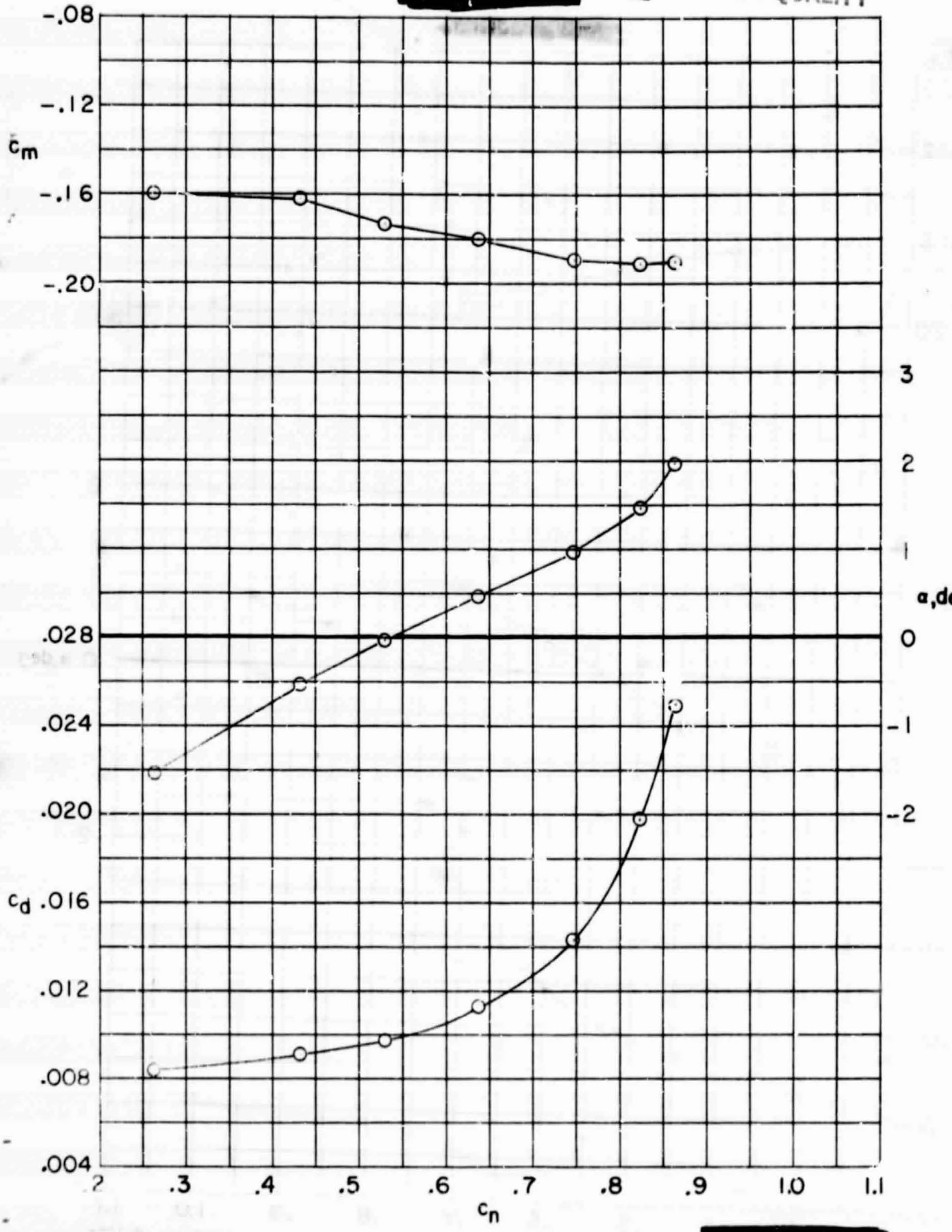

[redacted]

(i) M = 0.76.

Figure 7.- Continued.

[redacted]

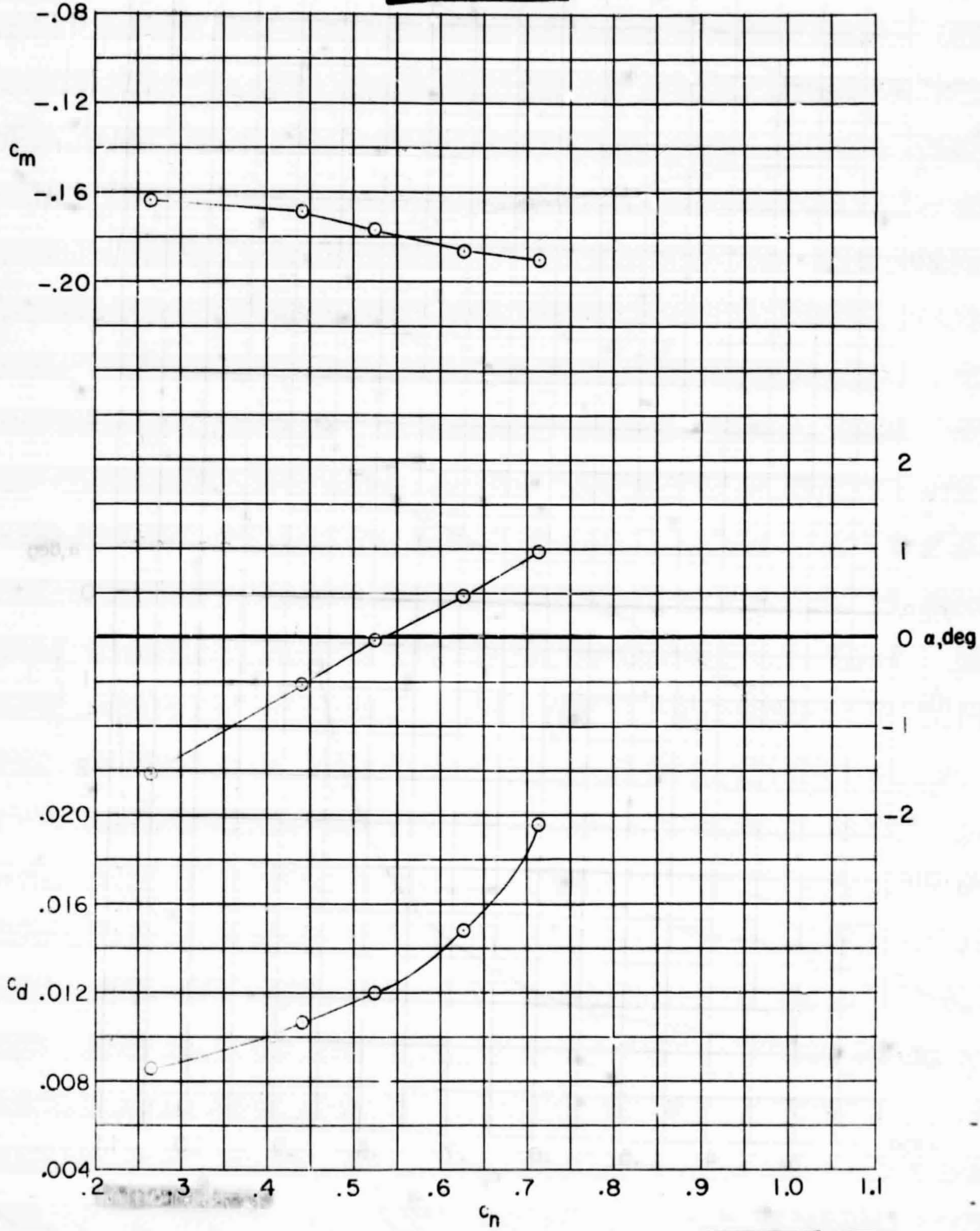

[redacted]

(j) M = 0.77.

Figure 7. - Continued.

[redacted]

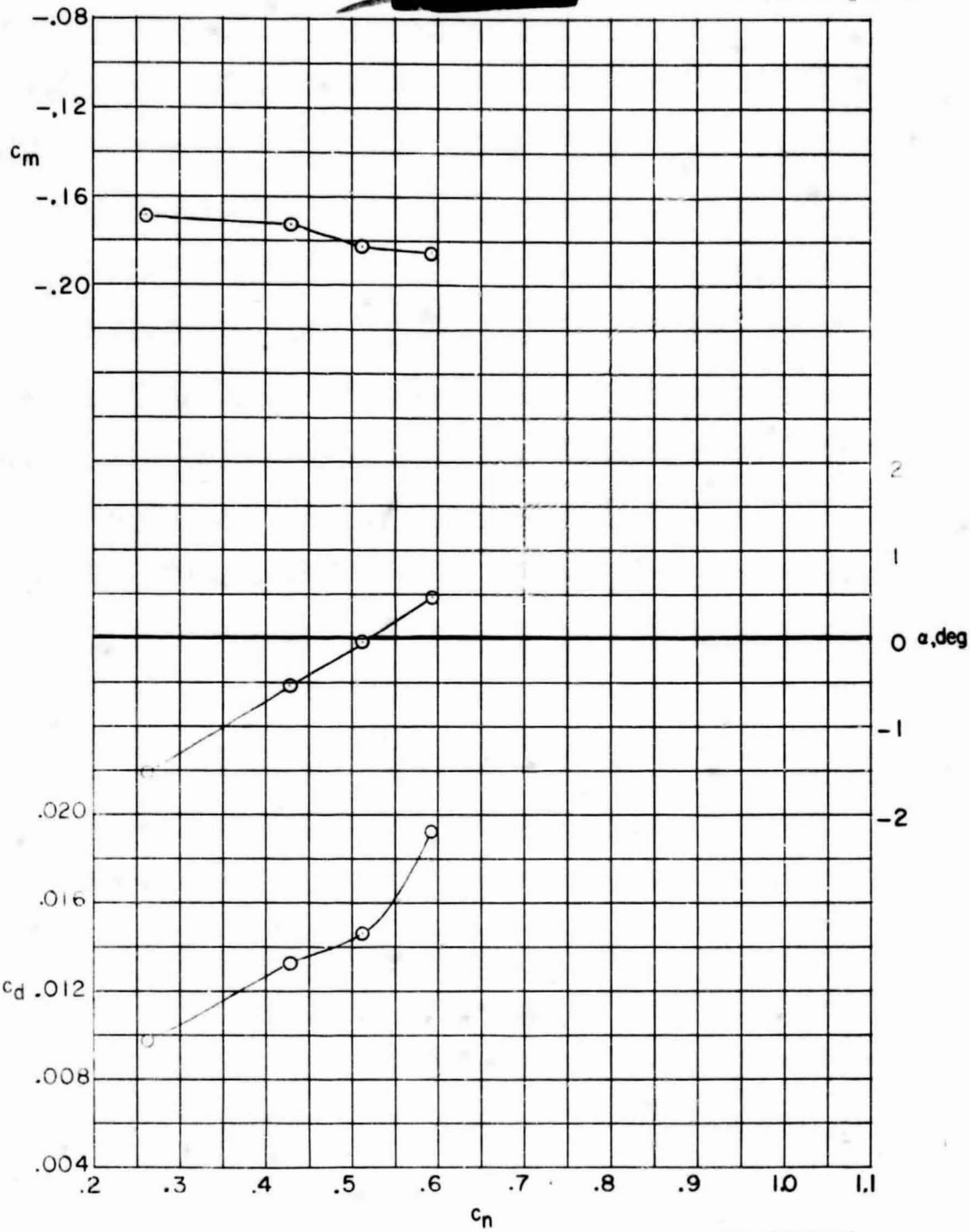

[redacted]

(k) M = 0.78.

Figure 7.- Concluded.

[redacted]

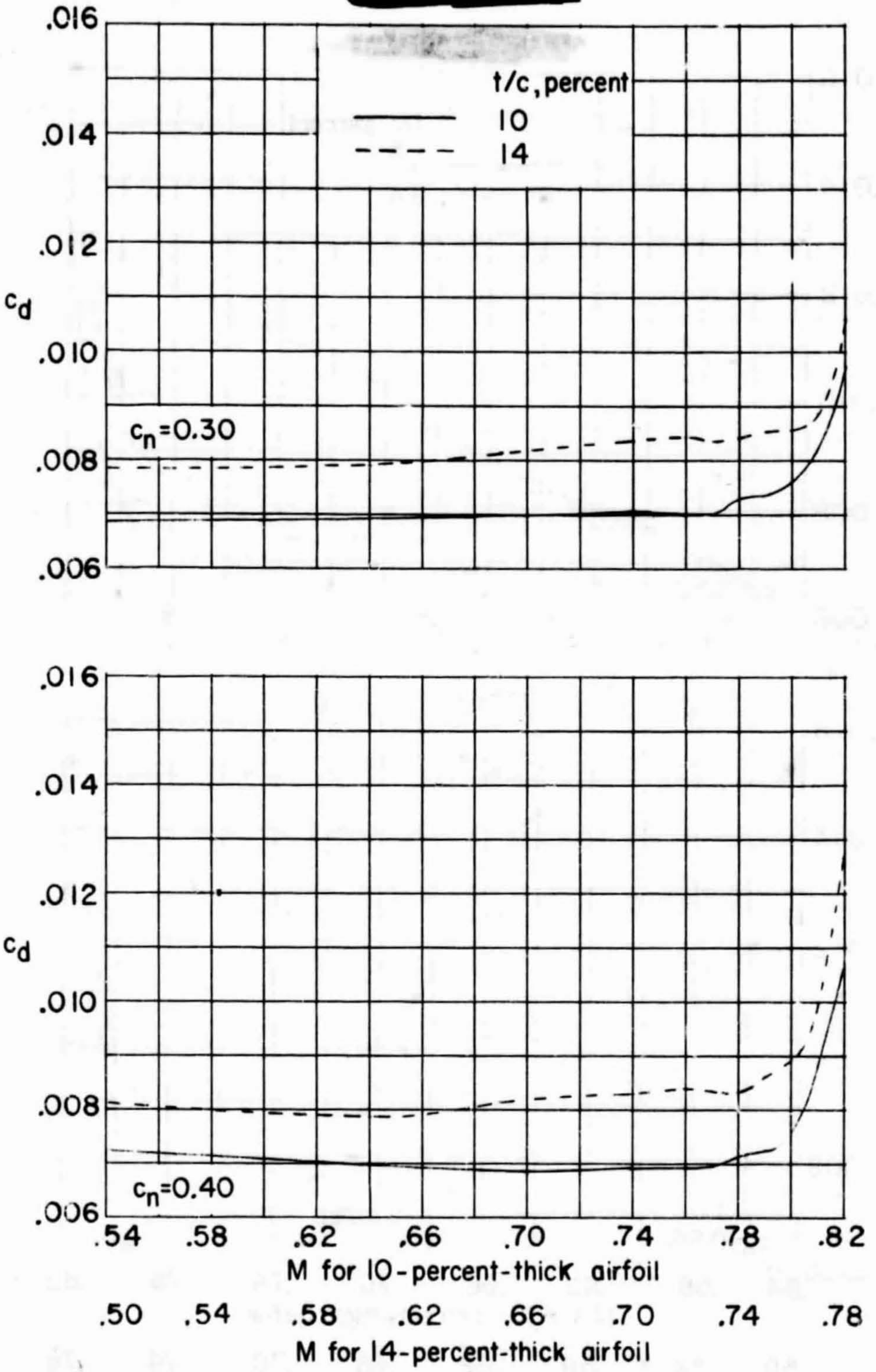

(a) c_n = 0.30 and 0.40.

Figure 8. - Variation of measured section drag coefficient with Mach number of 14- and 10-percent thick supercritical airfoils.

[redacted]

[redacted]

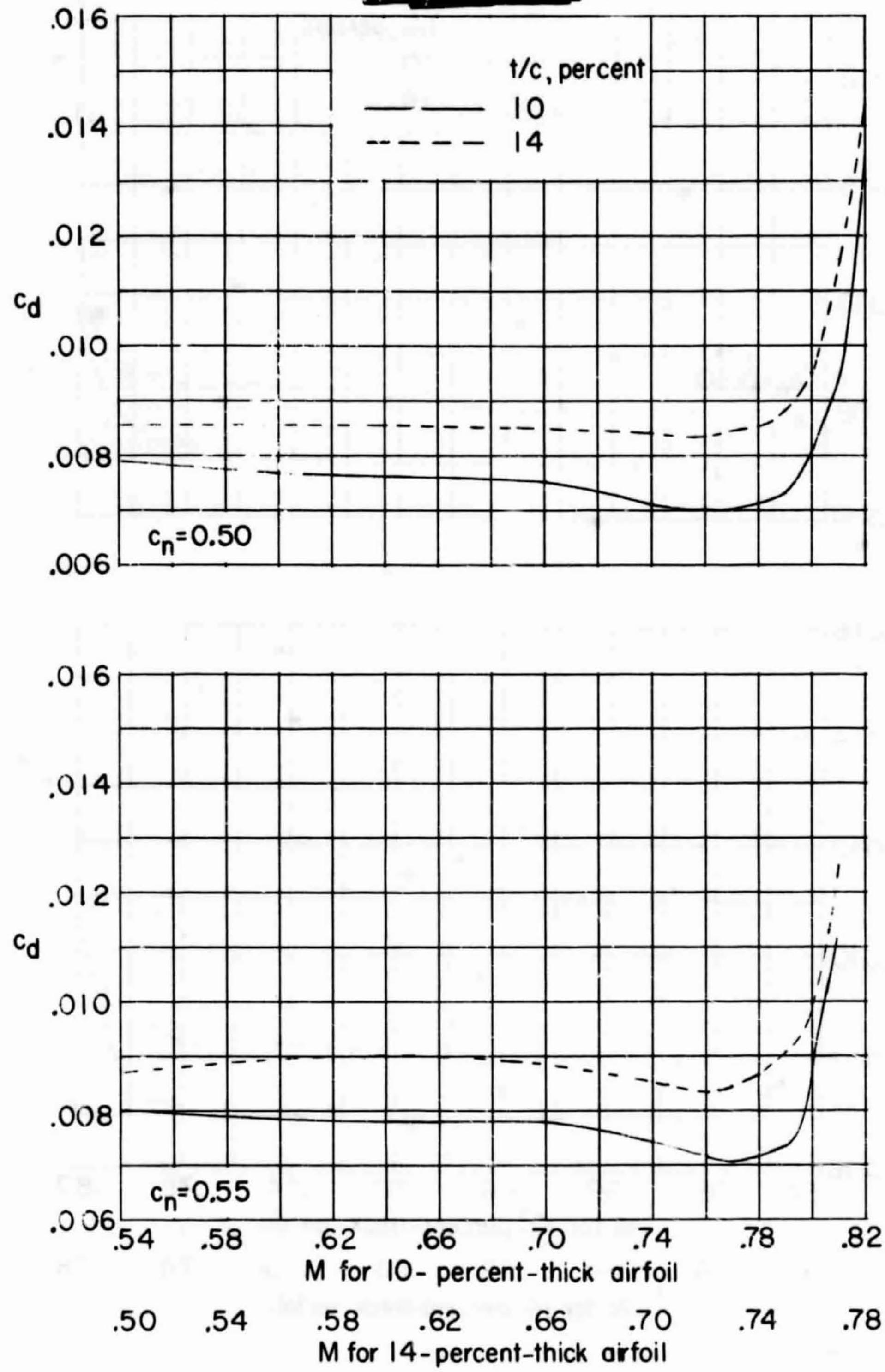

(b) c_n = 0.50 and 0.55.

Figure 8.- Continued.

[redacted]

[redacted]

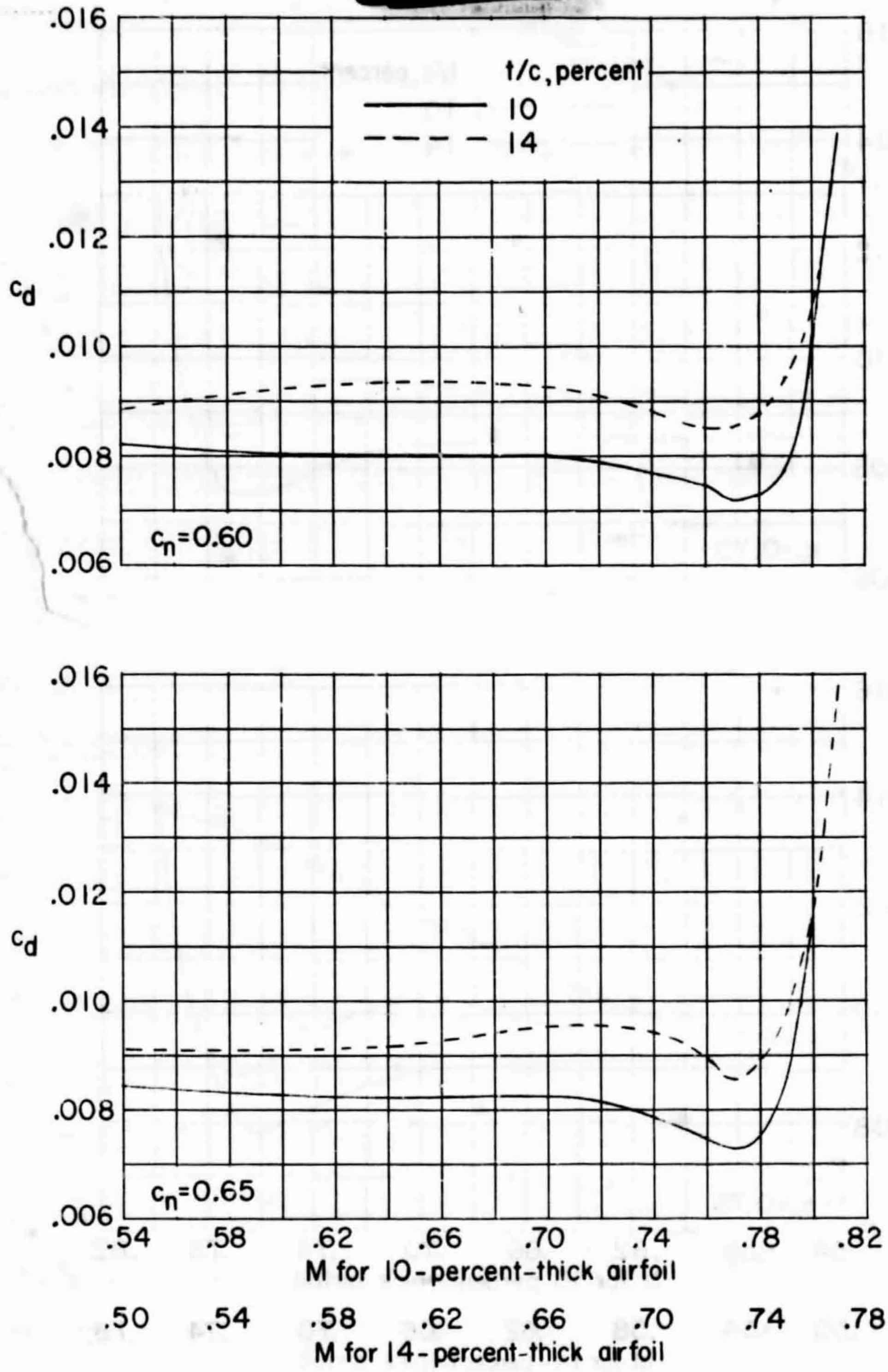

(c) c_n = 0.60 and 0.65.

Figure 8. - Continued.

[redacted]

[redacted]

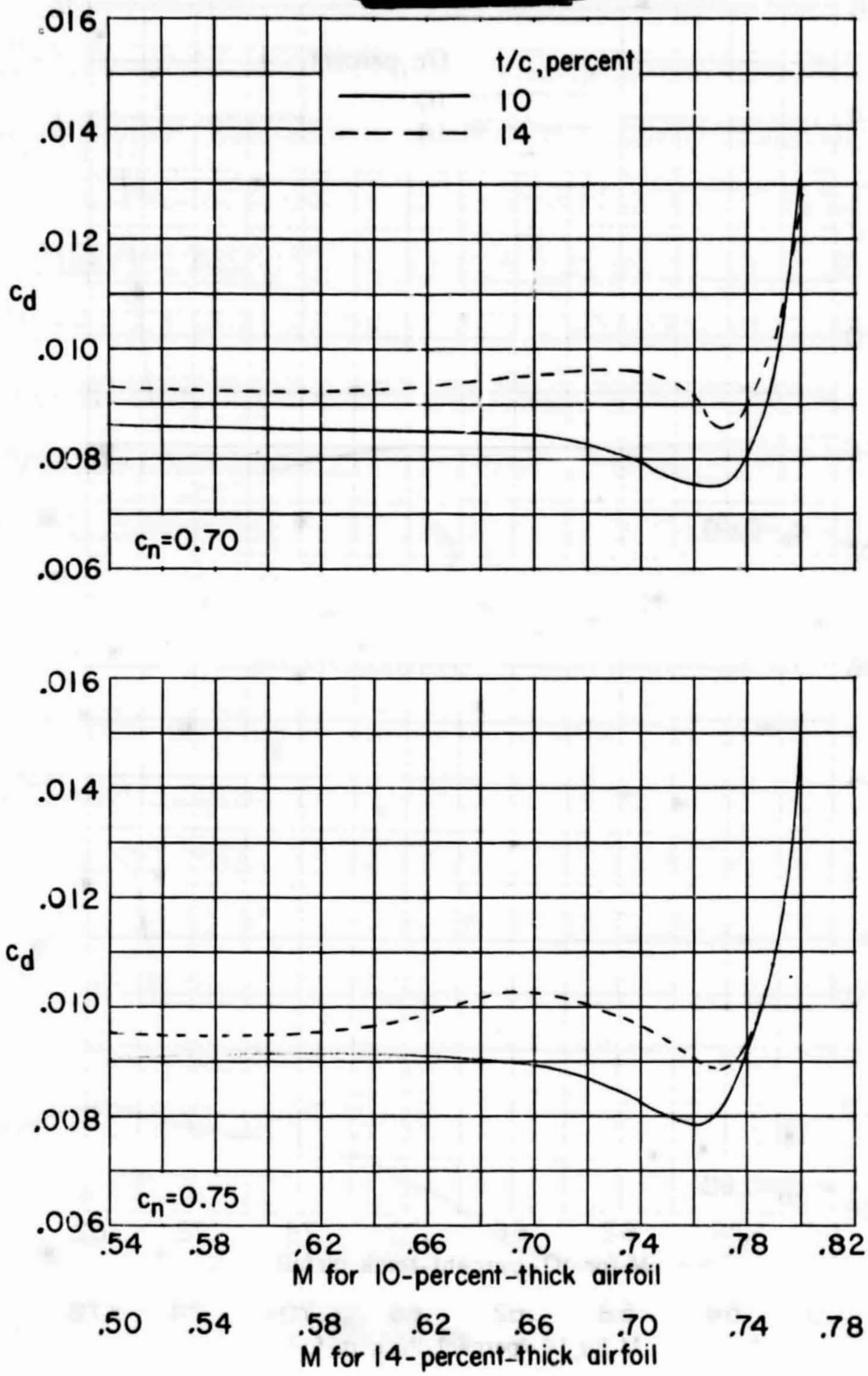

(d) c_n = 0.70 and 0.75.

Figure 8.- Continued.

[redacted]

[redacted]

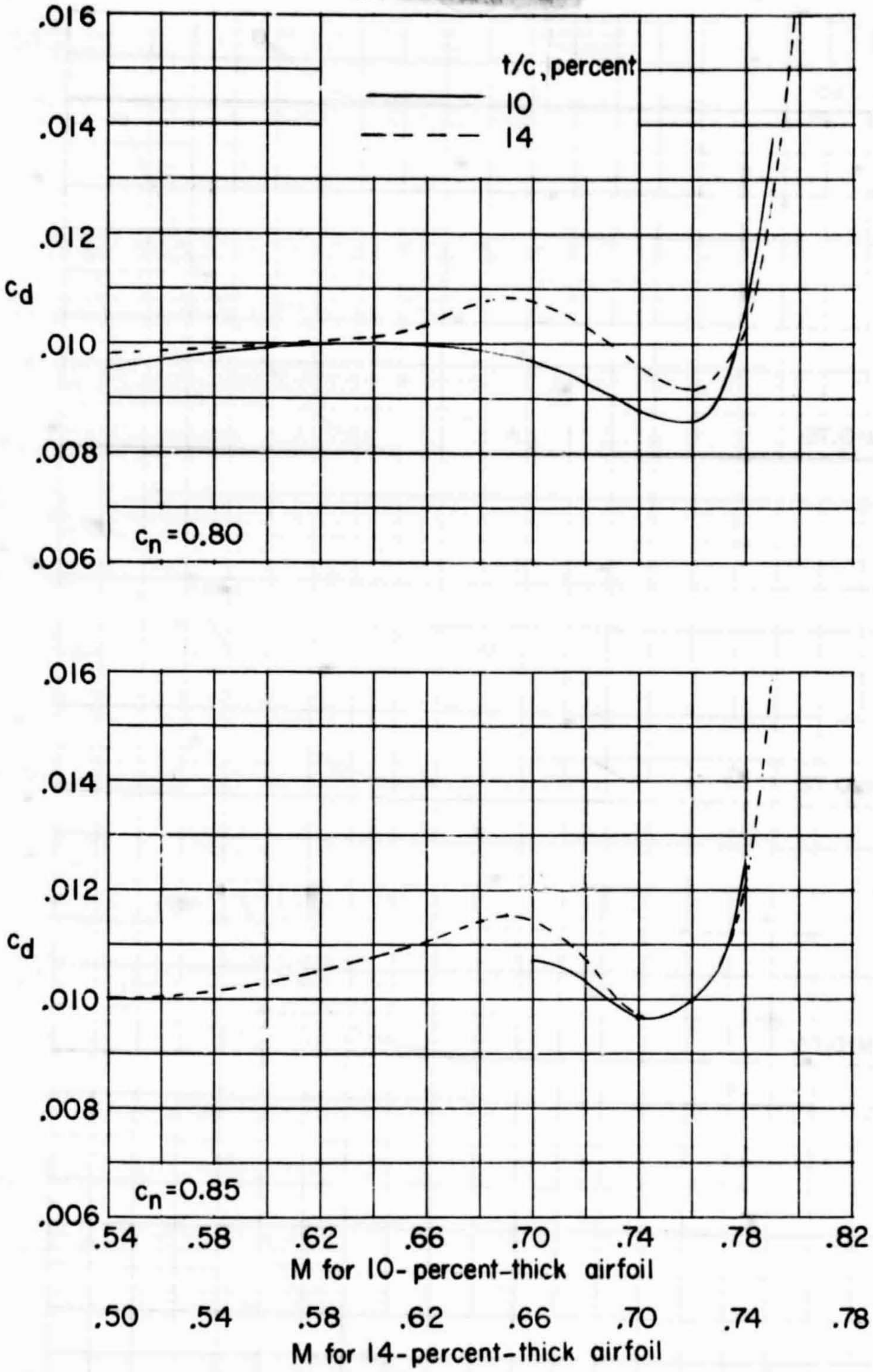

(e) c_n = 0.80 and 0.85.

Figure 8.- Concluded.

[redacted]

ORIGINAL PAGE IS
OF POOR QUALITY

[redacted]

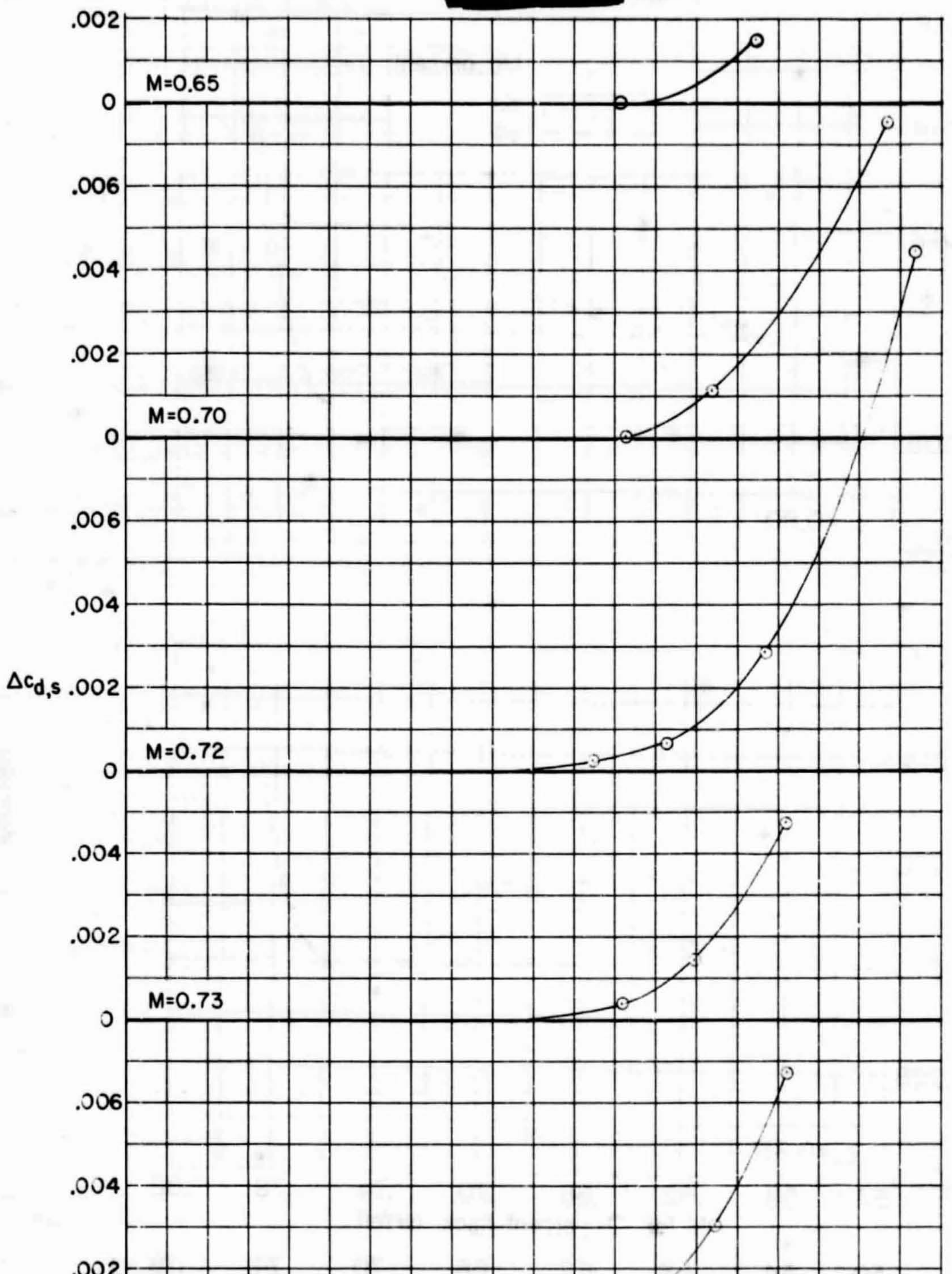

Figure 9. - Drag increment due to shock-wave losses of 14-percent-thick supercritical airfoil.

[redacted]

[redacted]

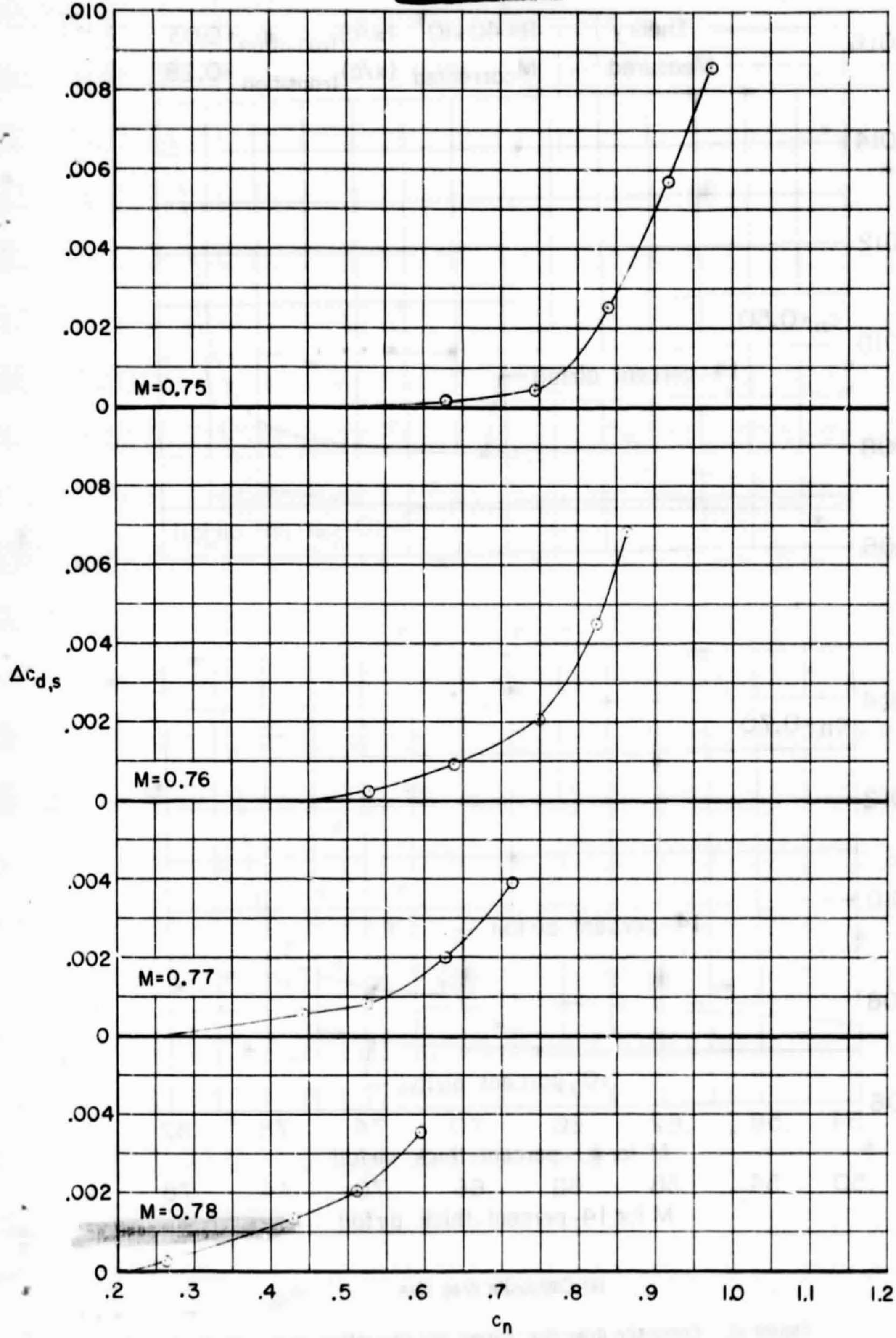

Figure 9. - Concluded.

[redacted]

SC(2)-0714

Low Mach Numbers

(M = 0,1 to M = 0,32)

- NASA TM-81912 -

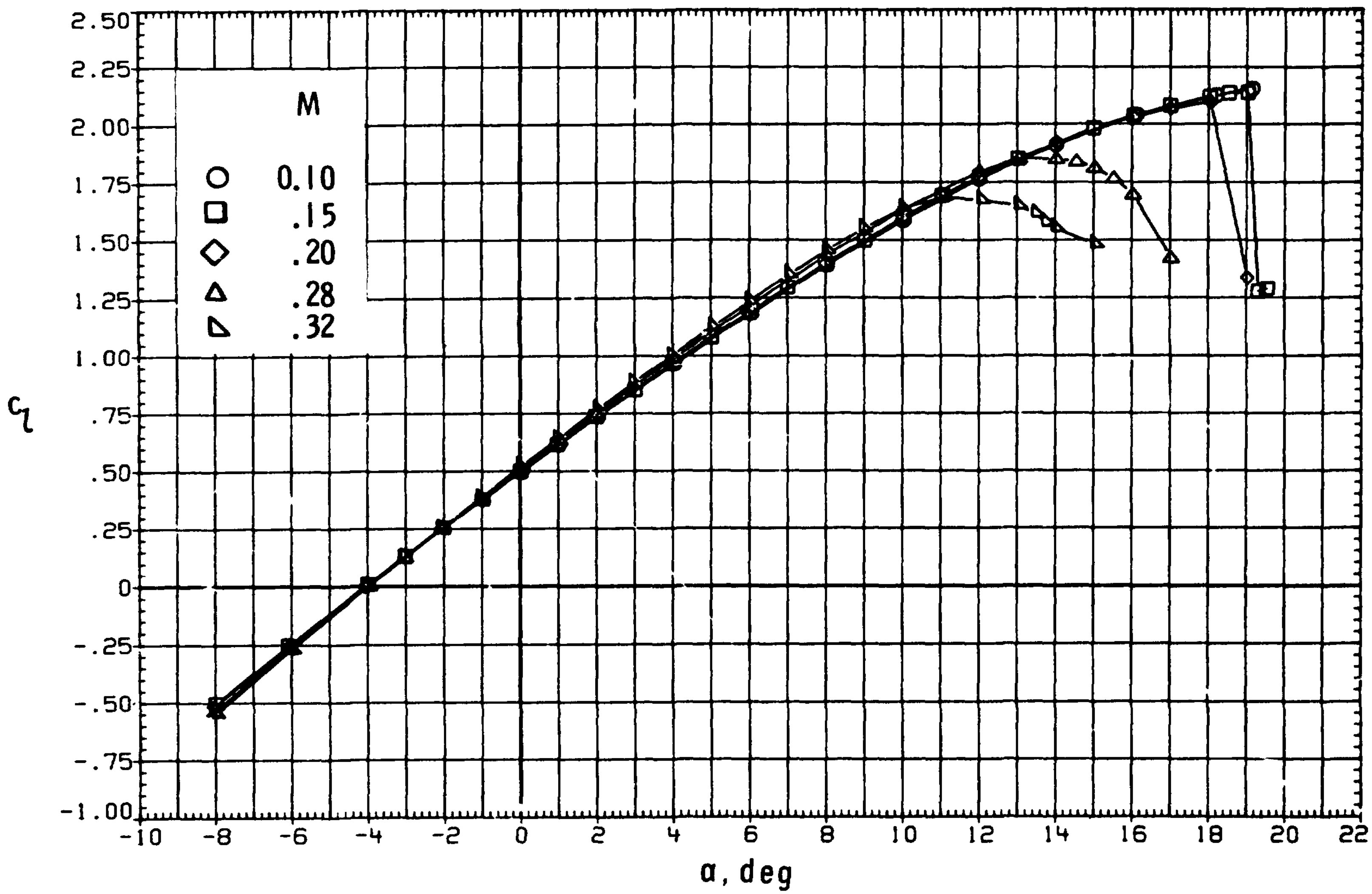

Figure 18.- Effect of Mach number on section characteristics; $R = 6.0 \times 10^6$, transition fixed.

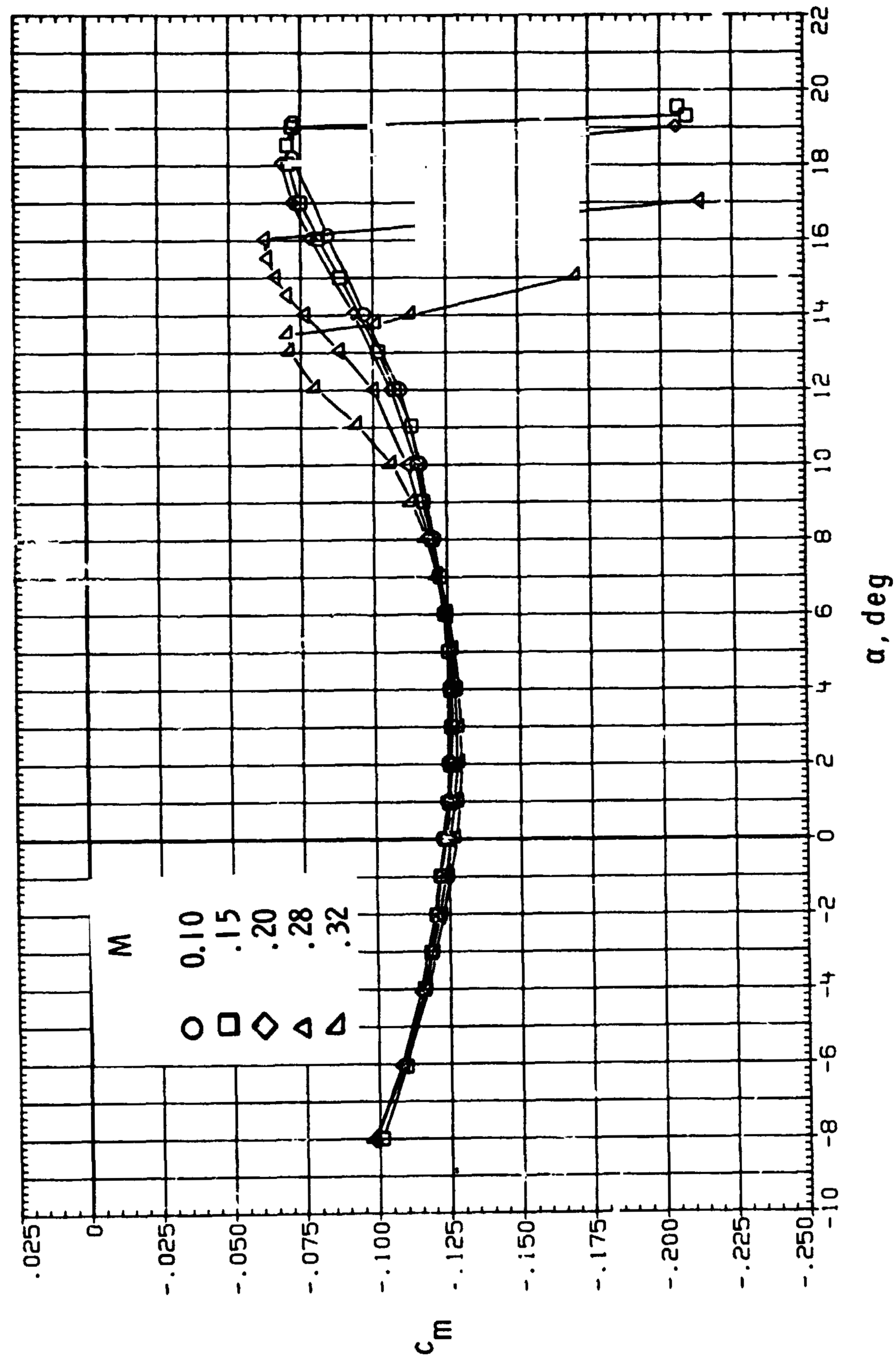

Figure 18.- Continued.

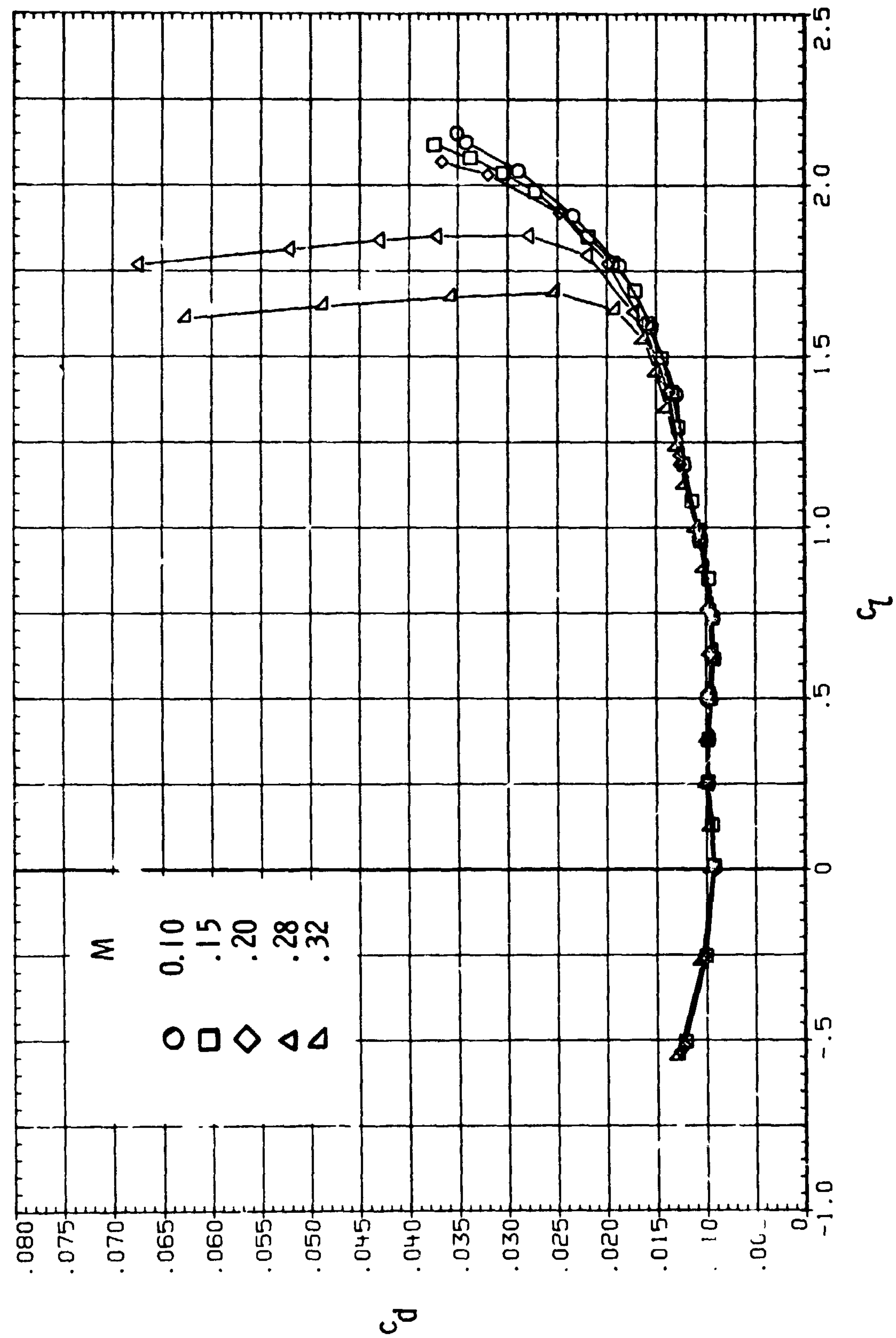

Figure 18.- Continued.

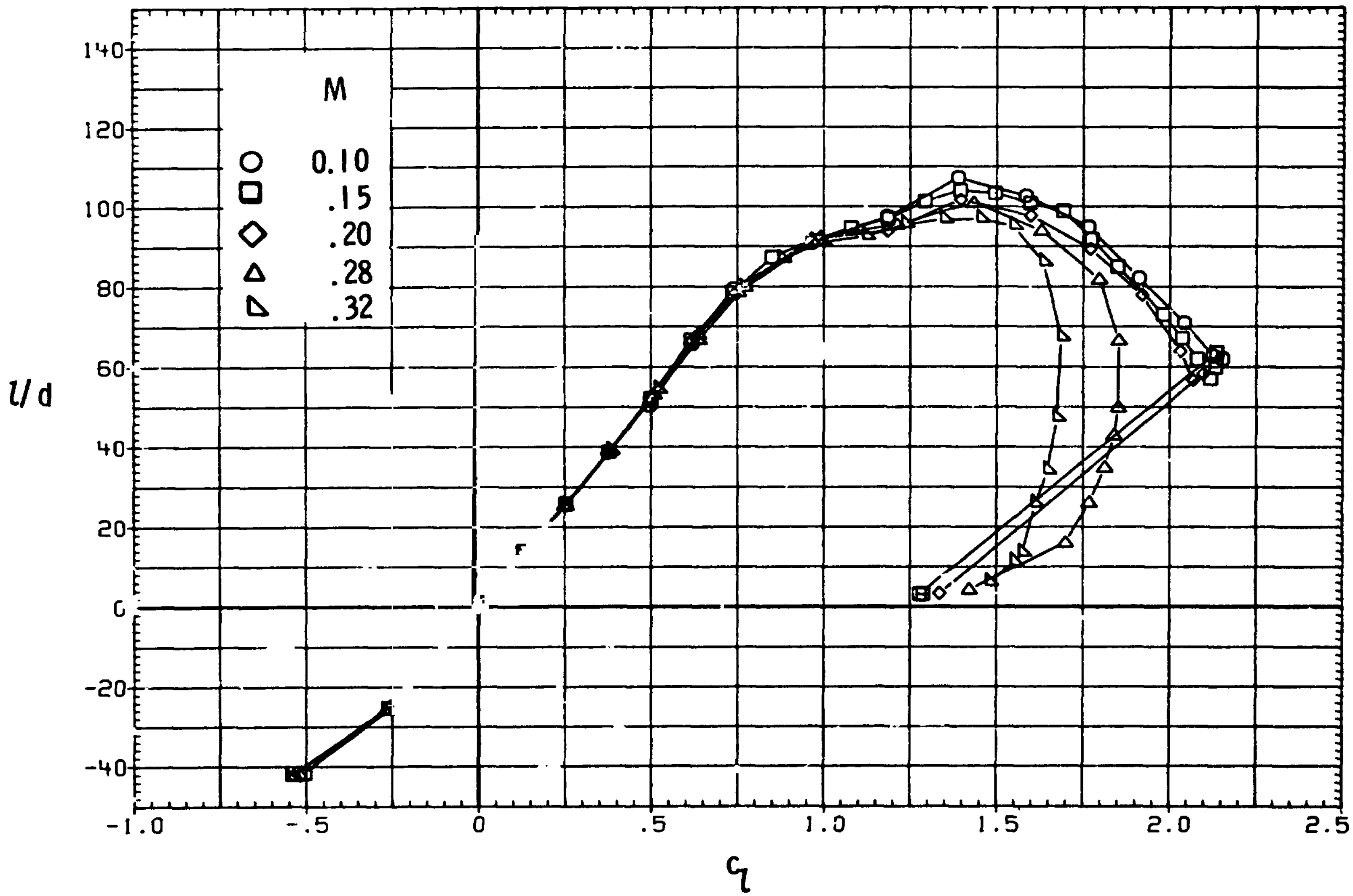

Figure 18.- Concluded.

SC(3)-0712(B)

NASA

Year	1985
Reference	NASA TM-86371
t/c	0,12
$c_{l,design}$	0,7
Transition	fixed at 0,05c

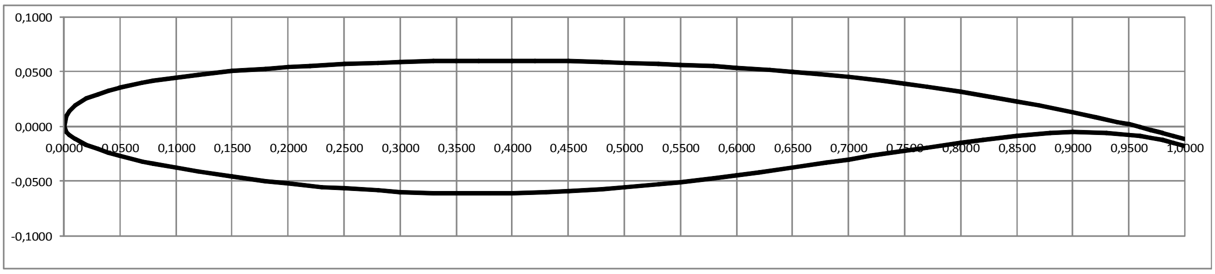

TABLE II. DESIGN AND MEASURED AIRFOIL COORDINATES

Upper surface		
x/c	z_{design}/c	z_{meas}/c
0.002	0.0092	0.0074
.005	.0141	.0131
.010	.0190	.0181
.020	.0252	.0247
.030	.0294	.0291
.040	.0327	.0325
.050	.0354	.0352
.070	.0397	.0397
.080	.0415	.0415
.100	.0446	.0445
.120	.0471	.0471
.150	.0504	.0504
.180	.0530	.0529
.200	.0544	.0544
.220	.0557	.0556
.250	.0572	.0572
.280	.0584	.0584
.300	.0590	.0589
.330	.0596	.0596
.350	.0599	.0599
.370	.0601	.0600
.400	.0601	.0601
.420	.0600	.0600
.450	.0596	.0596
.480	.0590	.0589
.500	.0584	.0583
.530	.0573	.0572
.550	.0564	.0563
.580	.0549	.0548
.600	.0537	.0536
.630	.0516	.0515
.650	.0500	.0499
.670	.0482	.0481
.700	.0451	.0450
.730	.0416	.0415
.750	.0390	.0389
.770	.0362	.0360
.800	.0316	.0315
.830	.0266	.0264
.850	.0230	.0228
.870	.0192	.0190
.900	.0131	.0129
.920	.0088	.0086
.940	.0042	.0040
.950	.0018	.0016
.960	−.0007	−.0009
.970	−.0033	−.0035
.980	−.0060	−.0062
.990	−.0088	−.0090
1.000	−.0117	−.0118

Lower surface		
x/c	z_{design}/c	z_{meas}/c
0.002	−0.0051	−.0039
.005	−.0081	−.0077
.010	−.0116	−.0113
.020	−.0165	−.0162
.030	−.0204	−.0202
.040	−.0238	−.0235
.050	−.0266	−.0264
.070	−.0316	−.0314
.080	−.0338	−.0336
.100	−.0377	−.0375
.120	−.0412	−.0410
.150	−.0458	−.0456
.180	−.0498	−.0496
.200	−.0521	−.0520
.230	−.0550	−.0549
.250	−.0566	−.0565
.280	−.0585	−.0584
.300	−.0595	−.0594
.330	−.0605	−.0604
.350	−.0609	−.0608
.380	−.0610	−.0609
.400	−.0608	−.0607
.430	−.0600	−.0599
.450	−.0591	−.0591
.480	−.0573	−.0572
.500	−.0558	−.0557
.530	−.0530	−.0529
.550	−.0509	−.0508
.580	−.0472	−.0471
.600	−.0446	−.0445
.620	−.0419	−.0418
.650	−.0376	−.0375
.680	−.0331	−.0329
.700	−.0299	−.0298
.720	−.0267	−.0266
.750	−.0221	−.0220
.770	−.0191	−.0190
.800	−.0149	−.0147
.820	−.0123	−.0121
.850	−.0088	−.0086
.880	−.0059	−.0057
.900	−.0049	−.0046
.930	−.0055	−.0051
.950	−.0074	−.0069
.960	−.0088	−.0082
.970	−.0105	−.0099
.980	−.0126	−.0120
.990	−.0150	−.0143
1.000	−.0177	−.0167

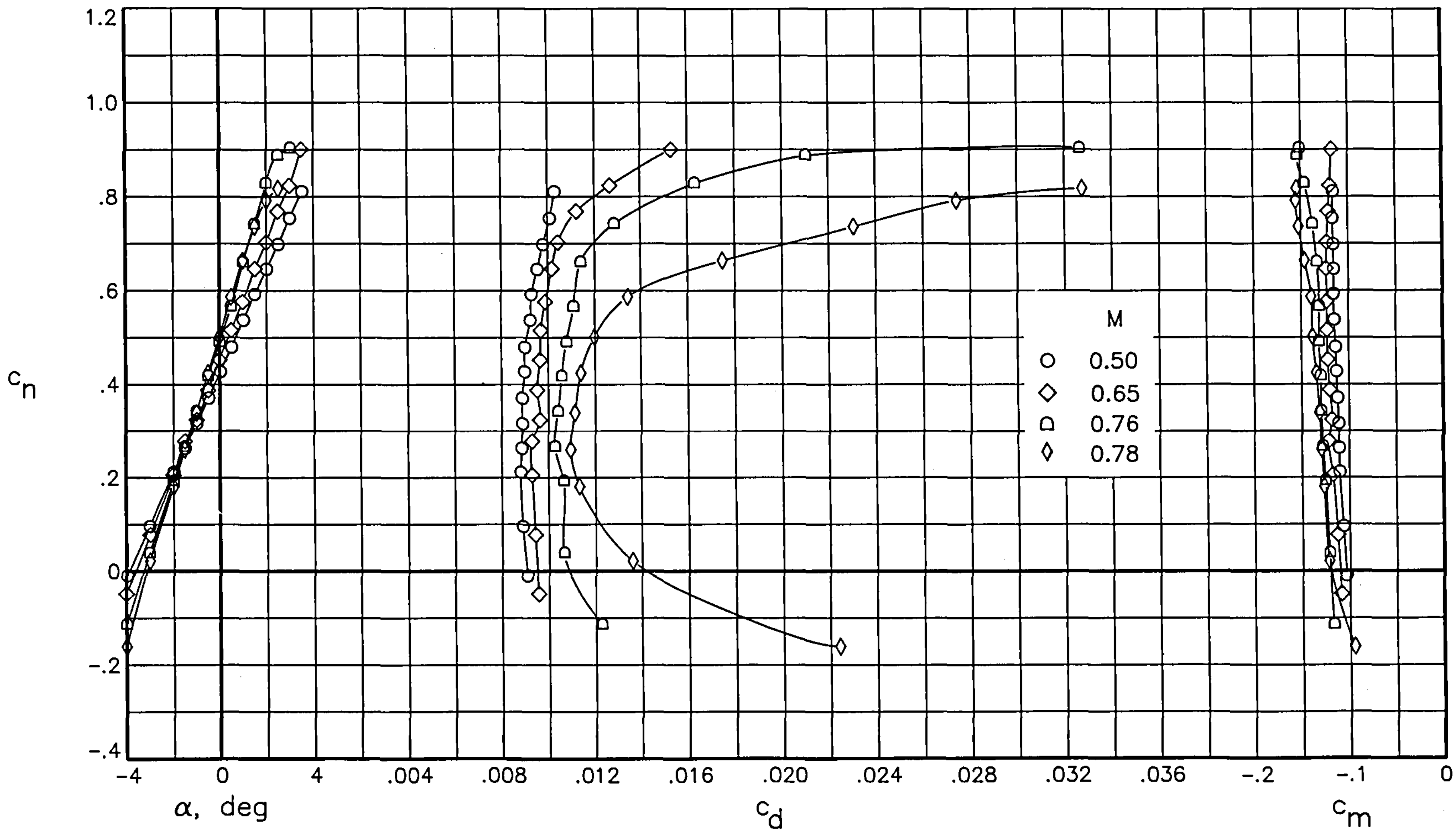

Figure 40. Effect of Mach number on aerodynamic characteristics of airfoil with fixed transition at $R \approx 7.0 \times 10^6$.

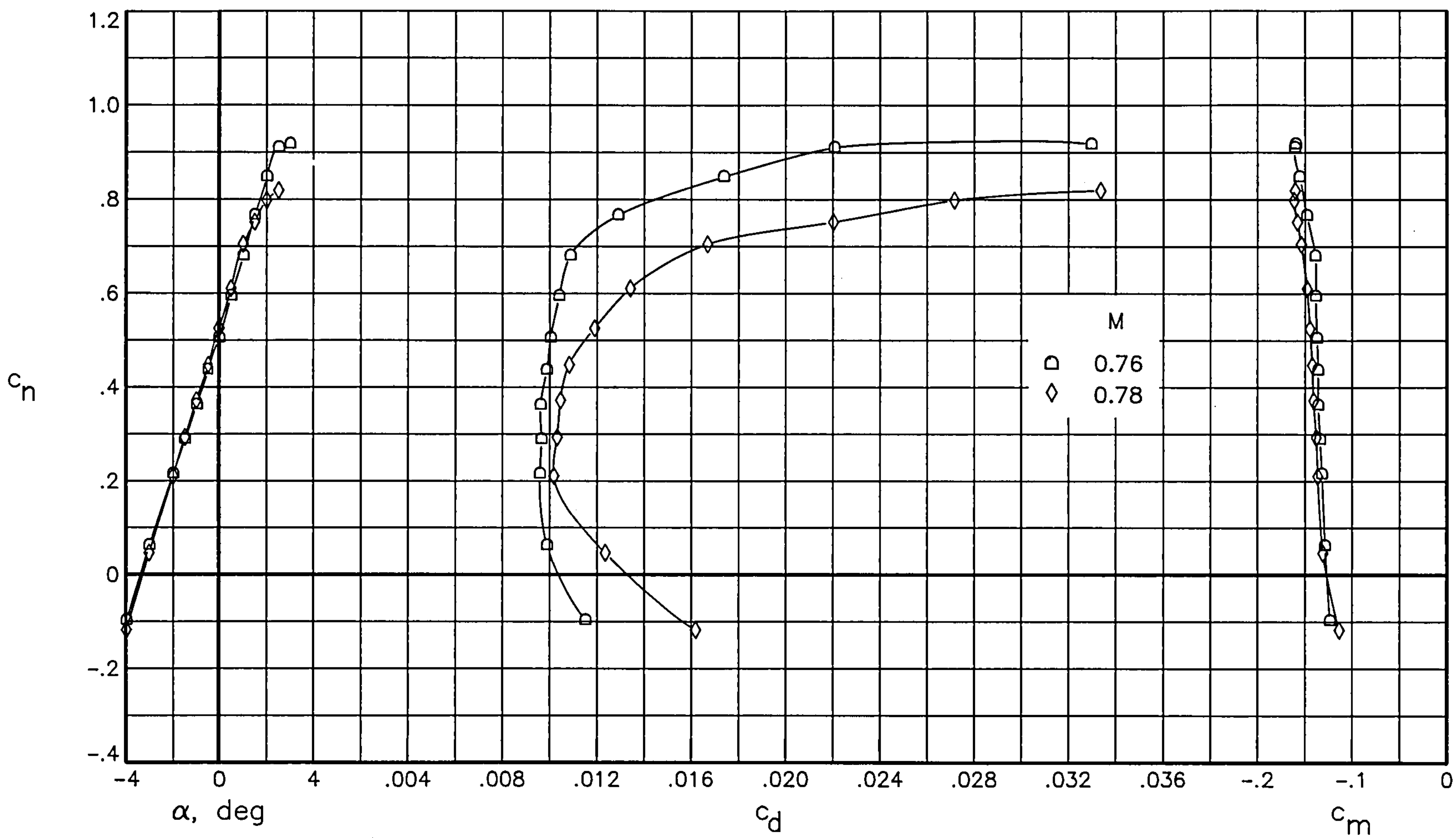

Figure 41. Effect of Mach number on aerodynamic characteristics of airfoil with fixed transition at $R \approx 10.0 \times 10^6$.

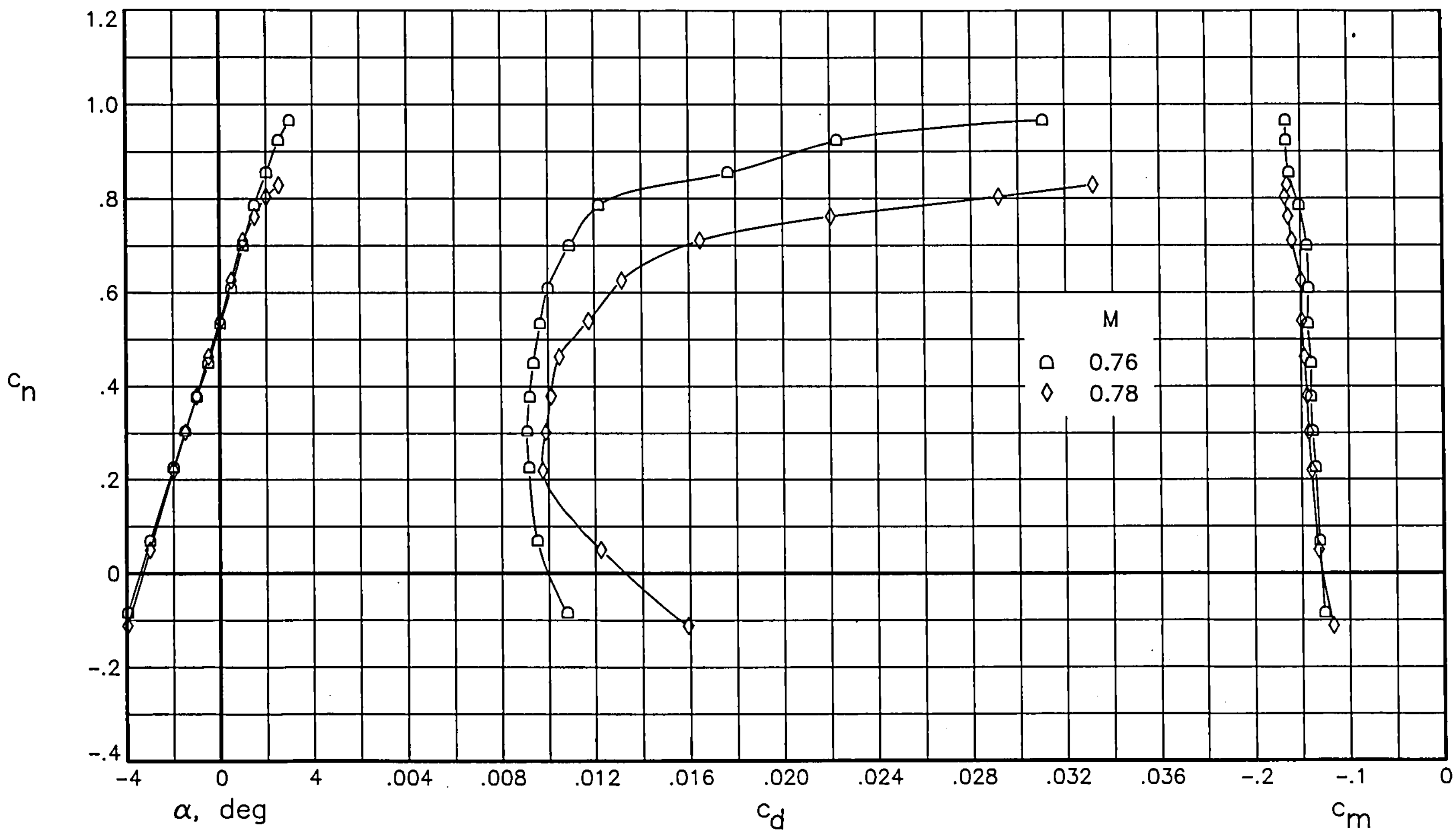

Figure 42. Effect of Mach number on aerodynamic characteristics of airfoil with fixed transition at $R \approx 15.0 \times 10^6$.

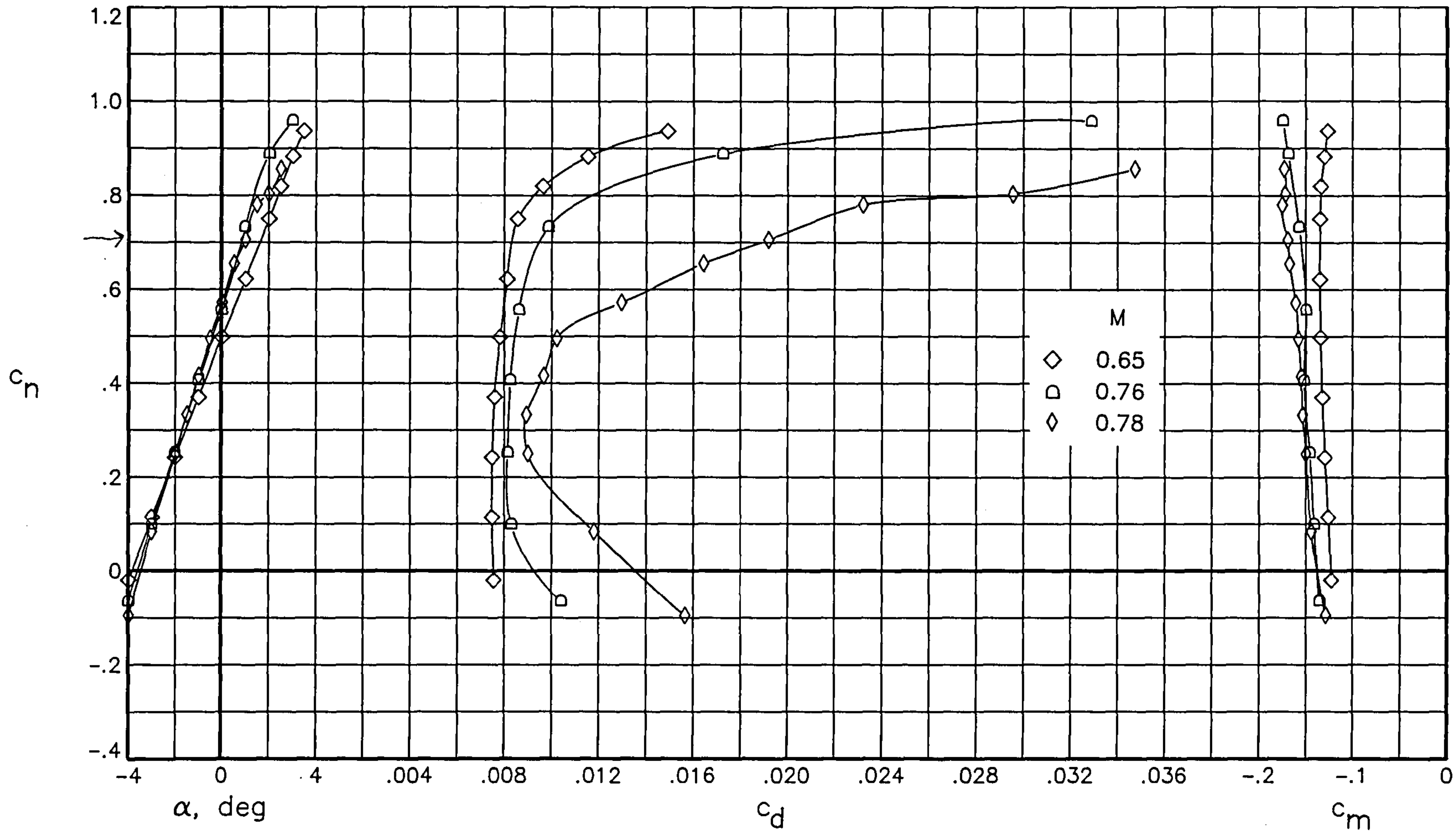

Figure 43. Effect of Mach number on aerodynamic characteristics of airfoil with fixed transition at $R \approx 30.0 \times 10^6$.

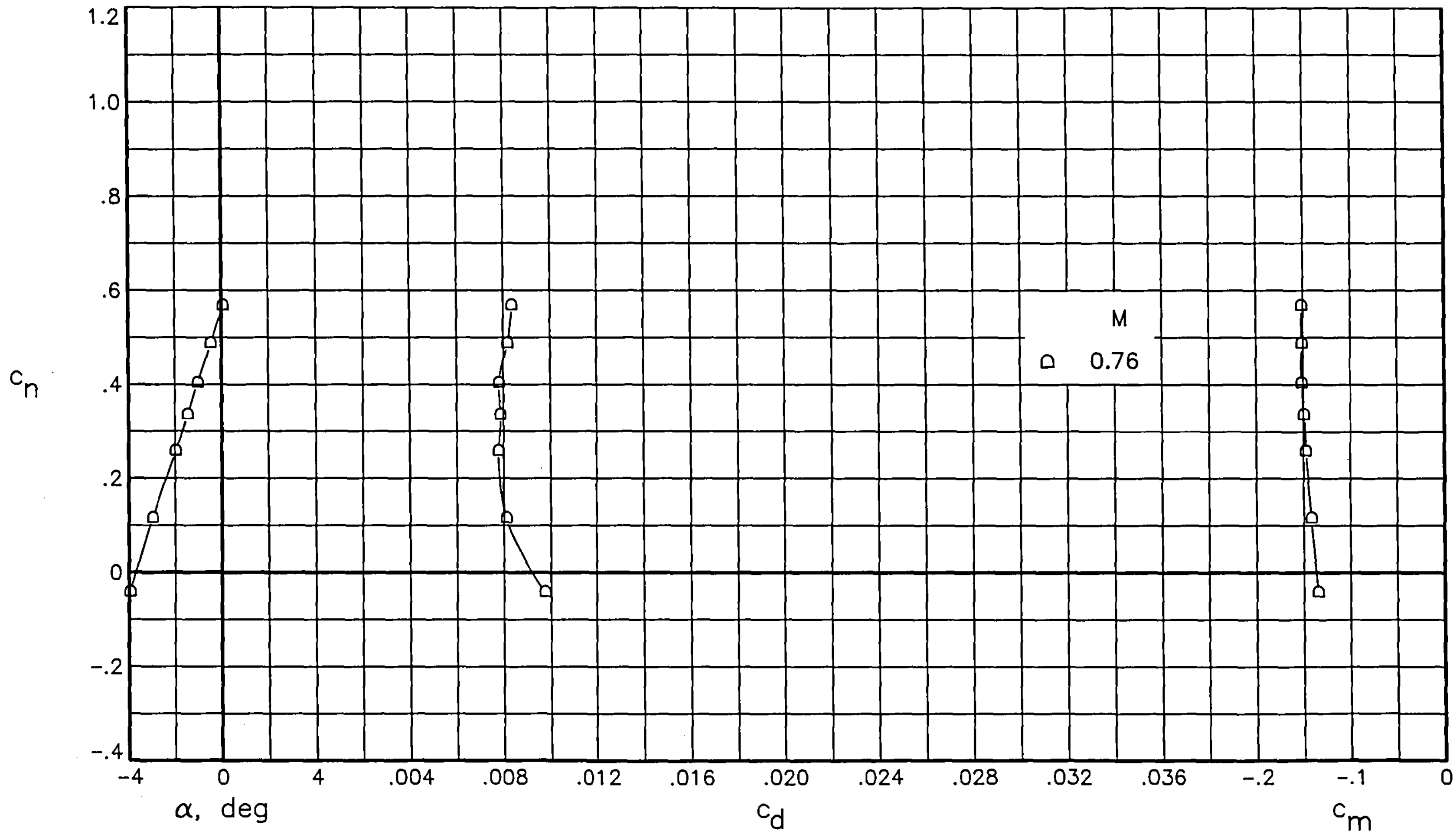

Figure 44. Effect of Mach number on aerodynamic characteristics of airfoil with fixed transition at $R \approx 40.0 \times 10^6$.

SKF 1.1

Versuchsanstalt für Luft- und Raumfahrt e.V. (DFVLR)

Year	1979
Reference	AGARD-AR-138
t/c	0,1207
$c_{l,design}$	0,532
M_{design}	0,769
Transition	if fixed: 0,3c upper surface 0,25c lower surface

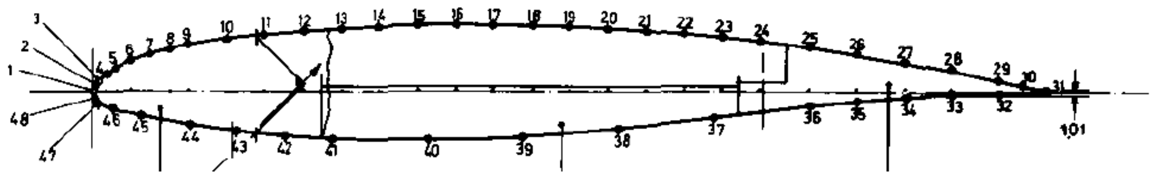

Table 5.1 Design coordinates for the airfoil SKF 1.1

Basic airfoil - Upper surface

Note: For actual model coordinates see Table 5.2

No.	x (mm)	z (mm)
1	0.000	0.179
2	0.001	0.348
3	0.011	0.517
4	0.028	0.685
5	0.053	0.852
6	0.094	1.051
7	0.145	1.247
8	0.207	1.440
9	0.279	1.630
10	0.361	1.815
11	0.452	1.995
12	0.553	2.171
13	0.693	2.386
14	0.845	2.593
15	1.009	2.791
16	1.182	2.981
17	1.364	3.164
18	1.553	3.339
19	1.876	3.612
20	2.210	3.870
21	2.553	4.117
22	3.048	4.450
23	3.553	4.768
24	4.046	5.063
25	4.546	5.346
26	5.052	5.618
27	5.545	5.868
28	6.043	6.109
29	6.545	6.341
30	7.052	6.564
31	7.670	6.823
32	8.293	7.073
33	8.920	7.311
34	9.551	7.539
35	10.243	7.777
36	10.940	8.003
37	11.640	8.217
38	12.344	8.421
39	13.050	8.615
40	13.945	8.848
41	14.842	9.068
42	15.742	9.276
43	16.644	9.473
44	17.549	9.660
45	18.645	9.874
46	19.742	10.076
47	20.842	10.266
48	21.944	10.466
49	23.048	10.616
50	24.377	10.810
51	25.709	10.993
52	27.041	11.165
53	28.375	11.328
54	29.710	11.482
55	31.045	11.628
56	32.756	11.804
57	34.468	11.967
58	36.181	12.119
59	37.895	12.261
60	39.610	12.394
61	41.325	12.517
62	43.041	12.632
63	45.040	12.756
64	47.039	12.870
65	49.038	12.975
66	51.038	13.071
67	53.038	13.159
68	55.039	13.239
69	57.438	13.325
70	59.837	13.402
71	62.236	13.469
72	64.635	13.526
73	67.035	13.575
74	70.034	13.624
75	73.034	13.660
76	76.033	13.683
77	79.033	13.695
78	82.032	13.696
79	85.031	13.687
80	88.030	13.669
81	91.029	13.642
82	94.028	13.608
83	97.027	13.564
84	100.026	13.510
85	103.025	13.444
86	105.026	13.392
87	107.026	13.331
88	109.026	13.262
89	111.025	13.184
90	113.024	13.095
91	115.022	12.994
92	116.738	12.899
93	118.453	12.794
94	120.168	12.681
95	121.881	12.558
96	123.595	12.427
97	125.307	12.287
98	127.019	12.139
99	129.021	11.954
100	131.022	11.759
101	133.022	11.553
102	135.021	11.337
103	137.019	11.112
104	139.016	10.877
105	141.019	10.633
106	143.020	10.378
107	145.020	10.115
108	147.019	9.842
109	149.016	9.560
110	151.013	9.268
111	153.016	8.966
112	155.017	8.653
113	157.018	8.332
114	159.017	8.001
115	161.014	7.662
116	163.010	7.314
117	165.412	6.886
118	167.813	6.447
119	170.212	5.999
120	172.610	5.543
121	175.006	5.081
122	179.506	4.198
123	184.004	3.304
124	190.002	2.102
125	195.501	0.989
126	200.000	0.071

Lower surface

No.	x (mm)	z (mm)
1	200.000	- 0.945
2	197.751	- 0.847
3	195.501	- 0.762
4	193.668	- 0.703
5	191.836	- 0.656
6	190.003	- 0.620
7	188.503	- 0.600
8	187.003	- 0.589
9	185.503	- 0.587
10	184.004	- 0.595
11	182.718	- 0.600
12	181.432	- 0.631
13	180.146	- 0.661
14	178.861	- 0.699
15	177.576	- 0.745
16	176.291	- 0.800
17	175.006	- 0.864
18	173.504	- 0.949
19	172.003	- 1.046
20	170.502	- 1.155
21	169.002	- 1.273
22	167.503	- 1.402
23	166.005	- 1.539
24	164.507	- 1.683
25	163.010	- 1.835
26	160.608	- 2.090
27	158.208	- 2.356
28	155.809	- 2.633
29	153.410	- 2.916
30	151.013	- 3.205
31	145.014	- 3.944
32	139.016	- 4.698
33	127.019	- 6.220
34	124.021	- 6.598
35	121.023	- 6.971
36	118.023	- 7.336
37	115.023	- 7.688
38	113.025	- 7.915
39	111.027	- 8.134
40	109.028	- 8.345
41	107.028	- 8.548
42	105.027	- 8.743
43	103.025	- 8.925
44	101.028	- 9.105
45	99.029	- 9.272
46	97.030	- 9.430
47	95.031	- 9.578
48	93.030	- 9.716
49	91.029	- 9.844
50	89.031	- 9.962
51	87.032	- 10.070
52	85.033	- 10.167
53	83.033	- 10.254
54	81.033	- 10.331
55	79.033	- 10.396
56	77.319	- 10.444
57	75.605	- 10.484
58	73.892	- 10.515
59	72.178	- 10.538
60	70.464	- 10.552
61	68.749	- 10.558
62	67.035	- 10.554
63	65.321	- 10.542
64	63.607	- 10.521
65	61.893	- 10.492
66	60.179	- 10.453
67	58.465	- 10.407
68	56.752	- 10.351
69	55.039	- 10.288
70	53.038	- 10.205
71	51.038	- 10.111
72	49.038	- 10.007
73	47.039	- 9.894
74	45.040	- 9.771
75	43.041	- 9.638
76	41.325	- 9.516
77	39.610	- 9.386
78	37.895	- 9.246
79	36.181	- 9.097
80	34.468	- 8.938
81	32.756	- 8.767
82	31.045	- 8.586
83	29.444	- 8.407
84	27.843	- 8.219
85	26.244	- 8.023
86	24.645	- 7.818
87	23.048	- 7.606
88	21.671	- 7.417
89	20.296	- 7.220
90	18.922	- 7.015
91	17.549	- 6.801
92	16.047	- 6.554
93	14.548	- 6.295
94	13.050	- 6.023
95	12.173	- 5.855
96	11.297	- 5.681
97	10.423	- 5.499
98	9.550	- 5.307
99	8.714	- 5.110
100	7.881	- 4.900
101	7.052	- 4.676
102	6.381	- 4.481
103	5.714	- 4.275
104	5.052	- 4.056
105	4.549	- 3.879
106	4.049	- 3.693
107	3.553	- 3.498
108	3.050	- 3.286
109	2.553	- 3.060
110	2.296	- 2.933
111	2.043	- 2.800
112	1.795	- 2.656
113	1.553	- 2.502
114	1.364	- 2.367
115	1.181	- 2.223
116	1.008	- 2.069
117	0.844	- 1.905
118	0.692	- 1.731
119	0.553	- 1.548
120	0.461	- 1.408
121	0.376	- 1.264
122	0.300	- 1.116
123	0.232	- 0.964
124	0.173	- 0.808
125	0.122	- 0.649
126	0.081	- 0.487
127	0.048	- 0.322
128	0.023	- 0.156
129	0.007	0.011

Table 5.6 DFVLR 1x1 Meter tests. Aerodynamic coefficients[1)]

Run	M_∞	α_g^o	Re · 10^{-6}	c_L	c_m	c_D	Transition	Configuration
60	0.760	2.5	2.31	0.5687	-0.0935	0.0106	Free	Basic airfoil
63	0.760	5.0	2.31	0.8048	-0.0971	0.0296	Free	
84	0.760	2.5	2.33	0.5606	-0.0868	0.0121	220K, 30/25L[3)]	
87	0.760	5.0	2.33	0.7803	-0.0899	0.0316	220K, 30/25L	
157	0.760	2.5	3.61	0.5772	-0.0922	0.0121	Free	
160	0.760	5.0	3.59	0.7879	-0.0986	0.0384	Free	Basic airfoil
234	0.70	0.0	2.22	0.7605	-0.2599	0.0141	Free	5[2)]
235	0.701	3.0	2.22	1.1806	-0.2552	0.0183		
236	0.700	5.0	2.22	1.4795	-0.2667	0.0407		
237	0.700	7.0	2.22	1.4795	-0.2409	0.0993		
240	0.760	0.0	2.32	0.8085	-0.2917	0.0197		
241	0.760	3.0	2.31	1.2230	-0.3150	0.0412		
242	0.759	5.0	2.31	1.3241	-0.2930	0.0578		
243	0.761	7.0	2.31	1.3811	-0.2741	0.1088		
223	0.600	3.0	2.01	1.0543	-0.2333	0.0139		
229	0.650	3.0	2.12	1.1154	-0.2419	0.0150		
230	0.650	6.0	2.12	1.4738	-0.2211	0.0362	Free	5
271	0.600	3.0	2.03	0.8430	-0.1563	0.0141	Free	4[2)]
277	0.650	3.0	2.13	0.8876	-0.1615	0.0149		
278	0.650	6.0	2.12	1.2941	-0.1560	0.0321	Free	4

Table 5.7 ONERA S3MA tests. Aerodynamic coefficients[1)]

Run	M_∞	α_g^o	Re · 10^{-6}	c_L	c_m	c_D	Transition	Configuration
9617	0.703	2.07	7.34	1.149	-0.2517	0.0224	Free	5[2)]
	0.703	4.08	7.25	1.446	-0.2604	0.0401		
9618	0.702	6.03	7.28	1.461	-0.2525	0.1079		
9621	0.760	2.05	7.73	1.206	-0.3031	0.0354		
	0.761	4.07	7.73	1.253	-0.2728	0.0681		
9606	0.499	2.05	5.55	0.997	-0.2286	0.0107		
9610	0.600	2.06	6.61	1.038	-0.2390	0.0122		
9612	0.649	2.06	6.97	1.076	-0.2442	0.0128		
9625[4)]	0.702	2.11	7.52	1.398	-0.3126	0.0756		
	0.702	4.06	7.51	1.300	-0.2691	0.1404	Free	5
9573	0.760	2.04	3.50	0.6037	-0.0965	0.0127	Free	Basic arifoil
9589	0.760	2.10	7.60	0.6180	-0.0935	0.0128		

Airbus TA11 Airfoil

(η = 0,55)

Year	1992
t/c	0,111

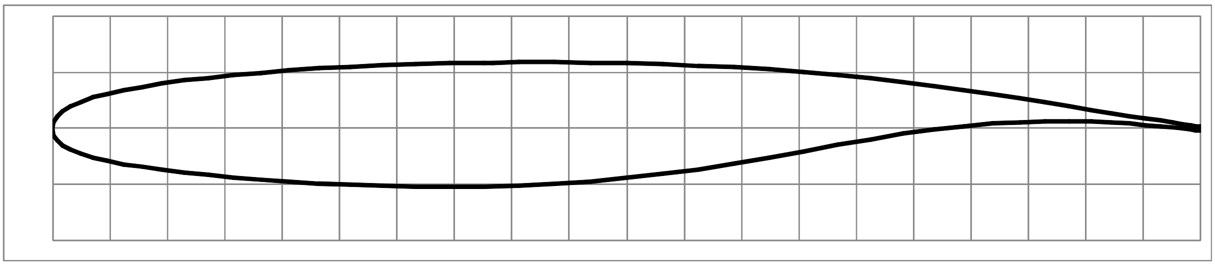

x/c	y_u/c	x/c	y_l/c
0,000000	0,000000	0,000000	0,000000
0,000967	0,005744	0,000967	-0,005606
0,003943	0,010954	0,003943	-0,010579
0,008856	0,015671	0,008856	-0,015030
0,015708	0,019992	0,015706	-0,019006
0,024472	0,023980	0,024472	-0,022574
0,035112	0,027670	0,035112	-0,025824
0,047586	0,031138	0,047586	-0,028792
0,061847	0,034391	0,061647	-0,031563
0,077836	0,037450	0,077836	-0,034182
0,095492	0,040313	0,095492	-0,036695
0,114743	0,043012	0,114743	-0,039101
0,135516	0,045539	0,135516	-0,041376
0,157726	0,047883	0,157726	-0,043504
0,181288	0,050025	0,181268	-0,045467
0,206107	0,051965	0,206107	-0,047235
0,232087	0,053692	0,232087	-0,048770
0,259123	0,055193	0,259123	-0,050038
0,287110	0,056463	0,287110	-0,051007
0,315938	0,057493	0,315938	-0,051639
0,345492	0,058279	0,345492	-0,051860
0,375655	0,058814	0,375655	-0,051567
0,383842	0,058912	0,406309	-0,050677
0,406309	0,059066	0,437333	-0,049135
0,437333	0,059089	0,468605	-0,046897
0,468605	0,058818	0,500000	-0,043962
0,500000	0,058267	0,531395	-0,040343
0,531395	0,057426	0,562667	-0,036056
0,562667	0,056291	0,593691	-0,031127
0,593691	0,054852	0,624345	-0,025692
0,624345	0,053045	0,654508	-0,020005
0,654508	0,050800	0,684062	-0,014414
0,684062	0,048115	0,712690	-0,009227
0,712890	0,045051	0,740877	-0,004658
0,740877	0,041687	0,767913	-0,000838
0,767913	0,038108	0,793893	0,002175
0,793893	0,034399	0,818712	0,004374
0,818712	0,030653	0,842274	0,005795
0,842274	0,026957	0,864484	0,006511
0,864464	0,023390	0,885257	0,006625
0,885257	0,020020	0,904508	0,006250
0,904508	0,016693	0,922164	0,005507
0,922164	0,014037	0,938153	0,004518
0,938153	0,011465	0,952414	0,003396
0,952414	0,009184	0,964888	0,002246
0,964868	0,007197	0,975528	0,001154
0,975528	0,005510	0,984292	0,000190
0,984292	0,004122	0,991144	-0,000596
0,991144	0,003038	0,996057	-0,001172
0,996057	0,002261	0,999013	-0,001521
0,999013	0,001794	1,000000	-0,001638
1,000000	0,001638		

References

AGARD-AR-138 ADVISORY GROUP FOR AEROSPACE RESEARCH AND DEVELOPMENT; NORTH ATLANTIC TREATY ORGANIZATION: *Experimental Data Base for Computer Program Assessment* : *Report of the Fluid Dynamics Panel Working Group 04*. Neuilly sur Seine : NATO, 1979 (AGARD-AR-138)

NACA TN 4279 HUNTON, Lynn W.; National Advisory Committee for Aeronautics: *Effects of Fixing Transition on the Transonic Aerodynamic Characteristics of a Wing-Body Configuration at Reynolds Numbers from 2.4 to 12 Million*. Washington : NACA, 1958 (NACA TN 4279). – Technical Note

NASA TM-81912 HARRIS, Charles D.; MCGHEE, Robert J., ALLISON, Dennis O., National Aeronautics and Space Administration: *Low Speed Aerodynamic Characteristics of a 14-Percent-Thick NASA Phase 2 Supercritical Airfoil Designed for a Lift Coefficient of 0.7*. Washington : NASA, 1980 (NASA TM X-72712). – Technical Memorandum

NASA TM-81922 JOHNSON, JR., William G.; HILL, Acquilla S.; RAY, Edward J; et. al.; National Aeronautics and Space Administration: *High Reynolds Number Tests of a Boeing BAC I Airfoil in the Langley 0.3-Meter Transonic Cryogenic Tunnel*. Washington : NASA, 1982 (NASA TM-81922, L-15011). – Technical Memorandum

NASA TM-85663 JENKINS, Renaldo V.; National Aeronautics and Space Administration: *Reynolds Number Tests of an NPL 9510 Airfoil in the Langley 0.3-Meter Transonic Tunnel*. Washington : NASA, 1983 (NASA TM-85663). – Technical Memorandum

NASA TM-85732 PLENTOVICH, E. B.; LADSON, Charles L.; HILL, Acquila S.; National Aeronautics and Space Administration: *Tests of a NACA 65_1-213 Airfoil in the NASA Langley 0.3-Meter Transonic Cryogenic Tunnel*. Washington : NASA, 1984 (NASA TM-85732). – Technical Memorandum

NASA TM-85739 JENKINS, Renaldo V.; JOHNSON, JR., William G.; HILL, Acquila S.; et. al.; National Aeronautics and Space Administration: *Data from Tests of a R4 Airfoil in the Langley 0.3-Meter Transonic Cryogenic Tunnel*. Washington : NASA, 1984 (NASA TM-85739). – Technical Memorandum

NASA TM-86273 DRESS, David A.; STANEWSKY, Egon; MCGUIRE, Peggy; et. al.; National Aeronautics and Space Administration: *High Reynolds Number Tests of the CAST 10-2/DOA 2 Airfoil in the Langley 0.3-Meter Transonic Cryogenic Tunnel – Phase II*. Washington : NASA, 1984 (NASA TM-86273). – Technical Memorandum

NASA TM-86371 JOHNSON, JR, William G.; HILL, Acquila S.; EICHMANN, Otto; National Aeronautics and Space Administration: *High Reynolds Number Tests of a NASA SC(3)-0712(B) Airfoil in the Langley 0.3-Meter Transonic Cryogenic Tunnel*. Washington : NASA, 1985 (NASA TM-86371, L-15909). – Technical Memorandum

NASA TM-87600 JOHNSON, JR, William G.; HILL, Acquila S.; National Aeronautics and Space Administration: *Pressure Distributions From High Reynolds Number Tests of a Boeing BAC I Airfoil in the 0.3-Meter Transonic Cryogenic Tunnel*. Washington : NASA, 1985 (NASA TM-87600, L-16010). – Technical Memorandum

NASA TM-89102 MINECK, Raymond E.; LAWING, Pierre L.; National Aeronautics and Space Administration: *High Reynolds Number Tests of the NASA SC(2)-0012 Airfoil in the 0.3-Meter Transonic Cryogenic Tunnel*. Washington : NASA, 1987 (NASA TM-89102, L-16259). – Technical Memorandum

NASA TM X-72711 HARRIS, Charles D.; National Aeronautics and Space Administration: *Aerodynamic Characteristics of the 10-Percent-Thick NASA Supercritical Airfoil 33 Designed for a Normal-Force Coefficient of 0.7*. Washington : NASA, 1975 (NASA TM X-72711). – Technical Memorandum

NASA TM X-72712 HARRIS, Charles D.; National Aeronautics and Space Administration: *Aerodynamic Characteristics of a 14-Percent-Thick NASA Supercritical Airfoil Designed for a Normal-Force Coefficient of 0.7*. Washington : NASA, 1975 (NASA TM X-72712). – Technical Memorandum

NASA TP-2969 HARRIS, Charles D.; National Aeronautics and Space Administration: *NASA Supercritical Airfoils* : *A Matrix of Family-Related Airfoils*. Washington : NASA, 1975 (NASA TP-2969, L-16625). – Technical Paper

NASA TP 3579 ALLISON, Dennis O.; MINECK, Raymond E.; National Aeronautics and Space Administration: *Assessment of Dual-Point Drag Reduction for an Executive-Jet Modified Airfoil Section*. Washington : NASA, 1996 (NASA TP-3579, L-17500). – Technical Paper

NTRS 2011 NASA Technical Reports Server (NTRS). URL: http://ntrs.nasa.gov (2011-12-19)